TREHALOSE-6-PHOSPHATE IS REQUIRED FOR METABOLISM AND VIRULENCE IN THE HUMAN FUNGAL PATHOGEN *ASPERGILLUS FUMIGATUS*

by

Srisombat Puttikamonkul

A dissertation submitted in partial fulfillment
of the requirements for the degree

of

Doctor of Philosophy

in

Immunology and Infectious Diseases

MONTANA STATE UNIVERSITY
Bozeman, Montana

July 2012

APPROVAL

of a dissertation submitted by

Srisombat Puttikamonkul

This dissertation has been read by each member of the dissertation committee and has been found to be satisfactory regarding content, English usage, format, citation, bibliographic style, and consistency and is ready for submission to The Graduate School.

Dr. Robert A. Cramer Jr.

Approved for the Department of Immunology and Infectious Diseases

Dr. Mark T. Quinn

Approved for The Graduate School

Dr. Carl A. Fox

STATEMENT OF PERMISSION TO USE

In presenting this dissertation in partial fulfillment of the requirements for a doctoral degree at Montana State University, I agree that the Library shall make it available to borrowers under rules of the Library. I further agree that copying of this dissertation is allowable only for scholarly purposes, consistent with "fair use" as prescribed in the U.S. Copyright Law. Requests for extensive copying or reproduction of this dissertation should be referred to ProQuest Information and Learning, 300 North Zeeb Road, Ann Arbor, Michigan 48106, to whom I have granted "the exclusive right to reproduce and distribute my dissertation in and from microform along with the non-exclusive right to reproduce and distribute my abstract in any format in whole or in part."

Srisombat Puttikamonkul

July 2012

ACKNOWLEDGEMENTS

I am so grateful for the fellowship supported by the Royal Thai Government. I am also thankful for funding provided by NIH-COBRE and the Montana State University Agricultural Experiment Station. I wish to express my special gratitude and appreciation to my advisor Dr. Robert A. Cramer Jr. for his patience, exceptional support and guidance. I would like to express my special thanks to my graduate committee members Dr. Allen G. Harmsen, Dr. Mark A. Jutila, Dr. Jovanka M. Voyich-Kane, and Dr. John E. Sherwood for taking time to provide critical direction and advice throughout my graduate education. Dr. Richard J. Smith, and Dr. Brian Bothner as graduate representatives, also generously providing input and their time. I would like to thank all current and past members of the Cramer lab including Kari Cramer, Dr. Sven D. Willger, Dr. Nora Grahl, Dr. Jean Cornish, Peggy Lehmann, Dr. Bridget Barker, Dr. Dawoon Chung, Sara Blosser, Kelly Shepardson, and Brittney Hendrickson for contributing to an outstanding research environment. I am also grateful for the support of our collaborating investigators Dr. John R. Perfect, Dr. Brian Bothner, Dr. David S. Perlin, Dr. Jean-Paul Latge, Dr. Agnieszka Rynda-Apple, Dr. Joshua J. Obar, Dr. Jonathan Hilmer, Dr. Vishu Kumar Amanianda, Navid Movahed, Steven Park, and Padmaja Paderu. Thanks to employees of the Animal Resources Center at Montana State University for Animal assistance. Finally, I am grateful to my family and friends for their love and support. I would like to express my deepest thanks to my husband, Songklod Puttikamonkul for his love, support, and always encouraging me to overcome the difficulties.

TABLE OF CONTENTS

TABLE OF CONTENTS-CONTINUED

TABLE OF CONTENTS-CONTINUED

TABLE OF CONTENTS-CONTINUED

TABLE OF CONTENTS-CONTINUED

LIST OF TABLES

LIST OF FIGURES

LIST OF FIGURES-CONTINUED

LIST OF FIGURES-CONTINUED

ABSTRACT

High mortality rates associated with Invasive Pulmonary Aspergillosis (IPA), commonly caused by the mold *Aspergillus fumigatus*, have dramatically increased in immunocompromised patients during the past 30 years. With limited antifungal drugs available and inconsistent outcomes associated with current antifungal drug treatment, much effort is being focused on new antifungal drug development. *A. fumigatus* has evolved multifactorial mechanisms to survive various stress conditions encountered in environment and *in vivo* during infection. Targeting the biochemical pathways utilized by the fungus to adapt to stress conditions is one proposed approach for development of new antifungal drugs. Biosynthesis of the disaccharide trehalose is one such target that is not found in mammals. This dissertation aimed to characterize the role of the trehalose biosynthesis pathway in the biology and virulence of *A. fumigatus*. My objectives were to identify the function of putative enzyme encoding genes involved in the TPS1/TPS2 pathway and establish the contribution of each protein to the virulence of *A. fumigatus* in clinically relevant IPA murine models.

My data suggests that the Trehalose-6-phosphate intermediate of the TPS1/TPS2 pathway plays a critical role in regulating fungal metabolic homeostasis and integrity of fungal cell wall. A mutant deficient in the TPS2 ortholog, OrlA, displayed increased sensitivity to cell wall perturbing drugs and importantly was attenuated in virulence in two murine models of IPA. My data further suggests that the attenuated virulence phenotype is directly linked to these changes in the fungal cell wall that alter the innate immune response to this fungal strain. In contrast, trehalose itself while having a general role in stress protection does not have a role in virulence in IPA models. Finally, my data suggest intricate links between the mobilization of trehalose and accumulation of T6P that also affect fungal metabolism and cell wall homeostasis via the activity of trehalose phosphorylase enzymes. In conclusion, my data supports the hypothesis that the trehalose biosynthesis pathway is a potential target for antifungal drug development in *A. fumigatus* particularly at the level of TPS2 activity. However, the underlying host immune status must also be taken into account when targeting this key fungal metabolic pathway.

CHAPTER ONE

BACKGROUND

Introduction to Aspergillosis

Problem Statement

Currently, infections caused by the mold *Aspergillus fumigatus* are growing in significance and frequency [1,2]. Importantly, there are limited effective and non-toxic antifungal drugs available to treat *Aspergillus* infections as fungi are eukaryotic organisms that have similar genetic compositions to humans. Recent reports have also observed increases in resistance against the limited number of antifungal drugs [3]. In particular, at least 27% of metazoan specific genes have detectable homologues in other eukaryotes, including *Saccharomyces cerevisiae* [4]. Indeed, many genes and gene products found in fungi are found in humans. Among seven eukaryotic genomes, approximately 40% of eukaryotic orthologous groups (KOG) have shown protein enrichment in housekeeping functions, particularly translation and RNA processing and these conserved KOGs are often essential for survival [5]. Consequently, most of the effective drugs against fungi are harmful and cause toxicity when used therapeutically in humans. Thus, much effort is being placed on identifying alternate antifungal drug targets and compounds that directly and specifically inhibit fungal growth without interfering with host cells, such as the trehalose biosynthetic pathway [6]. The traholse pathway has been examined in multiple fungal species as a possible target for therapy, but not in *A. fumigatus,* and was found to be essential for full virulence in fungal murine models.

Therefore, we believe that trehalose biosynthesis pathway plays a protective role and prevent *in vivo* environmental stresses in a successful pathogen *A. fumigatus*.

Aspergillus spp.

The *Aspergilli* are filamentous fungi (molds), which are multicellular eukaryotes with a relatively simple life cycle. The first description of *Aspergillus* was defined by Micheli in 1729, he described this mold by illustrating the pattern of beautiful conidial heads of *Aspergillus* with radiating conidia that resembled an aspergillum (a device used for sprinkling holy water in Roman Catholic masses) [2,7]. *Aspergillus* species are ascomycetes classified in the subdivision Deuteromycotina because most of these molds do not have a sexual reproductive phase. Over 200 species have been classified in the genus *Aspergillus* and new species continue to be described [8].

Among *Aspergillus* isolates from large diagnostic reference hospital centers, *Aspergillus fumigatus* is by far the most common species (50-60%), followed by *A. flavus, A. niger* and *A.terreus* (10-15% each), whereas *A. nidulans, A. ustus* and other rare *Aspergillus spp.* typically each represents <2% of isolates obtained from patients [9,10]. Many *Aspergillus spp.* have long been used in food production, industrial fermentation, and agriculture. On the other hand, a few, such as *A. fumigatus*, *A. flavus, A. niger, A. nidulans*, and *A. terreus*, are so called opportunistic fungal pathogens, causing life threatening invasive aspergillosis (IA) in immunosuppressed patients, in which *A. fumigatus* is one of the leading causes of infectious disease [2].

Aspergillus fumigatus is a saprophytic fungus found in soil where it decomposes and recycles organic matter [11]. This species has long been considered an asexual reproductive fungus, but recently a fully functional sexual reproductive cycle was discovered [12]. In 2009, a group of scientists in Ireland found the sexual life cycle and structures (cleistothecia and ascospores) of *A. fumigatus* produced on particular oat media and under non-disturbed cultivation conditions. Despite the presence of a sexual cycle, identification of *A. fumigatus* is based predominantly upon the morphology of asexual reproductive structures; conidia and conidiophores. The organism is characterized by green echinulate conidia (2.5 to 3 μm in diameter) produced in chains basipetally (the youngest conidium being at the base and the oldest being at the tip of the chain) from greenish conidiogenous cells; phialides. The phialides are 6 to 8 by 2 to 3 mm in size and borne directly on broadly clavate vesicles (20 to 30 mm in diameter) in the absence of metulae (Figure 1.1) [13,14].

This mold is disseminated in the air and can become a serious opportunistic pathogen to humans by causing a range of illness including chronic allergy type diseases and deadly invasive lung infections in immune-deficient patients [15]. Particularly, due to the “respirable-sized spores”, *A. fumigatus* is capable of bypassing initial structural immune defense mechanisms and entering the small airway inside the lung after inhalation. The inhaled conidia are normally eliminated by a competent innate immune response; however in immunocompromised patients or patients with pre-existing lung damage conidia are able to germinate, develop into hyphae, and colonize and damage the

integrity of the pulmonary epithelium as shown in the infectious life cycle of *A. fumgatus* (Figure 1.2) [16,17].

The genome of a clinical isolate *A. fumigatus* (AF293) has been fully sequenced by a whole genome random sequencing method. It revealed that this organism possesses a 29.4 Mb genome, which consists of eight chromosomes containing 9,926 predicted genes [18]. An additional clinical isolate was also sequenced, *A. fumigatus* A1163, and contained 99.8% identity to AF293 at the nucleotide level [19]. Moreover, the comparison of the genome of both *A. fumigatus* isolates and two closely related but rarely pathogenic species; *Neosartorya fischeri* and *A. clavatus,* suggested that *A. fumigatus* may possess lineage-specific genes that contribute to metabolic versatility and pathogenicity during *in vivo* infection.

Invasive Aspergillosis (IA)

Invasive aspergillosis is an emerging disease mainly found in immunocompromised individuals, such as organ transplant patients under long-term treatment with immunosuppressive drugs. This disease is most often caused by the fungal pathogen, *A. fumigatus*. In the past 30 years, there has been a substantial increase in the number of transplantation patients, more aggressive chemotherapy for myeloma, breast cancer, autoimmune disease, and the emergence of AIDS. A greater prevalence of risk factors among patients was associated with prolonged granulocytopenia. As the duration of granulocytopenia increased, the rate of development of IA increased [20]. The mortality from opportunistic fungal infections exceeds 50%, and has been reported to be

as high as 95% in leukemia patients and bone-marrow transplant patients infected with *Aspergillus* species [21,22].

Therapeutic Treatment

During the late twentieth century, only two antifungal agents, amphotericin B and itraconazole, were used as effective agents for treatment of invasive aspergillosis [1]. Amphotericin B was a gold standard for primary treatment of aspergillosis until 2000 [10]. High antifungal failure rate observed in the treatment of 595 IA patients reflects the actual clinical outcome achieved and confirms that mortality from IA in severely immunosuppressed patients remains high even when treated with amphotericin B [9]. Recently, voriconazole, a new broad-spectrum triazole, has been shown to be significantly superior to conventional amphotericin B and is now the drug of choice for treating IA [10,23]. A guideline from the Infectious Diseases Society of America (IDSA) now recommends the use of voriconazole as the primary therapy for invasive aspergillosis [24]. The largest randomized controlled trial demonstrates that voriconazole is more effective than amphotericin B deoxycholate, and improves survival (71% vs. 58%) with fewer severe drug-related adverse events compared to the standard approach of therapy with amphotericin B [23]. Additionally, late diagnosis often impedes successful treatment especially with less effective antifungal drugs [22]. IA remains a devastating infection despite voriconazole use. Mortality rates are over 90% in untreated patients. In contrast, mortality rates are usually around 30% - 50% in IA patients treated with voriconazole depending on the patients underlying condition [23]. The emerging significance and high mortality rates associated with IA has generated great interest in the

scientific community to elucidate the pathogenesis mechanisms of *A. fumigatus*. In addition, the whole-genome sequence availability of *A. fumigatus* allows the study of important metabolic pathways regarding virulence during infection. An increased understanding of the virulence mechanisms of this organism may facilitate the rational design of novel therapeutic strategies [15,16,18].

Antifungal Drugs

Triazoles are synthetic compounds that inhibit the synthesis of ergosterol from lanosterol in the fungal cell membrane [24]. The most effective azole drug for IA treatment is voriconazole which is approved by the Food and Drug Administration (FDA). Voriconazole, also called Vfend, is a broad-spectrum triazole that is active against various yeasts and molds, including *Aspergillus* species. Azoles have a toxic effect on mammalian cytochrome P450 functions causing hepatotoxicity and visual disturbances [25]. However, initial therapy with voriconazole leads to better responses and improved survival in patients with IA, and results in fewer severe side effects than the standard approach of initial therapy with amphotericin B. [23].

Amphotericin B is a natural polyene macrolide antibiotic which binds to ergosterol in fungal cell membrane leading to the formation of ion channels and thus fungal cell death. Since Amphotericin B also binds to cholesterol in mammalian cell membrane, it causes a severe adverse side effect against host cells that results in cellular injury and organ dysfunction particularly in the kidneys [24].

Echinocandins are antifungal agents acting on the cell wall by inhibiting β-glucan synthesis through inhibition of the target gene *fksA*. Caspofungin is the only echinocandin that is approved by FDA as salvage therapy for IA [25].

Antifungal Drugs Resistance

Resistance to the triazoles has been documented and more prevalent in particular areas of the world with two different patterns. First, azole resistance has occurred in the environment where this saprophytic fungus is exposed to azole fungicides used in agriculture and subsequently fungi becoming cross resistant to medical triazoles has been observed in European countries [3,26,27,28]. Second, the most common resistance mechanism that has been proposed in *A. fumigatus* is the acquired resistance during long-term azole therapy in patients with Aspergilloma [3]. The emergence of azole cross resistance is a devastating outcome in IA treatment and increased multi-azole resistance has become a global problem. The number of available drugs for treating IA is limited and the triazoles are the only class of antifungal drugs that can be administered orally. It is therefore of great interest to study new promising antifungal drug target and elucidating a potential class of specific antifungal drug that overcome adverse drug related outcomes and substitution of limited therapeutic options. Identifying and characterizing such a new drug target was a major objective of this dissertation research.

Fungal Virulence Attributes

A. fumigatus has evolved mechanisms to survive in environments by conferring a competitive advantage against microorganisms that share the same ecological niche [29],

which implies that the virulence of *A. fumigatus* relies on multifactorial adaptation to environmental conditions. Key traits for fungal virulence and survival during human infection include the following mechanisms discussed below [13,30].

High Temperature Growth

Survival at elevated temperatures of a human host is essential for fungal virulence [31]. The ability to grow at 37^{o}C is a key characteristic that distinguishes mammalian pathogenic species from nonpathogenic ones. Indeed, human pathogenic fungi are capable of growing at 35-37^{o}C. Although most *Aspergillus* species are incapable of growing at 37^{o}C, *A. fumigatus* is able to survive at temperatures up to 70^{o}C [2,11,32]. Due to their high temperature growth, *Asperigillus spp*. are commonly found in tropical areas [33].

Growth Rate

Each *Aspergillus* species grows at a different rate, and the most rapidly growing organism is *A. fumigatus*. Related to this, it has been reported that fungal growth rate is likely one of the key factors to determine rates of disease progression and pathogenicity [2].

Size and Surface Features of Conidia

Aspergillus spp. produce conidia commonly less than 3 μm in diameter [33], and the small size enable conidia to penetrate deeply into the lung. The surface of conidia is covered with hydrophobic proteins, RodA that are covalently bound to conidial cell wall.

The RodA proteins play a role in masking *A. fumigatus* to avoid recognition by the immune system. [34].

Secretion of Extracellular Proteases

Proteinases produced by *A. fumigatus* include metalloproteinases, alkaline proteinases, and elastases. To be able to survive in environmental niches or host cells, *A. fumigatus* has evolved nutrient uptake mechanisms involving the secretion of extracellular proteases. Most saprophytic fungi secrete extracellular enzymes and proteases that have major roles in degrading organic matter in the environment [35]. Likewise, the secreted enzymes utilized to obtain nutrients from the host during infection also cause destruction of host cells. Main components of lung tissue are collagen and elastin. The presence of elastins is likely linked to the increased elastase activity *A. fumigatus* adapted to growth in host environments. Although the presence of elastases and acid proteinase activity is not clearly correlated with development of invasive disease caused by *Aspergillus spp.*, 95.6% of a total 45 isolated *A. fumigatus* strains appear to possess elastase activity [36]. A number of proteases secreted by *A. fumigatus* presumably have functional redundancy. However, a role of the proteases in virulence in *A. fumigatus* remains controversial. More recently, PrtT, a transcription factor that controls expression of multiple extracellular proteases has been characterized in *A. niger*. In *A. fumigatus*, deletion of the PrtT homolog resulted in loss of secreted proteases activity. Although culture filtrates from a PrtT mutant reduced the killing of lung epithelial cells, disruption of PrtT did not affect virulence in a neutropenic murine model of aspergillosis [37].

Secondary Metabolites

Aspergillus species produce a remarkable number of highly diverse secondary metabolites, which facilitate adaptation to diverse ecological niches [38]. In addition, it has been reported that production of secondary metabolites are associated with pathogenicity in *A. fumigatus*. For example, a deletion of *laeA*, a gene encoding a putative methyltransferase that broadly regulates secondary metabolism, significantly impaired virulence in a murine IA model [39]. In addition, transcriptional profiling of *A. fumigatus* at the onset of invasive infection revealed that expression of genes involved in secondary metabolism were up-regulated during infection, which suggested a potential link between production of secondary metabolites and fungal responses to host immunity. An epipolythiodioxopiperazine, gliotoxin, is a mycotoxin produced by *A. fumigatus* and synthesis of gliotoxin is transcriptionally regulated in part by LaeA. Giotoxin has pleiotropic effects on various mammalian cell lines; at nanomolar concentrations it downregulates an oxidative burst by interfering with assembly of the NADPH oxidase complex [40]. Moreover, gliotoxin has been shown to reduce phagocytic activities of macrophages and neutrophils by inhibiting activation of the transcription factor NF-kB, a central regulator of inflammatory responses [41]. At higher concentrations (micromolar), gliotoxin induces apoptosis of macrophages [42]. Although PMNs remain resistant to gliotoxin-mediated apoptosis, phagocytosis and ROS production of PMNs is inhibited by gliotoxin. [43]. The role of gliotoxin in *A. fumigatus* virulence remains somewhat controversial as its importance for virulence appears linked to the underlying immune system status of the host [44,45,46].

Detoxifying Enzyme Production

Detoxification of hydrogen peroxide (H_2O_2) depends on iron because catalases and peroxidases require heme as a cofactor. Consistently, in iron-depleted conditions, *A. fumigatus* is more sensitive to hydrogen peroxide than in iron-replete conditions. Detoxification of hydrogen peroxide by catalases was proposed as a strategy of fungi to cope with stresses caused by reactive oxygen species (ROS) that phagocytic cells produce. *A. fumigatus* produces three active catalases; one conidial catalase and two mycelial catalases. A mutant lacking the conidial catalase (CatA) has increased sensitivity to H_2O_2 but no difference in susceptibility when tested in both a macrophage killing assay and in rat model of aspergillosis relative to wild type [47]. A double knock-out mutant lacking both mycelial catalases (Cat1 and Cat2) has attenuated virulence in a rat model [47]. ROS has been repeatedly described as playing an essential role in fungal killing. Regardless of NADPH oxidase function, internalization of conidia by AM rapidly occurred *in vitro* after 15 minutes of incubation [48]. Following engulfment of conidia by AM, ROS production is generated in response to the swollen conidia inside the phagolysosome and mediating the killing of *A. fumigatus*. Accordingly, AM from either corticosteroids immunosuppressed host or a mouse model of CGD (p47phox-/-) displayed a reduction of fungal killing which is associated with ROS production. Thus, human patients with a defective NADPH oxidase system or chronic granulomatous disease (CGD) are prone to recurrent infections of bacteria and fungi [49]. Invasive aspergillosis is the leading cause of mortality in CGD patients, reflecting the role of phagocyte NADPH oxidase in host defense against *A. fumigatus* [50]. Given that

NADPH oxidase and ROS production are essential for killing of fungal conidia by AM, *A. fumigatus* utilizes the superoxide dismutases (SOD) detoxification mechanism of extremely reactive superoxide anions produced by the NADPH oxidase complex. This mechanism has been considered as a putative fungal virulence factor as the *A. fumigatus* SOD mutants were more sensitive *in vitro* to oxidative stress and killing by AM of immunocompetent mice, however SOD was not required for fungal virulence in the immunocompromised mice.

Siderophore Biosynthesis

During infection, both animal hosts and invading microbes utilize strategies to withhold iron from surrounding organisms. Iron is essential for metabolism by serving as a cofactor for catalases, oxygenases, and peroxidases among other critical metabolic processes like respiration. Therefore, iron plays an important part in resistance against oxidative stress. However, overload of iron can also be toxic and cause adverse effects to both pathogens and hosts. In the mammalian hosts, iron is tightly bound by carrier proteins such as transferrin, which can result in limited iron availability for microbial growth. Most aerobic bacteria and fungi have genes encoding iron transport systems that become induced under iron limitation [51,52]. *A. fumigatus* lacks specific uptake systems for host iron sources such as heme, ferritin, or transferrin. Instead, it employs two high-affinity iron uptake systems, reductive iron assimilation (RIA) and siderophore-assisted iron uptake, both of which are induced upon iron starvation [53]. Siderophores are ferric iron-specific chelators which are synthesized during iron starvation [54]. Most fungi utilize intracellular siderophores as an iron storage compound. In *A. fumigatus*, a null

mutant of *sidA* encoding ornithine-N5-monooxygenase is unable to produce both intra- and extracellular siderophores, and importantly exhibited attenuated virulence in a neutropenic mouse model. These data suggest that siderophores are crucial for virulence of *A. fumigatus*. [53].

Hypoxia Adaptation

Recent studies have uncovered a sterol regulatory element binding protein (SrbA) as a regulator of hypoxia adaptation in *A. fumigatus*. A null mutant of *srbA* grows normally in normoxia (atmospheric oxygen 21%) but is incapable of growing in hypoxic conditions (1% O_2, 5% CO_2, 94% N_2). This mutant shows increased susceptibility to azole drugs, abnormal hyphal polarity, and avirulence in murine models of aspergillosis [55]. This finding suggests that an ability to grow in hypoxic conditions is an essential attribute of *A. fumigatus* to cause lethal disease. In addition, three immunologically distinct murine models of IA have shown that hypoxic microenvironments occur in the lung during infection [56], which supports hypoxia adaptation regulated by SrbA as critical for A. *fumigatus* virulence.

Melanin

Conidial melanins are pigments formed by oxidative polymerization of phenolic compounds. The polyketide polymers of melanins are synthesized during spore formation by deposition of a dense layer on the conidial surface [57]. Melanin protects conidia from oxidative damage by acting as a reactive oxygen intermediate (ROI) scavenger against oxidative damage by host leukocytes [58]. Deletion of *pksP,* encoding a type I polyketide

synthase, is essential for melanin biosynthesis and results in hypovirulence of *A. fumigatus*. Moreover, these results suggest that melanin may play a modulatory role in impeding the capability of host immune cells to respond to specific ligands on *A. fumigatus* [59,60]. Recently, a novel potential function of melanin was demonstrated in the protection against mammalian apoptosis through a sustained PI3K/Akt signaling pathway of infected macrophages [61].

Carbon Metabolism

Assimilation of available carbon sources is essential for fungal survival. It has been demonstrated that in host cells rich carbon sources like glucose are limited and only poor two carbon sources such as acetate and fatty acids are available. A role of alternative carbon metabolism utilized by the glyoxylate cycle, which requires isocitrate lyase (ICL) is essential and induced in persistent growth of *Candida albicans* inside phagosomes [62]. An increased expression of ICL was observed in *A. fumigatus* after being exposed to host macrophages, however ICL is dispensable for virulence in neutropenic IA murine models [63,64]. A transcriptional profile of conidia and hyphae exposed to host neutrophils revealed that a pool of genes involved in carbon metabolism was upregulated in conidia, which suggested that fungal metabolic reprogramming is employed to survive within host environments [30,65].

Discovery of Trehalose and Its Role in Fungi

As eukaryotic organisms, fungi including *A. fumigatus* share similar genes and metabolic pathways with humans [5]. This characteristic of fungi is partly responsible for

the limited effectiveness of antifungal drugs. Therefore, development of antifungal drugs targeting a fungal metabolic pathway that is absent in mammals is an attractive proposition. One example of a specific metabolic pathway found in fungi but not in mammals is the trehalose biosynthesis pathway.

Trehalose was incidentally discovered in Ergot in 1832 by H.A.L. Wiggers. In 1858, M. Berthelot found the same sugar in cocoons of beetles called ‘trehala’, which inspired the name of this sugar as ‘trehalose’. Trehalose is synthesized and stored in a wide variety of organisms such as bacteria, fungi, plants, insects, and some other invertebrates, but is not produced by mammals [66,67,68]. Genetic analyses using mutants of genes in the trehalose synthesis pathway have revealed many important roles of this sugar in bacteria and fungi.

Unlike other disaccharides, trehalose has particular properties related to the reducing ends of sugar molecules. Formation of a glycosidic bond by an α-α-(1→1) linkage between two molecules of glucose increases the stability at high temperature and resistance to acidic hydrolysis [69]. Trehalose undergoes two mechanisms of water replacement and glass formation mechanisms, which make trehalose an appropriate membrane and biomolecule stabilizer [70,71,72]. In the water replacement mechanism, trehalose replaces water by establishing hydrogen bonds with membranes and/or macromolecules during dehydration or freezing [70]. In the glass formation mechanism, trehalose is the only sugar that can remain in a glass-like state when completely dehydrated [71]. Staying in a glassy state, trehalose is thought to prevent biomolecules

from being denatured during dehydration and to retain functional activities of biomolecules until water is available for rehydration.

Energy Storage

Trehalose is primarily thought to serve as a storage carbohydrate due to the presence of a trehalase enzyme, which hydrolyzes and converts trehalose into two molecules of glucose. This also serves as a control point of trehalose concentration in the cell. In yeast, glucose may be supplied to the cell by the breakdown of trehalose via trehalase and is used as an energy source for cell recovery when cell membranes are damaged by severe heat shock that can disturb uptake of glucose from the medium [73]. However, this is surprising since yeast already contains glycogen as a storage carbohydrate. Energy reserves normally accumulate when nutrients are abundant, and storage for future starvation as glycogen is produced during exponential phase of growth. By contrast, trehalose is not produced until glucose levels are nearly exhausted and cells grow into stationary phase. In addition, starvation for nitrogen, phosphate and sulfur also induce trehalose accumulation in yeasts [74]. Moreover, glycogen is the sole source of energy that is utilized first during prolonged incubation in stationary phase, and trehalose is degraded long after glycogen stores are depleted. Trehalose may be an important carbohydrate source for reproductive propagules of fungi and is found abundantly in mature ascospores in yeast [75]. In, a filamentous fungus model, *A. nidulans* conidia showe a high concentration of trehalose, which rapidly degrades upon induction of conidial germination [76]. Thus, these data suggest that trehalose and glycogen may play distinct roles in fungal physiology [74].

Stress Protectant

A great variety of species producing trehalose are able to withstand almost complete desiccation and become fully active when the water is available. These patterns are found in plants (*Selaginella lepidophylla*), brine shrimp (*Artemia*), nematode (*Aphelenchus avenae*) and yeast (*S. cerevisiae*) [67,68]. The organisms presumably share a common mechanism for surviving dehydration. Survival of these species in the absence of water has correlated with the synthesis of trehalose. Similarly, yeast cells contain little trehalose in log phase growth and thus show poor survival in dehydration. However, when they accumulate trehalose, the desiccated yeast cells show improved survival. Moreover, when *S. cerevisiae* and *Schizosaccharomyces pombe* in log phase were subjected to heat shock, they rapidly synthesized trehalose and increased their ability to survive [77,78,79], implicating accumulation of trehalose as a key factor in survival at high temperature and dehydration. Additionally, trehalose can stabilize dry membranes more efficiently than other disaccharides, and also preserves labile proteins during drying [67].

Thus, it is clear that trehalose is much more than simply a storage compound as discussed above. A number of studies have revealed additional roles of trehalose as a general stress protectant against a variety of stress conditions in bacteria. For example, to protect cells from cold, an *E. coli* mutant strain that shows no trehalose production dies much earlier than wild type at 4^{o}C [80]. In contrast to most bacteria, *Mycobacterium tuberculosis* and *M. smegmatis* possess three pathways for synthesis of trehalose, which suggests critical roles of trehalose require the presence of multiple pathways in

Mycobacteria [81,82]. A mutant lacking all three pathways was unable to proliferate at elevated temperature even with supplemented trehalose. Therefore, trehalose is vital for growth and entry into stationary phase in this important human pathogen. [82]. In addition, trehalose is a basic component of a number of different glycolipids and this special cell wall lipid makes *M. tuberculosis* tolerant to anti-tubercular drugs [83].

Mechanism of Trehalose Biosynthesis in the Model Yeast *Saccharomyces cerevisiae*

Five different pathways of trehalose biosynthesis have been identified in various organisms [83,84]. In Baker's yeast this sugar is synthesized through a pathway elucidated by Cabib and Leloir almost 50 years ago [85]. Yeast synthesizes trehalose in a two-step reaction as shown in Figures 1.3 and 1.4. These reactions are carried out by a protein complex consisting of four subunits [86,87,88]:

(1) a 56-kDa subunit of trehalose 6 phosphate synthase encoded by *tps1*

(2) a 100-kDa subunit of trehalose 6 phosphate phosphatase encoded by *tps2*

(3) a 123-kDa subunit of regulatory protein encoded by *tsl1* (trehalose synthase long chain)

(4) a homologue of *tsl1*, regulatory protein encoded by *tps3*

Yeast two hybrid analyses to study *in vivo* interactions among Tps1, Tps2, Tsl1 and Tps3 revealed that both Tsl1 and Tps3 can interact with Tps1 and Tps2 [89]. All subunits are required for optimal enzyme activity and among the four genes studied *tps1* is necessary and sufficient for growth on glucose and fructose. Despite the sequence similarity shared by all proteins, none of the others can take over the function of Tps1.

Synthesis of trehalose starts with transferring of a glucosyl residue from uridine-diphospho-glucose to glucose-6-P to provide T6P that is subsequently dephosphorylated to eventually yield trehalose [88] (Figure 1.3).

(1) UDP-glucose + G6P → Trehalose-6-phosphate (T6P); this reaction is catalyzed by Tps1

(2) T6P → Trehalose + Pi ; this reaction is catalyzed by Tps2

Loss of Tps1 in yeast has severe effects on glucose metabolism including overactive hexokinase activity, and an increased flux of glucose into glycolysis [88]. Blazquez *et al*. [90] suggested that a *tps1* mutant lacks T6P-synthase enzyme activity to produce T6P, a potent inhibitor of hexokinase. Therefore, loss of this inhibition in the mutant causes a growth defect on glucose media. Disruption of *tps2* had no effects on T6P-synthase activity, but caused complete loss of T6P-phosphatase activity and accumulation of T6P instead of trehalose upon heat shock or transition to stationary phase. In wild type, heat shock induced an increase in T6P-phosphatase activity and accumulation of *tps2* mRNA transcripts [91]. Remarkably, a phenotype of the *tps2* mutant includes thermosensitive growth, which may be caused by excessive accumulation of T6P at elevated temperatures [88,91].

Alternate Trehalose Biosynthesis Pathways

The most common trehalose biosynthesis pathway among organisms is the two enzymatic TPS/TPP pathway as described above (Figure 1.3 and 1.4A). Four more alternate trehalose biosynthetic pathways have evolved in bacteria and some fungi as they utilized trehalose as osmotic active compounds, cryoprotectant, or thermoprotectant when

exposed to extreme conditions and enable survival until conditions are favorable again [84] (Figure 1.4).

In the second mechanism (Figure 1.4B), trehalose synthase (TS) catalyzes the conversion of maltose directly to trehalose in one step. This biosynthetic pathway has been characterized in bacteria such as *Pseudomonas stutzeri* [92], *Pimelobacter sp.*[93], *Mycobacterium smegmatis* [94], *Arthrobacter aurescens* [95] and *Enterobacter hormaechei* [96]. TS has strict substrate specificity for maltose, without requiring cofactors, and the optimum pH for enzymatic activities is around 7.5. In addition, this enzyme also catalyzes the reverse reaction for conversion of trehalose to maltose, but the equilibrium is favorably to the direction of trehalose synthesis.

The third mechanism is TreY/TreZ pathway involving conversion of maltooligosaccharides to maltooligosyl trehalose by intramolecular transglucosylation of the terminal glucose (Figure 1.4C). A trehalose portion of the intermediates is then cleaved by a second enzyme to give trehalose plus a shorter maltooligosaccharide [97]. An interesting thermostable version of the enzyme was purified from *Sulfolobus acidocaldarius*, and this enzyme has an extra gene encoding glycogen debranching enzyme (TreX) in the same operon [98].

In the fourth pathway (Figure 1.4D), trehalose phosphorylase (TreP) catalyses the reversible hydrolysis of trehalose in the presence of inorganic phosphate, and has been detected in green algae *Euglena gracilis* and some basidiomycete fungi such as *Agaricus bisporus.* [99,100]. There is uncertainty about the participation of the TreP enzyme in the synthesis or degradation of trehalose, since the biosynthetic reaction has only been shown

in vitro. Nevertheless, trehalose phosphorylase probably performs both synthesis and degradation as shown in *A. bisporus* that has no detectable activities of trehalase or trehalose synthase [99]. In addition, trehalose phosphorylase from *Catellatospora furruginea* showed the highest enzyme activity among actinomycetes which was able to catalyze both phosphorolysis and biosynthesis of trehalose [100].

Recently, an additional biosynthetic pathway of trehalose was characterized in the hyperthermophilic archaeon *Thermococcus litoralis* [101]. This pathway involves the trehalose glycosyltransferring synthase (TreT), which catalyses reversible formation of trehalose from ADP-glucose and glucose (Figure 1.4E). It can also use UDP-glucose and GDP-glucose as substrates, although it is less efficient to synthesize trehalose. TreT transfers glucose moiety from ADP-glucose and joins it at position 1 of another glucose molecule to form trehalose.

Finally, trehalose is degraded by trehalase (TreH) into two glucose molecules (Figure 1.4F). Increased TreH activity during germination has been characterized in *Aspergillus* fungi [102,103]. In mammals including rabbits and humans, intestinal TreH is most probably involved in hydrolysis of ingested trehalose and has been characterized [104,105].

Trehalose-6-Phosphate (T6P)

T6P, the intermediate of TPS/TPP pathway plays a critical role in the regulation of carbon flux into glycolysis in *S. cerevisiae*. Tps1 mutants of *S. cerevisiae* were unable to grow on glucose media due to dysregulated glycolysis in the absence of T6P [106]. Lack of Tps1 caused the sequestration of Pi as a consequence of sugar phosphates

hyperaccumulating and inhibition of ATP synthesis that leads to glycolysis arrest. In addition, lack of Tps2 in *S. cerevisiae* confirmed that high T6P level prior to glucose addition diminished sugar influx into glycolysis by inhibiting hexokinases activity [107]. However, Noubhani *et al.* proposed that the observed phenotypes of *tps2* mutant including an increased respiration rate, cytochrome content and cAMP relative to wild type are likely associated with protein interaction of hexokinase Hxk2 and Tps1 which regulate glucose influx into glycolysis. [108]. Although, a dimorphic yeast *Yarrowia lipolytica* that was diverged from ancestral yeast showed high sensitivity of hexokinase to T6P, a Tps1 mutant of *Y. lipolytica* exhibits normal growth in glucose media. This phenotype could be explained by the presence of T6P insensitive glucokinase constituting roughly 80% of the glucose phosphorylating capacity in *Y. liplolytica* [109].

Hexose Kinases

The initial step in sugar utilization is sugar uptake and conversion of sugar to sugar phosphate using hexose kinases. Hexoses including glucose and fructose are activated by soluble glucokinase and hexokinase. Both glucokinase and hexokinase are present in *A. nidulans*, *A. niger*, *A. fumigatus*, and *S. cerevisiae* as requirements for growth on glucose [110,111,112,113]. In *A. niger*, glucokinase possesses a very high specificity for glucose with a specific activity of 233 U/mg and a Km value of 63 µM, whereas the activation of fructose was not favorable due to a relatively high Km (120 mM) [113]. In contrast to glucokinase, purified *A. niger* hexokinase showed a specific activity of 220 U/mg for fructose and a Km of 2 mM but was also significantly active with glucose (specific activity of 20 U/mg; Km of 0.35 mM). Another distinguishing

feature of those enzymes included that only hexokinase activity was inhibited by T6P. Recently, catalytic glucokinase and hexokinase was characterized in *A. fumigatus*, and both enzymes displayed different biochemical properties with different roles during growth and development [111]. Glucokinase efficiently activates glucose and mannose but activates fructose only to a minor extent. Among tested hexose sugars, hexokinase has high efficiency for fructose activation. Interestingly, expression of both enzymes is associated with specific developmental states. Glucokinase was abundantly expressed in the resting conidia and steadily declined during germination, whereas hexokinase was highly induced during germination and constantly expressed in mycelia [111].

Trehalose Biosynthesis Pathway and Pathogenesis in Human and Plant Fungal Pathogens

Candida albicans

The increasing prevalence of resistance strains for candidiasis treatment indicates an urgent need for new antifungal agents. Genes encoding key enzymes in the trehalose pathway have been studied in *C. albicans*; a *tps1/tps1* mutant strain has a defect in trehalose production at stationary phase and after heat shock without a growth defect at 30^{o}C comparable to wild type. However at 42^{o}C it grows normally on galactose or glycerol but is not able to grow on glucose or fructose [114]. *C. albicans* can shift from yeast to hyphal form when cultured at 37^{o}C in the presence of newborn calf serum. This transition is severely impaired in this *tps1/tps1* mutant, and no hypha formation is observed in the glucose medium culture. Additionally, the mutant shows significantly decreased virulence compared to wild type in mice infection studies [114]. Similarly,

disruption of *tps2* in *C. albicans* causes decreased virulence and hyperaccumulation of T6P, a toxic intermediate agent that may interfere with yeast cell wall assembly [115]. Surprisingly, this mutant still produced substantial levels of trehalose by an unknown mechanism [6]. This result is similar to that of a *tps2* (designated *orlA)* mutant in *A. fumigatus* (this dissertation), but different from a *tps2* mutant in *S. cerevisiae* [91,116].

Cryptococcus neoformans

Recent studies in this human pathogen suggested that the presence of the trehalose pathway during infection is required for fungal survival in the host. Although both *tps1* and *tps2* genes are required for high temperature (37^{o}C) growth and glycolysis, growth defect of the mutants under these conditions is suppressed when cultured on media containing sorbitol [117]. It is hypothesized that both sugars (trehalose and sorbitol) act as stress protectants during exposure to high temperatures. Disruption of *tps2* results in toxic accumulation of T6P and corresponding cell death after 6 hours of growth at 37^{o}C. Attenuation in virulence of a *tps1* mutant strain in the invertebrate *C. elegans*, *in vivo* low temperature, and avirulence in both rabbits and mice support the hypothesis that the trehalose pathway in *C. neoformans* is involved in more host survival mechanisms than simply high-temperature stresses and glycolysis [117]. Accordingly, the function of trehalose synthesis pathway in the *Cryptococcus gattii* strain R265, a highly virulent strain from the Vancouver Island outbreak in immunocompetent humans, is essential for stress tolerance and virulence. The *C. gattii tps1* and *tps2* mutants have similar phenotype to *C. neoformans*, the accumulation of T6P is toxic and directly linked to the control of glycolysis in this species. Moreover, *C. gattii* tps1 mutant has additional defects in

melanin and capsule production which suggests that the trehalose synthesis pathway plays a central role in the virulence components of *C. gattii* via multiple mechanisms [118].

Magnaporthe grisea

To date, the trehalose pathway has not been fully elucidated in a filamentous human fungal pathogen [116,119]. However, more evidence for the implication of the trehalose biosynthesis pathway in fungal virulence comes from results with *M. grisea*, a filamentous fungus responsible for rice blast disease. *M. grisea tps1* mutants fail to synthesize trehalose, sporulate very poorly, and are unable to invade the host plant due to lack of functional appressoria, a structure needed for fungal invasion of plants [120]. Also recent studies have shown that trehalose metabolism may exert important regulatory roles in the development of multicellular eukaryotes. In fungi, Tps1 is a central regulator for integration of carbon and nitrogen metabolism in fungi. Moreover, the activity of Tps1 in *M. grisea* requires an associated regulator protein Tps3, which is also essential for pathogenicity [121]. Wilson *et al.* demonstrated that trehalose synthesis is not required for plant infection by *M. oryzae*, but Tps1 protein itself is necessary for its regulatory functions and for its role in fungal virulence [122]. Since the MgTps1 mutant cannot grow on nitrate, they further showed that Tps1 regulates at the transcriptional level nitrogen source utilization genes. The role of Tps1 in nitrogen metabolism and pathogenesis is associated with its ability to increase NADPH production in the oxidative pentose phosphate pathway (PPP) via activation of glucose-6-phosphate dehydrogenase (G6PDH) for activity of nitrate reductase and growth on nitrate, and (ii) Tps1 directly

binds NADPH and thereby inactivates NADP-dependent transcriptional repressors of virulence associated genes during appressorium-mediated plant infection.

Fungal Cell Wall

As alluded to above, alterations in the trehalose pathway may also alter the structure and function of the fungal cell wall, which has important implications for fungal virulence. The fungal cell wall is an insoluble rigid structure that provides protective functions and supports morphology in fungi. It is also a dynamic structure that continuously changes during growth depending on the culture conditions and environmental stresses [123,124]. Cell wall composition is a combination of polysaccharides that varies among fungal species. *S. cerevisiae* is versatile and well characterized for both biochemical and genetic studies. This organism is a model of other fungal organisms in all functional roles including fungal cell wall research [125]. The yeast cell wall consists mainly of polysaccharides made up of three fundamental sugars, glucose, mannose, and N-acetylglucosamine. In fungal pathogens, polysaccharide network of the cell wall mainly consists of β-1,3-glucan cross-linked to chitin and this complex network also covalently binds to other polysaccharides with a variation of the specific linkage of the individual fungus. Cell wall composition is organized into two layers according to their solubility in hot alkali solution. Fibrillar skeleton of cell wall structure is alkali-insoluble compartment of glucan-chitin covalent linkage, and the alkali-soluble components are amorphous cement present in the entire cell wall [126]. The heterogeneous polymers of polysaccharide composition varies between species, for

instance β-1,3/1,4-glucan is present in *A. fumigatus* whereas β-1,6-glucan is mainly present in *C. albicans* [124]. The fungal cell wall is specialized for fungal survival and a potential intriguing drug target due to its absence in humans. A comprehensive understanding of the interactions between the host membrane receptors and the fungal cell wall components remains poorly understood [126].

Host Responses

The lung is constantly exposed to a wide range of microorganisms and innocuous particles. The innate immune system is a constitutive defense mechanism that is robustly active against pathogens, including *A. fumigatus*. Normally, immunocompetent hosts eliminate inhaled conidia through innate immune system mediated mechanisms. Alveolar macrophages (AM) are prominent resident cells responsible for phagocytosis and fungal clearance [127]. On the other hand, escaped conidia transform into germlings and hyphae which strongly trigger recruitment of neutrophils to the site of infection [128].

Macrophages

Macrophages are major resident phagocytic cells in the lung, and involved in pulmonary innate immunity as effector cells. After inhalation of airborne *A. fumigatus* conidia, immunocompetent/healthy hosts are protected by the activation of AM. Engulfment of conidia lasts 2 hr and after 6 hr of phagocytosis, killing of *A. fumigatus* conidia occurs [48]. A functional NADPH oxidase is required for production of reactive oxidant intermediates (ROI) and the killing of *A. fumigatus* conidia by AM, which play

an essential role in clearing *A. fumigatus* conidia from the lung [48,129]. However, the exact mechanisms by which AMs kill fungal conidia remain to be fully elucidated.

Neutrophils

Polymorphonuclear Neutrophils (PMNs) are normally recruited during inflammation and together with AMs are responsible for phagocytosis of *A. fumigatus* conidia. The conidia that escape phagocytosis may germinate into hyphae. Unlike conidia, hyphae are too large to be engulfed by AM and are primarily targeted by PMNs. PMNs aggregate around hyphae and damage hyphae by released ROI, antimicrobial peptides and degranulation. The importance of PMNs for antifungal defense can be inferred from the propensity of patients with severe prolonged neutropenia to develop IA [20].

Reactive Oxygen Species (ROS)

One of the most powerful host defense mechanism against microbial pathogens utilized by phagocytes is ROS production. ROS includes superoxide anion (O_2^-), hydrogen peroxide (H_2O_2), the hydroxyl radical (OH^o) and hypochlorus acid (HOCl). NADPH oxidase is a multi-component enzyme system located in the plasma membrane of activated cells and responsible for ROS production upon cell activation. NADPH oxidase is composed of both membrane bound proteins (cytochrome b_{558} consist of gp91phox and p22phox) and several cytosolic protein subunits (p67phox, p47phox, p40phox, and Rac) [130]. Patients that have defective NADPH oxidase activity, a genetic

disease termed Chronic Granulamatous Disease (CGD) are susceptible to infections by *A. fumigatus* and other fungi and bacteria.

NET Formation

Neutrophil extracellular traps (NETs) are extruded nuclear DNA produced by dying PMNs. It is a highly dynamic web studded with fungicidal proteins that restricts hyphal growth [131]. Conidia and germ tubes of *A. fumigatus* are able to trigger the formation of NETs; however NET formation *per se* is not sufficient for killing fungi [132]. NET formation is a highly dynamic process and has been observed *in vivo* with 2 photon microscopy of *in vivo Aspergillus*-infected lungs. The exact role and nature of NET formation remains controversial with increasing data suggesting that NETs are an important part of the innate immune system's response to invading pathogens [133,134,135]. Restoration of NET formation in CGD neutrophils by gene therapy restored their ability to control *A. fumigatus* infection. The data demonstrates the critical role of calprotectin, zinc chelator, as the major NET component in antifungal activity against *A. fumigatus* [153].

Host Receptors and Fungi

Innate immune recognition is based on the detection of molecular structures unique to microorganisms [136]. Pattern recognition receptors (PRRs) can be expressed on host cell surfaces and in intracellular compartments, with secretion into the bloodstream being unusual. Each host receptor has a broad specificity and can potentially bind to a large number of molecules that have a common structural motif or pattern

[137,138]. Host receptors have the ability to recognize either carbohydrate endogenous to the animal or those that are presented by microbial invaders. A large number of animal lectins have been isolated and shown to have roles in biological recognition events [139]. C-type lectins represent an important recognition mechanism for oligosaccharides at cell surfaces. Binding of specific sugar structures by lectins mediates biological events including cell-cell adhesion, innate immune responses, and phagocytosis to potential pathogens [140].

Dectin-1 Receptor; a type II transmembrane protein that belongs to the NK-like C-type lectin-like receptor family, is a pattern recognition receptor for β-glucans [141]. Dectin-1 binds to the β-glucan-rich surface of *S. cerevisiae*, *C. albicans*, *Pneumocystis carinii*, and *Coccidioides posadasii*. Dectin-1 activation results in phagocytic, proinflammatory, and antimicrobial responses. PRRs have an important role in antifungal defense. The contribution of Dectin-1-mediated signals to innate immune defense against *A. fumigatus* infection requires surface exposed β-glucan [142]. Live conidia expose β-glucan on the conidial cell wall as they swell and extend into hyphae, which induces rapid neutrophil recruitment, production of proinflammatory cytokines, such as tumor necrosis factor (TNF)-α, interleukin (IL)-2, IL10, IL6, and IL23. Blockage of Dectin-1 by an antibody partially inhibits induction of proinflammatory cytokines response [128]. Accordingly, the importance of the Dectin-1 receptor in antifungal immunity is further demonstrated in the Dectin-1 knockout mice, generated in the 129/Sv background mice. Taylor *et al.* have shown that deficiency of Dectin-1 rendered mice susceptible to infection with *C. albicans* by impaired leukocyte responses and increased fungal burden.

Moreover, naïve Dectin-1 knockout mice without immunosuppression are more susceptible to *A. fumigatus* emphasizing that Dectin-1 was critical for innate defense against *A. fumigatus* [143]. Regarding mouse genetic background, various strains of wild type mice express different Dectin-1 isoforms. The C57BL/6 mice and 129/SvEv mice express a smaller isoform of Dectin-1B, whereas BALB/c mice present comparable levels of both Dectin-1A and Dectin-1B transcripts [144]. Despite fungal burden consistently being increased among all different genetic backgrounds of Dectin-1 knockout mice, varied susceptibility to *A. fumigatus* infection has been reported [143,144,145].

Toll Like Receptors are one of the PRR types and constitute a major surveillance and defense mechanism against microbial invaders. Originally identified in Drosophila, the Toll like receptor (TLR) consists of a family of at least 11 proteins which recognize specific microbial structures [146]. TLR2 and TLR4 have been implicated in recognition of *A. fumigatus* conidia and hyphae [128]. Ligation of microbial ligands and host TLRs initiate the signaling cascades mediated by the intracellular adaptor MyD88 and TRIF which leads to activation of NF-kB transcription factor and result in specific patterns of gene expression [146]. The involvement of TLRs in the recognition of *A. fumigatus* by macrophages has been clarified via use of specific TLR knockout mice. Unlike naïve knockout mice, the TLR knockout mice treated with cyclophosphamide show higher susceptibility to *A. fumigatus* lung infection [147].

Animal Models of Invasive Aspergillosis

Murine models of *A. fumigatus* were used to investigate the virulence of various fungal mutants, to evaluate the efficacy of antifungal drugs, and to determine cytokine and T cell responses against fungal infection [13]. To reproduce a human immunosuppressed patient condition, including patients who underwent transplantation and chemotherapy, similar drug regimens are used in the neutropenic and corticosteroid mouse models. In contrast, to study fungal infection in the context of genetic deficiency in CGD patients, a specific gene knockout was generated in the C57/BL6 murine background.

Neutropenic Model

This model of IA is characterized by a severe depletion of neutrophil cells and used to study IA found in severe immunosuppressed patients including bone marrow transplant patients [56]. To induce neutropenia in the murine model, either a single drug treatment of cyclophosphamide or combination treatment of cyclophosphamide and triamcinolone (corticosteroid) is employed for immunosuppression. This treatment is sufficient to induce profound and sustained neutropenia and allow successful invasive fungal infection [56,148]. Immune suppressor drugs are not only utilized for induction of neutropenia, but depletion of granulocytes by the monoclonal antibody RB6-8C5 (RB6) is used for creating susceptibility to fungal infection as well. Differences of the pathogenesis of experimental IPA in response to individual method for immunosuppression are very important in interpreting experimental results. The

coadministration of MAb RB6 and cyclophosphamide influences the outcomes of increased fungal burden, and less inflammation with lower lethal inoculum than the individual administration of either RB6 or cyclophosphamide. With regard to RB6 depletion, the death of immunosuppressed mice is partly due to an inflammatory response caused by neutrophil recovery on day three post infection [149].

Corticosteroid Model

Patients who have gone through high dose corticosteroid treatment for graft versus host disease or autoimmune type diseases are highly susceptible to invasive fungal infection [56]. Although corticosteroid treatment has no effect on the internalization of conidia by AM, ROS production is inhibited in mice treated with corticosteroid. Corticosteroids allow for the development of invasive aspergillosis in immunosuppressed mice [48]. Unlike the chemotherapy model, the animals that are immunosuppressed by corticosteroid therapy have an extensive influx of PMNs into the lungs and fungal proliferation. Therefore, different mechanisms of host defense occur depending on the immunosuppressive treatment used and the infectious dose. Death in the corticosteroid model of IPA is largely due to recruited immune cells that have been rendered non-functional from treatment and add to the lung damage caused by fungal growth likely through an inhibitory effect on NF-KB [150].

xCGD Model

This genetically deficient murine model was generated to reproduce chronic granulomatous disease (CGD) found in humans. CGD is an inherited immune deficiency

disease where phagocytes are unable to produce ROS. CGD is associated with recurrent bacterial and fungal infections during childhood. In addition to bacterial pathogens, *A. fumigatus* is one of the most common pathogens encountered in CGD patients and is a frequent cause of mortality [151]. The most frequent form of CGD is the X-linked gp91phox-deficient form, and approximately 70% of all CGD cases have mutations in the large subunit of the oxidase cytochrome b_{558}. Pollock et al., created a homologous recombinant mouse model of the X-linked gp91phox deficient form of CGD [152]. These animals are more susceptible to infections with the human fungal pathogens *Staphylococcus aureus* and *A. fumigatus*.

Objective

The primary goal of this study was to characterize the role of the trehalose biosynthesis pathway in *A. fumigatus* virulence. This biosynthetic pathway generates trehalose, a disaccharide sugar, from two molecules of glucose [glucose-6-phosphate (G6P) and UDP-glucose]. Trehalose plays a major role as a stress protectant compound and storage carbohydrate [103]. Trehalose is required by fungal cells to contend with diverse stresses such as heat shock, osmolarity shock, starvation and desiccation [117]. Importantly, the trehalose pathway has been observed to be required for stress responses and fungal virulence in other human pathogenic fungi including *C. neoformans, C. gattii,* and *C. albicans* [115,117,118].

However, to date, the trehalose biosynthesis pathway and function of trehalose have not been fully studied in *A. fumigatus*. It has been shown that *in vivo* host

environmental conditions in response to fungal infection are stressful and influence substantial fungal metabolic changes to overcome microenvironment challenges and establish fungal infection. Understanding the mechanisms which *A. fumigatus* utilizes to survive in mammalian host environment will potentially lead to improved patient outcomes. We hypothesize that the trehalose pathway is a key stress response pathway in *A. fumigatus* and is one attribute that allows this mold to cause lethal disease. Accordingly, determining the role of the catalytic and regulatory genes involved in trehalose biosynthesis in *A. fumigatus* was sought by utilizing bioinformatics data analysis to identify putative orthologs based on known regulators in *S. cerevisiae* and *A. nidulans*, and molecular genetics and animal models of IPA to uncover mechanisms and test my hypothesis.

Initially, the examination of the *A. fumigatus* trehalose pathway was begun by generation of an individual null mutation of putative genes in the pathway. Preliminary data showed interesting phenotypes exhibited by a particular null mutant lacking Trehalose-6-Phosphate Phosphatase (TPS2) enzyme OrlA; T6PP (designated Δ*orlA*) was influenced by the accumulation of Trehalose-6-Phosphate (T6P), regardless of persistent trehalose production. Accordingly, further hypothesis was that T6P accumulation is toxic to the glycolytic pathway through the inhibition of hexokinase activity wich results in an insufficiency of a critical precursor for fungal cell wall biosynthesis in *A. fumigatus*. I further demonstrated that critical enzymes and regulatory protein subunits were required for cell wall integrity of *A. fumigatus*. Two murine models of IPA were utilized and confirmed the attenuated virulence of Δ*orlA*.

Questions remain with regard to the mechanism behind the virulence attenuation in murine models of IPA. Given that T6PP encoding enzyme genes (*tps2* orthologs) are now known to be required for fungal virulence in the three most frequently encountered fungal pathogens of human mycoses, it provides a rationale for pursuing further research on this *A. fumigatus orlA* mutant that could lead to a better understanding of how this pathway affects fungal virulence.

No current knowledge explains how the trehalose pathway contributes to fungal virulence mechanisms in human fungal pathogens. One of the major findings of this study is that the attenuated virulence of *A. fumigatus* Δ*orlA* is related to alteration of cell wall composition and levels of accumulated T6P intermediate. To further explore this question, the initial host responses mediated by interaction of host immune cells and Δ*orlA* is addressed. Pathogenesis (animal models, *in vitro* assay) and FACS analysis of Δ*orlA* in the xCGD mice suggests that the influx of recruited PMNs and reduction of fungal growth are partially mediated by the altered cell wall composition of Δ*orlA*. A further examination of cell wall composition revealed decreased levels of chitin and increased levels of β-glucan in the Δ*orlA* cell wall. Depletion of PMNs in the xCGD murine model demonstrated that PMNs play a major role as the primary mechanism for antifungal activity in response to the absence of OrlA, whereas *in vivo* fungal growth per se is probably only playing a slight role in the attenuated virulence phenotype of Δ*orlA*. The conclusive *in vitro* evidence confirmed that fungal clearance of Δ*orlA* in xCGD mice was via functionally intact ROS independent mechanisms. Collectively, the interaction of the altered fungal cell wall and host cells prevent growth of Δ*orlA in vivo*; however such

interaction constitutively increased the influx of PMNs and caused exacerbation of disease and further mortality. These findings further our understanding of the outcome of antifungal host responses that depend upon the fungal cell wall interaction. Moreover, they raise intriguing questions about the development of new therapeutic strategies targeting the trehalose biosynthesis pathway to overcome the emerging antifungal drug resistance and limited therapeutic tools available for IPA in immunocompromised patients.

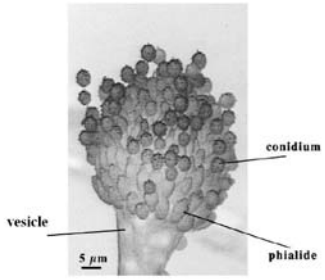

Figure 1.1. Scanning electron microscope image of *Aspergillus* conidiophores showing the stem cell; phialides, and conidia.

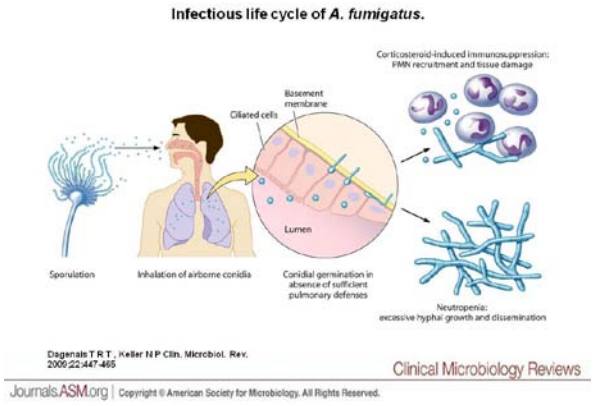

Figure 1.2. Infectious life cycle of *A. fumigatus*. *Aspergillus* is ubiquitous in the environment, and asexual reproduction leads to the production of airborne conidia. Inhalation by specific immunosuppressed patient groups results in conidium establishment in the lung, germination, and either PMN-mediated fungal control with significant inflammation (corticosteroid therapy) or uncontrolled hyphal growth with a lack of PMN infiltrates and, in severe cases, dissemination (neutropenia) [17].

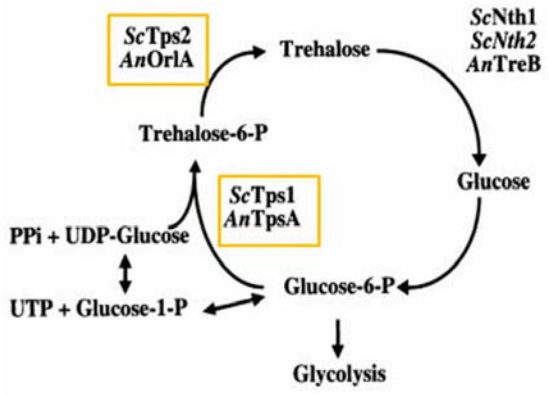

Figure 1.3. Trehalose metabolism in fungi. *Sc*Tps1 and *An*TpsA, trehalose-6-phosphate synthase; *Sc*Tps2 and *An*OrlA, trehalose-6-phosphate phosphatase; *Sc*Nth2 and *An*TreB, neutral trehalase; *Sc, S. cerevisiae; An, A.nidulans*.

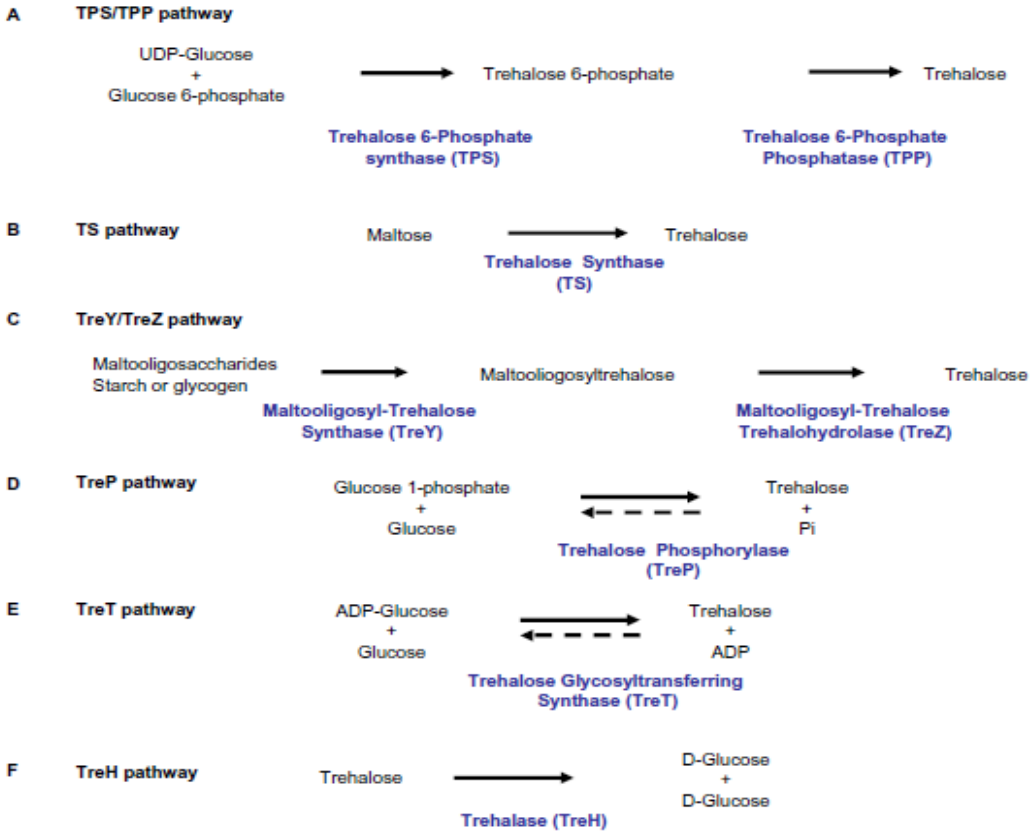

Figure 1.4. Trehalose biosynthesis pathways. Enzymes responsible for each reaction are indicated in blue [84].

Literature Cited

1. Denning DW (1996) Therapeutic outcome in invasive aspergillosis. Clin Infect Dis 23: 608-615.

2. Denning DW (1998) Invasive aspergillosis. Clin Infect Dis 26: 781-803; quiz 804-785.

3. Verweij PE, Snelders E, Kema GH, Mellado E, Melchers WJ (2009) Azole resistance in *Aspergillus fumigatus*: a side-effect of environmental fungicide use? Lancet Infect Dis 9: 789-795.

4. Babenko VN, Krylov DM (2004) Comparative analysis of complete genomes reveals gene loss, acquisition and acceleration of evolutionary rates in Metazoa, suggests a prevalence of evolution via gene acquisition and indicates that the evolutionary rates in animals tend to be conserved. Nucleic Acids Res 32: 5029-5035.

5. Koonin EV, Fedorova ND, Jackson JD, Jacobs AR, Krylov DM, et al. (2004) A comprehensive evolutionary classification of proteins encoded in complete eukaryotic genomes. Genome Biol 5: R7.

6. Van Dijck P, De Rop L, Szlufcik K, Van Ael E, Thevelein JM (2002) Disruption of the *Candida albicans* TPS2 gene encoding trehalose-6-phosphate phosphatase decreases infectivity without affecting hypha formation. Infect Immun 70: 1772-1782.

7. Micheli PA (1729) Nova plantarum genera juxta Tournefortii methodum disposita. Florence, Italy: Bernardo Paperini.

8. Patterson T, F. (2003) Aspergillosis; Dismukes WE, Pappas, P. G., Sobel, J. D., editor. New York: Oxford University Press. 519 p.

9. Patterson TF, Kirkpatrick WR, White M, Hiemenz JW, Wingard JR, et al. (2000) Invasive aspergillosis. Disease spectrum, treatment practices, and outcomes. I3 *Aspergillus* Study Group. Medicine (Baltimore) 79: 250-260.

10. Maschmeyer G, Haas A, Cornely OA (2007) Invasive aspergillosis: epidemiology, diagnosis and management in immunocompromised patients. Drugs 67: 1567-1601.

11. Brakhage AA, Langfelder K (2002) Menacing mold: the molecular biology of *Aspergillus fumigatus*. Annu Rev Microbiol 56: 433-455.

12. O'Gorman CM, Fuller HT, Dyer PS (2009) Discovery of a sexual cycle in the opportunistic fungal pathogen *Aspergillus fumigatus*. Nature 457: 471-474.

13. Latge JP (1999) *Aspergillus fumigatus* and aspergillosis. Clin Microbiol Rev 12: 310-350.

14. Gugnani HC (2003) Ecology and taxonomy of pathogenic *aspergilli*. Front Biosci 8: s346-357.

15. McDonagh A, Fedorova ND, Crabtree J, Yu Y, Kim S, et al. (2008) Sub-telomere directed gene expression during initiation of invasive aspergillosis. PLoS Pathog 4: e1000154.

16. Richie DL, Hartl L, Aimanianda V, Winters MS, Fuller KK, et al. (2009) A role for the unfolded protein response (UPR) in virulence and antifungal susceptibility in *Aspergillus fumigatus*. PLoS Pathog 5: e1000258.

17. Dagenais TR, Keller NP (2009) Pathogenesis of *Aspergillus fumigatus* in Invasive Aspergillosis. Clin Microbiol Rev 22: 447-465.

18. Nierman WC, Pain A, Anderson MJ, Wortman JR, Kim HS, et al. (2005) Genomic sequence of the pathogenic and allergenic filamentous fungus *Aspergillus fumigatus*. Nature 438: 1151-1156.

19. Fedorova ND, Khaldi N, Joardar VS, Maiti R, Amedeo P, et al. (2008) Genomic islands in the pathogenic filamentous fungus *Aspergillus fumigatus*. PLoS Genet 4: e1000046.

20. Gerson SL, Talbot GH, Hurwitz S, Strom BL, Lusk EJ, et al. (1984) Prolonged granulocytopenia: the major risk factor for invasive pulmonary aspergillosis in patients with acute leukemia. Ann Intern Med 100: 345-351.

21. Romani L (2004) Immunity to fungal infections. Nat Rev Immunol 4: 1-23.

22. Kontoyiannis DP, Bodey GP (2002) Invasive aspergillosis in 2002: an update. Eur J Clin Microbiol Infect Dis 21: 161-172.

23. Herbrecht R, Denning DW, Patterson TF, Bennett JE, Greene RE, et al. (2002) Voriconazole versus amphotericin B for primary therapy of invasive aspergillosis. N Engl J Med 347: 408-415.

24. Walsh TJ, Anaissie EJ, Denning DW, Herbrecht R, Kontoyiannis DP, et al. (2008) Treatment of aspergillosis: clinical practice guidelines of the Infectious Diseases Society of America. Clin Infect Dis 46: 327-360.

25. Segal BH (2009) Aspergillosis. N Engl J Med 360: 1870-1884.

26. Snelders E, van der Lee HA, Kuijpers J, Rijs AJ, Varga J, et al. (2008) Emergence of azole resistance in *Aspergillus fumigatus* and spread of a single resistance mechanism. PLoS Med 5: e219.

27. Mortensen KL, Mellado E, Lass-Florl C, Rodriguez-Tudela JL, Johansen HK, et al. Environmental study of azole-resistant *Aspergillus fumigatus* and other aspergilli in Austria, Denmark, and Spain. Antimicrob Agents Chemother 54: 4545-4549.

28. Snelders E, Camps SM, Karawajczyk A, Schaftenaar G, Kema GH, et al. Triazole Fungicides Can Induce Cross-Resistance to Medical Triazoles in *Aspergillus fumigatus*. PLoS One 7: e31801.

29. Tekaia F, Latge JP (2005) *Aspergillus fumigatus*: saprophyte or pathogen? Curr Opin Microbiol 8: 385-392.

30. Cooney NM, Klein BS (2008) Fungal adaptation to the mammalian host: it is a new world, after all. Curr Opin Microbiol 11: 511-516.

31. Casadevall A (2005) Fungal virulence, vertebrate endothermy, and dinosaur extinction: is there a connection? Fungal Genet Biol 42: 98-106.

32. Bhabhra R, Askew DS (2005) Thermotolerance and virulence of *Aspergillus fumigatus*: role of the fungal nucleolus. Med Mycol 43 Suppl 1: S87-93.

33. Pitt JI (1994) The current role of *Aspergillus* and *Penicillium* in human and animal health. J Med Vet Mycol 32 Suppl 1: 17-32.

34. Aimanianda V, Bayry J, Bozza S, Kniemeyer O, Perruccio K, et al. (2009) Surface hydrophobin prevents immune recognition of airborne fungal spores. Nature 460: 1117-1121.

35. St Leger RJ, Joshi L, Roberts DW (1997) Adaptation of proteases and carbohydrates of saprophytic, phytopathogenic and entomopathogenic fungi to the requirements of their ecological niches. Microbiology 143 (Pt 6): 1983-1992.

36. Alp S, Arikan S (2008) Investigation of extracellular elastase, acid proteinase and phospholipase activities as putative virulence factors in clinical isolates of *Aspergillus* species. J Basic Microbiol 48: 331-337.

37. Sharon H, Hagag S, Osherov N (2009) Transcription factor PrtT controls expression of multiple secreted proteases in the human pathogenic mold *Aspergillus fumigatus*. Infect Immun 77: 4051-4060.

38. Keller NP, Turner G, Bennett JW (2005) Fungal secondary metabolism - from biochemistry to genomics. Nat Rev Microbiol 3: 937-947.

39. Bok JW, Balajee SA, Marr KA, Andes D, Nielsen KF, et al. (2005) LaeA, a regulator of morphogenetic fungal virulence factors. Eukaryot Cell 4: 1574-1582.

40. Tsunawaki S, Yoshida LS, Nishida S, Kobayashi T, Shimoyama T (2004) Fungal metabolite gliotoxin inhibits assembly of the human respiratory burst NADPH oxidase. Infect Immun 72: 3373-3382.

41. Pahl HL, Krauss B, Schulze-Osthoff K, Decker T, Traenckner EB, et al. (1996) The immunosuppressive fungal metabolite gliotoxin specifically inhibits transcription factor NF-kappaB. J Exp Med 183: 1829-1840.

42. Waring P, Eichner RD, Mullbacher A, Sjaarda A (1988) Gliotoxin induces apoptosis in macrophages unrelated to its antiphagocytic properties. J Biol Chem 263: 18493-18499.

43. Orciuolo E, Stanzani M, Canestraro M, Galimberti S, Carulli G, et al. (2007) Effects of *Aspergillus fumigatus* gliotoxin and methylprednisolone on human neutrophils: implications for the pathogenesis of invasive aspergillosis. J Leukoc Biol 82: 839-848.

44. Cramer RA, Jr., Gamcsik MP, Brooking RM, Najvar LK, Kirkpatrick WR, et al. (2006) Disruption of a nonribosomal peptide synthetase in *Aspergillus fumigatus* eliminates gliotoxin production. Eukaryot Cell 5: 972-980.

45. Kupfahl C, Heinekamp T, Geginat G, Ruppert T, Hartl A, et al. (2006) Deletion of the gliP gene of *Aspergillus fumigatus* results in loss of gliotoxin production but has no effect on virulence of the fungus in a low-dose mouse infection model. Mol Microbiol 62: 292-302.

46. Sugui JA, Pardo J, Chang YC, Zarember KA, Nardone G, et al. (2007) Gliotoxin is a virulence factor of *Aspergillus fumigatus*: gliP deletion attenuates virulence in mice immunosuppressed with hydrocortisone. Eukaryot Cell 6: 1562-1569.

47. Paris S, Wysong D, Debeaupuis JP, Shibuya K, Philippe B, et al. (2003) Catalases of *Aspergillus fumigatus*. Infect Immun 71: 3551-3562.

48. Philippe B, Ibrahim-Granet O, Prevost MC, Gougerot-Pocidalo MA, Sanchez Perez M, et al. (2003) Killing of *Aspergillus fumigatus* by alveolar macrophages is mediated by reactive oxidant intermediates. Infect Immun 71: 3034-3042.

49. Mamishi S, Parvaneh N, Salavati A, Abdollahzadeh S, Yeganeh M (2007) Invasive aspergillosis in chronic granulomatous disease: report of 7 cases. Eur J Pediatr 166: 83-84.

50. Almyroudis NG, Holland SM, Segal BH (2005) Invasive aspergillosis in primary immunodeficiencies. Med Mycol 43 Suppl 1: S247-259.

51. Ratledge C, Dover LG (2000) Iron metabolism in pathogenic bacteria. Annu Rev Microbiol 54: 881-941.

52. Philpott CC (2006) Iron uptake in fungi: a system for every source. Biochim Biophys Acta 1763: 636-645.

53. Schrettl M, Bignell E, Kragl C, Sabiha Y, Loss O, et al. (2007) Distinct roles for intra- and extracellular siderophores during *Aspergillus fumigatus* infection. PLoS Pathog 3: 1195-1207.

54. Schrettl M, Bignell E, Kragl C, Joechl C, Rogers T, et al. (2004) Siderophore biosynthesis but not reductive iron assimilation is essential for *Aspergillus fumigatus* virulence. J Exp Med 200: 1213-1219.

55. Willger SD, Puttikamonkul S, Kim KH, Burritt JB, Grahl N, et al. (2008) A sterol-regulatory element binding protein is required for cell polarity, hypoxia adaptation, azole drug resistance, and virulence in *Aspergillus fumigatus*. PLoS Pathog 4: e1000200.

56. Grahl N, Puttikamonkul S, Macdonald JM, Gamcsik MP, Ngo LY, et al. *In vivo* hypoxia and a fungal alcohol dehydrogenase influence the pathogenesis of invasive pulmonary aspergillosis. PLoS Pathog 7: e1002145.

57. Calvo AM, Wilson RA, Bok JW, Keller NP (2002) Relationship between secondary metabolism and fungal development. Microbiol Mol Biol Rev 66: 447-459, table of contents.

58. Jacobson ES (2000) Pathogenic roles for fungal melanins. Clin Microbiol Rev 13: 708-717.

59. Chai LY, Netea MG, Sugui J, Vonk AG, van de Sande WW, et al. *Aspergillus fumigatus* conidial melanin modulates host cytokine response. Immunobiology 215: 915-920.

60. Brakhage AA, Liebmann B (2005) *Aspergillus fumigatus* conidial pigment and cAMP signal transduction: significance for virulence. Med Mycol 43 Suppl 1: S75-82.

61. Volling K, Thywissen A, Brakhage AA, Saluz HP Phagocytosis of melanized *Aspergillus* conidia by macrophages exerts cytoprotective effects by sustained PI3K/Akt signalling. Cell Microbiol 13: 1130-1148.

62. Lorenz MC, Fink GR (2001) The glyoxylate cycle is required for fungal virulence. Nature 412: 83-86.

63. Ebel F, Schwienbacher M, Beyer J, Heesemann J, Brakhage AA, et al. (2006) Analysis of the regulation, expression, and localisation of the isocitrate lyase from *Aspergillus fumigatus*, a potential target for antifungal drug development. Fungal Genet Biol 43: 476-489.

64. Schobel F, Ibrahim-Granet O, Ave P, Latge JP, Brakhage AA, et al. (2007) *Aspergillus fumigatus* does not require fatty acid metabolism via isocitrate lyase for development of invasive aspergillosis. Infect Immun 75: 1237-1244.

65. Sugui JA, Kim HS, Zarember KA, Chang YC, Gallin JI, et al. (2008) Genes differentially expressed in conidia and hyphae of *Aspergillus fumigatus* upon exposure to human neutrophils. PLoS One 3: e2655.

66. Thevelein JM (1984) Regulation of trehalose mobilization in fungi. Microbiol Rev 48: 42-59.

67. Crowe JH, Hoekstra FA, Crowe LM (1992) Anhydrobiosis. Annu Rev Physiol 54: 579-599.

68. Singer MA, Lindquist S (1998) Thermotolerance in *Saccharomyces cerevisiae*: the Yin and Yang of trehalose. Trends Biotechnol 16: 460-468.

69. Richards AB, Krakowka S, Dexter LB, Schmid H, Wolterbeek AP, et al. (2002) Trehalose: a review of properties, history of use and human tolerance, and results of multiple safety studies. Food Chem Toxicol 40: 871-898.

70. Sano F, Asakawa N, Inoue Y, Sakurai M (1999) A dual role for intracellular trehalose in the resistance of yeast cells to water stress. Cryobiology 39: 80-87.

71. Crowe LM, Reid DS, Crowe JH (1996) Is trehalose special for preserving dry biomaterials? Biophys J 71: 2087-2093.

72. Sun WQ, Leopold AC, Crowe LM, Crowe JH (1996) Stability of dry liposomes in sugar glasses. Biophys J 70: 1769-1776.

73. Nwaka S, Mechler B, Destruelle M, Holzer H (1995) Phenotypic features of trehalase mutants in *Saccharomyces cerevisiae*. FEBS Lett 360: 286-290.

74. Lillie SH, Pringle JR (1980) Reserve carbohydrate metabolism in *Saccharomyces cerevisiae*: responses to nutrient limitation. J Bacteriol 143: 1384-1394.

75. Kane SM, Roth R (1974) Carbohydrate metabolism during ascospore development in yeast. J Bacteriol 118: 8-14.

76. Fillinger S, Chaveroche MK, van Dijck P, de Vries R, Ruijter G, et al. (2001) Trehalose is required for the acquisition of tolerance to a variety of stresses in the filamentous fungus *Aspergillus nidulans*. Microbiology 147: 1851-1862.

77. De Virgilio C, Simmen U, Hottiger T, Boller T, Wiemken A (1990) Heat shock induces enzymes of trehalose metabolism, trehalose accumulation, and thermotolerance in *Schizosaccharomyces pombe*, even in the presence of cycloheximide. FEBS Lett 273: 107-110.

78. Hottiger T, Schmutz P, Wiemken A (1987) Heat-induced accumulation and futile cycling of trehalose in *Saccharomyces cerevisiae*. J Bacteriol 169: 5518-5522.

79. Winkler K, Kienle I, Burgert M, Wagner JC, Holzer H (1991) Metabolic regulation of the trehalose content of vegetative yeast. FEBS Lett 291: 269-272.

80. Kandror O, DeLeon A, Goldberg AL (2002) Trehalose synthesis is induced upon exposure of *Escherichia coli* to cold and is essential for viability at low temperatures. Proc Natl Acad Sci U S A 99: 9727-9732.

81. Murphy HN, Stewart GR, Mischenko VV, Apt AS, Harris R, et al. (2005) The OtsAB pathway is essential for trehalose biosynthesis in *Mycobacterium tuberculosis*. J Biol Chem 280: 14524-14529.

82. Woodruff PJ, Carlson BL, Siridechadilok B, Pratt MR, Senaratne RH, et al. (2004) Trehalose is required for growth of *Mycobacterium smegmatis*. J Biol Chem 279: 28835-28843.

83. Elbein AD, Pan YT, Pastuszak I, Carroll D (2003) New insights on trehalose: a multifunctional molecule. Glycobiology 13: 17R-27R.

84. Avonce N, Mendoza-Vargas A, Morett E, Iturriaga G (2006) Insights on the evolution of trehalose biosynthesis. BMC Evol Biol 6: 109.

85. Cabib E, Leloir LF (1958) The biosynthesis of trehalose phosphate. J Biol Chem 231: 259-275.

86. Vuorio OE, Kalkkinen N, Londesborough J (1993) Cloning of two related genes encoding the 56-kDa and 123-kDa subunits of trehalose synthase from the yeast *Saccharomyces cerevisiae*. Eur J Biochem 216: 849-861.

87. Elliott B, Haltiwanger RS, Futcher B (1996) Synergy between trehalose and Hsp104 for thermotolerance in *Saccharomyces cerevisiae*. Genetics 144: 923-933.

88. Gancedo C, Flores CL (2004) The importance of a functional trehalose biosynthetic pathway for the life of yeasts and fungi. FEMS Yeast Res 4: 351-359.

89. Reinders A, Burckert N, Hohmann S, Thevelein JM, Boller T, et al. (1997) Structural analysis of the subunits of the trehalose-6-phosphate synthase/phosphatase complex in *Saccharomyces cerevisiae* and their function during heat shock. Mol Microbiol 24: 687-695.

90. Blazquez MA, Lagunas R, Gancedo C, Gancedo JM (1993) Trehalose-6-phosphate, a new regulator of yeast glycolysis that inhibits hexokinases. FEBS Lett 329: 51-54.

91. De Virgilio C, Burckert N, Bell W, Jeno P, Boller T, et al. (1993) Disruption of TPS2, the gene encoding the 100-kDa subunit of the trehalose-6-phosphate synthase/phosphatase complex in *Saccharomyces cerevisiae*, causes accumulation of trehalose-6-phosphate and loss of trehalose-6-phosphate phosphatase activity. Eur J Biochem 212: 315-323.

92. Lee JH, Lee KH, Kim CG, Lee SY, Kim GJ, et al. (2005) Cloning and expression of a trehalose synthase from *Pseudomonas stutzeri* CJ38 in *Escherichia coli* for the production of trehalose. Appl Microbiol Biotechnol 68: 213-219.

93. Nishimoto T, Nakano M, Nakada T, Chaen H, Fukuda S, et al. (1996) Purification and properties of a novel enzyme, trehalose synthase, from *Pimelobacter sp*. R48. Biosci Biotechnol Biochem 60: 640-644.

94. Pan YT, Koroth Edavana V, Jourdian WJ, Edmondson R, Carroll JD, et al. (2004) Trehalose synthase of *Mycobacterium smegmatis*: purification, cloning, expression, and properties of the enzyme. Eur J Biochem 271: 4259-4269.

95. Xiuli W, Hongbiao D, Ming Y, Yu Q (2009) Gene cloning, expression, and characterization of a novel trehalose synthase from *Arthrobacter aurescens*. Appl Microbiol Biotechnol 83: 477-482.

96. Yue M, Wu XL, Gong WN, Ding HB (2009) Molecular cloning and expression of a novel trehalose synthase gene from *Enterobacter hormaechei*. Microb Cell Fact 8: 34.

97. Yamamoto T, Maruta K, Watanabe H, Yamashita H, Kubota M, et al. (2001) Trehalose-producing operon treYZ from *Arthrobacter ramosus* S34. Biosci Biotechnol Biochem 65: 1419-1423.

98. Maruta K, Mitsuzumi H, Nakada T, Kubota M, Chaen H, et al. (1996) Cloning and sequencing of a cluster of genes encoding novel enzymes of trehalose biosynthesis from thermophilic archaebacterium *Sulfolobus acidocaldarius*. Biochim Biophys Acta 1291: 177-181.

99. Wannet WJ, Op den Camp HJ, Wisselink HW, van der Drift C, Van Griensven LJ, et al. (1998) Purification and characterization of trehalose phosphorylase from the commercial mushroom *Agaricus bisporus*. Biochim Biophys Acta 1425: 177-188.

100. Aisaka K, Masuda T (1995) Production of trehalose phosphorylase by *Catellatospora ferruginea*. FEMS Microbiol Lett 131: 47-51.

101. Qu Q, Lee SJ, Boos W (2004) TreT, a novel trehalose glycosyltransferring synthase of the hyperthermophilic archaeon *Thermococcus litoralis*. J Biol Chem 279: 47890-47897.

102. Horikoshi K, Ikeda Y (1966) Trehalase in conidia of *Aspergillus oryzae*. J Bacteriol 91: 1883-1887.

103. d'Enfert C, Fontaine T (1997) Molecular characterization of the *Aspergillus nidulans treA* gene encoding an acid trehalase required for growth on trehalose. Mol Microbiol 24: 203-216.

104. Ruf J, Wacker H, James P, Maffia M, Seiler P, et al. (1990) Rabbit small intestinal trehalase. Purification, cDNA cloning, expression, and verification of glycosylphosphatidylinositol anchoring. J Biol Chem 265: 15034-15039.

105. Ishihara R, Taketani S, Sasai-Takedatsu M, Kino M, Tokunaga R, et al. (1997) Molecular cloning, sequencing and expression of cDNA encoding human trehalase. Gene 202: 69-74.

106. Bell W, Klaassen P, Ohnacker M, Boller T, Herweijer M, et al. (1992) Characterization of the 56-kDa subunit of yeast trehalose-6-phosphate synthase and cloning of its gene reveal its identity with the product of CIF1, a regulator of carbon catabolite inactivation. Eur J Biochem 209: 951-959.

107. Hohmann S, Bell W, Neves MJ, Valckx D, Thevelein JM (1996) Evidence for trehalose-6-phosphate-dependent and -independent mechanisms in the control of sugar influx into yeast glycolysis. Mol Microbiol 20: 981-991.

108. Noubhani A, Bunoust O, Bonini BM, Thevelein JM, Devin A, et al. (2009) The trehalose pathway regulates mitochondrial respiratory chain content through hexokinase 2 and cAMP in *Saccharomyces cerevisiae*. J Biol Chem 284: 27229-27234.

109. Flores CL, Gancedo C, Petit T Disruption of *Yarrowia lipolytica* TPS1 gene encoding trehalose-6-P synthase does not affect growth in glucose but impairs growth at high temperature. PLoS One 6: e23695.

110. Flipphi M, van de Vondervoort PJ, Ruijter GJ, Visser J, Arst HN, Jr., et al. (2003) Onset of carbon catabolite repression in *Aspergillus nidulans*. Parallel involvement of hexokinase and glucokinase in sugar signaling. J Biol Chem 278: 11849-11857.

111. Fleck CB, Brock M *Aspergillus fumigatus* catalytic glucokinase and hexokinase: expression analysis and importance for germination, growth, and conidiation. Eukaryot Cell 9: 1120-1135.

112. Steinbock F, Choojun S, Held I, Roehr M, Kubicek CP (1994) Characterization and regulatory properties of a single hexokinase from the citric acid accumulating fungus *Aspergillus niger*. Biochim Biophys Acta 1200: 215-223.

113. Panneman H, Ruijter GJ, van den Broeck HC, Driever ET, Visser J (1996) Cloning and biochemical characterisation of an *Aspergillus niger* glucokinase. Evidence for the presence of separate glucokinase and hexokinase enzymes. Eur J Biochem 240: 518-525.

114. Zaragoza O, Blazquez MA, Gancedo C (1998) Disruption of the *Candida albicans* TPS1 gene encoding trehalose-6-phosphate synthase impairs formation of hyphae and decreases infectivity. J Bacteriol 180: 3809-3815.

115. Zaragoza O, de Virgilio C, Ponton J, Gancedo C (2002) Disruption in *Candida albicans* of the TPS2 gene encoding trehalose-6-phosphate phosphatase affects cell integrity and decreases infectivity. Microbiology 148: 1281-1290.

116. Puttikamonkul S, Willger SD, Grahl N, Perfect JR, Movahed N, et al. (2010) Trehalose 6-phosphate phosphatase is required for cell wall integrity and fungal virulence but not trehalose biosynthesis in the human fungal pathogen *Aspergillus fumigatus*. Mol Microbiol 77: 891-911.

117. Petzold EW, Himmelreich U, Mylonakis E, Rude T, Toffaletti D, et al. (2006) Characterization and regulation of the trehalose synthesis pathway and its importance in the pathogenicity of *Cryptococcus neoformans*. Infect Immun 74: 5877-5887.

118. Ngamskulrungroj P, Himmelreich U, Breger JA, Wilson C, Chayakulkeeree M, et al. (2009) The trehalose synthesis pathway is an integral part of the virulence composite for *Cryptococcus gattii*. Infect Immun 77: 4584-4596.

119. Al-Bader N, Vanier G, Liu H, Gravelat FN, Urb M, et al. (2010) Role of trehalose biosynthesis in *Aspergillus fumigatus* development, stress response, and virulence. Infect Immun 78: 3007-3018.

120. Foster AJ, Jenkinson JM, Talbot NJ (2003) Trehalose synthesis and metabolism are required at different stages of plant infection by *Magnaporthe grisea*. EMBO J 22: 225-235.

121. Wilson RA, Jenkinson JM, Gibson RP, Littlechild JA, Wang ZY, et al. (2007) Tps1 regulates the pentose phosphate pathway, nitrogen metabolism and fungal virulence. EMBO J 26: 3673-3685.

122. Wilson RA, Gibson RP, Quispe CF, Littlechild JA, Talbot NJ An NADPH-dependent genetic switch regulates plant infection by the rice blast fungus. Proc Natl Acad Sci U S A 107: 21902-21907.

123. Latge JP (2007) The cell wall: a carbohydrate armour for the fungal cell. Mol Microbiol 66: 279-290.

124. Fontaine T, Simenel C, Dubreucq G, Adam O, Delepierre M, et al. (2000) Molecular organization of the alkali-insoluble fraction of *Aspergillus fumigatus* cell wall. J Biol Chem 275: 27594-27607.

125. Cabib E, Roh DH, Schmidt M, Crotti LB, Varma A (2001) The yeast cell wall and septum as paradigms of cell growth and morphogenesis. J Biol Chem 276: 19679-19682.

126. Latge JP (2010) Tasting the fungal cell wall. Cell Microbiol 12: 863-872.

127. Balloy V, Chignard M (2009) The innate immune response to *Aspergillus fumigatus*. Microbes Infect 11: 919-927.

128. Hohl TM, Van Epps HL, Rivera A, Morgan LA, Chen PL, et al. (2005) *Aspergillus fumigatus* triggers inflammatory responses by stage-specific beta-glucan display. PLoS Pathog 1: e30.

129. Brakhage AA, Bruns S, Thywissen A, Zipfel PF, Behnsen J Interaction of phagocytes with filamentous fungi. Curr Opin Microbiol 13: 409-415.

130. El-Benna J, Dang PM, Gougerot-Pocidalo MA, Elbim C (2005) Phagocyte NADPH oxidase: a multicomponent enzyme essential for host defenses. Arch Immunol Ther Exp (Warsz) 53: 199-206.

131. Bruns S, Kniemeyer O, Hasenberg M, Aimanianda V, Nietzsche S, et al. Production of extracellular traps against *Aspergillus fumigatus* in vitro and in infected lung tissue is dependent on invading neutrophils and influenced by hydrophobin RodA. PLoS Pathog 6: e1000873.

132. McCormick A, Heesemann L, Wagener J, Marcos V, Hartl D, et al. NETs formed by human neutrophils inhibit growth of the pathogenic mold *Aspergillus fumigatus*. Microbes Infect 12: 928-936.

133. Bianchi M, Hakkim A, Brinkmann V, Siler U, Seger RA, et al. (2009) Restoration of NET formation by gene therapy in CGD controls aspergillosis. Blood 114: 2619-2622.

134. Urban CF, Reichard U, Brinkmann V, Zychlinsky A (2006) Neutrophil extracellular traps capture and kill *Candida albicans* yeast and hyphal forms. Cell Microbiol 8: 668-676.

135. Hasenberg M, Behnsen J, Krappmann S, Brakhage A, Gunzer M Phagocyte responses towards *Aspergillus fumigatus*. Int J Med Microbiol 301: 436-444.

136. Janeway CA, Jr. (1989) Approaching the asymptote? Evolution and revolution in immunology. Cold Spring Harb Symp Quant Biol 54: 1-13.

137. Medzhitov R, Janeway CA, Jr. (1997) Innate immunity: impact on the adaptive immune response. Curr Opin Immunol 9: 4-9.

138. Medzhitov R (2007) Recognition of microorganisms and activation of the immune response. Nature 449: 819-826.

139. Drickamer K, Taylor ME (1993) Biology of animal lectins. Annu Rev Cell Biol 9: 237-264.

140. Kerrigan AM, Brown GD Syk-coupled C-type lectins in immunity. Trends Immunol 32: 151-156.

141. Brown GD, Gordon S (2001) Immune recognition. A new receptor for beta-glucans. Nature 413: 36-37.

142. Brown GD, Herre J, Williams DL, Willment JA, Marshall AS, et al. (2003) Dectin-1 mediates the biological effects of beta-glucans. J Exp Med 197: 1119-1124.

143. Werner JL, Metz AE, Horn D, Schoeb TR, Hewitt MM, et al. (2009) Requisite role for the dectin-1 beta-glucan receptor in pulmonary defense against *Aspergillus fumigatus*. J Immunol 182: 4938-4946.

144. Heinsbroek SE, Taylor PR, Rosas M, Willment JA, Williams DL, et al. (2006) Expression of functionally different dectin-1 isoforms by murine macrophages. J Immunol 176: 5513-5518.

145. Cunha C, Di Ianni M, Bozza S, Giovannini G, Zagarella S, et al. Dectin-1 Y238X polymorphism associates with susceptibility to invasive aspergillosis in hematopoietic transplantation through impairment of both recipient- and donor-dependent mechanisms of antifungal immunity. Blood 116: 5394-5402.

146. Dennehy KM, Ferwerda G, Faro-Trindade I, Pyz E, Willment JA, et al. (2008) Syk kinase is required for collaborative cytokine production induced through Dectin-1 and Toll-like receptors. Eur J Immunol 38: 500-506.

147. Bellocchio S, Montagnoli C, Bozza S, Gaziano R, Rossi G, et al. (2004) The contribution of the Toll-like/IL-1 receptor superfamily to innate and adaptive immunity to fungal pathogens in vivo. J Immunol 172: 3059-3069.

148. Zuluaga AF, Salazar BE, Rodriguez CA, Zapata AX, Agudelo M, et al. (2006) Neutropenia induced in outbred mice by a simplified low-dose cyclophosphamide regimen: characterization and applicability to diverse experimental models of infectious diseases. BMC Infect Dis 6: 55.

149. Stephens-Romero SD, Mednick AJ, Feldmesser M (2005) The pathogenesis of fatal outcome in murine pulmonary aspergillosis depends on the neutrophil depletion strategy. Infect Immun 73: 114-125.

150. Yamamoto Y, Gaynor RB (2001) Therapeutic potential of inhibition of the NF-kappaB pathway in the treatment of inflammation and cancer. J Clin Invest 107: 135-142.

151. Roos D, de Boer M, Kuribayashi F, Meischl C, Weening RS, et al. (1996) Mutations in the X-linked and autosomal recessive forms of chronic granulomatous disease. Blood 87: 1663-1681.

152. Pollock JD, Williams DA, Gifford MA, Li LL, Du X, et al. (1995) Mouse model of X-linked chronic granulomatous disease, an inherited defect in phagocyte superoxide production. Nat Genet 9: 202-209.

153. Bianchi M, Niemiec MJ, Siler U, Urban CF, Reichenbach J Restoration of anti-Aspergillus defense by neutrophil extracellular traps in human chronic

granulomatous disease after gene therapy is calprotectin-dependent. J Allergy Clin Immunol 127: 1243-1252 e1247.

CHAPTER TWO

TREHALOSE 6-PHOSPHATE PHOSPHATASE IS REQUIRED FOR CELL WALL INTEGRITY AND FUNGAL VIRULENCE BUT NOT TREHALOSE BIOSYNTHESIS IN THE HUMAN FUNGAL PATHOGEN *ASPERGILLUS FUMIGATUS*

Contribution of Authors and Co-Authors

Manuscript in Chapter 2

Author: Srisombat Puttikamonkul

Contributions: Designed the study and conducted the experiment, analyzed data, and wrote the manuscript.

Co-authors: Sven D. Willger, and Nora Grahl

Contributions: Assisted with study design and discussed the results and implications and edited the manuscript at all stages.

Co-author: Navid Movahed, and Brian Bothner,

Contributions: Assisted with LCMS experimental study and discussed the results and implications and commented on the manuscript.

Co-author: Steven Park, Padmaja Paderu, and David S. Perlin

Contributions: Assisted with RT-PCR analysis study and discussed the results and implications and commented on the manuscript.

Co-author: John R. Perfect

Contributions: Discussed the results and implications and commented on the manuscript.

Co-author: Robert A. Cramer Jr

Contributions: Obtained funding, assisted with study design, and discussed the results and implications and commented on the manuscript and edited the manuscript at all stages.

Manuscript Information Page

Srisombat Puttikamonkul, Sven D. Willger, Nora Grahl, Navid Movahed, Brian Bothner, Steven Park, Padmaja Paderu, David S. Perlin, John R. Perfect, Robert A. Cramer Jr

Journal Name: Molecular Microbiology

Status of Manuscript:
___Prepared for submission to a peer-reviewed journal
___Officially submitted to a peer-reviewed journal
___Accepted by a peer-reviewed journal
_x_Published in a peer-reviewed journal

Published by Blackwell Publishing Ltd.
Volume 77, Issue4, pages 891-911, August 2010

Abstract

The trehalose biosynthesis pathway is critical for virulence in human and plant fungal pathogens. In this study, we tested the hypothesis that trehalose-6-phosphate phosphatase (T6PP) is required for *Aspergillus fumigatus* virulence. A mutant of the *A. fumigatus* T6PP, OrlA, displayed severe morphological defects related to asexual reproduction when grown on glucose (1%) minimal media. These defects could be rescued by addition of osmotic stabilizers, reduction in incubation temperature, or increase in glucose levels (>4%). Subsequent examination of the mutant with cell wall perturbing agents revealed a link between cell wall biosynthesis and trehalose-6-phosphate (T6P) levels. As expected, high levels of T6P accumulated in the absence of OrlA resulting in depletion of free inorganic phosphate (Pi) and inhibition of hexokinase activity. Surprisingly, trehalose production persisted in the absence of OrlA. Further analyses revealed that *A. fumigatus* contains two trehalose phosphorylases that may be responsible for trehalose production in the absence of OrlA. Despite a normal growth rate under *in vitro* growth conditions, the *orlA* mutant was virtually avirulent in two distinct murine models of invasive pulmonary aspergillosis. Our results suggest that further study of this pathway will lead to new insights into regulation of fungal cell wall biosynthesis and virulence.

Introduction

Trehalose (α-D-glucopyranosyle α-D-glucopyranoside) is synthesized and stored in a wide variety of organisms such as bacteria, fungi, plants, insects, and some

invertebrates [1,2,3]. Unlike these other organisms, humans are unable to produce trehalose but can utilize trehalose through a trehalase enzyme [4,5,6]. Importantly, fungal mutants of enzymes at different key steps in the trehalose biosynthesis pathway are required for human and plant fungal pathogenesis [7,8,9,10,11]. Thus, the lack of human orthologs and the importance of trehalose biosynthesis in human and plant fungal pathogenesis has led to the hypothesis that this pathway is a promising antifungal drug target.

Mechanisms of trehalose biosynthesis in fungi have been extensively studied in the model yeast *Saccharomyces cerevisiae*. In *S. cerevisiae*, trehalose is synthesized in a two-step reaction (TPS/TPP) that is carried out by a four-subunit protein complex [4,12,13,14]. A glucosyl residue from uridine-diphospho-glucose (UDP-glucose) is transferred to glucose-6-phosphate (G6P) by trehalose-6-phosphate synthase (Tps1p) resulting in production of trehalose-6-phosphate (T6P). T6P is subsequently dephosphorylated by trehalose-6-phosphate phosphatase (Tps2p) to obtain trehalose (reviewed in [4]. Additionally, there are two regulatory subunits in the protein complex (Tsl1p and Tps3p) that participate in these reactions by interacting with the Tps1p and Tps2p complex [15,16]. All subunits are required for optimal enzymatic activity.

Five routes of trehalose biosynthesis have now been described in various organisms [17]. With regard to the pathogenic fungi, it seems that the TPS/TPP pathway is the primary route utilized, though mechanistic details have yet to be carried out to the extent that they have in *S. cerevisiae*. Some fungi have been reported to utilize the trehalose phosphorylase (TP) pathway for trehalose biosynthesis. For example, the basidiomycete

mushrooms *Grifola frendosa* and *Pleurotus ostreatus* use TP to produce trehalose from G1P and glucose [18,19]. TP activity also appears to play a key role in trehalose metabolism in *Agaricus bisporus* due to a lack of trehalose synthase and trehalase activity [20]. Importantly, this pathway of trehalose biosynthesis is negatively regulated by free inorganic phosphate (Pi) [20].

Trehalose has been primarily thought to serve as a storage carbohydrate in fungi due to the presence of a trehalase enzyme, which hydrolyzes trehalose into two molecules of glucose [2,21]. Trehalose also functions as an important stress protectant against a variety of stress conditions including dehydration, heat and cold shock, oxidative stress, and antimicrobial drug treatments [1,2,12,22,23,24,25,26]. Moreover, trehalose may be an important carbohydrate source for reproductive propagules of fungi. Trehalose is abundant in mature ascospores in yeast, and *Aspergillus nidulans* conidia have high concentrations of trehalose that is rapidly degraded upon induction of conidial germination [27,28]. Recently, a regulator of conidiogenesis, VosA, was identified in *A. nidulans* and also found to regulate genes involved in trehalose biosynthesis in conidia [29]. Perhaps most intriguingly, there is a growing understanding of the role that genes, proteins, and intermediate metabolites involved in trehalose biosynthesis are playing as key regulators of basic carbon metabolism in fungi [12,30,31,32].

With regard to fungal pathogenesis, the trehalose pathway has been characterized in three human pathogenic yeast (*Cryptococcus neoformans, Cryptococcus gattii,* and *Candida albicans*) and one filamentous fungal plant pathogen, *Magnaporthe grisea* [7,8,9,10,11,30,33]. However, studies on the trehalose pathway of the most common

cause of human invasive mold infections, *Aspergillus fumigatus*, have not been undertaken. In this study, we have begun a comprehensive examination of the trehalose biosynthesis pathway in this important human pathogenic fungus by identifying and functionally characterizing the T6P phosphatase OrlA, (*S. cerevisiae* Tps2p ortholog). Our results confirm previous suggestions that the trehalose biosynthesis pathway is a promising antifungal drug target, and also suggest a critical role for this pathway in regulating key aspects of *A. fumigatus* biology including glycolytic flux, cell wall integrity, and virulence.

Methods

Strains and Media

Aspergillus fumigatus strain CEA17 (a uracil auxotroph strain lacking *pyrG*) was used to generate the *orlA* mutant strain (Δ*orlA*; *orlA*::*A. parasiticus pyrG*) [34]. The corresponding wild-type strain CEA10 (CBS144.89) was utilized throughout this study (kind gift of Dr. Jean-Paul Latge). All strains were routinely grown in glucose minimal medium (GMM) containing a final concentration of 1% glucose, if not stated otherwise, with or without uridine and uracil at 37°C [35]. Conidia were harvested after growth on sorbitol minimal media (SMM, 1.2 M sorbitol, 1% glucose) for 3 days, using SMM for standard media in all experiments (with the exception of the virulence studies) due to the restricted ability of the *orlA* mutant to generate conidia on GMM. For the virulence studies, wild-type and reconstituted strain conidia were obtained from GMM. An examination of conidia from the wild-type and reconstituted strains grown on SMM did

not reveal any significant differences in morphology, viability or germination rates compared with GMM (data not shown). FMM is a minimal media that contain 1% fructose in substitution of glucose to determine the ability of fungal strains to utilize fructose as a sole carbon source.

Strain Construction

Mutant and reconstituted strains were generated by standard fungal protoplast transformation of *A. fumigatus* uracil auxotroph strain CEA17. PCR generated gene replacement or reconstitution constructs were utilized. BLAST searches of the A1163 genome sequence at The Central *Aspergillus* Data REpository (C*A*DRE) database retrieved the *orlA* open reading frame (AFUB_043350) [36]. The 2,999 bp *orlA* gene was replaced by a gene replacement construct of ~5kb. The replacement construct was generated by cloning homologous sequences (900 bp upstream and 951 bp downstream) of the *orlA* locus into plasmid pJW24 (gift from Dr. Nancy Keller) flanking the *A. parasiticus pyrG gene* [34]. This plasmid was then used as a template to amplify the replacement cassette and 10 µg of this PCR product was used for protoplast transformation. Polyethylene glycol mediated protoplast transformation was essentially performed according to the procedure described by Yelton et al. [37]. To reconstitute the wild-type *orlA* gene back into the *orlA* mutant background, a reconstitution construct was generated by cloning a ~5.3 kb fragment of *orlA* from the wild-type strain CEA10 into fungal transformation vector pBC-Hygro (gift from Kevin McCluskey, Fungal Genetics Stock Center), which contains the hygromycin B resistance gene as a selectable marker. 1,187bp of sequence upstream of the *orlA* coding sequence and 775bp downsteam of the

coding sequence were utilized. Subsequent transformants were selected on hygromycin B (150 µg/ml) containing media.

Transformants were initially screened with PCR to identify potential transformants with homologous recombination events at the *orlA* locus. PCR positive transformants were single spore isolated to eliminate any potential heterokaryons. Lastly, all possible candidates were then verified by Southern blot analysis and a strain carrying a single insertion of the replacement construct at the *orlA* gene locus was selected for further characterization. For reconstitution transformations, hygromycin resistant colonies were selected and screened with PCR and Southern blot analysis to identify a transformant with a single ectopic insertion of the reconstitution construct. Real time reverse transcriptase PCR was used to confirm expression of the re-introduced gene [38].

Conidia Production and Morphology

Equal amounts of conidia from the respective strains ($1x10^3$) were plated on two different media, GMM and SMM, and incubated at 37°C for 4 days prior to harvesting and counting. Total conidia production was assessed in triplicate and repeated on three separate occasions. Average value and standard deviation are reported with a two-tailed Student's t-test analysis ($P<0.05$) by GraphPad Prism software version 5 (San Diego, CA).

Flow cytometry analysis (FACS) was utilized to evaluate the morphology of conidia in the *orlA* mutant compared to wild-type and reconstituted strains. Freshly harvested conidia in 0.01% Tween80 were counted and diluted to $1x10^5$ conidia/ml [39], samples were flowed through the BD FACS Diva Version 6.0 without other additional

preparation steps. Side scatter (SSC) and forward scatter (FSC) analyses were performed on the sorted conidia.

Trehalose Measurement

A. fumigatus strains were grown on SMM plates at 37°C for 3 days. A total of $2x10^8$ conidia were used for the trehalose assay as described by d'Enfert C. and Fontaine [40]. Briefly, the conidia solution was centrifuged and resuspended in 500 µl of distilled water and incubated at 100°C for 20 min. The conidial extract containing soluble trehalose was separated from cell debris by centrifugation at 11,000xg for 10 min and used as the cell free extract.

Cell free extracts were then tested for trehalose levels according to the Glucose Assay Kit protocols (Sigma Aldrich). Samples (100 µl) were incubated with 100 µl of 0.2M sodium citrate pH 5.5 (0.1M final concentration) and incubated at 37°C overnight with 3mU of porcine kidney trehalase. The same reaction without trehalase was used as a control and utilized to determine the basal level of glucose in each reaction. The concentration of trehalose in the assay reaction (presence of trehalase) was subtracted by levels of glucose found in the control reaction (without trehalase). This ensures that the response measured is due to presence of trehalose and not glucose in the extracts. Concentration was normalized to starting input. Results from triplicate experiments were averaged, standard deviation calculated, and statistical significance determined ($P<0.05$) with a two-tailed Student's t-test.

Trehalose-6-Phosphate (T6P) Measurement

Liquid Chromatography Mass Spectrometry (LCMS) was used for measurement of T6P. Conidia and mycelia extractions were performed by the method modified from Wilson et al. [30]. A total of $3x10^{10}$ conidia from 3 day old cultures grown on SMM were used for T6P measurement. Briefly, the frozen conidia pellet is ground to a fine powder using a mortar and pestle and dichloromethane was used for extraction of metabolites. Mycelia samples were prepared from a 75 ml liquid GMM culture of $1x10^7$ conidia/ml grown overnight at 37°C. After overnight incubation, the cultures were filtered, lyophilized, ground with a mortar and pestle, and the subsequent powder weighed. For extraction, fungal powder was added to 10 ml of a Methanol: Dichloromethane: Water (6 : 2.5 : 1.5) solution and incubated at 4°C for 30 min. The suspension was centrifuged at 1,240×g for 20 min and the supernatant transferred to a new tube. Re-extraction of the sample pellet in 5 ml of fresh extraction solution was performed and the supernatant added to the previous supernatant. The pooled supernatant was then mixed with 7.5 ml of dichloromethane and 7.5 ml of water and centrifuged at 3,440×g for 20 min. The aqueous phase was collected and lyophilized overnight until completely dry. Resuspension of the dried samples was performed in 1 ml of deionized water and stored at -20°C until performing LCMS analysis.

LCMS was performed using an Agilent 1100 series LC system (Agilent Technologies, CA, USA) consisting of a vacuum degasser, autosampler, and a binary pump equipped with two tandem Luna Cartridges, Luna HILIC, 3µ, 200A°, 4x2.0mm (Phenomenex Inc.). The mobile phases were 100% water (solvent A) and 100%

acetonitrile (solvent B). A stepwise-gradient from 95% B to 10% B (25°C) at a flow rate of 0.2ml/min was used with a total run time of 9 min. The LC was directly interfaced to the ESI source of a microTOF (Bruker Daltonics, Bremen, Germany) mass spectrometer without splitting, operated in negative mode. Quantitation was achieved by analyzing samples in triplicate and using T6P-EIC (extracted ion chromatograms). Standard curves were constructed using a Trehalose 6-phosphate (Sigma) standard. The concentration of T6P was normalized to the input weight of fungal tissue for each sample. Results from triplicate experiments were averaged, standard deviation calculated, and statistical significance determined ($P \leq 0.05$) with a two-tailed Student's t-test.

Microscopic Analysis

A modified slide culture method adapted from Johnson [41] and Harris [42] was used to visualize the conidia and conidiophores of the *orlA* mutant compared to the wild-type and reconstituted strains with light microscopy. Briefly, a thin layer of solid media was cut in blocks approximately 10 mm^2, aseptically removed and placed on the glass slide which was placed on a support in a sterile 60 mm plastic petri dish. Each side of an agar block was inoculated with conidia of the respective strains. A sterile cover glass slip was placed on the inoculated agar and sterile water was added into the slide culture chamber to maintain humidity. This apparatus was incubated at 37°C until adequate growth and conidiogenesis had occurred (approximately 2-3 days). Both the cover slip and glass slide were carefully taken from the agar block and a drop of fungal mounting medium (lactophenol cotton blue, Sigma) was applied to each specimen. The slides were subsequently observed utilizing a light microscope.

Cell Wall Perturbation Agents

Several cell wall inhibitors were utilized for cell wall integrity tests: congo red (CR, Sigma Aldrich), calcofluor white (CFW, Sigma Aldrich), and Nikkomycin Z (NK, Sigma Aldrich) [43,44,45]. CR, CFW or NK were added into GMM at final concentrations of 1mg/ml, 25 µg/ml and 0.1 mM respectively. $1x10^6$ conidia (in a 5µl drop) of each test strain were placed on the center of each plate. The radial growth rates at 37°C of all strains were measured every 24 hours for a period of 5 days for each fungal strain in triplicate.

Quantitative Real-Time PCR

Respective *A. fumigatus* strains were cultured in liquid GMM for 6.5 and 24 hrs. At the respective time point, the germlings and mycelia were collected with vacuum filtration and lyophilized with a freeze drier (Labconco) prior to homogenization with 0.1 mm glass beads. Total RNA was extracted using the TRIsure reagent (Bioline) according to the manufacturer's protocol and subsequently further purified with the Qiagen RNeasy Plant Mini Kit (Qiagen). Genomic DNA contamination was further removed with Turbo DNase I treatment (Ambion). RNA integrity was confirmed with an Agilent Bioanalyzer. Quantitative real-time PCR analysis of cell wall biosynthesis genes was performed as previously described [46]**.** Primers for the individual cell wall biosynthesis genes are also as listed in Cramer *et al.*, 2008. qRT-PCR experiments were performed in duplicate and the fold expression data presented in Table 1 represents the mean and standard deviation of two biological replicates**.**

For mRNA abundance of the *orlA* and trehalose phosphorylase genes, conidia were produced on SMM plates (30 ^{o}C, 37 ^{o}C, and 45^{o}C) and harvested with 0.01% Tween80. Total conidia were centrifuged and lyophilized overnight prior to homogenization with 0.1 mm glass beads. Total RNA extraction and subsequent processing were as described above. 500 ng of DNase treated total RNA was reverse transcribed with the Quantitect Reverse Transcriptase kit (Qiagen). qRT-PCR was subsequently performed as we have previously described [38]. A no DNA template control was used in each analysis. Each sample was tested in triplicate and data was normalized to the actin reference gene and relative to the wild-type control grown at low temperature (30^{o}C) [47]. The results presented are from biological duplicate experiments and statistical significance was determined with an unpaired two-tailed student T-test.

Hexokinase and Pyruvate Decarboxylase Assays

1×10^{7} conidia/ml of the respective test strains were cultured in liquid GMM at 37°C for approximately 20 hr (which is the culture time that T6P accumulated in the *orlA* mutant). Mycelia was harvested by vacuum filtration, immediately frozen in liquid nitrogen and homogenized with 0.1 mm glass beads in 50mM Triethanolamine buffer pH 7.6 [48]. All procedures were conducted at 4°C. The homogenate was centrifuged at 13,000 rpm for 20 min at 4°C. The supernatant was transferred to a new pre-chilled tube and 25 µl of supernatant was used for the hexokinase assay following the manufacturer's protocol (Sigma Aldrich) [49]. Hexokinase activity was determined by measuring NADPH production at an absorption intensity of 340 nm with equilibration to 25°C. The ΔA340nm/minute was obtained from the maximum linear rate of kinetic measurements

for approximately 5 minutes [30]. Protein concentration in the extracted supernatant was quantified with the Bradford Reagent and used to normalize the data. Data presented are the mean and standard deviation of three biological replicates.

For pyruvate decarboxylase activity assays, the protocol of Lockington et al. was essentially followed [50]. Briefly, respective test strains were cultured overnight (~12 hours) at 37°C in liquid GMM (LGMM). Equal amounts of germlings were then incubated in fresh liquid GMM either under normoxic (20% O_2) or hypoxic (1% O_2) conditions for 48 hours at 37°C in LGMM. Cell free extracts from mycelium were collected as described for the hexokinase assay with the exception that the buffer for extraction was 100 mM KH_2PO_4, 2 mM $MgCl_2$, and 1 mM DTT**.** Pyruvate decarboxylase activity was determined by measuring the reduction of NADH at A_{340nm} and equilibrated to 37°C. Kinetic measurements were performed for 5 minutes and the maximum linear rate was calculated for each unit of enzyme. Data presented are the mean and standard deviation of two biological replicates.

Pi Assay

Conidia and mycelia of wild type, the *orlA* mutant and reconstituted strains were grown at 30, 37 and 45^{o}C. All strains were grown on SMM plates and a pellet of $2x10^9$ conidia was lyophilized overnight prior to homogenization with 0.1 mm glass beads. The mycelia was cultured in 50ml liquid GMM at inoculums of $1x10^7$conidia/ml overnight. Mycelia were then harvested, washed with sterile water, and collected with vacuum filtration prior to lyophilization and homogenization. Either 50mg of powdered mycelia or powder of $2x10^9$ conidia was then reconstituted in 1 ml and 0.5 ml of sterile water

respectively. The cell free extracts were prepared by vortexing and the clear supernatant was collected after centrifugation at 13,000 rpm for 10 minutes. Pi assay was measured by utilizing malachite green dye and molybdate, which forms a stable colored complex specifically with inorganic phosphate following the manufacturer's protocol; QuantiChrom Phosphate Assay Kit (BioAssay Systems). The cell free extracts were diluted to fall within the standard curve limits; 1:100 and 1:400 dilutions were optimized with conidia and mycelia samples respectively.

Murine Virulence Tests

Male CD1 mice (Charles River Laboratory, Raleign, NC) (6-8 weeks of age) were housed and supplied with food and antibiotic water ad libitum in the Animal Resources Center at Montana State University. Mice were immunosuppressed with intraperitoneal (IP) injections of cyclophosphamide (150 mg/kg) and subcutaneously (SC) with triamcinolone acetonide (Kenalog) (40 mg/kg) on days -2 and -1 respectively prior to infection. On days +3 and +6 post infection, the same dose of cyclophosphamide and Kenalog were repeated respectively. On day 0, groups of 10 mice were infected via the intranasal route with $1x10^6$ conidia of each *A. fumigatus* strain: *orlA* mutant, reconstituted (Rec-*orlA*), wild-type (CEA10), and a mock control group without conidia (the diluent; 0.01% Tween 80). For experiments with the X-CGD mice, 8-10 week old sex matched mice were utilized. Since the reconstitution strain was shown to have wild-type levels of virulence in the neutropenic model, only the wild-type and *orlA* mutant were compared in these animals (N = 10 each group). On day 0, mice were infected with $1x10^5$ conidia of the respective fungal strains.

Each mouse was observed twice daily for 14 days after *A. fumigatus* challenge. Mice were observed for standard signs of IPA including ruffled fur, hunched posture, difficulty breathing and weight loss accounting for more than 20% of body mass. Critically affected mice were humanely euthanized when it is clear recovery was not possible using the above criteria. A log rank test was used for pair wise comparisons of survival levels among the experimental groups, $P \leq 0.05$. Mouse experiments for each model were repeated on two separate occasions with similar results. Results presented are for one representative experiment for each model. All animal procedures and protocols were approved by the MSU Institutional Animal Care and Use Committee.

Histopathology

Additional murine experiments were conducted as described for histopathology analysis. In contrast to the survival study, 12 mice per group were used. At specific time points (days 1, 3, 5, 7, and 14 post-infections), two mice in each group were humanely euthanized. One lung was harvested from each mouse and fixed in 10% formalin prior to embedding in paraffin, 5 μm thick sections taken, and stained with either H&E (Hematoxylin and Eosin) or GMS (Gomori's Methenamine Silver) [51]. The other lung was kept at -80°C for additional analyses. Microscopic examination was performed on a Zeiss Axioscope2-plus microscope and engaged imaging system. Pictures were captured at 40x object-magnification and a reference bar is included in each image.

Results

Construction of Trehalose-6-Phosphate Phosphatase Mutant and Reconstituted Strains

To identify the putative trehalose-6-phosphate phosphatase gene involved in trehalose biosynthesis in *A. fumigatus*, we searched the genome sequence of *A. fumigatus* strain A1163 with the *A. nidulans* OrlA (AN3441) and S. cerevisiae Tps2p protein sequences using BLAST algorithms. Searches with both OrlA and Tps2p revealed a putative single ortholog in *A. fumigatus*, AFUB_043350, which we subsequently designated OrlA consistent with previous nomenclature in A. nidulans [52]. OrlA protein sequences from A. nidulans and *A. fumigatus* displayed 72% amino acid identity and 82% protein sequence similarity while *Sc* Tps2p and *Af* OrlA displayed 44% amino acid identity and 59% protein sequence similarity. Analysis of the *Af* OrlA protein sequence with InterPro revealed 3 highly conserved domains: a glycosyl transferase family 20 domain (amino acids 281-663), a trehalose phosphatase domain (amino acids 695-931), and a HAD-superfamily hydrolase subfamily IIB domain (amino acids 693-905). These results suggest that AFUB_043350 encodes the *A. fumigatus* trehalose-6-phosphate phosphatase, OrlA.

In order to determine the role of OrlA in *A. fumigatus* biology, we generated a null mutant of *orlA* by disruption of the coding sequence in the uracil/uridine auxotrophic *A. fumigatus* strain (CEA17) with the selectable marker pyrG from Aspergillus parasiticus as we have previously described [53] (Fig. 2.1). To confirm that phenotypes of the *orlA* mutant were solely due to loss of OrlA, we generated a reconstituted strain by

ectopic reintroduction of the wild-type *orlA* gene into the *orlA* mutant strain (Rec-*orlA* strain). All strains were rigorously confirmed by both PCR and Southern blot analyses (Fig. 2.1, and data not shown). All examined strains produced the expected hybridization signals when XbaI digested genomic DNA was hybridized with a DNA probe of the 5' (upstream) *orlA* ORF flanking sequence (Fig. 2.1A-C). The *orlA* mutant has a single band at 4,375 bp as expected for a clean disruption of the *orlA* open reading frame by the *A. parasiticus* pyrG marker (Fig. 2.1B-C). Subsequently, the reconstituted strain (Rec-*orlA*) contained hybridization bands corresponding to both the *orlA* mutant and wild-type alleles indicating successful ectopic reconstitution of the *orlA* gene in the *orlA* mutant background (Fig. 2.1A-C). mRNA abundance of the *orlA* gene was determined in all strains by qRT-PCR and expression of *orlA* was equivalent between the wild-type and Rec-*orlA* strains while absent in the *orlA* mutant (data not shown).

Abolished Asexual Reproduction and Abnormal Hyphal Morphology of the *orlA* Mutant

Although the *orlA* mutant has a wild-type like hyphal growth rate on glucose minimal media (GMM) at 37°C, we observed an almost complete loss of conidiation in the absence of *orlA* (Fig. 2.2A). When quantified, total conidia production of the *orlA* mutant on GMM at 37°C was significantly less than the wild-type and reconstituted strains ($P = 0.02$ and <0.01 respectively) (Fig. 2.2B). The conidiation defect could be partially rescued by growth at temperatures at or below 30°C and fully rescued on media containing an osmotic stabilizer (1.2 M sorbitol or 1% glycerol) (Fig. 2.2A-B and data not shown). We confirmed that temperature stress is a factor in the conidiation defect by

allowing growth of the mutant at 37°C for 2 days followed by a subsequent shift to lower temperatures (25°C and 30°C). We found that the *orlA* mutant was able to produce conidia on new tissue generated after the temperature shift to lower temperatures (data not shown).

Besides the effect of temperature on asexual reproduction, a temperature sensitive phenotype was observed at temperatures above 42°C. When subjected to heat stress (45°C) the *orlA* mutant displayed a significant decrease in growth in comparison with the wild-type and reconstituted strain when grown on both GMM and SMM media (data not shown). All strains grew better under high temperature stress when the osmotic stabilizing agent sorbitol was added to the media indicating that significant cell wall stress is placed on the fungus during high temperature growth. In the *orlA* mutant of *A. nidulans*, thermotolerance was completely suppressed as conidia were unable to germinate at high temperature (42°C) due to cell lysis [52,54]. However, conidia of the *orlA* mutant of *A. fumigatus* were able to survive and germinate at 45°C and we did not observe any cell lysis at these elevated temperatures. Taken together, these results strongly suggest that loss of trehalose-6-phosphate phosphatase activity severely impacted the ability of *A. fumigatus* to undergo asexual reproduction and tolerate temperature stress. We hypothesized that the ability of temperature and osmotic stabilizers to rescue these phenotypes suggested a possible defect in the cell wall of the *orlA* mutant.

To test our hypothesis we first examined the *orlA* mutant hyphal morphology using traditional slide cultures and lactophenol cotton blue stains (Fig. 2.3). Strikingly,

asexual reproduction was abolished in the absence of *orlA* as we found only conidiophores and vesicles produced on GMM with limited and abnormal phialide and conidia production (Fig. 2.3A). Abnormal hyphal morphology was also apparent when the *orlA* mutant was grown on GMM at 37°C. Mutant hyphae are clearly dysmorphic with shorter length compartments between septa and truncated hyphal tips with knobby, abnormal branching (Fig. 2.3A). When placed on high GMM (>4% glucose) or osmotic stabilizing media (Fig. 2.3B), these abnormal morphological phenotypes largely, but not completely, disappeared consistent with these culture conditions being able to restore conidiation. Interestingly, the ability of glucose to restore the conidiation defect of the mutant was dose dependent as restoration of conidiation started at around a concentration of 4% glucose and increased proportionately to the amount of glucose in the media (data not shown).

However, we observed that restoration of conidia production on high glucose media (10% glucose) or SMM resulted in conidia with abnormal morphology (Fig. 2.3B). The morphology of restored conidia of the *orlA* mutant grown on SMM media at 37°C are aberrant in shape and size as observed using light microscopy and confirmed by forward and side scatter measurements of conidia size and density using FACS analysis (Fig. 2.4).

Based on the FACS analysis, it is clear that a wide range of conidial morphologies is produced in the absence of *orlA*. This led us to question the viability and germination ability of the *orlA* mutant conidia. Conidia viability of all strains grown on SMM after incubation at 37°C did not differ after 10 days (all strains displayed a 60-70% survival

rate). However, after one month of incubation the *orlA* mutant conidia displayed an approximate 45% decrease in survival compared to day 3, whereas approximately 20% and 21% decreases in viability were observed in the wild-type and reconstituted strains respectively (data not shown).

When the ability of *orlA* mutant conidia from SMM plates at 37°C were examined for their ability to germinate in liquid GMM, we observed similar germination rates for all three strains with a slight but statistically insignificant trend for increased germination rates in the absence of *orlA* (data not shown). Thus, although dysmorphic, *orlA* mutant conidia are viable and have virtual wild-type levels of germination. Taken together, these morphological analyses of the *orlA* mutant suggest that loss of trehalose-6-phosphate phosphatase activity results in a defect in the cell wall that affects the ability of the fungus to form normal hyphae, asexual reproduction structures, and conidia.

Loss of *orlA* Results in Increased Sensitivity to Cell Wall Perturbing Agents

We next tested the hypothesis that the *orlA* mutant had a defect in the cell wall by utilizing several known cell wall perturbation agents. The mutant displayed wild-type levels of susceptibility to the echinocandin caspofungin, a specific β-1,3-glucan inhibitor, suggesting that β-1,3-glucan synthesis or content is not altered in the absence of OrlA. Susceptibility of the mutant to triazoles and amphotericin B was also tested and found to be the same as the wild-type and reconstituted strains (data not shown). Next, we tested the mutant's response to calcofluor white (CFW), congo red (CR), and Nikkomycin Z (NK). As observed in Figure 5, loss of *orlA* resulted in increased susceptibility to all three

cell wall perturbing agents compared to the wild-type and reconstituted strains (Fig. 2.5A-C). The growth rate (radius growth/day) of the reconstituted strain, but not the *orlA* mutant, was similar to the wild-type on all cell wall perturbing agents.

On CFW containing media, the growth rate of Rec-*orlA* (1.73±0.01) was comparable to CEA10 (1.65±0.03), while a decreased rate was observed in the *orlA* mutant (0.95±0.11). On NK, the *orlA* mutant (0.68±0.03) was again more susceptible than Rec-*orlA* (0.94±0.02) and CEA10 (1.09±0.03). Congo red had the strongest effect on the *orlA* mutant (Fig. 2.5A). Growth rates on CR containing media were similar in Rec-*orlA* (1.38±0.01) and CEA10 (1.27±0.03), but a drastic effect was observed on the *orlA* mutant (0.59±0.01). CR is thought to inhibit cell wall assembly enzymes that connect chitin to β-1,3-glucan and β-1,6-glucan. However, the mutant also displayed increased sensitivity to CFW and NK (Fig. 2.5B-C). CFW is an inhibitor of chitin polymer assembly while Nikkomycin Z is a chitin synthase inhibitor [43,44,45]. Taken together, these results suggest that β-1,3-glucan and β-1,6-glucan synthesis is likely unaffected, or at least not reduced, in the absence of OrlA. However, a significant defect either in the formation of the chitin-glucan matrix, which is critical for cell wall integrity, or actual chitin biosynthesis seems to be a consequence of OrlA loss.

We reasoned that the apparent cell wall defect in the *orlA* mutant could be due to alteration in the transcription of cell wall biosynthesis genes. To test this hypothesis, we examined the mRNA abundance of cell wall biosynthesis genes in the *orlA* mutant in comparison with the wild-type at two defined time points utilizing qRT-PCR (Table 1). 6.5 hours after conidial germination in liquid GMM at 37°C germ tubes had formed in

both the *orlA* mutant and wild-type strains. mRNA abundance of all 7 chitin synthase genes at 6.5 hours was not significantly altered in the *orlA* mutant compared to the wild-type. After 24 hours of growth in liquid GMM at 37°C, when both strains had formed masses of mycelia, chitin synthase mRNA abundance generally increased in the *orlA* mutant strain in comparison with the wild-type. However, it is unclear if the observed differences are biologically relevant. As expected from caspofungin's lack of an effect on the *orlA* mutant, no difference was observed between the wild-type and *orlA* mutant in the expression of the β-1,3- glucan synthase *fksA* at either time point. The most apparent differences in mRNA abundance at both 6.5 hours and 24 hours were observed in the three α-1,3-glucan synthases *agsA*, *agsB*, and *agsC*. In particular, the largest change in mRNA abundance was observed for *agsC*, which was increased over 16.35 (±7.6) fold in the absence of *orlA* at 24 hours. mRNA abundance changes in the cell wall remodeling enzymes *gelA*, *gelB*, and *gelC* (1,3-β -glucanosyltransferase) were also observed at 24 hours in the absence of *orlA*. However, inconsistencies between the replicates with these 3 genes prevent definitive conclusions from being drawn about the effect of OrlA loss on the mRNA abundance of these important cell wall remodeling enzyme encoding genes. Overall, we hypothesize that the general observed increases in mRNA abundance of the cell wall biosynthesis genes in the absence of *orlA* likely reflects the occurrence of alternations in the cell wall composition that results in positive transcriptional feedback of the required biosynthesis genes. Yet, the relatively modest increases in mRNA abundance may also suggest that the observed alterations in the *orlA* mutant cell wall occur due to changes in non-transcriptional based mechanisms.

Trehalose and Trehalose-6-Phosphate Production in the *orlA* Mutant is Altered

Based on knowledge of the *S. cerevisiae* trehalose biosynthesis pathway, the most likely hypothesis to explain the observed phenotypes of the *orlA* mutant is that loss of OrlA activity results in a significant increase in trehalose-6-phosphate (T6P) and subsequent loss of trehalose production. To test this hypothesis, we measured trehalose and T6P production in the wild-type, reconstituted, and *orlA* mutant strains. Surprisingly, we observed that *orlA* mutant conidia contained wild-type levels of trehalose when cultured at 37°C, and an approximate ~2 fold increase in trehalose content when exposed to high temperature stress (P value < 0.05) (Fig. 2.6A). This unexpected result raises the question whether OrlA is the trehalose-6-phosphate phosphatase in *A. fumigatus*.

However, liquid chromatography mass spectrometry (LCMS) analyses revealed that, as expected for a trehalose-6-phosphate phosphatase mutant, T6P accumulated in the *orlA* mutant to significant levels (2,400-4,700μM/gram conidia and 500-3,900 μM/gram mycelia) in both conidia and mycelia cultured at 30°C, 37°C, and 45°C (Fig. 2.6B) [55]. T6P levels were also found to increase with temperature suggesting that trehalose synthase activity encoded by *TPS1* orthologs is increased with temperature stress. Taken together, these results suggest that an alternate mechanism of trehalose biosynthesis exists in *A. fumigatus* in the absence of OrlA. Though unexpected, this result is not unprecedented as a similar persistence of trehalose biosynthesis was found in the *A. nidulans orlA* mutant [52] and a *C. albicans tps2/tps2* mutant [9].

A. fumigatus Contains Two Trehalose Phosphorylase Encoding Genes

Currently, the mechanism by which trehalose-6-phosphate phosphatase mutants in *Aspergillus* spp. and *C. albicans* generate trehalose is unknown. A preliminary microarray analysis of the *orlA* mutant revealed a significant increase in the mRNA abundance of a gene annotated as a trehalose synthase, CCG-9 (AFUB_062450) (data not shown). This gene is not part of the well-studied trehalose biosynthesis pathway in *S. cerevisiae*, but is part of a trehalose synthesizing enzyme family known as trehalose phosphorylases (TP) [18,56,57,58,59,60,61]. TPs are capable of producing trehalose from α or β-glucose-1-phosphate and have been found in a variety of organisms including bacteria, yeasts, green algae, and basidiomycete mushrooms [18,19]. *A. fumigatus* contains two putative TP encoding genes, the aforementioned AFUB_062450 and another gene, AFUB_037080. A third gene with putative sequence similarity to TPs was found, but appears to be a pseudogene based on current genome annotation. The predicted TP protein sequences have 36% similarity and both contain a highly conserved glycosyltransferase GTB type superfamily protein domain. In filamentous fungi, a TP encoding gene has been partially characterized in *Neurospora crassa* and named CCG-9 (clock controlled gene 9) [62]. AFUB_062450 has 32% sequence similarity while AFUB_037080 has 49% sequence similarity with *N. crassa* CCG-9.

We hypothesize that the persistence of trehalose biosynthesis in the *orlA* mutant is due to TP activity. Consequently, we examined the mRNA abundance of the two putative TP genes in conidia of both the *orlA* mutant and wild-type harvested from cultures grown on SMM at 30°C, 37°C, and 45°C (conditions in which the mutant produces wild-type

levels of trehalose). In comparison to wild-type conidia from cultures incubated at 30°C, conidia of both the wild-type and *orlA* mutant had mRNA abundance levels of AfuB_037080 with cultures from 30°C and 45°C having a significant increase in the *orlA* mutant (Fig. 2.7B). On the other hand, AFUB_062450 is the most abundant TP in the mutant conidia cultured at 30°C (Fig. 2.7A). In addition, AFUB_037080 mRNA was present at higher levels in the *orlA* mutant conidia under thermal stress conditions (37°C and 45°C) (Fig. 2.7B). mRNA abundance of *orlA* was essentially unchanged between the different temperature conditions, and no *orlA* mRNA was detected in the *orlA* mutant (Fig. 2.7C). These results suggest that increased TP mRNA levels could potentially explain the production of trehalose in the *orlA* mutant. Additional fungal genome analyses revealed putative TP orthologs in *A. nidulans* and other filamentous ascomycetes, but failed to identify a clear TP ortholog in *C. albicans*.

Potential Activation of TP Enzymes by
Depleted Free Pi Levels in the *orlA* Mutant

While the qRT-PCR data suggested slight increases in the mRNA levels of TP encoding genes in the *orlA* mutant, TP activity is also inhibited by high levels of free inorganic phosphate (Pi) [20]. We hypothesized that the accumulation of high T6P levels in the *orlA* mutant would result in sequestration of free Pi that could lead to induction of TP enzyme activity. To test this hypothesis, we measured levels of Pi in cell free extracts of the wild-type, *orlA* mutant and reconstituted strains incubated at 30°C, 37°C, and 45°C. We observed that in the mycelia, the *orlA* mutant contains less Pi than the wild type and reconstituted strains (P value <0.05 at all incubation conditions except at 30^{o}C)

(Fig. 2.8B). However, in conidia there was not a statistically significant difference between the fungal strains under thermal stress conditions with the exception of a higher Pi level in the *orlA* mutant at 30°C (Fig. 2.8A). The higher amount of Pi levels in the *orlA* mutant conidia may be a result of the difference in conidia size that we observed at 30°C (data not shown). Taken together, at similar conditions in which we observed the accumulation of T6P in the *orlA* mutant (Fig. 2.6B), associated Pi levels were consequently decreased in the absence of OrlA (Fig. 2.8B). This result suggests that Pi is sequestered by T6P which could induce the activation of TP enzymes. Confirmation of these results await further experimentation.

Hexokinase Activity is Decreased in
the *orlA* Mutant but Addition of GlcNAc to
Growth Medium does not Rescue Cell Wall Defects

T6P has been observed to inhibit hexokinase activity *in vitro* in several fungi. Thus, we hypothesized that the large accumulation of T6P in the *orlA* mutant would lead to decreased hexokinase activity. Cell free extracts from the *orlA* mutant displayed an approximate ~30% decrease in hexokinase activity in comparison with the wild-type and reconstituted strains (Fig. 2.9A). Importantly, this assay cannot distinguish between hexokinase and glucokinase activity. However, while glucose entry into glycolysis can be regulated by both hexokinase and glucokinase, fructose entry into glycolysis is solely regulated by hexokinase. Thus, we next tested the growth of the *orlA* mutant on fructose minimal media (FMM, 1% fructose). The *orlA* mutant grows slower than the wild-type and reconstituted strains when cultured on FMM. The radial growth rate (centrimeter diameter/day) of the *orlA* mutant was 1.27±0.00, the wild-type 2.20±0.03, and 2.16±0.05

in the reconstituted strain. This result confirms that hexokinase activity is likely significantly reduced in the *orlA* mutant.

To further examine whether glycolytic flux was potentially inhibited in the *orlA* mutant, we measured pyruvate decarboxylase (PDC) activity of the *orlA* mutant in comparison with the wild-type and reconstituted strains grown in liquid GMM at 37°C (Fig. 2.9B). The *orlA* mutant displayed a significant decrease in PDC activity suggesting decreased flux through the lower part of glycolysis occurs in the absence of OrlA. This result may be due to decreased levels of the glycolytic intermediates due to inhibition of hexokinase activity, or sequestration of free Pi in the absence of OrlA.

Since aminosugar biosynthesis is linked to intermediates of glycolysis, we next tested whether addition of N-acetylglucosamine (GlcNAc) to growth media could suppress the conidiation or hyphal morphology defect of the *orlA* mutant on GMM [52]. We tested GlcNAc at two concentrations (100 μg/ml and 1 mg/ml) in GMM and observed no change in the asexual conidiation or hyphal morphology defects of the *orlA* mutant at either concentration (data not shown). While a decrease in hexokinase activity in the *orlA* mutant is likely to result in a decrease in the needed precursors (Fructose-6-phosphate) for aminosugar biosynthesis, and therefore could explain the subsequent observed cell wall defects, this remains to be conclusively determined.

Loss of OrlA Function Results in Virulence Attenuation in Murine Models of Invasive Pulmonary Aspergillosis

Given the previous associations between the trehalose biosynthesis pathway and fungal virulence, we examined the virulence of the *A. fumigatus orlA* mutant,

reconstituted and wild-type strains in a chemotherapeutic murine model of invasive pulmonary aspergillosis. Despite the normal growth rate of the mutant at mammalian body temperature on glucose minimal media, the *orlA* mutant displayed a severe virulence attenuation in immunocompromised CD1 mice (Fig. 2.10A) (P value <0.0005 versus wild type and P=0.0007 versus reconstituted strain). Next, we examined the virulence of the *orlA* mutant in mice deficient in the gp91 Phox subunit of the NADPH oxidase (X-CGD mice) [63,64]. In this murine model, the *orlA* mutant also displayed a statistically significant decrease in virulence (P = 0.0005) (Fig. 2.10B). Importantly, X-CGD mice infected with the *orlA* mutant do eventually succumb to the infection. Culture of lung homogenates from X-CGD mice infected with the *orlA* mutant on day 10 of the infection revealed the persistence of the fungus in these animals. These striking results suggest that OrlA is part of the virulence arsenal of *A. fumigatus* and strongly supports our hypothesis that the trehalose pathway in *A. fumigatus* and other fungal pathogens is a potential global antifungal drug target.

To better understand the mechanism behind the virulence defect in the *orlA* mutant, we utilized histopathology analyses to visualize the host response and in vivo fungal burden during infection in the immunocompromised CD1 mouse model. On day 3-post infection, whole lung histopathology of mice infected with all 3 strains of fungus showed multiple sites of infection surrounded by leukocytes. At this time point, all mice exhibited symptoms of invasive pulmonary aspergillosis including ruffled fur, lethargy, and slightly labored breathing. No clear differences between the mutant and wild-type infected animals were observed in terms of lesion numbers (data not shown). However, a

closer examination of hematoxylin and Eosin (H&E) stained lungs revealed inflammation, drastic tissue damage, and hemorrhaging in the wild-type and reconstituted strains whereas *orlA* mutant infected mice had less inflammation and damage (Fig. 2.11 H&E staining). It is clear from the histopathology that the *orlA* mutant was able to germinate and develop hyphae in vivo in the lung, but it appears that the mutant stimulated a less aggressive inflammatory response which corresponded with slight decreases in fungal burden within given lesions (Fig. 2.11 GMS staining).

By day 7 post infection, all animals in the wild-type and reconstituted strain infected groups had perished and only *orlA* mutant infected mice survived. H&E and GMS staining revealed that the *orlA* mutant infected mice were able to partially clear the fungal infection as evidenced by contained, localized inflammatory lesions with minimal fungal growth (data not shown). The localized lesions surrounding the airways observed in *orlA* mutant infected mice were reminiscent of histopathology observed with mice infected with the *A. fumigatus* SREBP mutant, which cannot grow in low oxygen environments [53]. However, hypoxic growth of the *orlA* mutant was unaffected, and thus the mechanism behind the inability of the *orlA* mutant to proliferate throughout the host tissue and cause mortality is currently unknown.

Discussion

Continued advances in medical technologies that impair the host immune system and increased incidences of immunosuppressive diseases has resulted in substantial increases in invasive fungal infections over the last three decades [65,66]. Due to the

genetic similarity between humans and fungi, the antifungal drug arsenal available to treat fungal infections is relatively limited when compared to other infectious diseases. Moreover, as the use of available antifungal drugs has increased, resistant strains have and will continue to emerge [67,68,69,70]. Thus, in order to maintain our ability to thwart these often lethal infections, new antifungal agents are urgently needed. Biochemical pathways that are unique to fungi and absent in humans present ideal targets for antifungal drug development. The trehalose biosynthesis pathway in fungi is such a target.

Previous studies on the trehalose biosynthesis pathway in the human pathogenic fungi *C. neoformans*, *C. gattii*, and *C. albicans* have revealed the importance of this pathway in human fungal pathogenesis [7,8,9,10,33]. Broad spectrum antifungal agents that are effective against the majority of human pathogenic fungi are clearly desirable, and thus in this study we have started an examination of the trehalose biosynthesis pathway in the most common cause of invasive mold infections in humans, *A. fumigatus*.

Surprisingly, our bioinformatic analyses of genes encoding proteins predicted to be involved in trehalose biosynthesis in *A. fumigatus* revealed the presence of multiple functional copies of the trehalose-6-phosphate synthase (TPS1), which is different from findings in *A. nidulans*, *C. neoformans*, *C. albicans*, and the plant pathogenic fungus *Magnaporthe grisea* (Puttikamonkul *et al*. unpublished data). However, our analyses of the *A. fumigatus* genome revealed the presence of one putative trehalose-6-phosphate phophatase (T6PP) (TPS2 ortholog). Consequently, we began our examination of the *A. fumigatus* trehalose pathway by generation of a tps2 null mutant. Previously, a TPS2

ortholog was characterized in *A. nidulans* and named *orlA* [52]. Though the phenotype of our *A. fumigatus* T6PP mutant has different phenotypes than the *A. nidulans* mutant, most notably a continued ability to grow under high temperature without cell lysis, we elected to maintain the historical name of this gene and protein as *orlA*.

The first clear phenotype exhibited by the *Af orlA* mutant was a severe loss of conidiation on glucose minimal media (1% glucose). As observed in Fig. 2.2A, the mutant colony appears white in contrast to the blue-green pigmentation normally observed for *A. fumigatus* colonies. Microscopic examination of the mutant strain revealed that this lack of pigmentation was not due to loss of pigment production, but rather the inability to produce functional asexual reproductive structures. A similar, but less apparent, defect in conidiation was also reported for the *A. nidulans orlA* mutant [52].

Importantly, several environmental conditions could partially rescue the conidiation defect of the *Af orlA* mutant. First, we observed that conidiation could partially be restored during growth at temperatures at or below 30°C. Thus, while the *Af orlA* mutant does not display a lethal growth phenotype on glucose containing media at 37°C such as *C. neoformans*, *C. gattii*, and *S. cerevisiae* mutants, it does display a temperature sensitive phenotype. Second, we observed that conidiation could be almost fully restored on media that contained an osmotic stabilizer (either sorbitol or glycerol). Both of these phenotypes are consistent with previously reported phenotypes of the *An orlA* mutant [52]. In addition, the temperature sensitive phenotypes of the *C. neoformans* and *C. gattii* mutants could also be rescued with sorbitol. Third, addition of high levels of

glucose (>4%) could restore conidiation and morphological defects in a dose dependent manner. Taken together these results are consistent with the presence of a defect at the level of the cell wall in the *Af orlA* mutant, and also possibly suggest a defect in glycolysis at the point of glucose entry.

Further evidence for a major cell wall defect in the *orlA* mutant was observed upon microscopic examination of the *orlA* mutant hyphae, which displayed severe morphological defects when grown on GMM that could partially be rescued by growth on osmotic stabilizing media. When we examined the sensitivity of the mutant to agents known to target the fungal cell wall, we found that the mutant did not display an increased sensitivity to the β-1,3-glucan synthesis inhibitor caspofungin. However, exposure of the mutant to cell wall perturbing agents that either target chitin biosynthesis or the linkage of chitin polymers to β-1,3-glucan and β-1,6-glucan resulted in significant increases in susceptibility. Together, these results suggest that loss of OrlA results in a significant alteration in either chitin biosynthesis itself or the ability to properly assemble the cell wall matrix. This conclusion is also supported by decreased chitin levels found in the *An orlA* mutant when exposed to high temperature stress [52]. Interestingly, *C. albicans tps2* mutants also display a significant defect in cell integrity, which has been attributed to a defect in cell wall biosynthesis [7]. The *C. neoformans tps2* mutant displays a severe temperature sensitive growth phenotype (TS) in glucose media at 37°C that can be rescued with addition of sorbitol also implying that a defect in cell wall biosynthesis is responsible for the TS phenotype of this mutant [10].

A potential hypothesis to explain the *orlA* mutant phenotypes is that the predicted loss of trehalose biosynthesis due to blockage of T6PP results in the observed phenotypes as trehalose is a membrane and cell wall stabilizing agent. Yet several *tps2* mutants in fungi, including the *An* and *Af orlA* mutants, surprisingly still produce substantial amount of trehalose. Thus, it seems unlikely that defects in the production of trehalose itself are responsible for the observed phenotypes in the *Af orlA* mutant. It has been hypothesized that residual, non-specific phosphatase activity in the cell can dephosphorylate T6P into trehalose [9]. Given that *C. albicans tps2* mutants produce lower levels of trehalose than wild-type cells, this hypothesis seems plausible in this organism. However, in the *Af orlA* mutant we observed an increase in trehalose levels in response to heat shock in comparison with the wild-type strain.

Bioinformatic analyses of the *A. fumigatus* genome revealed that the number of genes involved in trehalose biosynthesis is expanded compared to *S. cerevisiae* and the pathogenic yeast studied to date (Puttikamonkul *et al.* unpublished data). Of great interest is the presence of at least two putative trehalose phosphorylase encoding genes in the *A. fumigatus* genome. Trehalose phosphorylase has been found to produce trehalose from glucose or α or β-glucose-1-phosphate in algae, bacteria, some yeasts, and basidiomycete mushrooms [18,19,58,59,60,71]. Interestingly, trehalose phosphorylase from the mushroom *Pleurotus sajor-caju* could complement the glucose growth and trehalose biosynthesis defect of a *S. cerevisiae tps1/tps2* double mutant [57]. In our study, we observed an increase in the mRNA abundance of both trehalose phosphorylase genes in the absence of *orlA* possibly suggesting that persistent TP activity explains the ability of

the *orlA* mutant to make wild-type levels of trehalose. It is also known that TP activity is inhibited by free inorganic phosphate. In theory, the accumulation of T6P in the absence of OrlA should lead to a significant decrease in free Pi levels in the cell. This could have two affects. First, it could lead to activation of the TP enzymes, and thus explain the persistence of trehalose in the *orlA* mutant. Second, Pi is a critical component of the lower portion of glycolysis, and thus the decreased PDC activity observed in the *olrA* mutant could also be explained by the decrease in available Pi. These alternatives, which may not be mutually exclusive, are being tested in our laboratory by generation of TP null mutants in the wild-type and *orlA* mutant backgrounds.

The relationship between TP encoding genes and genes of the better studied trehalose biosynthesis pathway (TPS1-TPS2-TPS3) remains to be determined. To date, a TP encoding gene has been partially characterized in *N. crassa* (CCG-9) where it was observed to be critical for clock control of fungal development [62]. However, the ability of the *ccg-9* null mutant (with an apparently intact Tps1p ortholog) to make trehalose was not examined and the role of TP enzymes in filamentous fungal biology remains to be explored. In Tps1 double mutants of *A. fumigatus* (*tpsA/tpsB*), trehalose production is completely absent (Puttikamonkul *et al.* unpublished data). However, in this *tps1* null mutant T6P levels are also removed and thus high free Pi levels, which would inhibit TP activity, are present. These results illustrate the complexity, differences, and importance of trehalose biosynthesis mechanisms among the fungi.

Since production of trehalose itself is not significantly affected in the *orlA* mutant, an alternative hypothesis to explain the *orlA* mutant phenotypes is that T6P inhibits/alters

cell wall biosynthesis. In *S. cerevisiae,* accumulation of T6P in the *tps2* mutant resulted in a temperature sensitive phenotype and inability of the mutant to grow on glucose. This led to the hypothesis that accumulation of T6P is toxic to yeast cells [72,73]. This toxicity is hypothesized to manifest itself through inhibition of hexokinase activity and subsequent mis-regulation of glycolysis or by sequestration of intracellular phosphate and subsequent intracellular acidification [31,32,74]. In the *An orlA* mutant, it was observed that glutamine:fructose-6-phosphate amidotransferase (GFAT) activity was reduced. GFAT is the first enzyme unique to aminosugar biosynthesis and thus N-acetylglucosamine (GlcNAc) could partially rescue some, but not all, of the mutant phenotypes [52]. Thus, it seems that T6P in *A. nidulans* may either directly or indirectly inhibit key enzymes involved in chitin biosynthesis.

A. fumigatus contains seven chitin synthase genes (*chsA – chsG)* which are split into 6 classes based on amino acid sequences [75,76]. Null mutants of *chsE and chsG* share the morphological and conidiation defect of the *Af orlA* mutant that can be rescued with an osmotic stabilizer [77,78,79]. Transcriptional profiling of cell wall biosynthesis genes in the *Af orlA* mutant background does not reveal a significant decrease in mRNA abundance in all known chitin synthases in the absence of *orlA.* Nevertheless, the chitin biosynthesis defects could occur at the post-transcriptional level and be due to the consequence of high T6P levels and/or depletion of free inorganic phosphate (Pi). Our data suggests that the accumulation of T6P in the *Af orlA* mutant may result in deregulation of glycolysis that could alter biosynthesis of GlcNAc, which is required for aminosugar biosynthesis.

Two key glycolysis intermediates are required to produce the UDP-GlcNAc required for chitin biosynthesis: glucose-6-phosphate and fructose-6-phosphate. Alteration in the levels or flux of these important carbohydrate metabolites could negatively impact the ability of the cell to produce appropriate levels of cell wall material. It has been shown that T6P can inhibit hexokinase activity *in vitro* in many fungal species [4,32,80]. In our study, we observed significant decreases in hexokinase activity and a growth defect on fructose minimal media, which suggests a possible alteration of flux through glycolysis in the absence of OrlA. This conclusion is also supported by the finding that high levels of glucose can suppress the *orlA* mutant phenotypes. Rescue by high glucose could be due to simple osmotic stabilization by the high glucose levels or, alternatively, high levels of glucose may overcome the inhibition of hexokinase activity and/or activation of glucokinase activity resulting in glucose-6-phosphate levels that restore aminosugar biosynthesis. A simple model is thereby proposed whereby accumulation of T6P in the absence of OrlA not only depletes available Pi levels, but also inhibits hexokinase activity thereby reducing the production of glucose-6-phosphate and fructose-6-phosphate. Regulation of glucose flux into glycolysis in *A. fumigatus* appears to be a highly regulated process as evidenced by the presence of no less than 6 putative hexokinase orthologs found in this filamentous fungus [81]. Future studies are focusing on the effect of T6P on glycolysis and cell wall biosynthesis in *A. fumigatus*.

Since the cell wall is a critical pathogen associated molecular pattern (PAMP), it is not surprising that the *orlA* mutant is attenuated in virulence in two distinct murine

models of invasive pulmonary aspergillosis. Given the normal growth rate of the mutant strain under standard *in vitro* conditions, the virulence defect of the mutant was surprising. Yet, this result is consistent with the attenuation in virulence of *C. albicans*, *C. gattii*, and *C. neoformans tps2* mutants [7,9,10,33]. In particular, *C. neoformans tps2* mutants have a severe TS growth phenotype due to build up of T6P and are unable to grow at 37°C, which would suggest avirulence in mammals [10]. Importantly, our results close the proverbial loop by showing that inhibition of *tps2* orthologs in the three most common human fungal pathogens results in virulence attenuation. Thus, development of a strategy to inhibit *tps2* function would likely have global applicability in treating invasive fungal infections.

Yet, questions remain with regard to the mechanism behind the virulence attenuation in the *Af orlA* mutant. Histopathological examinations of mice infected with the *orlA* mutant strain suggest that the mutant does not induce as strong an inflammatory response as the wild-type and reconstituted strains. This would be consistent with an alteration in the cell wall of the mutant strain. Moreover, while growth of the mutant strain *in vivo* was clearly observed throughout the infection, tissue proliferation seemed to be slightly decreased in comparison with the wild-type strain. This could be due to a simple inability of the mutant to grow *in vivo* in microenvironments with multiple stresses (possibly the result of glycolysis deregulation). Alternatively, the apparent alteration in cell wall composition of the mutant strain may influence how the host immune system is responding to (or “seeing”) the mutant. It is important to note that the virulence attenuation was also observed in mice deficient in the ability to generate an

ROS burst (X-CGD) but otherwise “normal” immunologically. In the X-CGD mice, the mutant was eventually able to cause mortality pointing to a delayed growth defect in the mutant either due to inhibition of fungal growth as a consequence of OrlA loss, or due to an alteration in the host response to the mutant strain. Studies are ongoing in our laboratory to assess the mechanism behind the virulence attenuation of the *orlA* mutant strain.

In conclusion, our results confirm previous suggestions that trehalose-6-phosphate phosphatase is a promising target for antifungal drug development. Given that *tps2* orthologs are now known to be required for fungal virulence in the three most frequently encountered causal agents of human mycoses, it seems logical to pursue research to better understand how this pathway affects fungal virulence. Since inhibition of *orlA* in *A. fumigatus* is not fungicidal per say, it may be that inhibition of this pathway in *A. fumigatus* would best be utilized in some form of combination therapy, as also previously suggested for *C. albicans* [9]. Yet, the association between the trehalose pathway and cell wall biosynthesis is intriguing given the clinical importance of the fungal cell wall both as a virulence factor and as a target of current antifungal drugs. Thus, it is likely that further in-depth analysis of the trehalose pathway in *A. fumigatus* and other pathogenic fungi will yield new insights into fungal biology and virulence that may prove fruitful for designing new therapeutic strategies to treat human mycoses.

Note

During the revision of this manuscript, a study was published by Nadia Al-Bader and colleagues comfirming that a tpsA/tpsB mutant is unable to produce trehalose during development and heat shock [82].

Acknowledgements

This work was supported by funding from the National Institutes of Health-NCRR COBRE grants 1P20RR020185 and 2P20RR020185 and the Montana State University Agricultural Experiment Station. Srisombat Puttikamonkul is funded through a Ph.D. fellowship from the Royal Thai Government. Dr. John Perfect is supported by Public Health Service Grant AI 73897. The authors would like to thank Dr. Kelly Craven, The Samuel Roberts Noble Foundation, Kevin Fuller and Dr. Judith Rhodes, University of Cincinnati, and members of the Cramer Laboratory for insightful discussions. Thanks to Dr. Allen Harmsen and laboratory members and Dr. Mark Quinn for technical advice and use of equipment at Montana State University, and the staff at the Animal Resources Center at Montana State University for their assistance and care of the animals used in this study.

Table 2.1. Quantitative Real-Time PCR analysis of cell wall biosynthesis genes in the *orlA* mutant and wild-type. mRNA abundance for each gene was normalized to β-tubulin in each strain and normalized mRNA abundance levels are from the *orlA* mutant relative to the wild-type strain at the respective time points (6.5 hours and 24 hours growth in glucose minimal media at 37°C). Data represents the average value of two biological replicates, each repeated in duplicate, and standard deviation.

			Fold Change	**Fold Change**
Gene	***Predicted Function***	***Location***	***6.5 hours***	***24 hours***
agsA	α-1,3-glucan synthase	Afu3g00910	0.25 (±1.9)	4.75 (±1.6)
agsB	α-1,3-glucan synthase	Afu2g11270	2.65 (±0.2)	1.45 (±0.1)
agsC	α-1,3-glucan synthase	Afu1g15440	3.95 (±0.2)	16.35 (±7.6)
chsA	chitin synthase A	Afu2g01870	-0.10 (±2.0)	3.35 (±0.2)
chsB	chitin synthase B	Afu4g04180	-0.20 (±1.8)	2.20 (±0.1)
chsC	chitin synthase C	Afu5g00760	0.05 (±1.8)	1.65 (±0.4)
chsD	chitin synthase D	Afu1g12600	-0.15 (±2.5)	1.30 (±0)
chsE	chitin synthase E	Afu2g13440	0.25 (±1.9)	2.85 (±1.5)
chsF	chitin synthase F	Afu8g05630	-1.95 (±5.3)	1.45 (±0.6)
chsG	chitin synthase G	Afu3g14420	-1.80 (±0.7)	1.70 (±0.8)
fksA	β-1,3-glucan synthase catalytic subunit	Afu6g12400	2.70 (±2.3)	1.65 (±0.8)
gelA	1,3-β-glucanosyltransferase	Afu2g01170	1.35 (±0.2)	8.10 (±3.4)
gelB	1,3-β-glucanosyltransferase	Afu6g11390	8.20 (±10.0)	9.45 (±11.1)
gelC	1,3-β-glucanosyltransferase	Afu2g12850	1.30 (±5.1)	5.65 (±6.6)

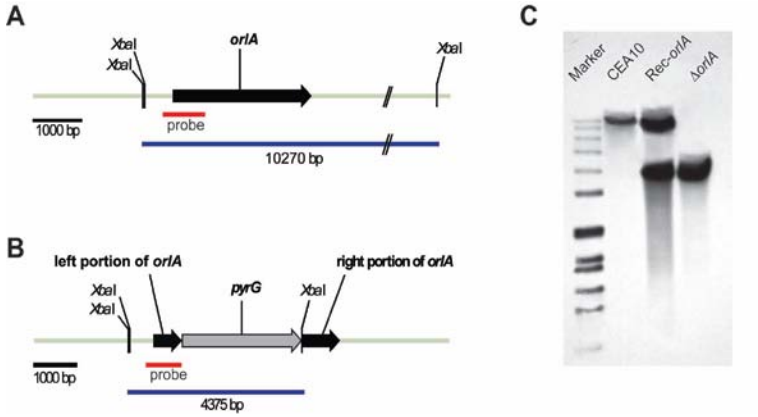

Figure 2.1. Generation of strains used in this study. (A) Locus of *orlA* gene in wild-type strain (CEA10) and (B) locus of *orlA* after successful introduction of gene replacement construct (C) Southern blot analysis of wild-type, reconstituted strain (Rec-*orlA*) and Δ*orlA* strains. The XbaI digested genomic DNA of all strains were separated on a 1% agarose gel, blotted, and hybridized with a 900 bp genomic DNA probe from the *orlA* upstream sequence. The expected fragment sizes of the *orlA* locus in the wild-type and *orlA* mutant were observed and are 10,270 bp and 4,375 bp respectively. The reconstituted strain (Rec-*orlA*) contains the expected hybridization signals for a single ectopic insertion of the wild-type allele of *orlA* (top) and maintenance of the disrupted *orlA* locus (bottom).

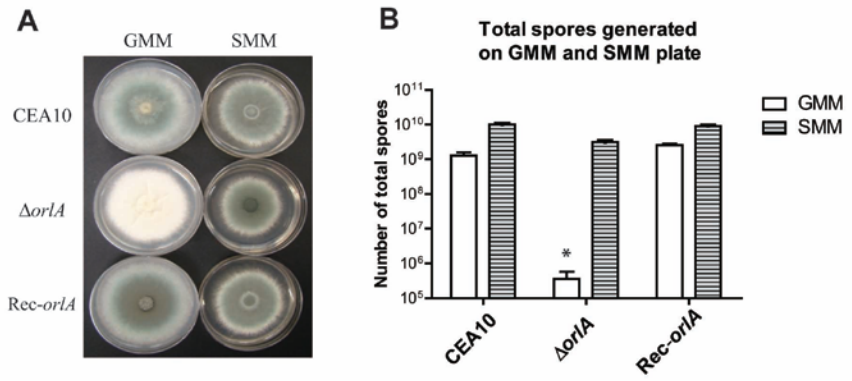

Figure 2.2. Colony morphology and conidia production in the absence of OrlA. (A) Normal growth rate but abolished asexual conidiation of the *orlA* mutant is observed on glucose minimal media (GMM) at 37°C. This defect could be recovered on 1.2M sorbitol minimal media (SMM) at 37°C. (B) Conidia production of wild-type, *orlA* mutant and *orlA* reconstituted strain on two different media GMM and SMM incubated at 37°C for 4 days prior to harvesting and counting. Data is the mean and standard deviation of three biological replicates. *Total conidia production of the mutant cultured on GMM is significantly less than the wild-type and reconstituted strains (P = 0.020 and 0.003 respectively).

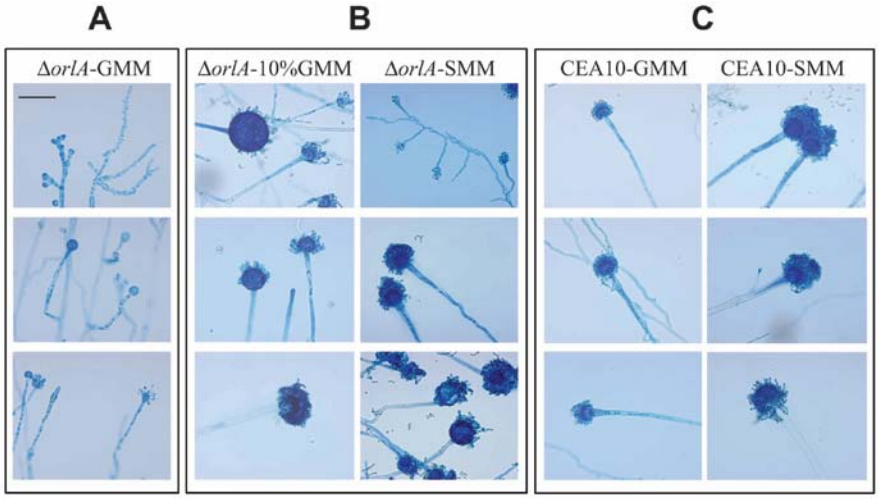

Figure 2.3. Hyphal morphology of the *orlA* mutant is altered. (A) Slide cultures and lactophenol cotton blue staining reveal dysmorphic hyphae and malformed asexual reproductive structures which formed vesicles lacking phialides in the *orlA* mutant grown on GMM at 37°C. (B) The ability to form normal hyphae, asexual reproductive structures, and conidia is restored in the *orlA* mutant grown on GMM containing 10% glucose or minimal media containing 1.2 M sorbitol (SMM) at 37°C. (C) Wild-type CEA10 generates normal hyphae and asexual reproductive structures when grown on GMM and SMM at 37°C. All representative pictures were captured under light microscopy at 400x magnification (reference bar = 50 µm).

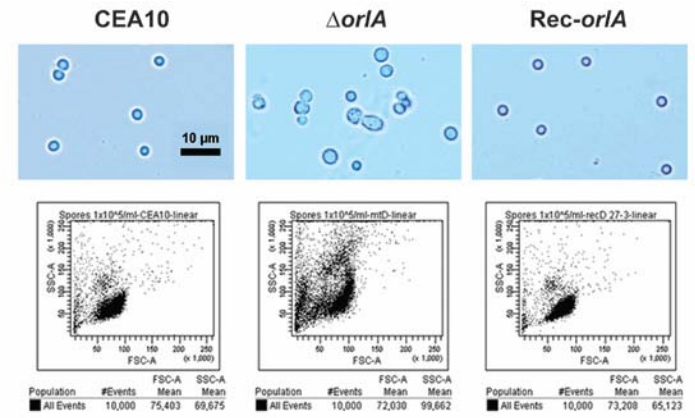

Figure 2.4. Flow cytometry analysis reveals a heterogeneous population of *orlA* mutant conidia from SMM when cultured at 37°C while wild-type (CEA10) and reconstituted strains (Rec-*orlA*) display a homogenous population of conidia. FACS analysis via forward and side scatter parameters of equal amounts (10,000 events) of conidia. Differences in conidia size and shape can be observed via light microscopic observation at 400x magnification. A reference bar is 10 µm length.

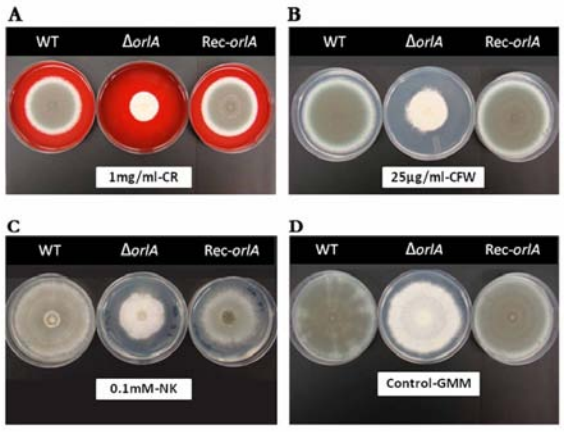

Figure 2.5. The *orlA* mutant is sensitive to cell wall perturbing agents. Cell wall defects were observed in the *orlA* null mutant cultured on GMM at 37°C containing various cell wall inhibitors. (A) Congo Red (CR) 1 mg/ml. (B) Calcofluor White (CFW) 25 µg/ml. (C) Nikkomycin Z (NK) 0.1mM. (D) GMM media without inhibitors was used as a control that represents the normal growth of all strains incubated at 37°C for 3 days. Concentrations presented are the optimum concentrations used to determine the growth defect of the *orlA* mutant (Δ*orlA*) compared to the wild-type (CEA10) and reconstituted strains (Rec-*orlA*). The experiment was repeated in biological triplicates with identical results.

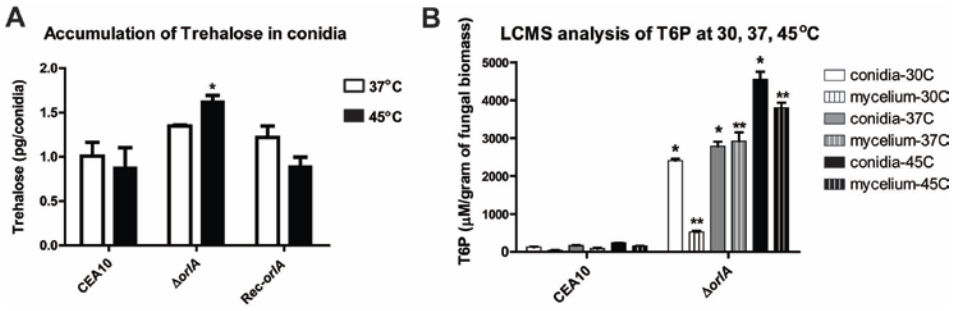

Figure 2.6. Production of trehalose and trehalose-6-phosphate (T6P). (A) Conidia for trehalose accumulation measurements were cultured at 37°C and 45°C. At 37°C, trehalose amounts found in the mutant were not significantly different from the wild-type and reconstituted strains; however at 45°C the mutant accumulated greater amounts of trehalose compared to the wild-type and reconstituted strains (*P =0.04 and 0.02 respectively. (B) T6P accumulation in conidia and mycelia were measured with LCMS from cell free culture extracts grown at 30°C, 37°C and 45°C. T6P concentration was back calculated from a T6P standard curve and normalized to the input weight of fungal biomass. In all conditions, T6P accumulated in conidia and mycelium of the *orlA* mutant and was significantly higher than the wild-type (CEA10) (*P<0.05 in conidia, **P<0.05 in mycelia).

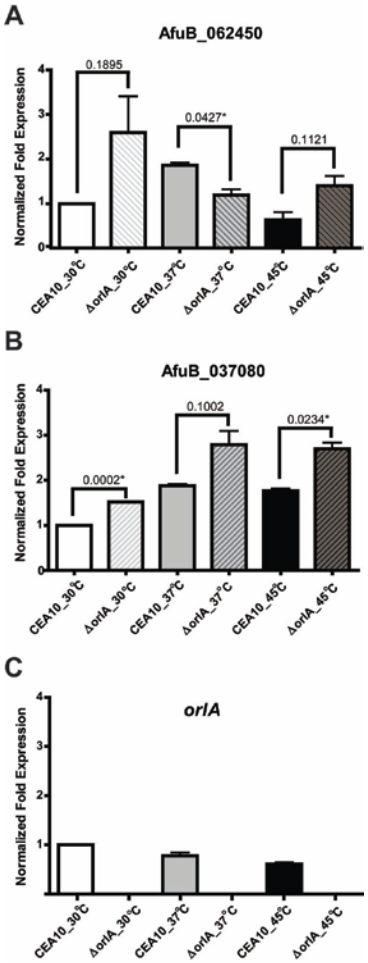

Figure 2.7. mRNA abundance of trehalose phosphorylase genes (A) AFUB_062450 (B) AFUB_037080 and (C) *orlA* was measured in conidia from the wild-type (CEA10) and *orlA* mutant. RNA samples were extracted from conidia cultured at 30^{o}C, 37^{o}C and 45^{o}C. mRNA abundance was normalized to actin and expression values are relative to the CEA10 sample at low temperature (30^{o}C). Results are the mean and standard deviation of two biological replicates and were calculated using the $2^{-\Delta\Delta Ct}$ method [47].

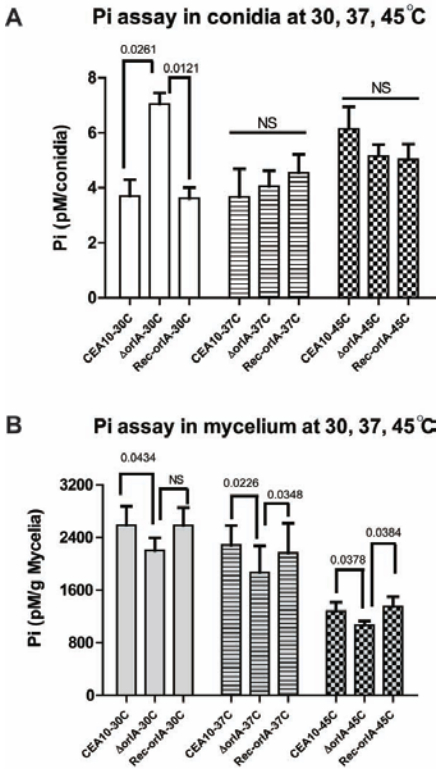

Figure 2.8. Free inorganic phosphate (Pi) is sequestrated by T6P in the absence of OrlA. Conidia (A) and mycelia (B) biomass for Pi assays were cultured at 30°C, 37°C and 45°C. At all conditions, Pi levels found in mycelia of the *orlA* mutant were significantly decreased from the wild-type and reconstituted strains (P value < 0.05 as indicated) where as an insignificant difference (NS; P value >0.05) was found in conidia cultured at 37°C and 45°C. However, at 30°C, a significant increase in Pi levels was found in the *orlA* mutant relative to wild type and reconstituted strains.

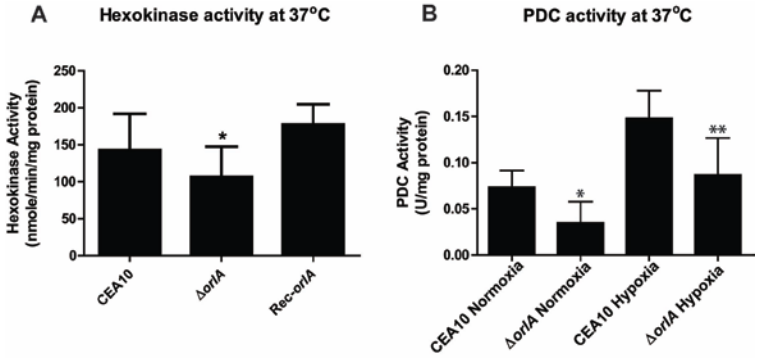

Figure 2.9. Key steps in glycolysis are altered in the absence of OrlA. (A) Hexokinase activity of the wild-type, the *orlA* mutant and the reconstituted strain indicates a decrease in hexokinase activity in the absence of *orlA* (P value = 0.04) relative to wild- type. Results presented are the mean and standard deviations from three independent experiments. (B) Pyruvate decarboxylase activity is decreased in the absence of OrlA also suggesting a potential decrease in glycolytic flux. Respective strains were grown in GMM at 37°C in normoxic (20% O_2) or hypoxic (1% O_2) conditions. Results presented are the mean and standard deviations from two independent experiments. *P = 0.03 **P = 0.05 (wild-type vs. mutant respectively for normoxia and hypoxia).

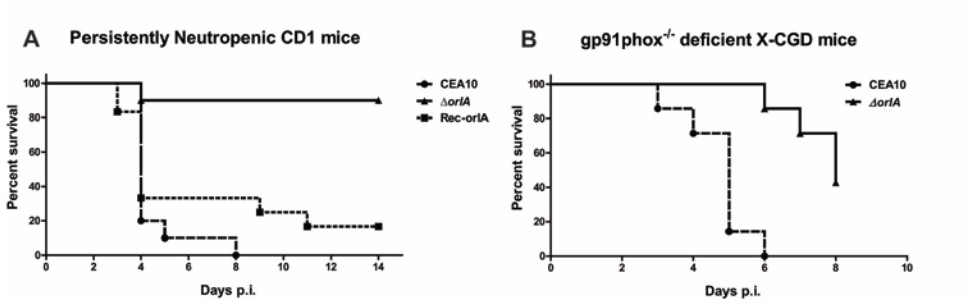

Figure 2.10. OrlA is a critical component of the *Aspergillus fumigatus* virulence arsenal. (A) Outbred CD-1 male mice (n = 10 each fungal strain or mock control) were immunosuppressed as described in the experimental procedures to generate persistently neutropenic mice. Mice were inoculated intranasally with 10^6 conidia/25 µl of wild-type CEA10, Δ*orlA*, or the *orlA* reconstituted strain Rec-*orlA*. A cohort of 10 mice was also mock infected with 0.01% Tween80 in sterile phosphate buffered saline. No mock infected animals perished in either experiment. Infection experiments were repeated two times with similar results. Log-Rank tests revealed that the survival curves between the mutant and wild-type CEA10 and mutant and reconstituted strain were statistically significant (P < 0.0001 and P = 0.0007, respectively). No significant difference was observed between the wild-type and reconstituted strains (P = 0.2659). (B) X-CGD murine model of IPA, mice were inoculated intranasally with 10^5 conidia/25 µl of wild type and *orlA* mutant. The delay in death of mice infected with the *orlA* mutant is statistically significant (P value = 0.0005).

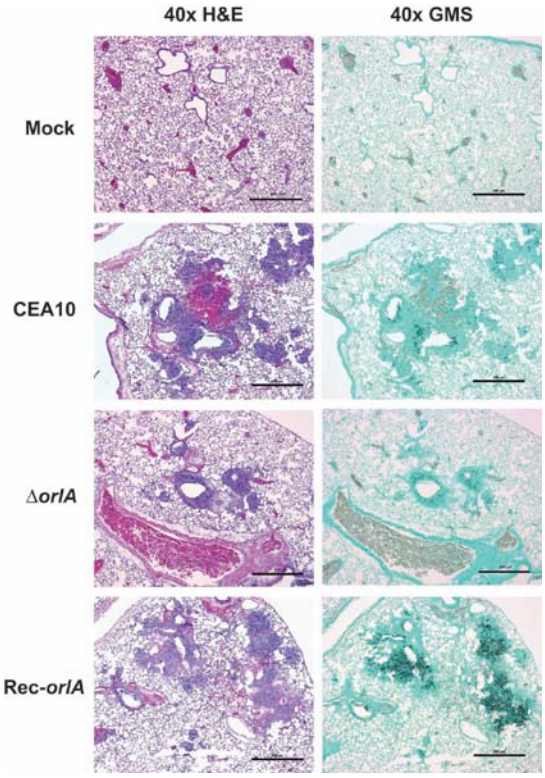

Figure 2.11. Histopathology from immunosuppressed CD1 mouse model observed on day 3 after infection. Mice were intranasally inoculated with 10^6 conidia and euthanized on day 3 post infection. Lung sections of representative infections stained with hematoxylin and eosin (H&E) or Gomori methenamine silver stain (GMS) are presented. Mock infected animals display normal healthy lung architecture with lack of necrosis, inflammation, and fungal elements. Wild-type (CEA10) and reconstituted strain infected lungs displayed significant numbers of inflammatory and necrotic lesions (H&E stains) surrounding sites infiltrated by fungal growth (black stained fungal hyphae as observed via GMS staining). Interestingly, the *orlA* mutant infected mice consistently contained less necrosis, inflammation, and fungal growth. Bar = 500 μm for 40x magnification.

Literature Cited

1. Crowe JH, Hoekstra FA, Crowe LM (1992) Anhydrobiosis. Annu Rev Physiol 54: 579-599.

2. Thevelein JM (1984) Regulation of trehalose mobilization in fungi. Microbiol Rev 48: 42-59.

3. Singer MA, Lindquist S (1998) Thermotolerance in *Saccharomyces cerevisiae*: the Yin and Yang of trehalose. Trends Biotechnol 16: 460-468.

4. Gancedo C, Flores CL (2004) The importance of a functional trehalose biosynthetic pathway for the life of yeasts and fungi. FEMS Yeast Res 4: 351-359.

5. Ishihara R, Taketani S, Sasai-Takedatsu M, Adachi Y, Kino M, et al. (2000) ELISA for urinary trehalase with monoclonal antibodies: a technique for assessment of renal tubular damage. Clin Chem 46: 636-643.

6. Murray IA, Coupland K, Smith JA, Ansell ID, Long RG (2000) Intestinal trehalase activity in a UK population: establishing a normal range and the effect of disease. Br J Nutr 83: 241-245.

7. Zaragoza O, de Virgilio C, Ponton J, Gancedo C (2002) Disruption in *Candida albicans* of the *TPS2* gene encoding trehalose-6-phosphate phosphatase affects cell integrity and decreases infectivity. Microbiology 148: 1281-1290.

8. Zaragoza O, Blazquez MA, Gancedo C (1998) Disruption of the *Candida albicans TPS1* gene encoding trehalose-6-phosphate synthase impairs formation of hyphae and decreases infectivity. J Bacteriol 180: 3809-3815.

9. Van Dijck P, De Rop L, Szlufcik K, Van Ael E, Thevelein JM (2002) Disruption of the *Candida albicans TPS2* gene encoding trehalose-6-phosphate phosphatase decreases infectivity without affecting hypha formation. Infect Immun 70: 1772-1782.

10. Petzold EW, Himmelreich U, Mylonakis E, Rude T, Toffaletti D, et al. (2006) Characterization and regulation of the trehalose synthesis pathway and its importance in the pathogenicity of *Cryptococcus neoformans*. Infect Immun 74: 5877-5887.

11. Foster AJ, Jenkinson JM, Talbot NJ (2003) Trehalose synthesis and metabolism are required at different stages of plant infection by *Magnaporthe grisea*. EMBO J 22: 225-235.

12. Elliott B, Haltiwanger RS, Futcher B (1996) Synergy between trehalose and Hsp104 for thermotolerance in *Saccharomyces cerevisiae*. Genetics 144: 923-933.

13. Vuorio OE, Kalkkinen N, Londesborough J (1993) Cloning of two related genes encoding the 56-kDa and 123-kDa subunits of trehalose synthase from the yeast *Saccharomyces cerevisiae*. Eur J Biochem 216: 849-861.

14. Cabib E, Leloir LF (1958) The biosynthesis of trehalose phosphate. J Biol Chem 231: 259-275.

15. Bell W, Sun W, Hohmann S, Wera S, Reinders A, et al. (1998) Composition and functional analysis of the *Saccharomyces cerevisiae* trehalose synthase complex. J Biol Chem 273: 33311-33319.

16. Reinders A, Burckert N, Hohmann S, Thevelein JM, Boller T, et al. (1997) Structural analysis of the subunits of the trehalose-6-phosphate synthase/phosphatase complex in *Saccharomyces cerevisiae* and their function during heat shock. Mol Microbiol 24: 687-695.

17. Avonce N, Mendoza-Vargas A, Morett E, Iturriaga G (2006) Insights on the evolution of trehalose biosynthesis. BMC Evol Biol 6: 109.

18. Saito K, Kase T, Takahashi E, Horinouchi S (1998) Purification and characterization of a trehalose synthase from the basidiomycete *grifola frondosa*. Appl Environ Microbiol 64: 4340-4345.

19. Kitamoto Y, Osaki, N., Tanaka, H., Sasaki, H., Mori, N. (2000) Purification and properties of a-glucose 1-phosphate-forming trehalose phosphorylase from basidiomycete, *Pleurotus ostreatus*. Mycoscience 41: 607-613.

20. Wannet WJ, Op den Camp HJ, Wisselink HW, van der Drift C, Van Griensven LJ, et al. (1998) Purification and characterization of trehalose phosphorylase from the commercial mushroom *Agaricus bisporus*. Biochim Biophys Acta 1425: 177-188.

21. Nwaka S, Mechler B, Destruelle M, Holzer H (1995) Phenotypic features of trehalase mutants in *Saccharomyces cerevisiae*. FEBS Lett 360: 286-290.

22. Elbein AD, Pan YT, Pastuszak I, Carroll D (2003) New insights on trehalose: a multifunctional molecule. Glycobiology 13: 17R-27R.

23. Sano F, Asakawa N, Inoue Y, Sakurai M (1999) A dual role for intracellular trehalose in the resistance of yeast cells to water stress. Cryobiology 39: 80-87.

24. Hottiger T, De Virgilio C, Hall MN, Boller T, Wiemken A (1994) The role of trehalose synthesis for the acquisition of thermotolerance in yeast. II. Physiological concentrations of trehalose increase the thermal stability of proteins *in vitro*. Eur J Biochem 219: 187-193.

25. Kandror O, DeLeon A, Goldberg AL (2002) Trehalose synthesis is induced upon exposure of *Escherichia coli* to cold and is essential for viability at low temperatures. Proc Natl Acad Sci U S A 99: 9727-9732.

26. Cao Y, Wang Y, Dai B, Wang B, Zhang H, et al. (2008) Trehalose is an important mediator of Cap1p oxidative stress response in *Candida albicans*. Biol Pharm Bull 31: 421-425.

27. Kane SM, Roth R (1974) Carbohydrate metabolism during ascospore development in yeast. J Bacteriol 118: 8-14.

28. Fillinger S, Chaveroche MK, van Dijck P, de Vries R, Ruijter G, et al. (2001) Trehalose is required for the acquisition of tolerance to a variety of stresses in the filamentous fungus *Aspergillus nidulans*. Microbiology 147: 1851-1862.

29. Ni M, Yu JH (2007) A novel regulator couples sporogenesis and trehalose biogenesis in *Aspergillus nidulans*. PLoS One 2: e970.

30. Wilson RA, Jenkinson JM, Gibson RP, Littlechild JA, Wang ZY, et al. (2007) Tps1 regulates the pentose phosphate pathway, nitrogen metabolism and fungal virulence. EMBO J 26: 3673-3685.

31. Thevelein JM, Hohmann S (1995) Trehalose synthase: guard to the gate of glycolysis in yeast? Trends Biochem Sci 20: 3-10.

32. Blazquez MA, Lagunas R, Gancedo C, Gancedo JM (1993) Trehalose-6-phosphate, a new regulator of yeast glycolysis that inhibits hexokinases. FEBS Lett 329: 51-54.

33. Ngamskulrungroj P, Himmelreich U, Breger JA, Wilson C, Chayakulkeeree M, et al. (2009) The trehalose synthesis pathway is an integral part of the virulence composite for *Cryptococcus gattii*. Infect Immun 77: 4584-4596.

34. d'Enfert C (1996) Selection of multiple disruption events in *Aspergillus fumigatus* using the orotidine-5'-decarboxylase gene, *pyrG*, as a unique transformation marker. Curr Genet 30: 76-82.

35. Shimizu K, Keller NP (2001) Genetic involvement of a cAMP-dependent protein kinase in a G protein signaling pathway regulating morphological and chemical transitions in *Aspergillus nidulans*. Genetics 157: 591-600.

36. Mabey JE, Anderson MJ, Giles PF, Miller CJ, Attwood TK, et al. (2004) CADRE: the Central Aspergillus Data REpository. Nucleic Acids Res 32: D401-405.

37. Yelton MM, Hamer JE, Timberlake WE (1984) Transformation of *Aspergillus nidulans* by using a trpC plasmid. Proc Natl Acad Sci U S A 81: 1470-1474.

38. Cramer RA, Jr., Gamcsik MP, Brooking RM, Najvar LK, Kirkpatrick WR, et al. (2006) Disruption of a nonribosomal peptide synthetase in *Aspergillus fumigatus* eliminates gliotoxin production. Eukaryot Cell 5: 972-980.

39. Ejzykowicz DE, Cunha MM, Rozental S, Solis NV, Gravelat FN, et al. (2009) The *Aspergillus fumigatus* transcription factor Ace2 governs pigment production, conidiation and virulence. Mol Microbiol 72: 155-169.

40. d'Enfert C, Fontaine T (1997) Molecular characterization of the *Aspergillus nidulans treA* gene encoding an acid trehalase required for growth on trehalose. Mol Microbiol 24: 203-216.

41. Johnson EA (1946) An Improved Slide Culture Technique for the Study and Identification of Pathogenic Fungi. J Bacteriol 51: 689-694.

42. Harris JL (1986) Modified method for fungal slide culture. J Clin Microbiol 24: 460-461.

43. Brun YF, Dennis CG, Greco WR, Bernacki RJ, Pera PJ, et al. (2007) Modeling the combination of amphotericin B, micafungin, and nikkomycin Z against *Aspergillus fumigatus in vitro* using a novel response surface paradigm. Antimicrob Agents Chemother 51: 1804-1812.

44. Kaur R, Ma B, Cormack BP (2007) A family of glycosylphosphatidylinositol-linked aspartyl proteases is required for virulence of *Candida glabrata*. Proc Natl Acad Sci U S A 104: 7628-7633.

45. Ram AF, Klis FM (2006) Identification of fungal cell wall mutants using susceptibility assays based on Calcofluor white and Congo red. Nat Protoc 1: 2253-2256.

46. Cramer RA, Jr., Perfect BZ, Pinchai N, Park S, Perlin DS, et al. (2008) Calcineurin target CrzA regulates conidial germination, hyphal growth, and pathogenesis of *Aspergillus fumigatus*. Eukaryot Cell 7: 1085-1097.

47. Livak KJ, Schmittgen TD (2001) Analysis of relative gene expression data using real-time quantitative PCR and the 2(-Delta Delta C(T)) Method. Methods 25: 402-408.

48. Anderson PJ, Karageuzian LN, Cheng HM, Epstein DL (1984) Hexokinase of calf trabecular meshwork. Invest Ophthalmol Vis Sci 25: 1258-1261.

49. Bergmeyer HU, Grassl M, Walter HE (1983). Methods of Enzymatic Analysis (Bergmeyer, HUed) 3rd ed. Deerfield Beach, FL: Verlag Chemie. pp. Volume II, 222-223.

50. Lockington RA, Borlace GN, Kelly JM (1997) Pyruvate decarboxylase and anaerobic survival in *Aspergillus nidulans*. Gene 191: 61-67.

51. Huppert M, Oliver DJ, Sun SH (1978) Combined methenamine-silver nitrate and hematoxylin & eosin stain for fungi in tissues. J Clin Microbiol 8: 598-603.

52. Borgia PT, Miao Y, Dodge CL (1996) The *orlA* gene from *Aspergillus nidulans* encodes a trehalose-6-phosphate phosphatase necessary for normal growth and chitin synthesis at elevated temperatures. Mol Microbiol 20: 1287-1296.

53. Willger SD, Puttikamonkul S, Kim KH, Burritt JB, Grahl N, et al. (2008) A sterol-regulatory element binding protein is required for cell polarity, hypoxia adaptation, azole drug resistance, and virulence in *Aspergillus fumigatus*. PLoS Pathog 4: e1000200.

54. Borgia PT, Dodge CL (1992) Characterization of *Aspergillus nidulans* mutants deficient in cell wall chitin or glucan. J Bacteriol 174: 377-383.

55. Lunn JE, Feil R, Hendriks JH, Gibon Y, Morcuende R, et al. (2006) Sugar-induced increases in trehalose 6-phosphate are correlated with redox activation of ADPglucose pyrophosphorylase and higher rates of starch synthesis in *Arabidopsis thaliana*. Biochem J 397: 139-148.

56. Saito K, Yamazaki H, Ohnishi Y, Fujimoto S, Takahashi E, et al. (1998) Production of trehalose synthase from a basidiomycete, *Grifola frondosa*, in Escherichia coli. Appl Microbiol Biotechnol 50: 193-198.

57. Han SE, Kwon HB, Lee SB, Yi BY, Murayama I, et al. (2003) Cloning and characterization of a gene encoding trehalose phosphorylase (TP) from *Pleurotus sajor-caju*. Protein Expr Purif 30: 194-202.

58. Eis C, Nidetzky B (1999) Characterization of trehalose phosphorylase from *Schizophyllum commune*. Biochem J 341 (Pt 2): 385-393.

59. Belocopitow E, Marechal LR (1970) Trehalose phosphorylase from *Euglena gracilis*. Biochim Biophys Acta 198: 151-154.

60. Aisaka K, Masuda T (1995) Production of trehalose phosphorylase by *Catellatospora ferruginea*. FEMS Microbiol Lett 131: 47-51.

61. Aisaka K, Masuda T, Chikamune T, Kamitori K (1998) Purification and characterization of trehalose phosphorylase from *Catellatospora ferruginea*. Biosci Biotechnol Biochem 62: 782-787.

62. Shinohara ML, Correa A, Bell-Pedersen D, Dunlap JC, Loros JJ (2002) *Neurospora* clock-controlled gene 9 (ccg-9) encodes trehalose synthase: circadian regulation of stress responses and development. Eukaryot Cell 1: 33-43.

63. Pollock JD, Williams DA, Gifford MA, Li LL, Du X, et al. (1995) Mouse model of X-linked chronic granulomatous disease, an inherited defect in phagocyte superoxide production. Nat Genet 9: 202-209.

64. Morgenstern DE, Gifford MA, Li LL, Doerschuk CM, Dinauer MC (1997) Absence of respiratory burst in X-linked chronic granulomatous disease mice leads to abnormalities in both host defense and inflammatory response to *Aspergillus fumigatus*. J Exp Med 185: 207-218.

65. Erjavec Z, Kluin-Nelemans H, Verweij PE (2009) Trends in invasive fungal infections, with emphasis on invasive aspergillosis. Clin Microbiol Infect 15: 625-633.

66. Varkey JB, Perfect JR (2008) Rare and emerging fungal pulmonary infections. Semin Respir Crit Care Med 29: 121-131.

67. Perlin DS, Mellado E (2008) Antifungal Mechanisms of Action and Resistance. In: Latge J-P, Steinbach WJ, editors. *Aspergillus fumigatus* and Aspergillosis. Washington, DC: ASM Press. pp. 568.

68. Verweij PE, Mellado E, Melchers WJ (2007) Multiple-triazole-resistant aspergillosis. N Engl J Med 356: 1481-1483.

69. White TC, Marr KA, Bowden RA (1998) Clinical, cellular, and molecular factors that contribute to antifungal drug resistance. Clin Microbiol Rev 11: 382-402.

70. Snelders E, van der Lee HA, Kuijpers J, Rijs AJ, Varga J, et al. (2008) Emergence of azole resistance in *Aspergillus fumigatus* and spread of a single resistance mechanism. PLoS Med 5: e219.

71. Belocopitow E, Marechal LR (1974) Metabolism of trehalose in *Euglena gracilis*. Partial purification and some properties of phosphoglucomutase acting on beta-glucose 1-phosphate. Eur J Biochem 46: 631-637.

72. De Virgilio C, Burckert N, Bell W, Jeno P, Boller T, et al. (1993) Disruption of TPS2, the gene encoding the 100-kDa subunit of the trehalose-6-phosphate synthase/phosphatase complex in *Saccharomyces cerevisiae*, causes accumulation of trehalose-6-phosphate and loss of trehalose-6-phosphate phosphatase activity. Eur J Biochem 212: 315-323.

73. Sur IP, Lobo Z, Maitra PK (1994) Analysis of PFK3--a gene involved in particulate phosphofructokinase synthesis reveals additional functions of TPS2 in *Saccharomyces cerevisiae*. Yeast 10: 199-209.

74. Blazquez MA, Stucka R, Feldmann H, Gancedo C (1994) Trehalose-6-P synthase is dispensable for growth on glucose but not for spore germination in *Schizosaccharomyces pombe*. J Bacteriol 176: 3895-3902.

75. Bernard M, Latge JP (2001) *Aspergillus fumigatus* cell wall: composition and biosynthesis. Med Mycol 39 Suppl 1: 9-17.

76. Munro CA, Gow NA (2001) Chitin synthesis in human pathogenic fungi. Med Mycol 39 Suppl 1: 41-53.

77. Mellado E, Aufauvre-Brown A, Gow NA, Holden DW (1996) The *Aspergillus fumigatus* chsC and chsG genes encode class III chitin synthases with different functions. Mol Microbiol 20: 667-679.

78. Mellado E, Dubreucq G, Mol P, Sarfati J, Paris S, et al. (2003) Cell wall biogenesis in a double chitin synthase mutant (chsG-/chsE-) of *Aspergillus fumigatus*. Fungal Genet Biol 38: 98-109.

79. Aufauvre-Brown A, Mellado E, Gow NAR, Holden DW (1997) *Aspergillus fumigatus* chsE: A Gene Related to CHS3 of Saccharomyces cerevisiae and Important for Hyphal Growth and Conidiophore Development but Not Pathogenicity. Fungal Genet Biol 21: 141-152.

80. Panneman H, Ruijter GJ, van den Broeck HC, Visser J (1998) Cloning and biochemical characterisation of *Aspergillus niger* hexokinase--the enzyme is strongly inhibited by physiological concentrations of trehalose 6-phosphate. Eur J Biochem 258: 223-232.

81. Flipphi M, Sun J, Robellet X, Karaffa L, Fekete E, et al. (2009) Biodiversity and evolution of primary carbon metabolism in *Aspergillus nidulans* and other Aspergillus spp. Fungal Genet Biol 46 Suppl 1: S19-S44.

82. Al-Bader N, Vanier G, Liu H, Gravelat FN, Urb M, et al. (2010) The role of trehalose biosynthesis in *Aspergillus fumigatus* development, stress response and virulence. Infect Immun.

CHAPTER THREE

THE TREHALOSE PATHWAY INTERMEDIATE, T6P, REGULATES CELL WALL COMPOSITION AND VIRULENCE IN *ASPERGILLUS FUMIGATUS*

Contribution of Authors and Co-Authors

Manuscript in Chapter 3

Author: Srisombat Puttikamonkul

Contributions: Designed the study and conducted the experiment, analyzed data, and wrote the manuscript.

Co-authors: Sven D. Willger, Nora Grahl, and Kelly Shepardson

Contributions: Assisted with study design, experiment, and discussed the results and implications

Co-author: Jonathan Hilmer, and Brian Bothner,

Contributions: Assisted with LCMS experimental study and discussed the results and implications and commented on the manuscript.

Co-author: Vishu Kumar Amanianda, and Jean-Paul Latge

Contributions: Assisted with cell wall analysis study and discussed the results and implications and commented on the manuscript.

Co-author: John R. Perfect

Contributions: Discussed the results and implications and commented on the manuscript.

Co-author: Robert A. Cramer Jr

Contributions: Obtained funding, assisted with study design, and discussed the results and implications and commented on the manuscript and edited the manuscript at all stages.

Manuscript Information Page

Srisombat Puttikamonkul, Kelly Shepardson, Sven D. Willger, Nora Grahl, Jonathan Hilmer, Brian Bothner, Vishu Kumar Amanianda, Jean-Paul Latge, John R. Perfect, Robert A. Cramer Jr

Journal Name: Blood

Status of Manuscript:
_x_Prepared for submission to a peer-reviewed journal
___Officially submitted to a peer-reviewed journal
___Accepted by a peer-reviewed journal
___Published in a peer-reviewed journal

Abstract

While a general understanding of the role of trehalose and its biosynthetic pathway in fungal metabolism exists, the mechanism(s) behind the attenuated fungal virulence of various trehalose pathway mutants is not well understood. We showed previously that TPS2/OrlA, a key enzyme in TPS1/TPS2 trehalose biosynthesis pathway is required for cell wall integrity and fungal virulence in *A. fumigatus.* In this study, we further tested the hypothesis that a significant *in vivo* attenuated virulence and *in vitro* impaired cell wall integrity of Δ*orlA* is influenced by the accumulation of trehalose pathway intermediate Trehalose-6-Phosphate (T6P). Here, we report that the mechanisms behind the attenuated virulence of the *A. fumigatus* TPS2 null mutant, Δ*orlA,* is mediated by an increased susceptibility of Δ*orlA* to PMN killing. The depletion of PMNs by RB6 MAb treatment of xCGD mice resulted in lose of *in vivo* protection from invasive fungal infection of Δ*orlA.* In the absence of PMNs, Δ*orlA* has increased fungal burden and restored virulence similar to wild type. To define T6P's role in fungal cell wall integrity and virulence, a series of multiple mutations were generated in the Δ*orlA* background to further understand the mechanisms of its attenuated virulence. Further characterization of regulatory protein subunits required for TPS1/TPS2 function strongly suggests that high accumulation of T6P is the key factor associated with morphological defects of the fungal cell wall in Δ*orlA*. Despite normal *in vivo* growth, Δ*orlA* has altered hyphal cell wall components that likely benefits antifungal host responses as we observed decreases or increases in key polysaccharides in the cell wall of this mutant. The particular changes in cell wall likely mediate the change in recruitment of PMNs and resulted in increased

susceptibility of the mutant to phagocytic killing. Therefore, our results shed light on host immune response mediated by T6P mediated changes in the fungal cell wall of *A. fumigatus*. In addition, this further understanding of mechanisms of host-fungus interactions will contribute to the development of new therapies and help shape concepts for future treatment strategies.

Introduction

Following *A. fumigatus* spore inhalation, a series of host initiated innate responses eliminates fungal spores in immunocompetent hosts [1,2,3,4,5]. In contrast, hosts with an underlying immunocompromised condition have increased incidences of Invasive Pulmonary Aspergillosis (IPA) [6,7]. With limited antifungal drugs available, and complicated outcomes even with standard antifungal treatment, much effort has been focused on new antifungal drug targeting of the fungal cell wall [1,7,8,9,10].

Pattern recognition receptors (PRRs) play an important role in the orchestration of an immune response by recognition of pathogen-associated molecular patterns (PAMPs) [11,12,13,14]. The β-glucans are generally found in fungi, plant, and some bacteria. In fungi, β-glucans are major carbohydrate components of the cell wall, in particularly, forms of β-1,3/ β-1,4/ and β-1,6, linkage polymers. However, only β-1,3, and β-1,4 glucans are found in the *A. fumigatus* cell wall [14]. Several receptors for β-glucans have been described. The most molecular detail on regulating immune responses has been described for Dectin-1 [15]. In addition, purified chitin from *C. albican* appears to be

immunologically inert in TLRs recognition, however chitin may act as an immunosuppressive agent by blocking Dectin-1 recognition [16,17].

Dectin-1 is a type II membrane receptor, C-type lectin, and predominantly expressed by myeloid cells, including monocytes, macrophages (AMs), neutrophils (PMNs), dendritic cells (DC), and a subset of T cells [13,15,18]. Following Dectin-1 recognition of β-glucans, an initiation of signal transduction occurrs to stimulate phagocytic activity, ROS production, and proinflammatory cytokines, such as TNF-α production to promote coordinated antifungal activities of the immune response [4,19,20,21].

PMNs are normally recruited during inflammation and together with AMs are responsible for phagocytosis of *A. fumigatus* conidia. Germinating, but not resting conidia, induce neutrophil recruitment to the airways. Consistent with this, β-glucan was detected using a soluble anti β-glucan antibody on the surface of swollen conidia and germlings, but not on resting spores [22,23]. PMNs aggregate around hyphae and damage hyphae by releasing reactive oxygen intermediates (ROI), antimicrobial peptides and degranulation. The importance of PMNs for antifungal defense can be inferred from the propensity of patients with severe prolonged neutropenia to develop IA [24].

One promising fungal metabolic pathway for drug targeting that does not exist in humans is the trehalose biosynthesis pathway. Among five biosynthesis pathways that various organisms utilize for trehalose production, the TPS1/TPS2 pathway is a well characterized pathway in *S. cerevisiae* [25,26,27]. The four-subunit protein complex include Tps1, Tps2, Tsl1, and Tps3 catalyzed two-step reaction results in disaccharide

trehalose production in *S. cerevisiae* [28,29,30,31]. Trehalose itself acts as a stress protectant in various types of organisms [32,33,34]. It has been shown that a single disruption of enzyme encoding genes in TPS/TPP pathway is sufficient to abolish trehalose production and decrease fungal virulence in other pathogenic fungi such as *Candida albicans, Cryptococcus neoformans, C. gattii, and Magnaprthe grisea* [35,36,37,38,39,40,41]. Unlike other fungi, multiple Tps1 encoding genes in *A. fumigatus* are required for trehalose production, stress response and thermotolerance [42]. Interestingly, an increase in fungal virulence was reported with this Tps1 mutant that was hypothesized to be associated with the altered cell wall that enhances resistance to macrophage phagocytosis [42]. In contrast to this reported Tps1mutant, the second key catalytic enzyme in the Trehalose biosynthesis pathway was characterized by our group. We found that Trehalose 6 Phosphate Phosphatase (Tps2/OrlA) is required for fungal virulence, but surprisingly not required for trehalose production in the human pathogen *A. fumigatus* [43]. To date, how the trehalose pathway contributes to fungal virulence mechanisms in human fungal pathogens is not well understood.

We previously showed that absence of OrlA led to persistent production of trehalose, although the intermediate T6P is highly accumulated as found in TPS2 mutants of other fungi [29,36,37,39,44]. Importantly, T6P accumulation is critical for regulation of fungal metabolism [45,46]. Hexokinase, a key glycolytic enzyme, is inhibited by T6P and previous phenotypic characterization of Δ*orlA* in *A. fumigatus* suggests that one ramification of T6P accumulation is an alteration of cell wall biosynthesis. In particular,

we hypothesize that T6P plays a regulatory role in the fungal cell wall biosynthesis and influences the protective responses against fungal infection.

In the present study, we uncover the role of two uncharacterized genes (*tslA, tslB*) which play a regulatory role in *A. fumigatus* trehalose biosynthesis pathway. To our knowledge, our finding is the first to demonstrate a linkage of the T6P intermediate to an increase in β-glucan content of the cell wall. We found that the host pathogen interaction mediated by this altered cell wall is the primary mechanism for antifungal activity and fungal clearance of the OrlA mutant. These findings raise intriguing questions about the development of a new therapeutic strategy targeting the trehalose biosynthesis pathway to overcome the emerging antifungal drug resistance and limited therapeutic tools available for IPA in immunocompromised patients.

Methods

Strains and Media

Aspergillus fumigatus strain CEA17 (a uracil auxotroph strain lacking *pyrG*) was used to generate single deletion mutant strains as listed in Table 3.1 [47]. The corresponding wild-type strain CBS144.89 was utilized throughout this study (kind gift of Dr. Jean-Paul Latge). The Δ*orlA* strain was generated in a previous study [43] and used as the background strain for additional deletion of putative regulatory subunit protein encoding genes; TslA, TslB. All strains (with the exception of the mutants generated by the Δ*orlA* background) were routinely grown in glucose minimal medium (GMM) containing a final concentration of 1% glucose, if not stated otherwise at 37°C [48]. Conidia were harvested after growth on appropriate solid media for 3 days at 37^{o}C.

All mutants having Δ*orlA* were grown in sorbitol minimal media (SMM; 1.2 M sorbitol, 1% glucose) and SMM was used as standard media in all experiments requiring conidia due to the restricted ability of Δ*orlA* to generate conidia on GMM.

Strain Construction

Mutant and reconstituted strains were generated by homologous recombination and standard polyethylene glycol mediated fungal protoplast transformation of *A. fumigatus* uracil auxotroph strain CEA17 and indicated mutants as shown in Table 3.2 [49]. PCR generated gene replacement constructs were utilized for specified mutations as stated in following strategies. Gene replacements and reconstituted strains were generated as we have previously described [43,50]. Real time reverse transcriptase PCR was used to confirm expression of the re-introduced gene [51]. To generate a double mutant strain, we utilized *pyrG* marker recycling approach. The particular single mutation strain for example Δ*orlA* was regenerated with a 1 kb-*Pst*I truncated *pyrG* homologous replacement construct. An additional *pyrG*+ knockout construct of a second GOI was generated as single mutation approach and transformed into the recreated (*pyrG*$^{-}$) single mutant strain to obtain the double mutant Δ*orlA(pyrG-)*Δ*tslA(pyrG+)* strain. Following *pyrG* recycling approach, we utilized *Hph*; hygromycin B marker to generate the third gene deletion by alternative overlapped PCR approach [52].

Trehalose Measurement

A. fumigatus strains were grown on SMM plates at 37°C for 3 days and fresh harvested conidia in 0.01% Tween80 solution were used for further analysis. A total of

$2x10^8$ conidia were used for the trehalose assay in conidia. Conidia were extracted in 500 µl of distilled water by boiling at 100°C for 20 min. The conidial extract containing soluble trehalose was separated from cell debris by centrifugation at 11,000xg for 10 min and used as the cell free extract as previously described [43].

In mycelium, overnight shaking cultures of $1x10^8$ conidia in 10 ml of LGMM at 37^oC were filtered and rinsed with sterile distilled water. Filtered mycelia were transferred into screw cap tubes, weighed, and flash frozen in liquid nitrogen. Five hundred microliters of sterile water was added to the fungal tissue tube containing 0.1mm glass beads and physically disrupted with a bead beater twice with 5 min. on ice interval. Mycelium homogenates were incubated at 100°C for 20 min. and crude extracts were subsequently collected after centrifugation at 11,000xg for 10 min. Cell free extracts were then used to measure trehalose production according to the Glucose Assay Kit protocols, (Sigma Aldrich) as described earlier [43]. Statistical significance ($P \leq 0.05$) was determined with a two-tailed Student's *t*-test.

LCMS Analysis of T6P

Mycelia extractions with Methanol:Dichloromethane:Water solution were performed as previously described [43]. Quantitation of [T6P extracts] was carried out via UHPLC-ESI-MS with an Agilent 1290 LC system coupled to an Agilent 6538 QTOF. The extracted material was thawed, vortexed, and diluted into a 50:50 solution of water and acetonitrile. Authentic standards were prepared via serial dilution into the same solvent. All samples were placed into capped autosampler vials and stored in a refrigerated autosampler at 4^oC during the course of the analysis. Chromatography was

performed using HILIC-type gradients with a Cogent Diamond Hydride Type-C silica column, 150mm x 2.1mm, 4µm (MicroSolv Technology). Solvent "A" consisted of water with 0.1% formic acid, and solvent "B" was acetonitrile with 0.1% formic acid, with a flow rate of 0.5 mL/min. The column was held in a thermostated compartment at 50^{o}C. The solvent gradient is as follows: pre-run equilibration and loading with 90% B, followed by a wash from injection until 1.0 min also at 90% B. From 1.0 to 5.0 minutes, a linear gradient from 90% to 25% B. From 5.0 to 8.0 min, held at 25% B. From 8.0 to 10 min, held at 90% B. [T6P] was found to elute at approximately 3.5 minutes. The column eluant was diverted to waste from 0 to 2.0 min, to the ESI source from 2 to 6 min, and again to waste from 6 to 10 minutes. Starting at 6.5 min during the second waste stage, the flow rate was increased to maximum possible within pressure limits for thorough washing and re-equilibration of the column.

Column eluant was introduced to the mass spectrometer via typical electrospray ionization source. The drying gas was reduced to 300^{o}C due to the high concentration of acetonitrile, with the nebulizer at 55 psig and drying gas at 12 L/min. The fragmentor was 120V and skimmer was 45V. Data was collected in negative mode, low mass range with high dynamic range option, with data collection of both profile and centroid from 25 to 1000 m/z, at a rate of 1 spectrum per second. The [T6P] peak was identified via accurate mass, retention time, and fragmentation patterns with comparison against the standard compound. The chromatographic separation was tested with the experimental samples using fragmentation scanning between 5 and 40V to ensure that there were no isobaric contaminants in the experimental samples which co-elute with [T6P].

Quantitation of [T6P] was carried out using the Agilent MassHunter Quantitative Analysis software package, using accurate mass based upon the [12-super] C peak. Based upon the standard curve for authentic [T6P], the effective limit of quantitation is approximately 1 ng per injection, using this method. For best results, sample dilutions were adjusted to achieve between 10 and 100 ng per injection. The concentration of T6P was normalized to the input weight of fungal tissue for each sample. Results from triplicate experiments were averaged, standard deviation calculated, and statistical significance was determined ($P \leq 0.05$) with a two-tailed Student's t-test.

Trehalose-6-Phosphate Phosphatase Enzyme Assays

The activity of T6PP was determined in mycelia extracts by measuring trehalose production in the reaction. Ten milliliters of a 20 hrs culture of $1x10^7$ conidia in LGMM at 37^{o}C were filtered, weighed, and flash frozen in liquid nitrogen. All procedures were conducted at 4°C. Two volumes (1:2, w/v) of 50mM Tris-HCl Buffer [53] was added to the fungal tissue tube containing 0.1mm glass beads and physically disrupted by bead beater twice with 5 min. on ice interval. The crude extract was subsequently collected after refrigerated centrifugation at 13,000rpm/15 min and immediately precleaned through G25 sephadex column following the manufacturer's protocol (GE Healthcare) prior to performing the T6PP assay in a total volume of 100 µl, using the modified procedure of De Virgilio *et al.* [29]. The reaction mixture contained the following components: 1.6mM T6P, 10mM $MgCl_2$, 25mM Sodium Phosphate Buffer, pH 6.0, and 50 µl of precleaned extract. Reactions were incubated at 30^{o}C for 20 min. and stopped by boiling in a water bath for 3 min. The amount of trehalose product generated in the

collected supernatant after centrifugation at 10,000rpm/5min was indirectly determined by measuring the liberated glucose after trehalase treatment as previously described in the trehalose measurement procedure [43]. Protein concentration in the extracted supernatant was quantified with the Bradford Reagent and used to normalize the data. Data presented are the mean and standard deviation of three biological replicates. Statistical significance ($P \leq 0.05$) was determined with a two-tailed Student's *t*-test.

Radial Growth Rate and Cell Wall Perturbation Agents

For growth test experiments on different carbon sources, all media contained trace element and salt solution as described in glucose minimal media [48]. MM is minimal media without carbon source, TMM is minimal media that contains 0.5% trehalose in place of glucose, and SMM is minimal media that contains 1.2M sorbitol, and 1% glucose. A 5µl drop of $1x10^6$ conidia of each test strain were placed on the center of each plate. Radial growth rates at 37°C of all strains were measured every 24 hours for a period of 5 days for each fungal strain in triplicate. Radial growth rate was generated from highest rate of all strains on day 4.

Cell wall inhibitors were utilized for cell wall integrity tests: Congo Red (CR, Sigma Aldrich), and Calcofluor White (CFW, Sigma Aldrich) [54]. CR and CFW were added into GMM at final concentrations of 1mg/ml, and 25 µg/ml respectively [43]. A 5µl drop of $1x10^6$ conidia of each test strain were placed on the center of each plate. The radial growth rates at 37°C of all strains were measured every 24 hours for a period of 7 days for each fungal strain in triplicate. Radial growth rate was generated from highest

rate of all strains on day 6. Results are an average of triplicate experiments, and statistical significance ($P \leq 0.05$) was determined with a two-tailed Student's *t*-test.

For nutrient versatility assay, fresh murine lung explants were placed on 1% agarose plate and standard Yeast Potato Dextrose plates were inoculated with 2,000 conidia in a 5 µl volume and incubated at 37^{o}C for 7 days as previously described [55].

Cell Wall Composition Analysis

A. fumigatus strains were grown in Sabouraud medium containing 5mM uridine for 20 hrs at 37^{o}C. The mycelia were collected by filtration, washed thoroughly with sterile water and subjected to cell wall monosaccharide analysis. The percentage of respective monosaccharide compositions in each strain was calculated as previously described [56]. Statistical significance ($P \leq 0.05$) was determined with a paired or unpaired two-tailed Student's *t*-test as indicated in figure.

Soluble Dectin-1 Staining

A. fumigatus conidia were adhered to sterile, 8-chamber well glass slides for 7 hrs in the 37^{o}C, CO_2 incubator. The hyphae were UV irradiated with a CL-1000 UV Crosslinker (energy power = 6,000x100µ J/cm2), blocked, and stained with conditioned media containing s-dectin-hFc (kind gift of Dr. Tobias M. Hohl) followed by DyLight 594 -conjugated, goat anti-human IgG1 [23]. After being washed, the glass slides were mounted by coverslips with Prolong mounting media (Molecular Probes). The slides were captured using an Olympus Deltavision microscope. Dectin-1 staining was measured by averaging the amount of edge staining, detected by the program, above the

signal threshold to the total area of each hypha. All hyphal measurements were conducted using ImageJ software (version 1.45). Negative staining control was performed by omitting primary antibody (s-dectin-hFc). The fluorescence result indicates the specificity of glucan bound s-dectin-hFc staining.

Bone Marrow Neutrophil Isolation

Neutrophils were isolated from mouse bone marrow, as previously described [57]. Femur and tibias from both hind legs were dissected from 8-10 week old C57BL/6 or xCGD mice. The extreme distal tip of each bone was cut off and marrow was flushed out of bone with a syringe of Murine Neutrophils Buffer (HBSS containing 0.1%FBS, and 1%Glucose). After dispersing cell clumps, the cell suspension was centrifuged at 600xg for 10 min, 4^{o}C. Leukocyte cells were resuspended in 3 ml of 45% percoll solution and loaded on top of a percoll density gradient of 2 ml of 50%, 55%, 62%, and 3 ml of 81% in 15ml polypropylene tube. A cell band formed between 81% and 62% layer was collected after 30 min centrifugation at 1,600xg, 10^{o}C. Neutrophils were transfered to enriched Tissue Culture media (TC media containing RPMI, 10% FBS, 5mM HEPES buffer, 1.1 mM L-glutamine, 0.5U/ml penicillin, and 50mg/ml streptomycin) in 50ml polypropylene tube, washed with HBSS and cells were diluted for counting. We obtained $2\text{-}5x10^{7}$ cells per mouse. Cell concentration for experiments was adjusted with TC media to obtain $5x10^{6}$ cells/ml and was kept on ice until performing *in vitro* PMN killing assay and PMN lysis assay with fungus.

Fungal Preparation for *in vitro* Assays

$1x10^5$ conidia/well in 200 µl of TC media were grown in 96 well plates for 16 hrs at 30^{o}C and shifted to 37^{o}C for another 2 hrs in an incubator to obtain an early hyphal growth stage. The hyphae were used for *in vitro* assays with bone marrow neutrophils as indicated in the specified *in vitro* PMN lysis and PMN killing sections below.

ELISA-TNF-α Production

Commercially available ELISA kits for TNF analysis (eBioscience, San Diego, California, United States) was used according to the manufactures' instructions. The limit of TNF detection was 15 pg/mL. Statistical significance ($P \leq 0.05$) was determined with a paired two-tailed Student's *t*-test.

In vitro PMN Lysis and LDH Determination

In vitro PMN lysis following co-incubation with live hyphae was determined by the release of Lactate Dehydrogenase enzyme (LDH) into the co-culture supernatant. In brief, a fungal plate of $1x10^5$ live hyphae grown-18 hrs per well as earlier described was added with 200 µl of $1x10^6$ bone marrow derived neutrophils in TC media (1:10 ratio) and co-incubation at 37^{o}C in CO_2 incubator. After 1 and 5 hrs of co-culture, supernatants were transferred to another 96 well plate for the LDH assay using the CytoTox 96 Non-Radioactive Cytotoxicity assay (Promega, Madison, WI, USA) according to the manufacturer's protocol.

In vivo released LDH in BAL samples was determined with a CytoTox 96 kit and using a standard LDH solution for this quantitatitve colorimetric test. Briefly, standards

were prepared as 2 fold serial dilutions in DPBS ranging from 0.02-1.44 Unit/ml. Fifty microliters of the standard or sample was added to individual wells in a 96 well plate and mixed with 50 µl of substrate mix, incubated in the dark at room temperature for 30 min. 50 µl of stop solution was added to each well, absorbance was determined at 490 nm within 1 hr. Statistical significance ($P \leq 0.05$) was determined with a two-tailed Student's *t*-test.

Murine Models Used for
Virulence Test and Host Responses

Male CD1 mice (Charles River Laboratory, Raleign, NC) (6-8 weeks of age) were housed and supplied with food and antibiotic water ad libitum in the Animal Resources Center at Montana State University. Two murine models of chemotherapeutic immunosuppression and Knockout mice were used as we have previously described [50]. For PMN depletion studies in xCGD mice; the Gr1-specific RB6-8C5 monoclonal antibody was utilized for PMN neutralization [58]. xCGD mice were intraperitoneally administered monoclonal Ab (250µg of RB6) one day prior to intranasal inoculation of $1x10^5$ conidia and every day throughout the course of infection in comparison to naïve xCGD mice.

Each *in vivo* mouse survival study was observed three times daily for 14 days after *A. fumigatus* challenge. Mice were observed for standard signs of IPA including ruffled fur, hunched posture, difficulty breathing and weight loss accounting for more than 20% of body mass. Critically affected mice were humanely euthanized when it was clear recovery was not possible using the above criteria. A log rank test was used for pair

wise comparisons of survival among the experimental groups, $P \leq 0.05$. Mouse experiments for each model were repeated at least on two separate occasions with similar results. Results presented are from one representative experiment for each model. All animal procedures and protocols were approved by the MSU Institutional Animal Care and Use Committee.

Flow Cytometry Analysis of Leukocyte Subsets

Analysis of leukocytes in the lung was performed using flow cytometry and appropriate cell markers. Mice were euthanized 2, 3, 4, or 5 days post-inoculation with respective *A. fumigatus* strains. Broncheo Alveolar Lavage samples (BAL) were obtained by 3 ml PBS perfusion and single cell suspensions were stained with a combination of the following fluorescence-conjugated mAbs (from BD Biosciences, San Jose, CA, or eBiosciences, San Diego, CA): anti-CD11b (PerCP-Cy5.5), anti-CD11c (FITC), anti-Ly6C (conjugated-biotin), anti-Ly6G (APC), anti-SiglecF (PE), anti-F4/80 (APC-Cy7), and secondary antibody PE-Cy7-Streptavidin. Unstained cells, and control cell suspensions were individually stained with a single Ab fluorochrome conjugate of each antibody fluorochrome used in the multiple stain reactions to compensate for the spill over in the emission spectrums for each fluorochrome prior to acquisition of 10,000 events per compensation tube.

Samples were analyzed on a Canto II fluorescence-activated cell sorter (FACS) instrument using Diva software (BD Bioscience). Analysis of gated leukocyte subsets was performed with FlowJo software Version 7.2.4. and the absolute number of each leukocyte subset was calculated from percentage of a gated cell type to the total number

of live cells in BAL samples. Statistical significance ($P \leq 0.05$) was determined with a two-tailed Student's *t*-test.

Histopathology

Additional murine experiments were conducted for histopathology analyses. At specific time points (days 2, 3, and 4 post-inoculation as indicated in respective figures), three mice in each group were humanely euthanized. One lung was harvested from each mouse and fixed in 10% formalin prior to embedding in paraffin, 5 μm thick sections taken, and stained with either H&E (Hematoxylin and Eosin) or GMS (Gomori's Methenamine Silver) [59]. The other lung was kept at -80°C for fungal burden analyses. Microscopic examination was performed on a Zeiss Axioscope2-plus microscope and engaged imaging system. Pictures were captured at 40x and 100x magnification as indicated in each image. For visualization of distributed fungal infection and inflammation throughout mouse lung, the entire lobe of mouse lung in Figure 3.1A was generated from combined sequential captured pictures using Adobe Photoshop 7.0.

Determination of *in vivo* Fungal
Burden and *in vitro* PMN Killing

uantitative fungal growth in the infected mouse lungs was performed after lungs were harvested at specific time point as indicated in figures. Lungs were chopped and immediately frozen in liquid nitrogen prior to lyophilization, and thoroughly homogenized with 0.1mm glass beads to obtain fine powdered mouse lungs. Total DNA was extracted using the E.N.Z.A. fungal DNA kit (Omega BioTek, Norcross, GA, USA)

according to the manufacturer's protocol. Real-time quantitative PCR was performed as previously described [60].

In vitro PMN killing was assessed by simultaneous quantitative determination of (i) fungal burden after 3 hrs-coincubation of live hyphae with bone marrow-derived neutrophils (killing) and (ii) following 3 hrs of PMN killing, the increase in fungal burden after 3hrs-recovery time in fresh medium without PMNs (recovery) was delineated. In brief, 200 µl of $1x10^6$ bone marrow neutrophils in TC media was added to a fungal plate of $1x10^6$ live hyphae-18 hrs grown per well as earlier described (1:1 ratio) and co-incubated at 37^oC. After 3 hrs of co-culture, PMNs were lysed with cold water and supernatant was discarded following 5 min. centrifugation at 4,400 rpm. Fungal tissue in each well was immediately lysed and extracted with TRIsure reagent (Bioline, Tauton, MA, USA) according to the manufacturer's instructions. To determine the recovery of fungus after 3 hrs of coincubation with PMN, fresh TC medium without PMNs was added into each well and fungal DNA extraction was then performed as above after 3 hrs growth at 37^oC. Genomic DNA obtained from TRIsure extraction was verified by amplification of 18s rRNA gene using conventional PCR. Quantitative fungal burden was analyzed in two sets: (i) extracted fungal DNA after 3 hrs-PMN co-incubation and (ii) after 3 hrs-recovery following 3 hrs-PMN killing. Additionally, a control fungus alone was grown in a different plate and fungal DNA extraction was utilized at 3 hrs and 6 hrs. The fold fungal growth after 3 hrs-recovery from incubation with the neutrophils was normalized to fungus alone. Reproducible data were obtained from two independent

experiments, and statistical significance ($P \leq 0.05$) was determined with a two-tailed Student's *t*-test.

Results

Impaired *in vivo* Fungal Burden of Δ*orlA* in Naïve xCGD Host is due to Host Response

Tps2 orthologs have been observed to play a pivotal role in fungal pathogenesis in four human fungal pathogens, including *Candida albicans, Cryptococcus gattii, Cryptococcus neoformans* and *Aspergillus fumigatus* [36,37,39,41,43]. However, the mechanism(s) by which Tps2 orthologs contribute to fungal pathogenesis is poorly understood. Here we utilized the *A.fumgitaus* Tps2 null mutant, Δ*orlA*, to further examine the role of this protein in fungal virulence. We began this work with two hypotheses that may or may not be mutually exclusive. On the one hand we hypothesized that loss of OrlA function leads to an *in vivo* fungal growth defect that attenuates virulence in murine models of IPA. However, an alternative hypothesis was that loss of OrlA function leads to increased fungal susceptibility to host mediated immune responses.

To initially examine whether the attenuated virulence of Δ*orlA* was due to defective *in vivo* fungal growth, we determined the *in vivo fungal* burden in lungs from an xCGD murine model of IPA inoculated with either Δ*orlA* or wild-type strains. Previous experiments have shown that the Δ*orlA* reconstituted strain recapitulates the wild-type phenotype in this animal model and thus this strain was not included in these studies to minimize use of animals. Histopathological analyses of lung sections of both groups display differences in the number of stained fungal hyphae (GMS) with Δ*orlA* inoculated

lungs having less hyphae, but a surprisingly similar level of inflammation as the wild-type as assessed qualitatively by H&E staining (Figure 3.1A). Correspondingly, fungal DNA increased (as measured by qRT-PCR of 18S rDNA) over the time course of infection and peaked on day 4 in wild type inoculated xCGD mice whereas fungal DNA peaked on day 3 in mice inoculated with Δ*orlA* and on day 4 was significantly reduced relative to wild type (Figure 3.1B). Taken together, these data suggest that levels of fungal growth are significantly reduced in xCGD mice inoculated with Δ*orlA*.

Increased Recruitment of Neutrophils in Response to Δ*orlA*

Given the apparent maintenance of the inflammatory response, despite a general decrease in fungal burden in the Δ*orlA* inoculated mice, we next examined the inflammatory response in more detail in our xCGD IPA model. We utilized fluorescence-activated cell sorting (FACS) to determine the populations of immune cells during the time course of infection between Δ*orlA* and the wild-type. Total leukocytes including neutrophils (CD11b+ CD11c-/ly6G+), macrophages (CD11b- CD11c+/siglecF+), inflammatory monocytes (CD11b- CD11c+/ly6C+), dendritic cells (CD11b- CD11c+/siglecF-), and eosinophils (CD11b+ CD11c-/siglecF+) were increased significantly over the 1-5 day time course of infection in Δ*orlA* compared to the wild type inoculated mice, which succumbed to death as early as day 4 post inoculation (Figure 3.2A-D and data not shown). In particular, a significant increase in the number of PMNs in the lungs was found on day 4 post inoculation (Figure 3.2B-C) and decreased on day 5 in the Δ*orlA* infected group (data not shown). Importantly, on day 3 post-inoculation

when fungal burden levels between the wild-type and Δ*orlA* were roughly equivalent (Figure 3.1B), an increase in PMN numbers was observed in the BAL samples of Δ*orlA* inoculated mice. Subsequently, on day 4 when Δ*orlA* presence in the lung was significantly decreased, a substantial increase in PMN levels were observed in the BAL samples of Δ*orlA* inoculated mice. Despite the substantial decrease in fungal burden in the lung, Δ*orlA* was able to induce significant amounts of TNF production, as measured in BAL samples, which is generally consistent with the increased numbers of leukocytes in the BAL samples from mice inoculated with this mutant (Figure 3.2E). Surprisingly, given the large number of leukocytes in the lung of Δ*orlA* inoculate mice, *in vivo* release of lactate dehydrogenase (LDH) in Δ*orlA* BAL fluid samples was consistently lower than the production of LDH mediated by the wild type strain (Figure 3.2F). Taken together, these data strongly suggest that loss of OrlA function alters host innate immune responses to *A. fumgiatus* particularly with regard to increased recruitment of neutrophils that lead to a subsequent decrease in *in vivo* Δ*orlA* fungal growth, lung damage, and virulence.

Δ*orlA* has Increased Susceptibility to Hyphal Damage by xCGD PMNs

The above data suggest that Δ*orlA* may increase PMN recruitment to the lung and that Δ*orlA* may have increased susceptibility to ROS independent PMN fungal killing mechanisms. However, a potential alternative hypothesis is that Δ*orlA* induces less PMN lysis at the site of infection than wild type *A. fumigatus.* To explore these mechanisms further, we next addressed whether Δ*orlA* was more susceptible to fungal killing by xCGD PMNs. PMNs were isolated from bone marrow of xCGD mice and an *in vitro*

PMN lysis assay was conducted by measurement of LDH levels in the supernatant of co-incubated PMNs with live hyphae. PMN lysis was slightly reduced in PMNs exposed to Δ*orlA* compared to wild type, but this slight difference was not statistically significant and thus likely does not account for the dramatic increase in PMN numbers *in vivo* (Figure 3.3A, P=0.24). Thus, increased PMN levels observed in xCGD murine lungs inoculated with Δ*orlA* is likely due to increased recruitment rather than differences in PMN lysis by the respective *A. fumigatus* strains. It is important to note that at the time of increased PMN recruitment in the lung of Δ*orlA* inoculated animals, that Δ*orlA* fungal burden is substantially less than wild type suggesting that Δ*orlA* directly stimulates the increased recruitment phenotype.

We next explored the antifungal activity of bone marrow-derived PMNs from xCGD or wild type C57BL/6 mice against hyphae of wild type, Δ*orlA*, or reconstituted Δ*orlA*. After co-incubation of live hyphae with bone marrow-derived PMNs for 3 hr, PMNs were removed from the culture and fungal growth was allowed to continue in fresh medium for 3 hr. Genomic DNA was then isolated from hyphae remaining in the culture wells and quantified by fungal burden qPCR analysis. A significant reduction in fungal burden was observed in wells containing Δ*orlA* than wild type or reconstituted strains regardless of whether isolated PMNs were from naïve C57BL/6 or xCGD mice (Figure 3.3B, P value $\leq$ 0.05). However, Δ*orlA* displayed increased susceptibility to killing by xCGD PMNs compared to the wild type and reconstituted strains. These results suggest that reduced fungal growth of Δ*orlA* during infection of xCGD mice is likely mediated by an undefined ROS independent mechanism of antifungal activity of PMNs.

PMNs Depletion in xCGD Mice
Restores Virulence of Δ*orlA*

To definitively determine whether increased susceptibility to *in vitro* PMN killing of Δ*orlA* reflects an *in vivo* protective role of PMNs against Δ*orlA* rather than a specific fungal growth defect, we depleted PMNs in the xCGD murine model with the GR1-specific RB6 monoclonal antibody. It should be noted that this antibody does partially deplete other GR1+ cells, such as some monocyte populations [58]. We hypothesized that PMN depletion would restore the virulence of Δ*orlA* if PMN mediated fungal killing and/or host damage was the primary mechanism for the attenuated virulence of Δ*orlA*. Depletion of PMNs restored the virulence of Δ*orlA* compared to the non-depleted xCGD mice inoculated with Δ*orlA* (Figure 3.4A). Virulence of the wild type strain was also slightly increased as evidenced by a decrease in the time to death in mice depleted with RB6. BAL samples of wild type strain infected animals with depleted PMNs also showed increases in LDH levels [61] and TNF production compared to Δ*orlA* (Figure 3.4B-C). These results correspond to the virulence phenotype and fungal burden in the infected lungs (Figure 3.4A, 3.5). PMN depletion was confirmed by monitoring PMN numbers in BAL samples taken on day 2 and RB6+ animals inoculated with both fungal strains displayed marked decreases in PMN numbers compared to naïve xCGD mice (Figure 3.4D).

The increased virulence of Δ*orlA* observed in PMN-depleted animals correlated with an increased fungal burden compared to non-depleted animals (Figure 3.5A). H&E stains demonstrated less inflammatory infiltrates in RB6-treated animals at sites of infection (Figure 3.5B), but correspondingly increased fungal elements observed with

GMS stains (Figure 3.5C) consistent with the increased fungal virulence observed in RB6 MAb-treated animals. These data also suggested that xCGD PMNs and possibly monocyte subsets retain ROS independent undefined fungal killing mechanisms. Taken together, we conclude that loss of OrlA function in *A. fumigatus* results in more efficacious killing of *A. fumigatus* by PMNs that leads to the attenuated virulence of Δ*orlA.*

In addition, we evaluated the hypothesis that PMN-mediated antifungal activity required for fungal killing was the primary mechanism for the attenuated virulence of Δ*orlA*. The inflammation or recruitment of leukocytes with reduced antifungal activity possibly through an inhibitory effect of corticosteroids on NF-κβ [62] demonstrated that impaired fungal growth per se was not the primary mechanism behinds the attenuated phenotype of Δ*orlA.* Accordingly, Δ*orlA* did indeed retain wild-type virulence in this model of IPA (P = 0.33; Figure 3.10-A). The increased fungal burden observed in lung homogenates is consistent with the histology of lung tissue from this model displayed a robust host inflammatory response and tissue damage on day 3 in Δ*orlA*- and wild type-inoculated animals (Figure 3.10, B-C). The increased fungal growth over time in both strains was not significantly different from each other but the pattern of growth was generally lower in Δ*orlA* than wild type. Taken together, the *in vivo* fungal growth of Δ*orlA* in the corticosteroid model of IPA indicates that functional leukocytes mainly mediated by PMNs are requisite for the attenuated virulence of Δ*orlA* rather than direct effect of fungal growth.

Putative Orthologs of Trehalose Biosynthesis Enzymes in *A. fumigatus*

We next sought to uncover the mechanism behind the ability of Δ*orlA* to recruit more PMNs to sites of infection, as well as its increased susceptibility to PMN killing. Based on our previous findings with Δ*orlA* that suggested altered cell wall composition, we hypothesized that loss of Δ*orlA* alters the cell wall of *A. fumigatus* to mediate these *in vivo* responses. To address this hypothesis, we used bioinformatics to identify candidate genes involved in the most widely distributed pathway of trehalose synthesis in fungi, the TPS1/TPS2 pathway (Figure 3.11) [25,26,27]. We utilized the genome database of *A. fumigatus* in CADRE (The Central *Aspergillus* Data Repository [63]), AspGD (*Aspergillus* Genome Database [64]), and together with available genomic information tools provided by NCBI (The National Center for Biotechnology Information [65]) for putative ortholog identification.

We were able to search putative orthologs of *S. cerevisiae* TPS1 protein in *A. fumigatus* A1163 whole genome sequence by using BLAST algorithms of amino acid sequences. Four trehalose-6-phosphate synthase encoding genes involved in trehalose biosynthesis (*Af-tpsA*, AFUB_001790; *Af-tpsB*, AFUB_021080; *Af-tpsC*, AFUB_099940; and *Af-tpsD*, AFUB_062010) were found containing similar conserved domains of GT1_TPS, a glycosyltransferase, that catalyses the synthesis of α, α-1,1-trehalose-6-phosphate (T6P) intermediate from glucose-6-phosphate using a UDP-glucose donor (Figure 3.11 and Table 3.1). Previously, four orthologs of TPS1 were identified and characterized in *A. fumigatus* strain AF293 [42]. Percent amino acid identities of Sc-Tps1

to Af-TpsA, and Af-TpsB orthologs (67%) are much greater than Af-TpsC and Af-TpsD orthologs (47%) in *A. fumigatus* A1163.

In *S. cerevisiae*, two regulatory subunits play an essential role in regulating TPS1/TPS2 enzyme activity by forming a four subunit enzyme complex with TPS1 and TPS2 [30,31]. Two putative genes; *tslA* (AFUB_089470) and *tslB* (AFUB_021090) were closely related to regulatory protein subunits Tsl1 and Tps3 found in *S. cerevisiae* (Table 3.1). Amino acid alignments of these genes revealed conserved domains similar to TPS2/OrlA that contained a glycosyl transferase, a trehalose phosphatase domain and HAD-superfamily hydrolase. Amino acid similarity of Af-TslA and Af-TslB to Af-OrlA was 38% and 34% respectively and both regulatory subunits are highly similar with 47% identity.

Regulatory Subunits of TPS1/TPS2 Enzymes are Partially Responsible for Persistent Trehalose Production in the Absence of OrlA

Persistent trehalose production with a substantial increase in T6P accumulation in mutants lacking OrlA underscores the complexity of trehalose biosynthesis in *A. fumigatus* [43]. We hypothesized that two uncharacterized genes; *tslA* (AFUB_089470) and *tslB* (AFUB_021090) may play important undefined roles in regulating trehalose production in *A. fumigatus*. Because similar conserved domains in OrlA were found in these regulatory subunits, we hypothesized they could have functional roles as Trehalose-6-Phosphate Phosphatases (T6PP). To test our hypothesis, we examined the role of *tslA* and *tslB* genes by generating single and double mutant strains in the Δ*orlA* background. A double mutant lacking both OrlA and TslA had a significant decrease in trehalose

production with 60-70% remaining relative to the Δ*orlA* background (Figure 3.6A-B). These data suggest that TslA is involved in trehalose production in *A. fumigatus*.

Given that TslA and TslB share 47% amino acid sequence identity and contained similar protein domains, they likely encode similar functional proteins in *A. fumigatus*. Therefore, we generated a Δ*tslB* mutation in the Δ*orlA* Δ*tslA* strain. Interestingly, T6PP activity was undetectable in the absence of both OrlA and the predicted regulatory proteins *(ΔorlA/ΔtslA/ΔtslB*), which suggested that one potential role of these genes is as a T6PP (Figure 3.6C). However, trehalose production remained in conidia of this triple mutant indicating that partial T6PP activity of TslA and TslB was not totally accountable for the persistent trehalose production in the absence of OrlA. Together our data suggest that trehalose may be produced in part by partial T6PP function of TslA and TslB regulatory subunits and an additional unidentified mechanism in *A. fumigatus*.

First Key Enzymatic Step in
TPS1/TPS2 Biosynthesis Pathway
is Critical for Trehalose Production

We next examined whether trehalose production could be completely ameliorated as reported in strain AF293, by genetic mutation of TPS1 orthologs [42]. Amino acid identity between the putative TPS1 orthologs; TpsA and TpsB in CBS144.89 is 79% and both proteins are predicted to contain the conserved GT1_TPS domain. As anticipated, fungal strains lacking a single deletion of either TPS1 ortholog (Δ*tpsA*, and Δ*tpsB*) were still able to produce trehalose in fungal conidia or mycelium compared to wild type CBS144.89 strain (Figure 3.6A-B). However, a double mutant lacking both *tpsA* and *tpsB* was generated and, as in strain AF293, found to completely lack trehalose production and

displayed increased sensitivity to temperature stress [42] (Figure 3.12). Reconstitution of Δ*tpsA*/Δ*tpsB* with either TpsA or TpsB is sufficient to restore trehalose production (Δ*tpsA*/Δ*tpsB*+*tpsA* and Δ*tpsA*/Δ*tpsB*+*tpsB*) (Figure 3.6A-B). Thus, total loss of trehalose biosynthesis can be achieved in *A. fumigatus* by elimination of trehalose synthase activity but not trehalose-6-phosphatae phosphatase activity.

Growth Defect of Mutants Lacking OrlA is Associated with T6P Accumulation

We next hypothesized that TslA and TslB, regulatory protein subunits are required for stabilizing TPS1/TPS2 enzyme activity to maximize the synthase/phosphatase enzymatic activities and that the accumulation of T6P in Δ*orlA* may be primarily responsible for the phenotypes it exhibits *in vitro* and *in vivo* [30,31]. LCMS analysis revealed a T6P level corresponding to levels of trehalose content (Figure 3.6A-B, D). Loss of the TslA protein had no effect on T6P accumulation relative to Δ*orlA*. However, both putative regulatory proteins are critical for full production of T6P as loss of these proteins greatly reduced production of T6P that is synthesized largely by TpsA and TpsB (Figures 3.10 and 3.6). Collectively, these trehalose and T6P quantitative data suggest that T6P is generated in wild type and single Tps1 mutants, but subsequently rapidly dephosphorylated to trehalose. Residual T6PP activity was found in the double mutant lacking TpsA and TpsB, however no trehalose production was found in this mutant which could be due to loss of the T6P substrate (Figure 3.6C).

In support of our hypothesis that T6P accumulation in Δ*orlA* is primarily responsible for the observed phenotypes of this mutant, loss of T6P accumulation through

deletion of TslA/TslB restored the majority of Δ*orlA* phenotypes (Figures 3.7&3.8). Radial growth assays of all generated mutants, including mutation of regulatory proteins TslA and TslB and mutations of TPS1 encoding genes *tpsA* and *tpsB,* was performed on four different media including Minimal media (MM), Trehalose minimal media (TMM), Glucose minimal media (GMM) and Sorbitol minimal media (SMM) (Figure 3.7A). All minimal media contain similar base components with different carbon sources ranging from zero (MM), 1% glucose (GMM), 0.5% trehalose (TMM), and 1.2M sorbitol (SMM). Analysis revealed a moderate, but significant reduction in growth rate of mutants lacking OrlA; Δ*orlA* and Δ*orlA*/Δ*tslA* strains. Loss of both TslA and TslB in Δ*orlA* was able to restore wild-type growth rates on GMM, MM, and TMM strongly suggesting that accumulation of T6P was responsible for the impaired growth rate of Δ*orlA.* As *in vitro* laboratory growth conditions likely do not mimic the nutrient sources available in the lung, we next tested the ability of Δ*orlA* to cope with complex mouse lung explants in comparison to rich medium containing broken down protein YPD media (Yeast extract/Peptone/Dextrose media [55]). This result suggested that both wild type and Δ*orlA* were able to grow on lung and control YPD media (Figure 3.7B). Taken together, these results suggest that accumulation of T6P in Δ*orlA* alters *A. fumigatus* growth rates and culture morphology *in vitro*.

T6P Accumulation Regulates Cell Wall Composition in *Aspergillus fumigatus*

In further support of a major regulatory role for T6P levels, loss of *tslA* and *tslB* in *Δ*orlA strikingly restored the conidiation defect on GMM that correlated with a

concomitant decrease in T6P levels in the mycelium (Figures 3.8A and 3.6D). Accordingly, the cell wall integrity of *ΔorlAΔtslAΔtslB* displayed an intermediate phenotype between the wild type and *ΔorlA* strains as measured by cell wall perturbing agents (Figure 3.8A-B). Quantification of radial growth on two different cell wall perturbing media containing Congo Red (CR) and Calcofluor White (CFW) further supported the solid media plate phenotypes (Figure 3.8B, 3.7A). Full wild type restoration of cell wall integrity was observed in the presence of functional OrlA (Rec-OrlA: *ΔorlAΔtslAΔtslB)*.

We next further examined the cell wall composition of Δ*orlA* given the importance of the fungal cell wall in virulence and responses to antifungal drugs [10,66,67,68]. Cell wall composition analyses revealed increased levels of β-glucan and α-glucan in the alkaline insoluble and soluble cell wall fractions of Δ*orlA*, respectively, whereas the percentage of chitin was decreased relative to wild type and reconstituted strains (Figure 3.8C). In addition, we utilized fluorescence microscopy to determine whether the increased β-glucan content in the Δ*orlA* cell wall was exposed by staining with soluble recombinant Dectin-1; a host receptor that has specific binding to fungal β-glucan [23]. A higher fluorescence intensity along the cell wall of Δ*orlA* was observed compared to the wild type strain suggesting that the increase in β-glucan composition leads to increased exposure (Figure 3.8D). Taken together, these results suggest a significant role for T6P in regulating cell wall homeostasis in *A.fumigatus*.

Loss of T6P Accumulation in Δ*orlA* Restores Fungal Virulence

As fungal β-glucan exposure is a critical pathogen associated molecular pattern that can alter host immune responses to fungal pathogens, we then hypothesized that the restoration of wild type cell wall morphology is essential for fungal virulence and we addressed this hypothesis in our xCGD murine model of IPA. Here, we observed that mortality occured in xCGD mice inoculated with Δ*orlA*, but was significantly delayed compared to the WT in agreement with our *in vivo* host response and fungal burden data (Figure 3.1-3.5, and Figure 3.9). Importantly, *ΔorlAΔtslAΔtslB* displayed virulence comparable to the wild type strongly suggesting that the Δ*orlA* virulence defect is due specifically to T6P accumulation (P value ≤ 0.05 in Δ*orlA* compared to the other strains, Figure 3.9). Maintenance of full virulence of the Tps1 double mutant Δ*tpsA/tpsB*, which lacks T6P accumulation and trehalose accumulation, in this murine model further supports a key role for T6P accumulation in mediating Δ*orlA* virulence.

Discussion

Previous studies have suggested that the trehalose biosynthesis pathway in human pathogenic fungi is a promising broad spectrum drug target due to both its essential role in fungal virulence and absence in humans [35,36,37,39,41,43]. While a general understanding of the role of trehalose and its biosynthetic pathway in fungal metabolism exists, the mechanism(s) behind the attenuated fungal virulence of various trehalose pathway mutants is not well understood. A full understanding of the implications of trehalose pathway inhibition in human pathogenic fungi is thus critical to fully evaluate

this pathway as an antifungal drug target. In further support of this rationale, both TPS1 and TPS2 null mutants in the human pathogenic yeast *C. albicans, C. neoformans, and C. gattii* display severely attenuated virulence in murine models [35,36,37,39,41]. In contrast, in the mold *A. fumigatus*, while inhibition of TPS2 (OrlA) results in attenuated virulence in chemotherapeutic and xCGD murine models [43], loss of TPS1 (TpsA/TpsB) function results in a hypervirulent strain in a corticosteroid murine model of invasive pulmonary aspergillosis [42] and persistent virulence in three additional immunologically distinct murine models of IPA (chemotherapeutic, corticosteroid, and xCGD) in Chapter 4. Thus, both the fungal pathogen itself and the underlying immune system status of the host likely play interdependent roles in determining the feasibility of targeting the trehalose pathway for broad spectrum antifungal drug development. Here, we sought to elucidate the mechanisms behind the attenuated virulence of the *A. fumigatus* TPS2 null mutant, Δ*orlA*.

We chose to pursue these inquiries utilizing the xCGD murine model of invasive pulmonary aspergillosis, due to the specific defect in NADPH oxidase activity in these animals that results in susceptibility to *A. fumigatus* challenge [69]. In contrast, the underlying immune system defects that lead to susceptibility in chemotherapeutic models of IPA characterized by cyclophosphamide use and corticosteroid models are less well defined and multi-faceted [62,70]. We observed that in our xCGD IPA model, Δ*orlA* inoculation results in a significant delay in mortality compared to wild type inoculation. In addition to *in vivo* attenuated virulence, cell wall integrity of Δ*orlA* is significantly impaired under *in vitro* stress environments, and we hypothesized that the observed

attenuated virulence phenotype in this murine model was due to a fungal growth defect. The initial examination of *in vivo* fungal growth with GMS staining of whole lung sections showed significantly less fungal growth and hyphal formation in the Δ*orlA*-inoculated mice compared to the wild type-inoculated mice. However, it was interesting that we observed a similar level of inflammation in the H&E stained histopathology between Δ*orlA*- and wild type-inoculated mice. We then considered that the differences in fungal growth on day 4 post inoculation was possibly due to Δ*orlA* being more susceptible to the immune response in xCGD mice. Accordingly, our results showed that 4 days after inoculation with Δ*orlA*, there was a significant increase in the number of leukocytes in BAL samples of the xCGD mice. Particularly, recruitment of PMNs was significant higher in the Δ*orlA* inoculated mice than wild type. *In vitro* PMN lysis also supported that the increase in PMNs was not due to a reduction of PMN lysis induced by Δ*orlA*.

Taken together, we hypothesized that the reduced virulence of this mutant is mediated by an increased susceptibility of Δ*orlA* to PMN killing. To address this hypothesis directly, we utilized a neutrophil-depleting RB6 monoclonal antibody [23]. Depletion of PMNs in our xCGD murine model clearly demonstrates that RB6-treated xCGD mice lost *in vivo* protection from invasive fungal infection of Δ*orlA*. In the absence of PMNs, Δ*orlA* had increased fungal burden and restored virulence similar to wild type. Bone marrow-derived PMNs from xCGD and wild type C57BL/6 mice damaged/killed hyphae of Δ*orlA* more effectively than wild type *A. fumigatus*, which was likely mediated by an undefined ROS-independent mechanism. Taken together, these

data strongly conclude that loss of OrlA function alters host innate immune responses and is a primary mechanism for the attenuated virulence of Δ*orlA* in this murine model.

The present findings have shown the antifungal activities mediated by ROS deficient PMNs can delay the colonization of *A. fumigatus* Δ*orlA*. However, the mechanism behind the OrlA-mediated depression of PMNs recruitment to sites of infection as well as the decreased susceptibility to PMN killing remains to be fully understood. One possible explanation includes the defective cell wall of Δ*orlA*. Importantly, our data suggest that the cell wall defect of Δ*orlA* is directly mediated by accumulation of the T6P intermediate. To further explore this hypothesis, we manipulated T6P levels *in vivo* by generating additional genetic mutations in Δ*orlA* to reduce T6P accumulation. Loss of the two putative trehalose synthase regulatory subunits in Δ*orlA* (Δ*orlA*;Δ*tslA*;Δ*tslB*) resulted in a loss of trehalose production and significant reduction in T6P levels. This triple mutant displayed normal conidiation levels on GMM media, cell wall integrity, and virulence in xCGD murine model of IPA. Taken together, these data strongly suggest that the two regulatory subunits are required for activity of T6P synthase to produce T6P and that persistent trehalose production in Δ*orlA* is largely the result of dephosphorylation of accumulated T6P and not through an alternative pathway as we had previously hypothesized [28,71].

The ramifications of T6P accumulation on fungal biology has been observed in *S. cerevisiae*, and other fungi [29,36,39,41,72]. The T6P intermediate is a known specific hexokinase inhibitor and plays a critical role in the control of glycolytic flux by restricting glucose influx at the level of glucose phosphorylation [72,73,74,75]. Fungi

utilize both glucokinase and hexokinase to convert sugar into sugar phosphate for glycolysis [75,76,77,78]. Recently, Fleck *et al.* showed that hexokinase genes are abundantly expressed during germination and constantly expressed in mycelia of *A. fumigatus* [75]. Therefore it is possible that a negative effect of T6P accumulation on regulation of glycolysis and cell wall biosynthesis is increased during hyphal growth of Δ*orlA*. Indeed, a strain with double loss of hexokinase and glucokinase in *A. fumigatus* also displays a severe cell wall defect in response to cell wall perturbing compounds, which indicates an essential role of hexose kinases for synthesis of the fungal cell wall [75].

To address whether T6P is the key factor associated with morphological defects of fungal cell wall, we performed exclusive cell wall analyses. We observed that the amount of N-acetylglucosamine polysaccharide or chitin decreased in *A. fumigatus* Δ*orlA*, which was consistent with findings in an *A. nidulans orlA* mutant [44]. To date, although there are no identified specific chitin receptors in myeloid cells of the immune system, research on chitin polysaccharides indicate that chitin recognition is complex and possibly associated with TLR2, Dectin-1, and mannose receptors [79]. Purified chitin from *C. albican* appears to be immunologically inert and does not have immunomodulatory capability on TLR2 and TLR4, though, however, acts as an immunosuppressive agent by blocking fungal recognition by Dectin-1 [16,17]. In this respect, the decreased chitin in Δ*orlA* may partially be a factor that stimulates an increased immune response that seems likely to be mediated through the increase in β-glucan composition during *in vivo* fungal growth. In addition to increased β-glucan

quantity in the Δ*orlA* cell wall, increased exposure of β-glucan was observed in Δ*orlA* as examined by specific soluble Dectin-1 straining [23]. Of note, we previously observed increased mRNA abundance of genes encoding 1,3 glucan synthase and glucanosyltransferase in Δ*orlA* [43].

In addition, the heteropolymer consisting of galactose and N-acetylgalactosamine named galactosaminogalactan (GG) was characterized in *A. fumigatus*, and it had an essential immunological role in induction of PMNs apoptosis and an immunosuppressive function that triggers disease in immunocompetent mice [80]. Of note, N-acetylgalactosamine (GalNAc) composition in Δ*orlA* is significantly lower than wild type. Thus, together with normal induction of PMN lysis data, our data suggest that the changes in Δ*orlA* cell wall likely mediate the change in the immune response that benefits antifungal host responses as we observed a decreased in key immunosuppressor polysaccharides; i.e. chitin, and GG. In addition to these polysaccharides, genes encoding α-1,3 glucan synthase and β-1,3 glucanosyltransferase were characterized in *A. fumigatus*. However, none of these fungal cell wall components have been further studied to understand a role in host response due to no significant impact on *in vitro* fungal viability and possibly its cell wall compensation [81,82]. Taken together, we speculate that the increased β-1,3 glucan in cell wall likely mediated the change in recruitment of PMNs and resulted in increased susceptibility of the mutant to phagocytic killing. However, we cannot directly attribute the attenuated virulence of Δ*orlA* simply to an increase in β-1,3 glucan exposure due to the complex nature of the cell wall and this will be a topic of future study.

Fungi evolved the cell wall integrity signaling pathway (CWI) in response to the presence of cell wall perturbing compounds [83,84]. The cell wall remodeling has been found crucial for integrity of cell wall, consists of alterations in both composition and architecture of the cell wall including the increased deposition of chitin, mannoprotein, increased expression of (α-) and (β-)1,3 glucan synthase [83,85,86,87]. Chitin or N-acetyl-D-glucosamine (GlcNAc) polymers are synthesized from Fructose-6-Phosphate (F6P), the key intermediate required for glycolysis [88]. Given the findings that accumulation of T6P in Δ*orlA* results in deregulation of glycolysis along with lower activity of pyruvate decarboxylase enzyme, we speculate that T6P may act as internal stress of the cell wall integrity pathway which result in the induction of (α-) and (β-)1,3 glucan in compensation to an unresponsive post-transcriptional level of chitin synthesis due to insufficient aminosugar precursor [43,88]. In addition, inhibition of Chitin synthase enzymes by genetic mutation results in increased glucan content in the cell wall of *C. albicans* [89]. Likewise, Glucose-1-Phosphate (G1P) is required as a substrate of UDP-glucose and glucan polymerization [90,91]. Of great interest, the alternative trehalose metabolic pathway (Trehalose Phosphorylase) may play an important role in the absence of OrlA. This reversible enzyme catalyzes the degradation of trehalose and generates glucose and G1P. Based on the metabolic reactions, G1P can be converted to G6P by Phosphoglucomutases enzymes and G6P is then recycled into glycolysis bypassing the key restricted conversion of glucose to G6P step. On the other hand, G1P is also needed for glucan synthesis regarding to the alteration of Δ*orlA* cell wall [92].

In conclusion, we have demonstrated a link between intracellular T6P accumulation from the canonical TPS1/TPS2 pathway and fungal cell wall integrity that directly impact the outcome of invasive pulmonary aspergillosis in a murine model of xCGD. The ROS-independent antifungal mechanism observed in xCGD phagocytes caused by loss of OrlA function is an intriguing avenue for further examination as a potential of immune-based strategy for IPA control in CGD patients [93,94]. For therapeutic purpose, targeting the trehalose pathway at the level of Tps2/OrlA will be a fine balance in patients with invasive pulmonary aspergillosis. It seems clear that the underlying status of the patient's immune system must be factored in when attempting to target this pathway that can directly alter fungal PAMPs. Thus, a further understanding of the mechanism by which T6P accumulation and trehalose biosynthesis affects fungal cell wall integrity and subsequent host immune response are vital to fully evaluating this pathway as an antifungal drug target for invasive pulmonary aspergillosis and perhaps other human fungal infections.

Acknowledgements

This work was supported by funding from the National Institutes of Health-NCRR COBRE grants and the Montana State University Agricultural Experiment Station. Srisombat Puttikamonkul is funded through a Ph.D. fellowship from the Royal Thai Government. The authors would like to thank Dr. Agnieszka Rynda-Apple, Department of Immunology and Infectious Diseases, Montana State University for helping with FACS analysis and members of the Cramer Laboratory for insightful

discussions. Thanks to Dr. Allen Harmsen and laboratory members and Dr. Mark Quinn for technical advice and use of equipment at Montana State University, and the staff at the Animal Resources Center at Montana State University for their assistance and care of the animals used in this study.

Table 3.1. Genome analyses reveal genes involved in trehalose biosynthesis and hydrolysis pathways found in *A. fumigatus* regarding the similar amino acid sequences to fungal model *S. cerevisiae* and filamentous fungal model *A. nidulans*.

Function	Locus ID	Organisms	Gene name	ORF length	References
Trehalose 6 Phosphate	TPS1	*S. cerevisiae*	Sc-tps1	495 aa	[72,95]
Synthase	AFUB_001790	A1163	Af-tpsA	515 aa	This study
	AFUB_021080	A1163	Af-tpsB	479 aa	This study
	AFUB_099940	A1163	Af-tpsC	475 aa	
	AFUB_062010	A1163	Af-tpsD	476 aa	
Trehalose 6 Phosphate	TPS2	*S. cerevisiae*	Sc-tps2	896 aa	[29]
Phosphatase	AN3441	*A. nidulans*	An-orlA	882 aa	[44]
	AFUB_043350	A1163	Af-orlA	949 aa	Chapter 2, [43]
Regulatory Subunit	TSL1	*S. cerevisiae*	Sc-tsl1	1098 aa	[28]
	TPS3	*S. cerevisiae*	Sc-tps3	1054 aa	[30,31]
	AFUB_089470	A1163	Af-tslA	919 aa	This study
	AFUB_021090	A1163	Af-tslB	918 aa	This study
Trehalose	AFUB_037080	A1163	Af-tpyA	694 aa	Chapter 4
Phosphorylase	AFUB_062450	A1163	Af-tpyB	667 aa	Chapter 4
Trehalase	AFUB_046050	A1163	Af-treA	1072 aa	
	AFUB_070450	A1163	Af-treB	775 aa	

Table 3.2. *Aspergillus fumigatus* mutant and complement strains are created and used in this study.

Strain	Genotype	References
Δ*orlA*	CEA17 *orlA*::PYRG	Chapter 2, [43]
Rec-*orlA*	CEA17 *orlA*::PYRG, *orlA*:HPH	Chapter 2, [43]
Δ*orlA* pyrG-	CEA17 *orlA*::PYRG$^-$	This study
Δ*orlA*Δ*tslA*	CEA17 *orlA*::PYRG$^-$, *tslA*::PYRG	This study
Δ*orlA*Δ*tslA*Δ*tslB*	CEA17 *orlA*::PYRG$^-$, *tslA*::PYRG, *tslB*::HPH	This study
Rec-*orlA*+Δ*orlA*Δ*tslA*Δ*tslB*	CEA17 *orlA*::PYRG$^-$, *tslA*::PYRG, *tslB*::HPH, *orlA*:BLE	This study
Δ*tpsA*	CEA17 *tpsA*::PYRG	This study
Δ*tpsB*	CEA17 *tpsB*::PYRG	This study
Δ*tpsA* pyrG-	CEA17 *tpsA*::PYRG$^-$	This study
Δ*tpsA*Δ*tpsB*	CEA17 *tpsA*::PYRG$^-$, *tpsB*::PYRG	This study
Δ*tpsA*Δ*tpsB*+*tpsA*	CEA17 *tpsA*::PYRG$^-$, *tpsB*::PYRG *tpsA*:HPH	This study
Δ*tpsA*Δ*tpsB*+*tpsB*	CEA17 *tpsA*::PYRG$^-$, *tpsB*::PYRG *tpsB*:BLE	This study

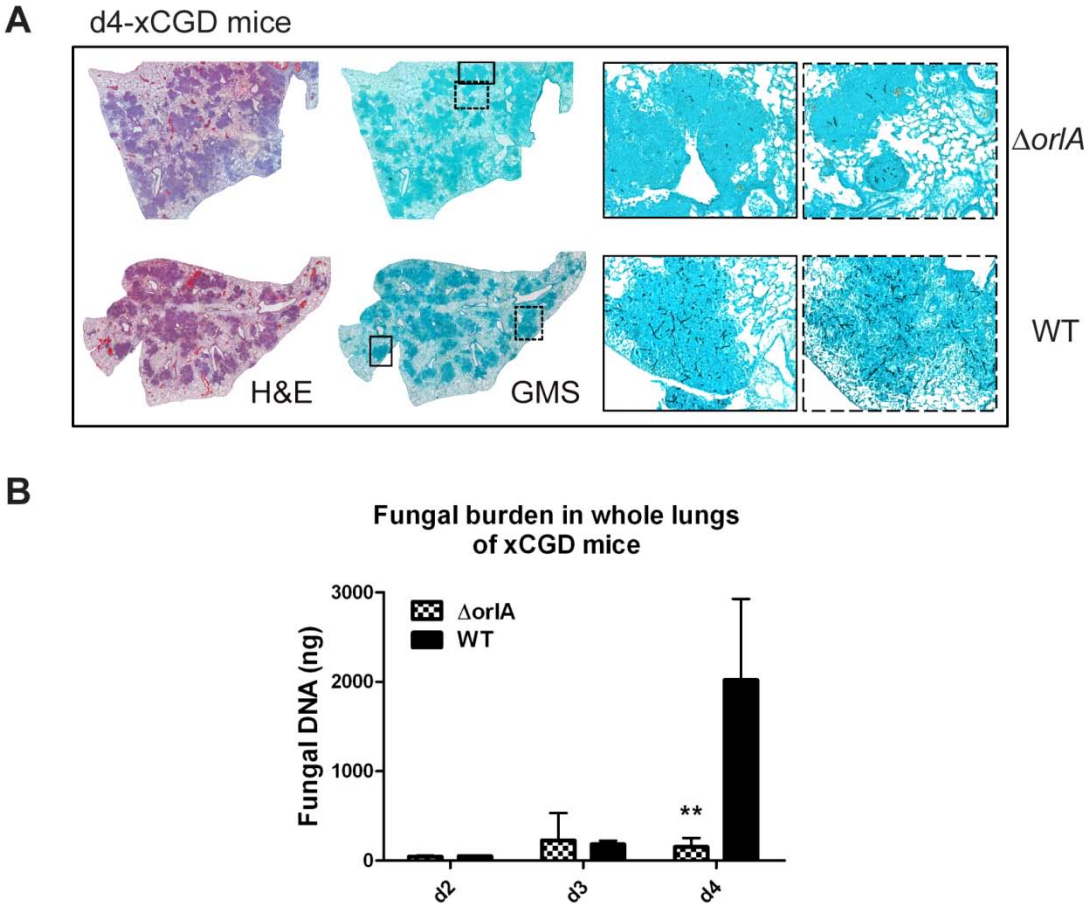

Figure 3.1. Loss of OrlA results in decreased fungal burden in xCGD murine model of Invasive Pulmonary Aspergillosis. *In vivo* lung histology and fungal burden of xCGD mice. A) Day 4 post-inoculation, H&E stained leukocyte infiltrates and GMS stained hyphae of the entire lobe of lung histology (40x). Solid and dashed squares represent 100 x magnification B) Day 2, 3 and 4 post-inoculation fungal burden qPCR analysis of *A. fumigatus* 18s rRNA gene. Data represent mean ± SD from two independent experiments (n=6 mice for each group), a significant decrease in fungal burden of Δ*orlA* inoculated xCGD mice relative to WT is observed on day 4 (**$P \leq 0.05$).

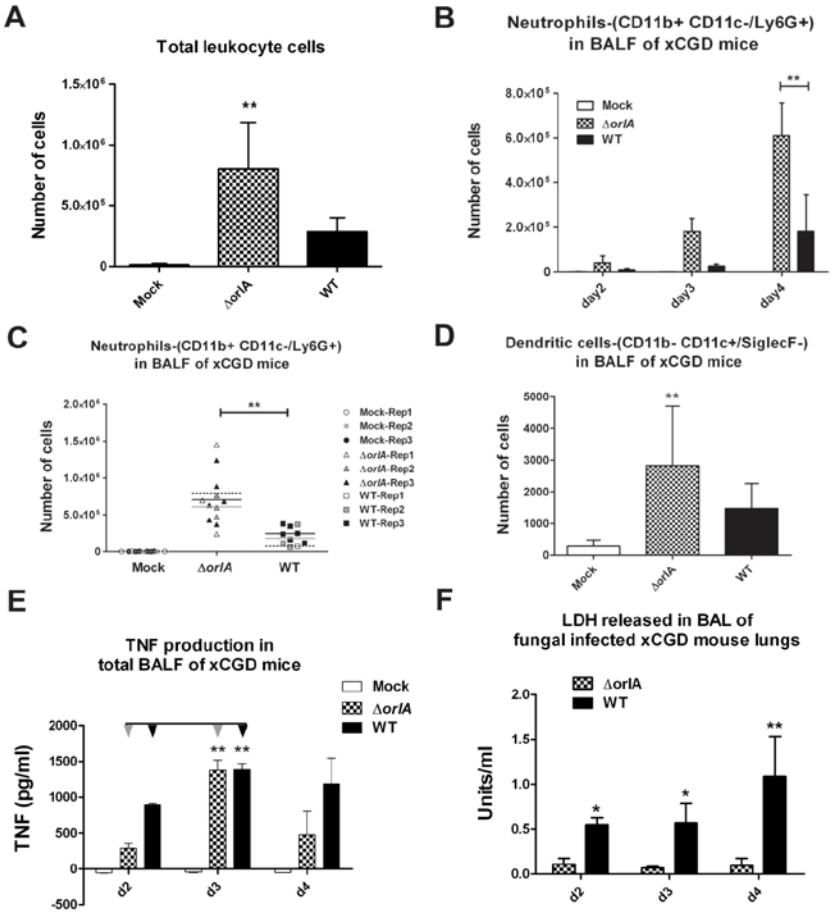

Figure 3.2. Neutrophil numbers and TNF production are increased in response to Δ*orlA* in xCGD murine model of Invasive Pulmonary Aspergillosis. A) xCGD mice were intranasally inoculated with $1x10^5$ conidia. Day 2, 3 and 4 post infection, mice were sacrificed and BAL samples were collected. Quantitation by flow cytometery shows a significant increase in total leukocytes in response to Δ*orlA* than WT CBS144.89 strain infected mice (***P* ≤ 0.05, n=6, day 4). B) Flow cytometry analysis measuring PMNs (neutrophils; CD11b+CD11c-/Ly6G+) in BAL fluid samples. Data from one representative experiment. A significant increase in PMNs in Δ*orlA* inoculated xCGD mice relative to WT is observed on day 4 (***P* ≤ 0.05). C) Cumulative quantitative data for PMN numbers from three independent studies on day 4 post infection (***P* ≤ 0.05, n=9). D) Beside neutrophils, dendritic cells (CD11b-CD11c+/SiglecF-) are significant elevated in Δ*orlA* inoculated xCGD mice relative to WT (***P* ≤ 0.05, n=6, day 4). E) ELISA analysis of TNF production in supernatants of BAL fluid. A significant increase in TNF production on day3 (***P* = 0.01) and decrease on day4 (*P* = 0.06) was observed in Δ*orlA* inoculated animals. F) *In vivo* release of Lactate Dehydrogenase (LDH) in BAL samples obtained from xCGD mice on d2, 3, and 4 post inoculation with wild type and Δ*orlA* strains indicating more lung damage is induced by WT infection than Δ*orlA (****P* ≤ 0.05, n=4, day 4; **P* = 0.06, n=3, day 2 and 3).

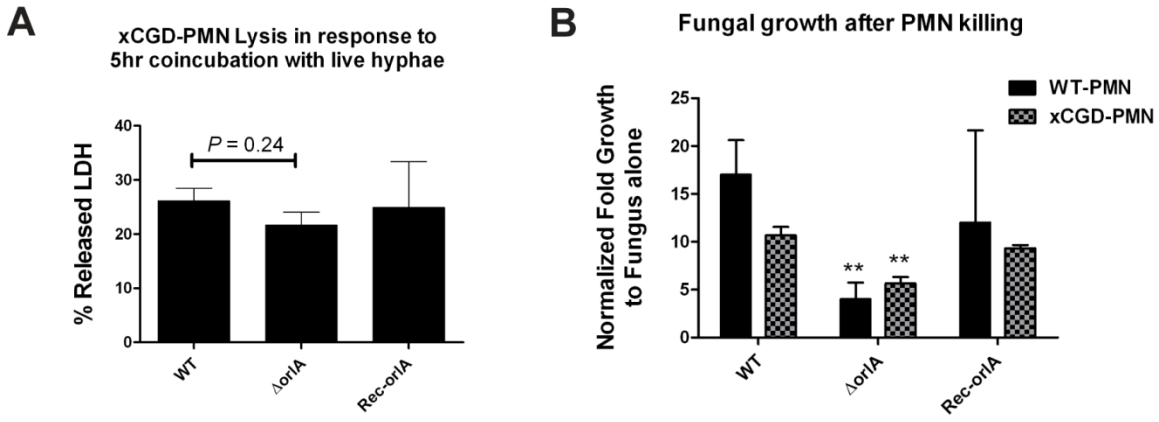

Figure 3.3. Δ*orlA* is more susceptible to damage induced by xCGD PMNs than Wild type *Aspergillus fumigatus.* A) *In vitro* PMNs Lysis assay was conducted in a 96 well plate. PMNs were isolated from bone marrow of xCGD mice and co-incubation with live hyphae and PMNs was at a 10:1 ratio with incubation at 37^{o}C in 5% CO2 for 5hr. After incubation, LDH release in the culture supernatant was measured. Δ*orlA* induced slightly less LDH production than wild type but this result was not significant (P = 0.24) . B) *In vitro* PMN killing of *A. fumigatus* strains was tested with PMNs obtained from wild type C57BL/6 and xCGD mice after a 3 hr co-incubation with PMNs (1:1 ratio). Fungal burden was analyzed via qPCR of *A. fumigatus* 18S rDNA after PMNs were removed from culture and fungi were allowed to grow in fresh media for an additional 3 hours. A significant decrease in fungal burden of Δ*orlA* was observed after co-incubation with either wild type or xCGD PMNs (**$P \leq 0.05$). Data was normalized to fungal burden of fungus grown alone in the absence of PMNs for each respective strain.

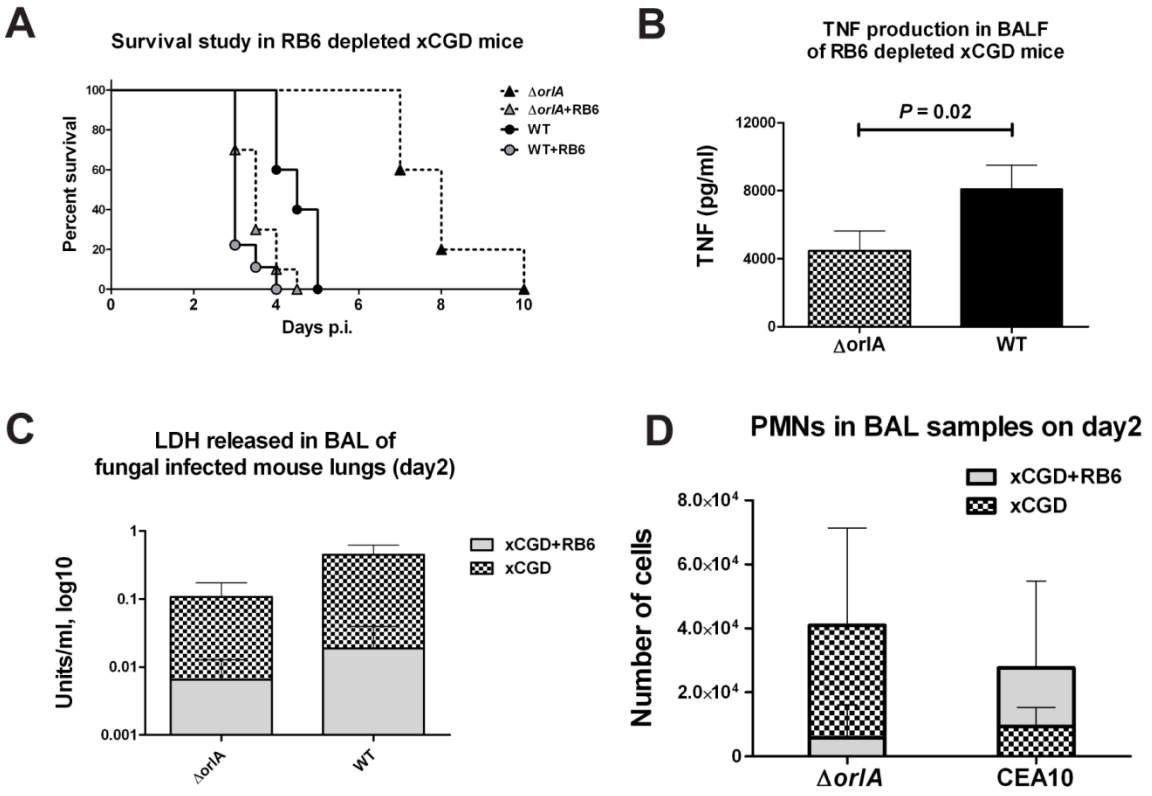

Figure 3.4. PMN Depletion in xCGD mice restores virulence of Δ*orlA*. A) Survival study of xCGD mice treated with intraperitoneal injection of monoclonal Ab RB6 (250µg of RB6) one day prior to intranasal inoculation of $1x10^5$ conidia and every day throughout course of infection in comparison to naïve xCGD mice. Log Rank Test $P \leq 0.01$; naïve vs RB6 treated mice of each respective strain indicates both strains are significant virulence in the absence of PMNs. Log Rank Test $P \leq 0.01$; Δ*orlA* vs WT in naïve xCGD mice indicates attenuated virulence of Δ*orlA* relative to WT in the presence of PMNs and $P > 0.05$; Δ*orlA* vs WT in RB6 treated xCGD mice indicates no significant different in virulence of Δ*orlA* and WT in the absence of PMNs. (B) ELISA analysis of TNF production induced by wild type and Δ*orlA* on day 2 post-inoculation in RB6 depleted animals ($P = 0.02$) C) *In vivo* Lactate Dehydrogenase (LDH) release in BAL samples suggesting that wild type *A. fumigatus* CBS144.89 caused greater lung damage than Δ*orlA* strain in both RB6 depleted animals and naïve xCGD mice ($P > 0.05$ and $P \leq 0.05$, respectively). A significant damage caused by WT occurred in naïve greater than RB6 treated mice, $P \leq 0.05$ and no significant damage caused by Δ*orlA*, $P > 0.05$ in this murine models. D) Flow cytometery analysis of PMNs population (Cd11b+Cd11c-/Ly6G+) in BAL samples suggesting that RB6 depletion causes lower PMN numbers into *Aspergillus* infected mouse lungs as expected from RB6 mediated PMN depletion.

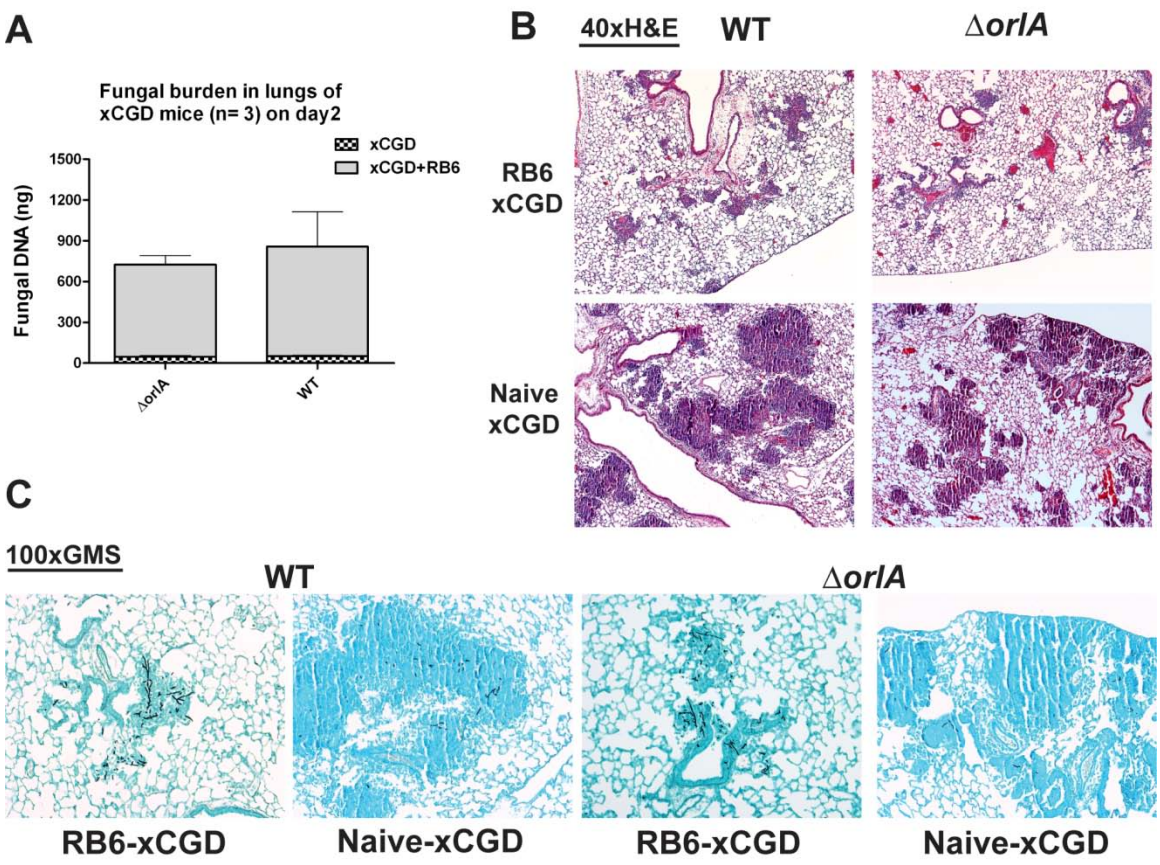

Figure 3.5. RB6 depleted mice show a large increase *in vivo* fungal burden and a concomitant diminished inflammatory response. A) Day 2 post infection, xCGD mice with and without RB6 depletion were sacrificed and fungal burden qPCR analysis of *A. fumigatus* 18s rRNA gene was performed on murine lungs. Δ*orlA* showed a slightly lower DNA fungal burden than in mice inoculation with WT strain, however this was not significant ($P > 0.05$). Depletion of PMNs allowed a substantial increase in fungal burden irrespective of the fungal strain used for inoculation ($P \leq 0.05$). B) Histopathology H&E stain in xCGD and RB6 treated xCGD animals shows less inflammation observed in RB6 treated mice inoculated with either the wild type or Δ*orlA* strain relative to control naïve xCGD mice (40 x magnification). C) Substantial increase in fungal burden as evidenced by increases in GMS stained hyphae corresponding to qPCR fungal burden data (100x magnification).

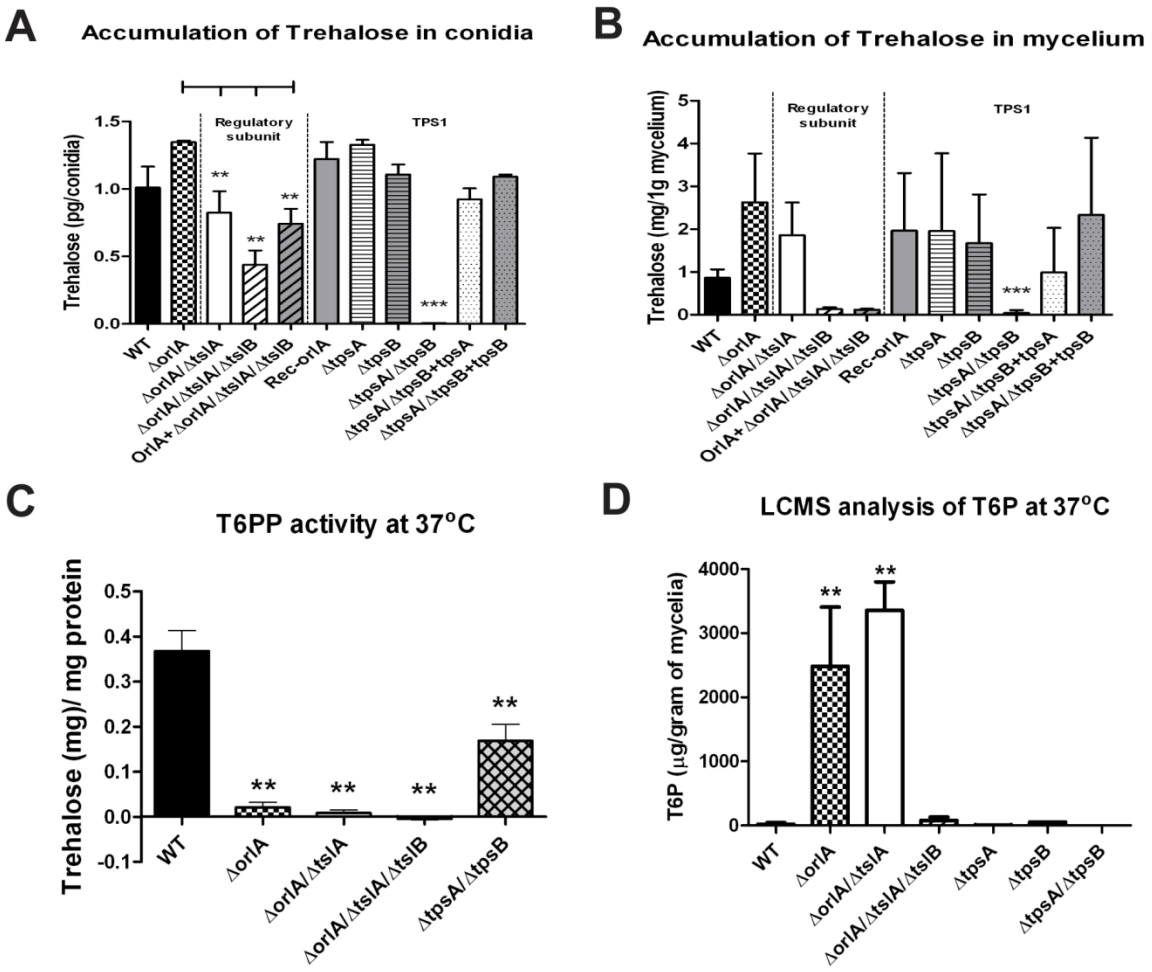

Figure 3.6. Loss of putative regulatory proteins TslA and TslB reduces Trehalose-6-phosphate accumulation and trehalose production in Δ*orlA* background. A-B) Quantitation of trehalose production via measuring of glucose production after trehalase enzyme treatment of cell free extracts in respective fungal strains. Conidia were harvested from cultures grown at 37^{o}C on Sorbitol Minimal Medium plates and B) Filtered mycelium biomass was obtained from 37^{o}C shake flask cultures in LGMM. Persistent trehalose production in Δ*orlA* is dramatically decreased in the absence of the two regulatory subunits (Δ*orlA* /Δ*tslA* /Δ*tslB*; ** $P \leq 0.05$ in comparison to Δo*rlA* strain) whereas abolished trehalose production is found in the Tps1 double mutant (Δ*tpsA*/Δ*tpsB*; *** $P \leq 0.05$ in comparison to wild type CBS144.89 strain. C) Trehalose-6-Phosphate Phosphatase enzyme activity assay of cell free mycelium extracts. No detectable T6PP activity was observed in the triple mutant Δ*orlA* /Δ*tslA* /Δ*tslB.* All mutants have significant decreased T6PP activity than WT, ** $P \leq 0.05$. D) Accumulation T6P intermediate in mycelial extracts quantified by LCMS analysis. Data are represented as mean+/- SD of three biological replicates.

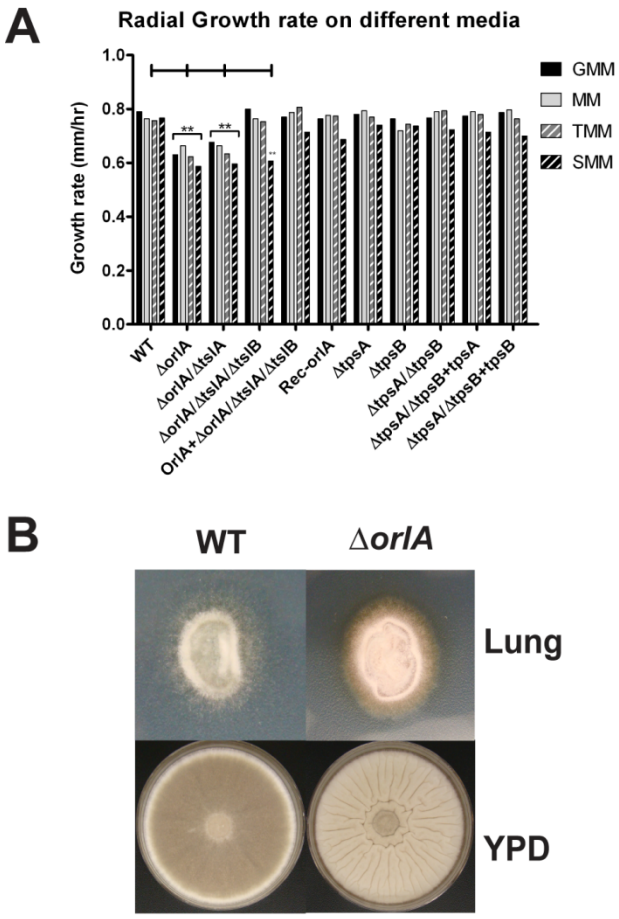

Figure 3.7. Loss of OrlA slightly attenuates *in vitro* growth on solid minimal media but not on lung explants or nutrient rich solid media. A) Radial growth assay was measured everyday after 5 □l of $1x10^6$ Conidia of test strains were placed on the center of specified minmal media: MM; minimal media without carbon source, TMM; 0.5% Trehalose minimal media, GMM; 1% Glucose minimal media and SMM; 1.2 M Sorbitol minimal media. An impaired growth rate of Δ*orlA* and Δ*orlA*/Δ*tslA* strains was observed on all tested media and is significant relative to wild type (**$P \leq 0.05$). Data are represented from the mean of three biological replicates. B) *In vitro* assay of nutritional versatility on a rich substrate Yeast Peptone Dextrose (YPD) media and mouse lung explants showing an aberrant morphological pattern but substantial growth of Δ*orlA* relative to wild type CBS144.89 strain.

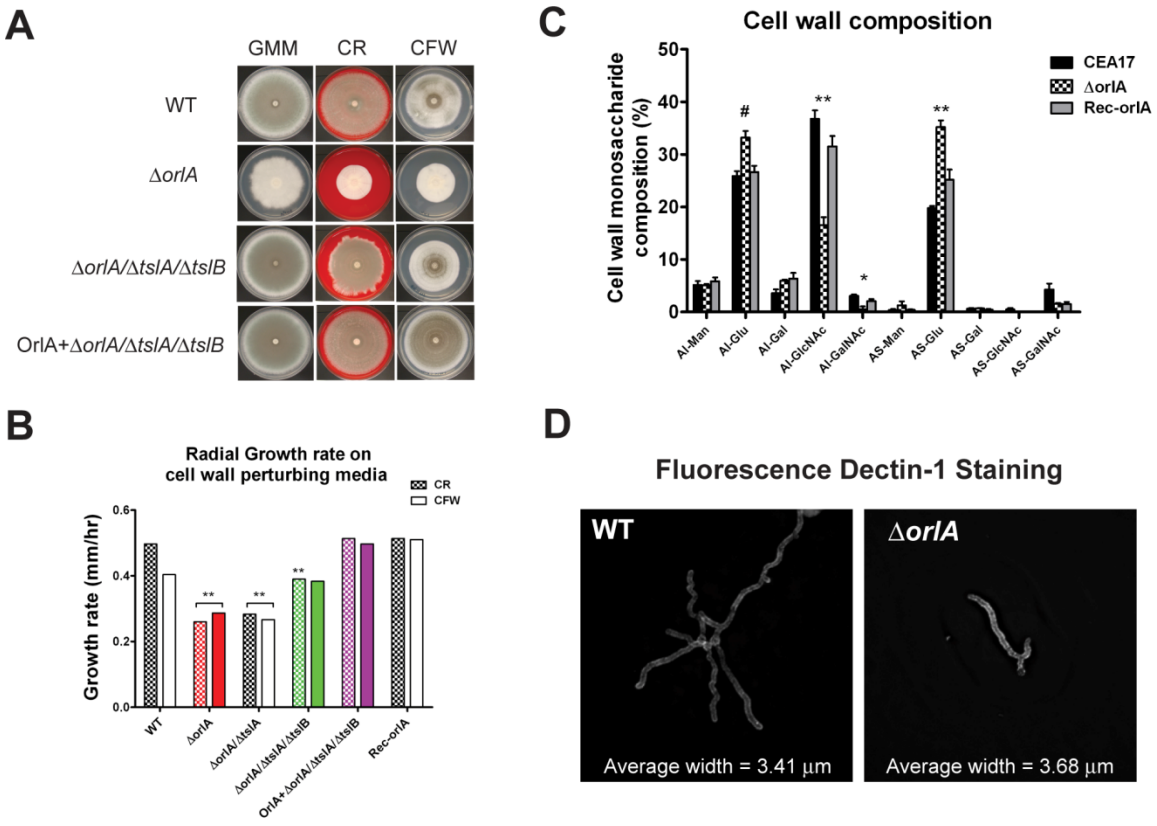

Figure 3.8. Loss of OrlA increases glucan content with a concomitant decrease in chitin that alters responses to cell wall perturbing agents mediated in part by T6P accumulation. A) Cell wall perturbing assay with concentrations of Congo Red (CR) (1mg/ml) and Calcofluor White (CFW) (25μg/ml) added to GMM agar. Plates were incubated at 37^{o}C for 6 days. A partial restoration of the wild type phenotype is observed in the mutant lacking both regulatory subunit proteins (TslA and TslB) in Δ*orlA* on both Congo Red (CR) and Calcofluor white (CFW). B) Growth rates of each fungal strain were generated from daily radial growth measurement as shown in A. C) Cell wall composition analyses showes the percentages of the Alkaline insoluble (AI) and Alkaline soluble fractions containing cell wall components: Man; Mannan, Glu; Glucose, Gal; Galactose, GlcNAc; N-acetylglucosamine, and GalNAc; N-acetylgalactosamine in comparison between CBS144.89 wild type, Δ*orlA*, and *orlA* reconstituted strain. Asterisks (**) indicate statistical significance between Δ*orlA* and respective strains; CEA17 and Rec-OrlA (pair t-test $P \leq 0.05$), and (*) asterisk indicates significant difference between Δ*orlA* and CEA17. Unpair t-test, (#) $P = 0.01$ indicates significant increase in β-glucan in Δ*orlA* relative to CEA17 background strain. D) Soluble dectin-1 staining shows a higher fluorescence in Δ*orlA* germlings relative to wild type CBS144.89.

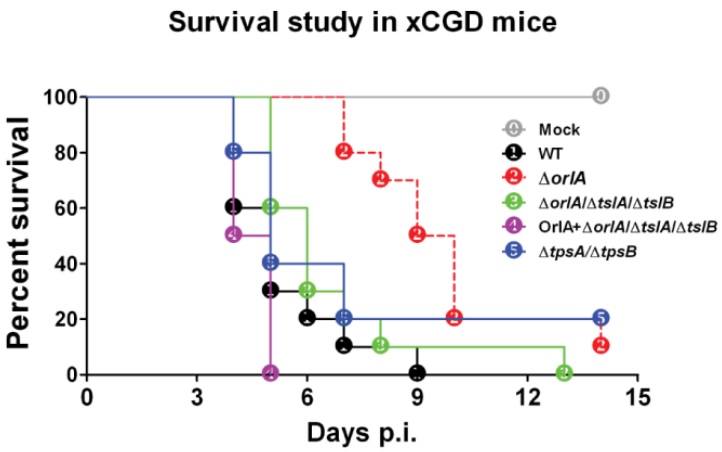

Figure 3.9. Increased β-glucan exposure and accumulation of T6P in Δ*orlA* cause *in vivo* attenuated fungal virulence in xCGD murine model of Invasive Aspergillosis. A) Survival analysis was performed in xCGD murine model of invasive pulmonary aspergillosis. Restored virulence and increased morbidity were observed in mice that were inoculated with Δ*orlA*/Δ*tslA*/Δ*tslB* (green dash line). Reconstitution of OrlA in this triple mutant (purple line) also demonstrated fully restored virulence and a non-significant difference to wild type *A. fumigatus* (P = 0.18). All tested strains are significantly virulent compare to Δ*orlA* (Log Rank Test, $P \leq 0.05$). Similar color codes represent tested strains in this virulence study and cell wall integrity analysis (Figure 3.8B), Red; Δ*orlA*, Green; Δ*orlA*/Δ*tslA*/Δ*tslB*, Purple; Rec-orlA (Δ*orlA*/Δ*tslA*/Δ*tslB*).

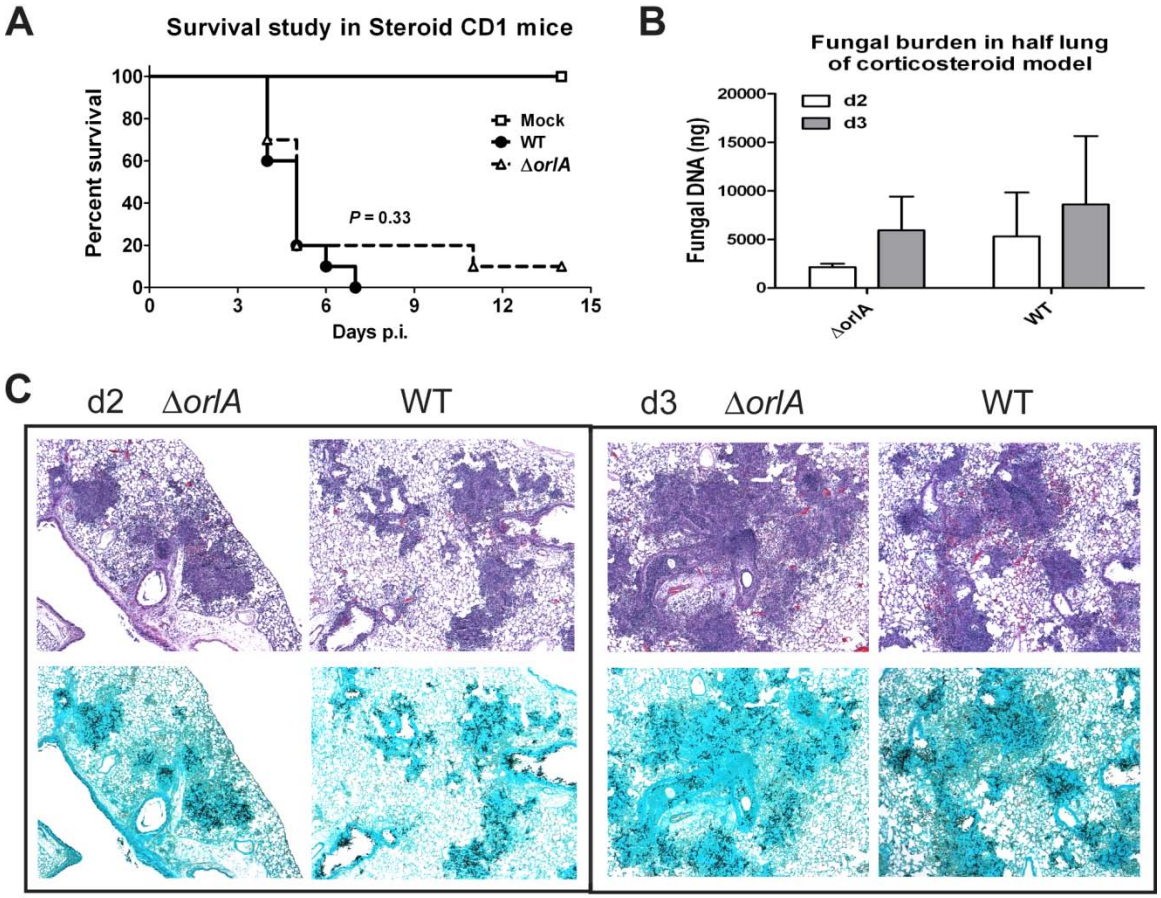

Figure 3.10. A) Survival study of corticosteroid immunosuppressed CD1 mice with $2x10^6$ conidia intranasal inoculation, Log Rank Test $P = 0.33$ indicates no significant difference in virulence between WT and Δ*orlA* in this model. B) Fungal burden qPCR analysis of *A. fumigatus* 18s rRNA gene in murine lungs, $P > 0.05$ for both time points indicating not significant difference in fungal burden between both strains on d2 and d3 in this murine model. C) Day 2 and 3 post infection in corticosteroid model standard H&E and GMS staining with 40x magnification.

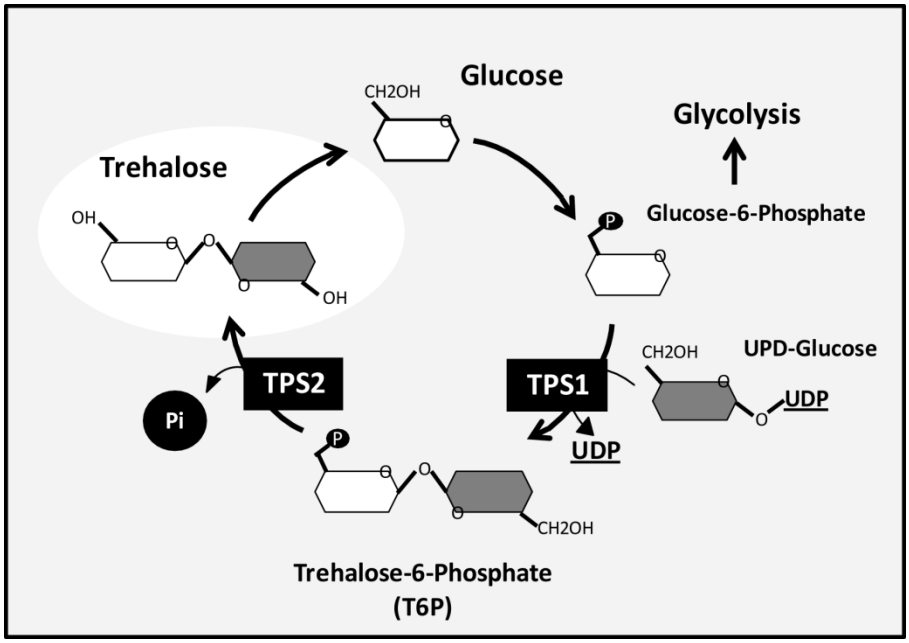

Figure 3.11. Schematic of the well characterized Trehalose biosynthesis pathway in *S. cerevisiae*. Trehalose is primarily synthesized by two enzymatic steps pathway (TPS1/TPS2). TPS1 or Trehalose-6-Phosphate Synthase transfers a glucosyl residue from UDP-glucose to Glucose-6-Phosphate to yield Trehalose-6-Phosphate (T6P). The intermediate T6P is subsequently dephosphorylated by the second catalytic enzyme, Trehalose-6-Phosphate Phosphatase; TPS2/OrlA, generating Trehalose sugar and free inorganic phosphate (Pi) products. Reserved disaccharide Trehalose is subsequently recycled into fungal metabolism by Trehalase enzymes (Table 3.1) and two molecules of glucose are converted to Glucose-6-Phosphate and reenter the glycolytic and trehalose biosynthesis pathways.

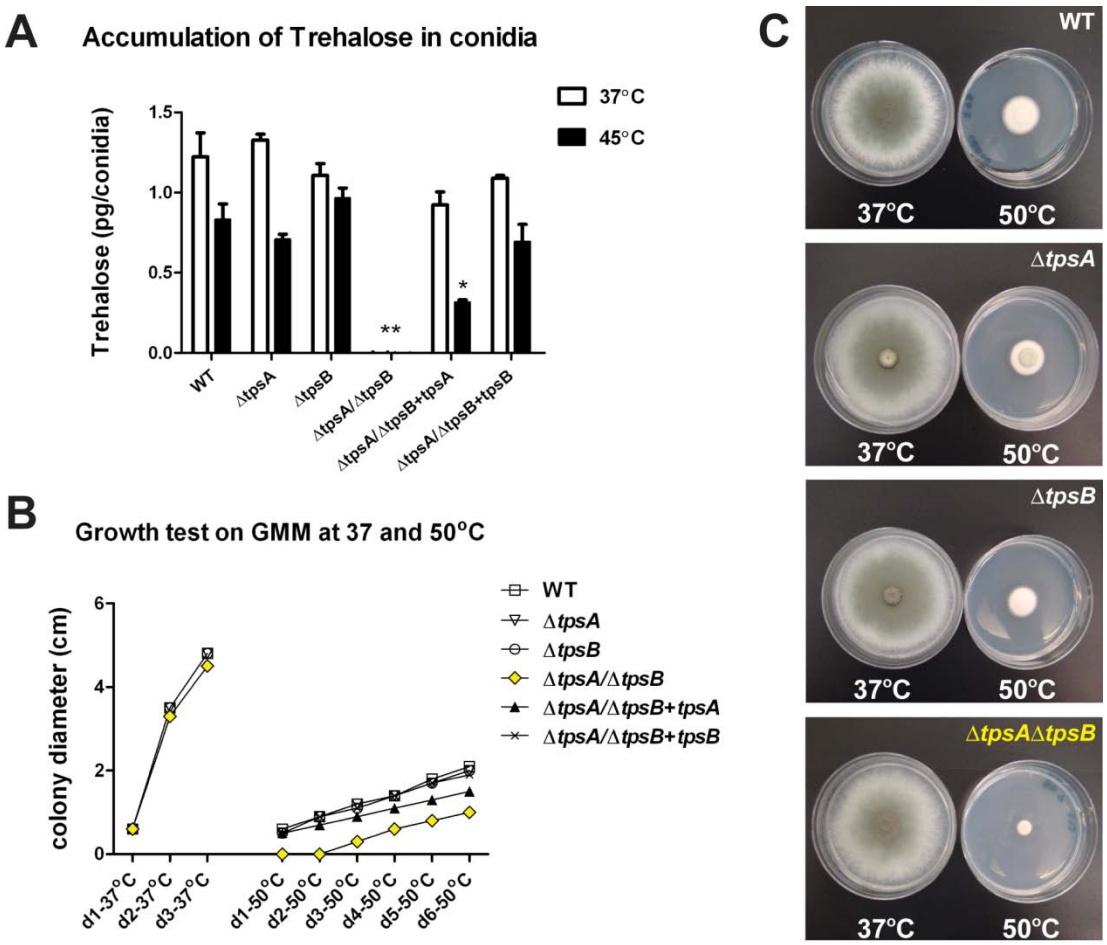

Figure 3.12. Trehalose is required for high temperature growth in *Aspergillus fumigatus*. A) Trehalose production in single mutants of Tps1 genes (TpsA and TpsB) are similar to wild type CBS144.89 strain. In contrast, double deletion of Tps1 (*tpsA*, *tpsB*) hads no accumulation of trehalose in the resting conidia in both conditions tested; $^{**}P \leq 0.05$ (glucose minimal media (GMM) at 37 ^{o}C, and SMM at 45^{o}C). B) Colony radial growth on GMM) after culture at 37^{o}C was similar in WT and mutants but high temperature (50^{o}C) incubation shows a growth defect in the double mutant lacking both *tpsA* and *tpsB* relative to wild type and single mutants. C) Growth on GMM plates shows wild type phenotype for all mutants at 37^{o}C and smaller colony size of double mutant *tpsA*/*tpsB* relative to WT and single mutants at 50^{o}C.

Literature cited

1. Maschmeyer G, Haas A, Cornely OA (2007) Invasive aspergillosis: epidemiology, diagnosis and management in immunocompromised patients. Drugs 67: 1567-1601.

2. Philippe B, Ibrahim-Granet O, Prevost MC, Gougerot-Pocidalo MA, Sanchez Perez M, et al. (2003) Killing of *Aspergillus fumigatus* by alveolar macrophages is mediated by reactive oxidant intermediates. Infect Immun 71: 3034-3042.

3. Hohl TM, Van Epps HL, Rivera A, Morgan LA, Chen PL, et al. (2005) *Aspergillus fumigatus* triggers inflammatory responses by stage-specific beta-glucan display. PLoS Pathog 1: e30.

4. Werner JL, Metz AE, Horn D, Schoeb TR, Hewitt MM, et al. (2009) Requisite role for the dectin-1 beta-glucan receptor in pulmonary defense against *Aspergillus fumigatus*. J Immunol 182: 4938-4946.

5. Cramer RA, Rivera A, Hohl TM Immune responses against *Aspergillus fumigatus*: what have we learned? Curr Opin Infect Dis 24: 315-322.

6. Denning DW (1998) Invasive aspergillosis. Clin Infect Dis 26: 781-803; quiz 804-785.

7. Kontoyiannis DP, Bodey GP (2002) Invasive aspergillosis in 2002: an update. Eur J Clin Microbiol Infect Dis 21: 161-172.

8. Walsh TJ, Anaissie EJ, Denning DW, Herbrecht R, Kontoyiannis DP, et al. (2008) Treatment of aspergillosis: clinical practice guidelines of the Infectious Diseases Society of America. Clin Infect Dis 46: 327-360.

9. Herbrecht R, Denning DW, Patterson TF, Bennett JE, Greene RE, et al. (2002) Voriconazole versus amphotericin B for primary therapy of invasive aspergillosis. N Engl J Med 347: 408-415.

10. Latge JP (2007) The cell wall: a carbohydrate armour for the fungal cell. Mol Microbiol 66: 279-290.

11. Romani L (2004) Immunity to fungal infections. Nat Rev Immunol 4: 1-23.

12. Balloy V, Chignard M (2009) The innate immune response to *Aspergillus fumigatus*. Microbes Infect 11: 919-927.

13. Reid DM, Gow NA, Brown GD (2009) Pattern recognition: recent insights from Dectin-1. Curr Opin Immunol 21: 30-37.

14. Latge JP (2010) Tasting the fungal cell wall. Cell Microbiol 12: 863-872.

15. Goodridge HS, Wolf AJ, Underhill DM (2009) Beta-glucan recognition by the innate immune system. Immunol Rev 230: 38-50.

16. Mora-Montes HM, Netea MG, Ferwerda G, Lenardon MD, Brown GD, et al. Recognition and blocking of innate immunity cells by Candida albicans chitin. Infect Immun 79: 1961-1970.

17. Chai LY, Vonk AG, Kullberg BJ, Verweij PE, Verschueren I, et al. *Aspergillus fumigatus* cell wall components differentially modulate host TLR2 and TLR4 responses. Microbes Infect 13: 151-159.

18. Tsoni SV, Brown GD (2008) beta-Glucans and dectin-1. Ann N Y Acad Sci 1143: 45-60.

19. Brown GD, Gordon S (2001) Immune recognition. A new receptor for beta-glucans. Nature 413: 36-37.

20. Brown GD, Herre J, Williams DL, Willment JA, Marshall AS, et al. (2003) Dectin-1 mediates the biological effects of beta-glucans. J Exp Med 197: 1119-1124.

21. Reeves EP, Lu H, Jacobs HL, Messina CG, Bolsover S, et al. (2002) Killing activity of neutrophils is mediated through activation of proteases by K+ flux. Nature 416: 291-297.

22. Steele C, Rapaka RR, Metz A, Pop SM, Williams DL, et al. (2005) The beta-glucan receptor dectin-1 recognizes specific morphologies of *Aspergillus fumigatus*. PLoS Pathog 1: e42.

23. Graham LM, Tsoni SV, Willment JA, Williams DL, Taylor PR, et al. (2006) Soluble Dectin-1 as a tool to detect beta-glucans. J Immunol Methods 314: 164-169.

24. Gerson SL, Talbot GH, Hurwitz S, Strom BL, Lusk EJ, et al. (1984) Prolonged granulocytopenia: the major risk factor for invasive pulmonary aspergillosis in patients with acute leukemia. Ann Intern Med 100: 345-351.

25. Avonce N, Mendoza-Vargas A, Morett E, Iturriaga G (2006) Insights on the evolution of trehalose biosynthesis. BMC Evol Biol 6: 109.

26. Cabib E, Leloir LF (1958) The biosynthesis of trehalose phosphate. J Biol Chem 231: 259-275.

27. Elbein AD, Pan YT, Pastuszak I, Carroll D (2003) New insights on trehalose: a multifunctional molecule. Glycobiology 13: 17R-27R.

28. Vuorio OE, Kalkkinen N, Londesborough J (1993) Cloning of two related genes encoding the 56-kDa and 123-kDa subunits of trehalose synthase from the yeast *Saccharomyces cerevisiae*. Eur J Biochem 216: 849-861.

29. De Virgilio C, Burckert N, Bell W, Jeno P, Boller T, et al. (1993) Disruption of TPS2, the gene encoding the 100-kDa subunit of the trehalose-6-phosphate synthase/phosphatase complex in *Saccharomyces cerevisiae*, causes accumulation of trehalose-6-phosphate and loss of trehalose-6-phosphate phosphatase activity. Eur J Biochem 212: 315-323.

30. Reinders A, Burckert N, Hohmann S, Thevelein JM, Boller T, et al. (1997) Structural analysis of the subunits of the trehalose-6-phosphate synthase/phosphatase complex in *Saccharomyces cerevisiae* and their function during heat shock. Mol Microbiol 24: 687-695.

31. Bell W, Sun W, Hohmann S, Wera S, Reinders A, et al. (1998) Composition and functional analysis of the *Saccharomyces cerevisiae* trehalose synthase complex. J Biol Chem 273: 33311-33319.

32. Thevelein JM (1984) Regulation of trehalose mobilization in fungi. Microbiol Rev 48: 42-59.

33. Crowe JH, Hoekstra FA, Crowe LM (1992) Anhydrobiosis. Annu Rev Physiol 54: 579-599.

34. Singer MA, Lindquist S (1998) Thermotolerance in *Saccharomyces cerevisiae*: the Yin and Yang of trehalose. Trends Biotechnol 16: 460-468.

35. Zaragoza O, Blazquez MA, Gancedo C (1998) Disruption of the *Candida albicans* TPS1 gene encoding trehalose-6-phosphate synthase impairs formation of hyphae and decreases infectivity. J Bacteriol 180: 3809-3815.

36. Zaragoza O, de Virgilio C, Ponton J, Gancedo C (2002) Disruption in *Candida albicans* of the TPS2 gene encoding trehalose-6-phosphate phosphatase affects cell integrity and decreases infectivity. Microbiology 148: 1281-1290.

37. Van Dijck P, De Rop L, Szlufcik K, Van Ael E, Thevelein JM (2002) Disruption of the *Candida albicans* TPS2 gene encoding trehalose-6-phosphate phosphatase

decreases infectivity without affecting hypha formation. Infect Immun 70: 1772-1782.

38. Foster AJ, Jenkinson JM, Talbot NJ (2003) Trehalose synthesis and metabolism are required at different stages of plant infection by *Magnaporthe grisea*. EMBO J 22: 225-235.

39. Petzold EW, Himmelreich U, Mylonakis E, Rude T, Toffaletti D, et al. (2006) Characterization and regulation of the trehalose synthesis pathway and its importance in the pathogenicity of *Cryptococcus neoformans*. Infect Immun 74: 5877-5887.

40. Wilson RA, Jenkinson JM, Gibson RP, Littlechild JA, Wang ZY, et al. (2007) Tps1 regulates the pentose phosphate pathway, nitrogen metabolism and fungal virulence. EMBO J 26: 3673-3685.

41. Ngamskulrungroj P, Himmelreich U, Breger JA, Wilson C, Chayakulkeeree M, et al. (2009) The trehalose synthesis pathway is an integral part of the virulence composite for *Cryptococcus gattii*. Infect Immun 77: 4584-4596.

42. Al-Bader N, Vanier G, Liu H, Gravelat FN, Urb M, et al. (2010) Role of trehalose biosynthesis in *Aspergillus fumigatus* development, stress response, and virulence. Infect Immun 78: 3007-3018.

43. Puttikamonkul S, Willger SD, Grahl N, Perfect JR, Movahed N, et al. (2010) Trehalose 6-phosphate phosphatase is required for cell wall integrity and fungal virulence but not trehalose biosynthesis in the human fungal pathogen *Aspergillus fumigatus*. Mol Microbiol 77: 891-911.

44. Borgia PT, Miao Y, Dodge CL (1996) The orlA gene from *Aspergillus nidulans* encodes a trehalose-6-phosphate phosphatase necessary for normal growth and chitin synthesis at elevated temperatures. Mol Microbiol 20: 1287-1296.

45. Blazquez MA, Lagunas R, Gancedo C, Gancedo JM (1993) Trehalose-6-phosphate, a new regulator of yeast glycolysis that inhibits hexokinases. FEBS Lett 329: 51-54.

46. Hohmann S, Bell W, Neves MJ, Valckx D, Thevelein JM (1996) Evidence for trehalose-6-phosphate-dependent and -independent mechanisms in the control of sugar influx into yeast glycolysis. Mol Microbiol 20: 981-991.

47. d'Enfert C (1996) Selection of multiple disruption events in *Aspergillus fumigatus* using the orotidine-5'-decarboxylase gene, *pyrG*, as a unique transformation marker. Curr Genet 30: 76-82.

48. Shimizu K, Keller NP (2001) Genetic involvement of a cAMP-dependent protein kinase in a G protein signaling pathway regulating morphological and chemical transitions in *Aspergillus nidulans*. Genetics 157: 591-600.

49. Yelton MM, Hamer JE, Timberlake WE (1984) Transformation of *Aspergillus nidulans* by using a trpC plasmid. Proc Natl Acad Sci U S A 81: 1470-1474.

50. Grahl N, Puttikamonkul S, Macdonald JM, Gamcsik MP, Ngo LY, et al. In vivo hypoxia and a fungal alcohol dehydrogenase influence the pathogenesis of invasive pulmonary aspergillosis. PLoS Pathog 7: e1002145.

51. Cramer RA, Jr., Gamcsik MP, Brooking RM, Najvar LK, Kirkpatrick WR, et al. (2006) Disruption of a nonribosomal peptide synthetase in *Aspergillus fumigatus* eliminates gliotoxin production. Eukaryot Cell 5: 972-980.

52. Yu JH, Hamari Z, Han KH, Seo JA, Reyes-Dominguez Y, et al. (2004) Double-joint PCR: a PCR-based molecular tool for gene manipulations in filamentous fungi. Fungal Genet Biol 41: 973-981.

53. Edavana VK, Pastuszak I, Carroll JD, Thampi P, Abraham EC, et al. (2004) Cloning and expression of the trehalose-phosphate phosphatase of Mycobacterium tuberculosis: comparison to the enzyme from *Mycobacterium smegmatis*. Arch Biochem Biophys 426: 250-257.

54. Ram AF, Klis FM (2006) Identification of fungal cell wall mutants using susceptibility assays based on Calcofluor white and Congo red. Nat Protoc 1: 2253-2256.

55. Feng X, Krishnan K, Richie DL, Aimanianda V, Hartl L, et al. HacA-independent functions of the ER stress sensor IreA synergize with the canonical UPR to influence virulence traits in *Aspergillus fumigatus*. PLoS Pathog 7: e1002330.

56. Richie DL, Hartl L, Aimanianda V, Winters MS, Fuller KK, et al. (2009) A role for the unfolded protein response (UPR) in virulence and antifungal susceptibility in *Aspergillus fumigatus*. PLoS Pathog 5: e1000258.

57. Lowell CA, Fumagalli L, Berton G (1996) Deficiency of Src family kinases p59/61hck and p58c-fgr results in defective adhesion-dependent neutrophil functions. J Cell Biol 133: 895-910.

58. Daley JM, Thomay AA, Connolly MD, Reichner JS, Albina JE (2008) Use of Ly6G-specific monoclonal antibody to deplete neutrophils in mice. J Leukoc Biol 83: 64-70.

59. Huppert M, Oliver DJ, Sun SH (1978) Combined methenamine-silver nitrate and hematoxylin & eosin stain for fungi in tissues. J Clin Microbiol 8: 598-603.

60. Li H, Barker BM, Grahl N, Puttikamonkul S, Bell JD, et al. The small GTPase RacA mediates intracellular reactive oxygen species production, polarized growth, and virulence in the human fungal pathogen *Aspergillus fumigatus*. Eukaryot Cell 10: 174-186.

61. Drent M, Cobben NA, Henderson RF, Wouters EF, van Dieijen-Visser M (1996) Usefulness of lactate dehydrogenase and its isoenzymes as indicators of lung damage or inflammation. Eur Respir J 9: 1736-1742.

62. Yamamoto Y, Gaynor RB (2001) Therapeutic potential of inhibition of the NF-kappaB pathway in the treatment of inflammation and cancer. J Clin Invest 107: 135-142.

63. Mabey JE, Anderson MJ, Giles PF, Miller CJ, Attwood TK, et al. (2004) CADRE: the Central Aspergillus Data REpository. Nucleic Acids Res 32: D401-405.

64. Arnaud MB, Cerqueira GC, Inglis DO, Skrzypek MS, Binkley J, et al. The *Aspergillus* Genome Database (AspGD): recent developments in comprehensive multispecies curation, comparative genomics and community resources. Nucleic Acids Res 40: D653-659.

65. Altschul SF, Gish W, Miller W, Myers EW, Lipman DJ (1990) Basic local alignment search tool. J Mol Biol 215: 403-410.

66. Cabib E, Roh DH, Schmidt M, Crotti LB, Varma A (2001) The yeast cell wall and septum as paradigms of cell growth and morphogenesis. J Biol Chem 276: 19679-19682.

67. Reese AJ, Yoneda A, Breger JA, Beauvais A, Liu H, et al. (2007) Loss of cell wall alpha(1-3) glucan affects Cryptococcus neoformans from ultrastructure to virulence. Mol Microbiol 63: 1385-1398.

68. Mouyna I, Morelle W, Vai M, Monod M, Lechenne B, et al. (2005) Deletion of GEL2 encoding for a beta(1-3)glucanosyltransferase affects morphogenesis and virulence in *Aspergillus fumigatus*. Mol Microbiol 56: 1675-1688.

69. Pollock JD, Williams DA, Gifford MA, Li LL, Du X, et al. (1995) Mouse model of X-linked chronic granulomatous disease, an inherited defect in phagocyte superoxide production. Nat Genet 9: 202-209.

70. Balloy V, Huerre M, Latge JP, Chignard M (2005) Differences in patterns of infection and inflammation for corticosteroid treatment and chemotherapy in experimental invasive pulmonary aspergillosis. Infect Immun 73: 494-503.

71. Gancedo C, Flores CL (2004) The importance of a functional trehalose biosynthetic pathway for the life of yeasts and fungi. FEMS Yeast Res 4: 351-359.

72. Bell W, Klaassen P, Ohnacker M, Boller T, Herweijer M, et al. (1992) Characterization of the 56-kDa subunit of yeast trehalose-6-phosphate synthase and cloning of its gene reveal its identity with the product of CIF1, a regulator of carbon catabolite inactivation. Eur J Biochem 209: 951-959.

73. Ruijter GJ, Panneman H, van den Broeck HC, Bennett JM, Visser J (1996) Characterisation of the *Aspergillus nidulans* frA1 mutant: hexose phosphorylation and apparent lack of involvement of hexokinase in glucose repression. FEMS Microbiol Lett 139: 223-228.

74. Panneman H, Ruijter GJ, van den Broeck HC, Visser J (1998) Cloning and biochemical characterisation of *Aspergillus niger* hexokinase--the enzyme is strongly inhibited by physiological concentrations of trehalose 6-phosphate. Eur J Biochem 258: 223-232.

75. Fleck CB, Brock M *Aspergillus fumigatus* catalytic glucokinase and hexokinase: expression analysis and importance for germination, growth, and conidiation. Eukaryot Cell 9: 1120-1135.

76. Flipphi M, van de Vondervoort PJ, Ruijter GJ, Visser J, Arst HN, Jr., et al. (2003) Onset of carbon catabolite repression in *Aspergillus nidulans*. Parallel involvement of hexokinase and glucokinase in sugar signaling. J Biol Chem 278: 11849-11857.

77. Steinbock F, Choojun S, Held I, Roehr M, Kubicek CP (1994) Characterization and regulatory properties of a single hexokinase from the citric acid accumulating fungus *Aspergillus niger*. Biochim Biophys Acta 1200: 215-223.

78. Panneman H, Ruijter GJ, van den Broeck HC, Driever ET, Visser J (1996) Cloning and biochemical characterisation of an *Aspergillus niger* glucokinase. Evidence for the presence of separate glucokinase and hexokinase enzymes. Eur J Biochem 240: 518-525.

79. Da Silva CA, Chalouni C, Williams A, Hartl D, Lee CG, et al. (2009) Chitin is a size-dependent regulator of macrophage TNF and IL-10 production. J Immunol 182: 3573-3582.

80. Fontaine T, Delangle A, Simenel C, Coddeville B, van Vliet SJ, et al. Galactosaminogalactan, a new immunosuppressive polysaccharide of *Aspergillus fumigatus*. PLoS Pathog 7: e1002372.

81. Henry C, Latge JP, Beauvais A alpha1,3 glucans are dispensable in *Aspergillus fumigatus*. Eukaryot Cell 11: 26-29.

82. Gastebois A, Fontaine T, Latge JP, Mouyna I (2010) beta(1-3)Glucanosyltransferase Gel4p is essential for *Aspergillus fumigatus*. Eukaryot Cell 9: 1294-1298.

83. Damveld RA, Arentshorst M, Franken A, vanKuyk PA, Klis FM, et al. (2005) The *Aspergillus niger* MADS-box transcription factor RlmA is required for cell wall reinforcement in response to cell wall stress. Mol Microbiol 58: 305-319.

84. Levin DE (2005) Cell wall integrity signaling in *Saccharomyces cerevisiae*. Microbiol Mol Biol Rev 69: 262-291.

85. Ram AF, Arentshorst M, Damveld RA, vanKuyk PA, Klis FM, et al. (2004) The cell wall stress response in *Aspergillus niger* involves increased expression of the glutamine : fructose-6-phosphate amidotransferase-encoding gene (gfaA) and increased deposition of chitin in the cell wall. Microbiology 150: 3315-3326.

86. de Nobel H, Ruiz C, Martin H, Morris W, Brul S, et al. (2000) Cell wall perturbation in yeast results in dual phosphorylation of the Slt2/Mpk1 MAP kinase and in an Slt2-mediated increase in FKS2-lacZ expression, glucanase resistance and thermotolerance. Microbiology 146 (Pt 9): 2121-2132.

87. Damveld RA, vanKuyk PA, Arentshorst M, Klis FM, van den Hondel CA, et al. (2005) Expression of agsA, one of five 1,3-alpha-D-glucan synthase-encoding genes in *Aspergillus niger*, is induced in response to cell wall stress. Fungal Genet Biol 42: 165-177.

88. Milewski S, Gabriel I, Olchowy J (2006) Enzymes of UDP-GlcNAc biosynthesis in yeast. Yeast 23: 1-14.

89. Munro CA, Whitton RK, Hughes HB, Rella M, Selvaggini S, et al. (2003) CHS8-a fourth chitin synthase gene of *Candida albicans* contributes to in vitro chitin synthase activity, but is dispensable for growth. Fungal Genet Biol 40: 146-158.

90. McIntosh M, Stone BA, Stanisich VA (2005) Curdlan and other bacterial (1-->3)-beta-D-glucans. Appl Microbiol Biotechnol 68: 163-173.

91. Clark AF, Villemez CL (1972) The Formation of beta, 1 --> 4 Glucan from UDP-alpha-d-Glucose Catalyzed by a Phaseolus aureus Enzyme. Plant Physiol 50: 371-374.

92. Mesak LR, Dahl MK (2000) Purification and enzymatic characterization of PgcM: a beta-phosphoglucomutase and glucose-1-phosphate phosphodismutase of *Bacillus subtilis*. Arch Microbiol 174: 256-264.

93. Cornish EJ, Hurtgen BJ, McInnerney K, Burritt NL, Taylor RM, et al. (2008) Reduced nicotinamide adenine dinucleotide phosphate oxidase-independent resistance to *Aspergillus fumigatus* in alveolar macrophages. J Immunol 180: 6854-6867.

94. Henriet SS, Hermans PW, Verweij PE, Simonetti E, Holland SM, et al. Human leukocytes kill *Aspergillus nidulans* by reactive oxygen species-independent mechanisms. Infect Immun 79: 767-773.

95. Londesborough J, Vuorio O (1991) Trehalose-6-phosphate synthase/phosphatase complex from bakers' yeast: purification of a proteolytically activated form. J Gen Microbiol 137: 323-330.

CHAPTER FOUR

TREHALOSE PHOSPHORYLASE IS REQUIRED FOR TREHALOSE MOBILIZATION AND FUNGAL GROWTH IN THE ABSENCE OF TREHALOSE 6 PHOSPHATE PHOSPHATASE IN *ASPERGILLUS FUMIGATUS*

Abstract

The persistent trehalose production observed in the absence of OrlA led to the hypothesis that an alternate trehalose biosynthesis pathway exists in *Aspergillus fumigatus*. This alternative pathway is characterized by the presence of two trehalose phosphorylase genes, *tpyA* and *tpyB.* This hypothesis was tested by generation of an *A. fumigatus* mutant that lacks OrlA and both Tpy enzyme encoding genes. Despite the loss of Tpy enzyme activity in the OrlA null mutant background, the triple mutant still produced significant amounts of trehalose, suggesting that Tpy enzymes are not responsible for the trehalose production in the *orlA* null mutant. Further enzyme assay analysis suggested that Tpy is involved in the mobilization of trehalose, or trehalose phosphorolysis, by a yet undetectable synthesis of trehalose that may be regulated by intracellular levels of inorganic phosphate. Further analysis of the trehalose synthase mutant, Δ*tps1*, strongly suggests that the TPS1/TPS2 pathway is the major producer of trehalose in *A. fumigatus*. Together with results previously reported in Chapter 3, we conclude that the persistent trehalose production observed in Δ*orlA* is likely generated by non-specific dephosphorylation of T6P or possibly another undefined trehalose biosynthesis pathway. Importantly, and in contrast to other human pathogenic fungi, the

results suggest that trehalose itself is not essential for *A. fumigatus* virulence in immunocompromised murine models of invasive pulmonary aspergillosis.

Introduction

Previously we have demonstrated that Trehalose-6-Phosphate Phosphatase (OrlA) catalyzes the second enzymatic step of the trehalose biosynthesis pathway but is not required for trehalose production in *A. fumigatus* [1] (Chapter 2 and 3). Thus, the main objective of the studies presented in this chapter is to further understand potential alternate mechanisms behind trehalose production in the human fungal pathogen *A. fumigatus.*

One putative mechanism involves the Tpy, or Trehalose Phosphorylase pathway, and has been well characterized in basidiomycete mushrooms [2,3]. Currently, Tpy enzymes have been characterized in various organisms such as alga, ascomycete yeast, basidiomycetes, and bacterial actinomycetes. These enzymes reversibly catalyze trehalose biosynthesis and trehalose phosphorolysis (Figure 1A) [2,4,5,6,7].

In the Ascomycete *Neurospora crassa*, characterization of Clock controlled gene 9 (Ccg-9) revealed extensive amino acid similarities to the Trehalose synthase/Phosphorylase of the basidiomycete *Grifola frondosa* [8]. The altered conidiophore morphology of the Ccg-9 null mutant suggested that Ccg-9 is involved in developmental morphogenesis of conidiation. Expression of Ccg-9 is upregulated during glucose deprivation, osmotic stress, and heat shock, which corresponds with the stress protectant role attributed to trehalose.

To date, the role of Tpy or Tpy homologs have not been characterized in other filamentous ascomycetes, such as *A. fumigatus*. In this study, we aim to further understand the role of trehalose in the biology and virulence of *A. fumigatus* by determining the mechanism of persistent trehalose production in Δ*orlA*.

Methods

Strains and Media

Aspergillus fumigatus strain CEA17 (a uracil auxotroph strain lacking *pyrG*) was used to generate single deletion mutants strain as listed in Table 1 [9]. The corresponding wild-type strain CBS144.89 was utilized throughout this study (the kind gift of Dr. Jean-Paul Latge). The Δ*orlA* strain was previously generated in Chapter 2 [1] and used as the background strain for additional deletion of putative genes involved in the trehalose phosphorylase alternate pathway; *tpyA*, *tpyB* genes. All strains (with the exception of the mutants generated by the Δ*orlA* background) were routinely grown in glucose minimal medium (GMM) containing a final concentration of 1% glucose, and if not stated otherwise, grown at 37°C [10]. Conidia were harvested after growth on appropriate solid media for 3 days at 37^{o}C. All mutants containing Δ*orlA* were grown in sorbitol minimal media (SMM; 1.2 M sorbitol, 1% glucose) and SMM was used as standard media in all experiments requiring conidia due to the restricted ability of Δ*orlA* to generate conidia on GMM.

Strain Construction

Mutant and reconstituted strains were generated by homologous recombination and standard polyethylene glycol mediated fungal protoplast transformation of *A. fumigatus* uracil auxotroph strain CEA17 and indicated mutants as shown in Table 2 [11]. PCR generated gene replacement constructs were utilized for specified mutations as stated in subsequent strategies. Gene replacements and reconstituted strains were generated as I have previously described [1,12,13]. Real time reverse transcriptase PCR was used to confirm expression of the re-introduced gene [14]. To generate a double mutant strain, I utilized a *pyrG*-marker recycling approach, in which a particular single mutation strain was regenerated with a 1 kb-*Pst*I truncated *pyrG* homologous replacement construct. An additional *pyrG+* knockout construct of a second GOI (gene-of-interest) was generated as a single mutation approach and transformed into the recreated (*pyrG*$^{-}$) single mutant strain to obtain the double mutant [ex. Δ*orlA(pyrG-)/*Δ*tpyA(pyrG+)]* strain. Following the *pyrG* recycling approach, I utilized *Hph*; a hygromycin B marker, to generate the third gene deletion by a nested PCR approach [13].

In vitro Germination Assay

Germination time courses were performed using shaking cultures in which $1x10^7$ conidia/ml were incubated in liquid GMM at 37^oC/300 rpm. To assess germination, 500 µl of culture was aliquoted at various timepoints following inoculation. These aliquots were homogenized briefly in a bead beater with 0.1mm glass beads, for 30 seconds at indicated timepoints every 30 min from 3-7 hrs of incubation. The percentage of germination was scored based on the visualization of germ tubes elongation from

conidia.. Statistical significance ($P \leq 0.05$) was determined via paired two-tailed Student's *t*-test.

In vitro Conidial Viability upon Cold Storage

Freshly harvested conidia were diluted with distilled water to obtain $2x10^3$ conidia/ml and store at 4^oC. 100 µl aliquots were taken on day 0, 3, 5, 10, 20, 30, 60, 90, and 120 after storage, and were spread onto Sabouraud plates (in triplicate). After overnight incubation at 37^oC, colonies were counted for viability, and recorded as percent survival when compared with day 0 [15]. Statistical significance ($P \leq 0.05$) was determined with a paired two-tailed Student's *t*-test.

Trehalose Measurement and
Trehalose Breakdown Determination

A. fumigatus strains were grown on SMM plates for 3 days at 37°C prior to harvesting conidia in 0.01% Tween80 for further analysis.Trehalose was measured from condial or mycelial cultures as described in chapter 3.

Trehalose hydrolysis was measured in conidia cultured in liquid GMM at 37^oC/300 rpm. Ten milliliters of $2x10^8$ conidia were harvested at indicated timepoints (0, 0.5, 1, 2, 4, and 6 hr) by centrifugation at 4,000 rpm/10 min. Following centrifugation, the conidial pellet was washing twice with distilled water and resuspended in 500 µl of distilled water. Trehalose extraction and measurement was performed as previously mentioned in chapter 3. Statistical significance ($P \leq 0.05$) was determined with a paired two-tailed Student's *t*-test.

LCMS Analysis of T6P

Mycelia extractions with Methanol:Dichloromethane:Water solution were performed as previously described [1]. Quantitation of [T6P extracts] was carried out via UHPLC-ESI-MS with an Agilent 1290 LC system coupled to an Agilent 6538 QTOF as previously described in chapter 3. The concentration of T6P was normalized to the input weight of fungal tissue for each sample. Results from triplicate experiments were averaged, standard deviation calculated, and statistical significance was determined ($P \leq 0.05$) with a paired two-tailed Student's t-test.

Trehalose-6-Phosphate Phosphatase
(T6PP) Enzyme Assays

The activity of T6PP was determined in mycelia extracts by measuring trehalose production in the reaction as previously described in chapter 3. Data presented are the mean and standard deviation of three biological replicates. Statistical significance ($P \leq 0.05$) was determined with a paired two-tailed Student's *t*-test.

Radial Growth Rate and Cell
Wall Perturbation Agents

Growth tests on different carbon sources (MM, GMM, TMM, and SMM), or cell wall inhibitors (CR, and CFW) were prepared and performed as previously described in chapter 3. Results are an average of triplicate experiments, and statistical significance ($P \leq 0.05$) was determined with a paired two-tailed Student's *t*-test.

Trehalose Phosphorylase (TPY) Enzyme Assays

Mycelial crude extracts were cultivated and prepared like the T6PP enzyme extraction exceptt that the extraction buffer consisted of two volumes (1:2, w/v) of 20 mM MES buffer, pH 6.8 containing 4mM EDTA, 2mM mercaptoethanol, and 40% (v/v) glycerol [5]. The phosphorolysis activity of the Tpy enzyme in the degradation of trehalose substrate into glucose and G1P products was determined by mesuring the amount of liberated glucose in the reaction which is proportional to the phosphorolysis activity of the Tpy enzyme. Following 30 min incubation at 30^{o}C, the 500 µl reaction mixtures containing 50 mM Trehalose, 50 mM Potassium Phosphate Buffer, pH 7.0, and 300 µl precleaned extract then underwent 3 min heat inactivation by boiling. Cell free extracts were then used to measure liberated glucose according to the Glucose Assay Kit protocols (Sigma Aldrich).

The contribution of Tpy to Trehalose synthesis was indirectly determined via the release of inorganic phosphate (Pi). 15 µl of precleaned crude extract was combined with two substrates, 50 mM glucose and 50 mM α-G1P, then assayed after 30 minutes at 30^{o}C. Total Pi generated in the reaction was quantified by total consumption in the purine nucleoside phosphorylase (PNP) enzymatic reaction method as described in EnzChek Phosphate Assay Kit (Molecular Probes). Experimental controls included a no-substrate and no-crude extract in order to determine the synthetic activity of the Tpy enzyme.

Alternatively, Trehalose synthesis activity was directly measured by glucose assay (Sigma Aldrich). After Trehalase treatment of the sample, Glucose and Trehalose

levels were monitored; where increase of Trehalose and decrease of Glucose substrate indicated new Trehalose synthesis.

Pi Assay

Inoculums of $1x10^7$conidia/ml were cultivated in 50ml liquid GMM at 37^oC overnight. Mycelia were then harvested, washed with sterile water, and collected with vacuum filtration prior to lyophilization. Dried mycelia tissues were powdered by mortar and pestle and 50 mg of powdered mycelia was then reconstituted in 1 ml of sterile water. The cell free extracts were prepared by vortexing and the clear supernatant was collected after centrifugation at 13,000 rpm for 10 minutes. Pi was measured by utilizing an enzyme assay with the purine nucleoside phosphorylase (PNP) method following the manufacturer's protocol as described in EnzChek Phosphate Assay Kit (Molecular Probes). The cell free extracts were diluted to fall within the standard curve limits; 1:40 dilutions were optimized with mycelia samples.

Virulence Test in Waxworm Model

Healthy *Galleria mellonella* larvae were inoculated with resting conidia by injecting 5 µl suspension of $1x10^5$ conidia into the haemocoel through the last pro-leg using a Hamilton syringe/needle (Hamilton, Reno, NV). Control waxworm larvae were inoculated with tween diluent. Twenty larvae were used for each group and larvae were maintained in wood shaving-filled Petri dishes in the dark at 37^oC and monitored for mortality daily [16]. The experiment was repeated independently; the mean value of three independent experiments was representing with log rank test statistic analysis.

Murine Virulence Tests

Two distinct therapeutically immunosuppresed murine models of CD1 mice (chemotherapeutic and corticosteroid) and one genetic knockout mouse model were used as previously described in chapter 2 and 3 [12]. A log rank test was used for pair wise comparisons of survival among the experimental groups, $P \leq 0.05$. Mouse experiments for each model were repeated at least twice with similar results. Results presented are from one representative experiment for each model. All animal procedures and protocols were approved by the MSU Institutional Animal Care and Use Committee.

Histopathology

Additional murine experiments were conducted for histopathology analyses at day four post-inoculation. Three mice in each group were humanely euthanized. Whole lungs were harvested from each mouse and fixed in 10% formalin prior to embedding in paraffin, 5 μm thick sections were taken, and stained with either H&E (Hematoxylin and Eosin) or GMS (Gomori's Methenamine Silver) [17]. Microscopic examination was performed on a Zeiss Axioscope2-plus microscope and engaged imaging system. Pictures were captured at 40x magnification as indicated in each image.

Results

TPY Pathway Does Not Play a Role in Trehalose Production of Δ*orlA*

Previous observations revealed an increase in the mRNA abundance of the uncharacterized *tpyA* and *tpyB* genes in the absence of Δ*orlA* (Table 4.1, and Chapter 2-

Figure 2.7). Thus, we hypothesized that Δ*orlA* is able to produce trehalose via TpyA and TpyB, in a putative alternative trehalose biosynthesis pathway, and that this alternative pathway is responsible for the persistent trehalose production observed in Δ*orlA.*

The amino acid sequences revealed by Bioinformatic identification indicate that TpyA and TpyB are larger in size than Tps1, but smaller than Tps2 enzymes and highly diverged (Table 4.1, Figure 4.1B) [18,19,20]. The amino acid sequences of the predicted Glycosyltransferase_GTB_type domain of *A. fumigatus* Tpy genes (AF_TpyA, AF_TpyB) were analyzed by multiple alignment with the GT1-Trehalose Phosphorylase domain of Basidiomycetes; *Pleurotus spp.*, *Grifola frondosa*, and *Schizophyllum commune* and a representative strain of bacteria, *Sulfolobus solfataricus* (Figure 4.2). The Glycosyltransferase_GTB_type domain of *A. fumigatus* had 54% similarity to the conserved GT1 Trehalose Phosphorylase domain of *G. frondosa* at amino acids level. Activity of Tpy enzymes has never been described in *S. cerevisiae*, it was however identified in yeast *Pichia fermentans, P. quercuum,* and *P. rhodanensis* without amino acid sequences analysis [7].

In addition, we analyzed the amino acid alignment of the Clock-controlled-9 protein of *Neurospora crassa,* which encodes a Trehalose Synthase that is predicted to be a Tpy homolog of the basidiomycete *G. frondosa* [8], and Ccg-9 homologs in *Magnaporthe oryzae,* and *A. nidulans* with AF_TpyA and AF_TpyB [21]. In *N. crassa,* Ccg-9 mRNA was induced upon encountering stress, and a Ccg-9 null mutant has both a conidiation and circadian rhythm defect [8]. The *ccg-9* homologs in *M. oryzae* and *A. nidulans* remain uncharacterized [21]. Based on domain homology, TpyA and TpyB may

possess similar Trehalose Phosphorylase enzyme activity, and be involved in the biosynthesis of trehalose.

To test the hypothesis that persistent trehalose production in Δ*orlA* was due to increased activity of Trehalose Phosphorylases (Tpy), null mutants of TpyA (AFUB_037080), and TpyB (AFUB_062450) were constructed in the Δ*orlA* background (Table 4.1 and 4.2). Both double mutant strains; *ΔorlA/ΔtpyA* and *ΔorlA/ΔtpyB* germinated significantly faster than the wild type strain and exhibited increased viability upon prolonged storage in water at 4^{o}C, and a significantly greater survival of colonies after 4 months storage (Figure 4.3A-B). Surprisingly, these null mutant strains contained a comparable amount of trehalose in conidia and mycelium to the parental Δ*orlA* strain (P>0.05), and a higher amount of trehalose than the wild type (P≤0.05, Figure 4.4A-B).

Accordingly, we next hypothesized that the two putative Tpy orthologs play a redundant role in trehalose production in the absence of OrlA. To address this hypothesis, we generated a triple mutant lacking OrlA, TpyA, and TpyB. In this strain, no defect in trehalose production or or impaired germination and viability was observed (Figure 4.3A-B, 4.4A-B). Additionally, residual activity of Trehalose-6-Phosphate Phosphatase (T6PP) was detected in all mutants derived from the Δ*orlA* background as expected (Figure 4.3C). In contrast to *A. fumigatus* wild type, all mutations of Tpy encoding enzymes in the absence of OrlA revealed substantial levels of T6P similar to the Δ*orlA* background (Figure 4.4D). Taken together, these data suggest that Tpy enzymes in *A. fumigatus* do not contribute to the persistent trehalose production in the absence of OrlA, and their loss does not affect the Tps1/Tps2 canonical trehalose biosynthesis pathway in *A. fumigatus*.

High Level of Intracellular Phosphate Ion
Regulates TPY Dependent Degradation of Trehalose

Unlike T6PP activity, in basidiomycete mushrooms the Tpy enzyme catalyzes reversible Trehalose synthesis and degradation [2,6]. Tpy activity in all mutants was determined by measuring both synthesis and degredation of trehalose metabolism. The Tpy/OrlA mutant (Δ*orlA*/Δ*tpyA*/Δ*tpyB*) had a significant decrease of liberated glucose, indicating trehalose degradation, when compared to the parental Δ*orlA* strain ($P \leq 0.05$). None of the mutants had a significant difference in Tpy enzyme activity of trehalose synthesis or liberated Pi level compared to wild type ($P > 0.05$, Figure 4.5A). Thus, as no difference in Tpy synthesis activity was observed among any of the strains, suggesting that either TypA/TpyB in *A. fumigatus* did not contribue to trehalose biosynthesis activity or that the reaction conditions were not sensitive enough to detect changes in synthesis activity (Figure 4.5B).

Activity of Tpy enzymes has been suggested to rely upon the level of intracellular inorganic phosphate (Pi) [2,6]. However, approximately 20-30 mM of Pi was detected in myeclium (Figure 4.5C), which was higher than the reported threshold level for Tpy synthesis activity to be inhibited by Pi (5 mM). Together, these data suggest that Tpy enzymes in *A. fumigatus* are important in trehalose degradation, particularly in the absence of OrlA (Δ*orlA*), but not in trehalose biosynthesis in *A. fumigatus* under the examined conditions.

Defective Trehalose Degradation
in The Absence of Tpy Genes

The above data suggests that Tpy enzymes may play an important role in trehalose degradation. To determine whether decreased Tpy activity of Δ*orlA*/Δ*tpyA*/Δ*tpyB* also indicates the *in vivo* capacity to break down trehalose in this strain, we next tested the ability of all mutants to utilize trehalose as a sole carbon source. Accordingly, lack of both putative orthologs of Tpy (Δ*orlA*/Δ*tpyA*/Δ*tpyB*) had a dramatic impairment in radial growth on minimal medium lacking a defined carbon source (thus only intracellular trehalose is available for initial growth) and minimal media containing 0.5% trehalose as an extracellular carbon source (Figure 4.6A). While the double mutant strains *ΔorlA/ΔtpyA* and *ΔorlA/ΔtpyB* showed a similar conidiation defect and normal growth rate to the parental *ΔorlA* strain on glucose minimal media (GMM), the triple mutant strain (*ΔorlA/ΔtpyA/ΔtpyB*) had a significant growth defect on GMM, MM, and TMM (Figure 4.6A-B). Similarly, the radial growth and conidiation defects of all mutants were dramatically restored on Sorbital minimal media as observed in the parental *ΔorlA* strain, (Figure 4.6A). Interestingly, cell wall homeostasis and colony morphology were significantly impaired to the parental Δ*orlA* in the Tpy pathway mutants (*ΔorlA/ΔtpyA/ΔtpyB*) and this more prominent phenotype was in contrast to those containing a functional Tpy pathway (Figure 4.6). These data further support my hypothesis that T6P accumulation and trehalose degradation is critical for cell wall formation in *A. fumigatus*. Taken together, the data suggests that Tpy enzymes play an important role in degradation of trehalose, and that the absence of Tpy enzymes impairs

both fungal metabolism and cell wall biosynthesis under conditions where trehalose is needed for growth.

In addition, loss of *tpyA* and *tpyB* in Δ*orlA* strikingly decreased the mobilization of accumulated trehalose in conidia during cultivaion inliquid glucose minimal media at 37^{o}C. In wild type, trehalose was completely consumed or degraded within 30 minutes of cultivation, whereas only 60% of accumulated trehalose was degraded after 4 hr of incubation in Δ*orlA* (Figure 4.7). In the *ΔorlA/ΔtpyA/ΔtpyB* strain, an additional decrease in the dagradation of Trehalose was observed compared to the parental Δ*orlA* background. This result supports the hypothesis that Tpy enzymes in *A. fumigatus* are involved in the degradation of trehalose.

Trehalose Product and Tps1 Do Not Contribute to *A. fumigatus* Virulence

We previously determined the role of Tps1 encoding genes on the trehalose production and showed that the two putative Tps1 orthologs, TpsA and TpsB, have overlapping function and are required for Tps1 activity to synthesize both T6P and trehalose (Chapter 3). We also observed that Tps1 mutants germinated significantly faster than wild type, whereas prolonged storage at 4^{o}C reduced their survival (Figure 4.8). However, because the loss of OrlA (Tps2) did not attenuate trehalose production in *A. fumigatus*, and with the marked accumulation of T6P in that strain, the question of whether trehalose itself was required for *A. fumigatus* remained. Here, in the *A. fumigatus CBS144.89* background, we next explored the hypothesis that Tps1 dependent trehalose

production is a key factor in the pathogenesis of *A. fumigatus* in immune compromised murine models of invasive pulmonary aspergillosis.

To further examine the role of trehalose in *A. fumigatus* virulence, we first tested the virulence phenotype of single and double mutants of the Tps1 encoding genes (*tpsA* and *tpsB)* in the invertebrate (*Galleria mellonella*) larvae [16,22]. All waxworms inoculated with Tps1 mutants and wild type displayed comparable levels of mortality between the respective groups, suggesting that the Tps1 mutants were not required for *A. fumigatus* virulence in this insect model (Figure 4.9). Next, we tested the virulence of the Tps1 mutants in three immunologically distinct murine models of IPA; xCGD mice, chemotherapeutic and corticosteroid models (as described previously in chapter 2 and 3). In all 3 murine models, the *tpsA/tpsB* double mutant displayed a wild type level of virulence as determined by mortality (Figure 4.10A-C). Histopathological lung sections analyzed with GMS staining revealed an aggressive infection of fungal hyphae and H&E stains showed substantial areas of inflammation and lung damage in mice inoculated with all examined strains (Figure 4.10D). Thus, these data suggest that neither Tps1 nor trehalose production itself is required for full virulence of *A. fumigatus* in the animal and insect models examined here.

Discussion

The TPS1/TPS2 pathway of trehalose biosynthesis has been well characterized in *S. cerevisiae* and bacteria, and there are four additional pathways that can produce trehalose from different monosaccharide substrates which have been studied in various

organisms [3,23]. In human yeast pathogens, TPS1 and TPS2 encoding genes have been initially characterized and it was reported that this pathway is responsible for trehalose production and was a significant contributator to fungal pathogenesis [24,25,26,27,28]. However, in the mold *A. fumigatus* I found (Chapter 2 and 3) that the Tps2 ortholog OrlA is required for virulence but dispensable for trehalose production [29]. Thus, a major question of my dissertation that remained was whether trehalose itself was critical for *A. fumigatus* biology and virulence as in the yeast pathogens *Candida albicans* and *Cryptococcus neoformans*. In this chapter, we characterized for the first time in a filamentous Ascomycete, the role of predicted Trehalose Phosphorylase enzymes in trehalose biosynthesis in the absence of OrlA.

Previously, intracellular concentrations of free inorganic phosphate (Pi) were shown to play a critical role in regulation of *in vivo* Trehalose phosphorylase (Tpy) activity. The degradation of trehalose appreared to be strictly dependent on a high Pi (Km=4.7mM) whereas the synthesis of trehalose was strongly inhibited by lower Pi concentrations (Ki=2mM) [2]. Despite the ability of Tpy enzymes to catalyze both degradation and synthesis activities *in vitro*, in the Basidiomycetes *Flammulina velutipes* and *Catellatospora ferruginea* only one active direction in either degradation or synthesis, is observed [4,6]. *Agaricus bisporus*, the Basidiomycete white button mushroom, relies solely on the Tpy pathway for trehalose metabolism due to absence of the canonical TPS1/TPS2 pathway and trehalase enzyme [2]. In this organism, Tpy can perform both synthesis and degradation of trehalose depending on the physiological conditions *in vivo*. Free Pi concentration varied from 2-5 mM in the mycelium, to 5-20

mM in the fruiting bodies, and correlated to the metabolism of trehalose in this mushroom. Trehalose is synthesized and accumulated in the mycelium (low Pi) until a threshold concentration is reached and translocated to the emerging fruiting bodies where it is degraded (high Pi) and yielding glucose and G1P energy source for development of the fruiting bodies.

In *A. fumigatus*, both genes encoding Tpy enzymes are required for trehalose degradation activity but appear to be dispensable in the direction of trehalose synthesis. Initially, I anticipated that the significant lower level of Pi observed in Δ*orlA* plays a stimulatory role and activation of trehalose biosynthesis in Δ*orlA* [1]. The result showed that the available free Pi in mycelium tissue that used in the enzyme assay was measured to be in the range of 25-30 mM. This amount is higher than required for an inhibitory effect of Pi (80% inhibition) on trehalose synthesis in *A. bisporus* [2]. Thus, the natural high Pi levels found in *A. fumigatus* may drive Tpy enzyme activity towards the degradation of trehalose in this human pathogen.

However, the synthesis of trehalose by Tpy has previously been reported to utilize both anomers (α and β) of G1P as substrate. Generally, the synthesis of trehalose by Tpy is from β-G1P and glucose as reported in bacteria and algae [6,30] while the α-G1P substrate is utilized by Basidiomycetes [2,5]. In my *in vitro* enzyme assay of Tpy synthesis activity in *A. fumigatus* cell free extracts, we used α-G1P as the substrate and no synthetic activity was directly measured from trehalose product whereas the indirect measurement of liberated Pi in the reaction was similar in all samples. Thus, we cannot

rule out that Tpy in *A. fumigatus* may have a role in synthesis activity using β-G1P as the substrate because of an unavailability of this compound during these studies.

Yet, additional studies with the Tpy null mutants in the OrlA background strongly suggest that Tpy enzymes in *A. fumigatus* are critical for trehalose degradation. Phosphorolysis of a substrate is a breakdown of the O-glycosidic linkage concomitant with glycosyl transfer to phosphate and yields the corresponding sugar 1-phosphate (i.e. G1P) as a high energy product. In contrast, hydrolysis of a sugar usually requires energy (i.e. ATP). For example, glucose produced from trehalose would often be converted to glucose 6-phosphate in a kinase catalyzed transformation [31]. With this context, phosphorolysis seems to be an energetically more economic way of utilizing disaccharide substrates than hydrolysis. Accordingly, enzymes catalyzing the phosphorolytic conversion of O-glycosidic substrates have often been identified in facultative anaerobic microorganisms. It is possible that regulation of the glycolytic pathway mediated by accumulation of T6P could also decrease ATP production. Therefore, the direction of the phosphorylase reaction in which O-glycoside is produced (synthesis) will be strongly disfavored as compared to phosphorolysis under conditions prevailing *in vivo* such as in the OrlA null mutant [31]. Our results suggest that Tpy tends to have Phosphorolysis activity to breakdown trehalose and provide the high energy G1P product.

Support for the important role of Tpy enzymes in conditions were ATP or energy generation may be inhibited such as in the presence of high T6P levels comes from the observation that loss of Tpy genes (Δ*orlA*/Δ*tpyA*/Δ*tpyB*) results in a dramatic impairment in *A. fumigatus* growth on minimal media with trehalose as the sole carbon source, and

also MM media without a carbon source, which indicates that this mutant was unable to utilize both extracellular and intracellular trehalose as a sole carbon source. Moreover, the accumulated trehalose in conidia of this triple mutant remained after the germination stage in which normally is rapidly degraded in the wild type [32]. Of interest, a similar impaired growth was observed on GMM, implying that degradation of trehalose by Tpy, yielding glucose and glucose-1-phosphate (G1P), is possibly very important in the absence of OrlA. Given that the accumulation of high T6P levels inhibits hexokinase activity, the glycolytic enzyme that catalyzes glucose to glucose-6-phosphate (G6P) [1,33,34,35,36], G1P that would be generated by Tpy dependent trehalose breakdown is likely critical for many fungal metabolic processes as G1P can be converted to G6P by Phosphoglucomutases enzymes (G1P→G6P). G6P would then be recycled into glycolysis and bypass the key regulated step of sugar phosphate conversion (glucose→G6P) that is inhibited in OrlA mutant [37]. In contrast, the hydrolysis of trehalose by trehalase results in two molecules of glucose, and requires energy for sugar phosphate conversion, causing a physiological stress to the fungal cell as hexokinase is inhibited by T6P. Consistently, as both glucose and intracellular trehalose unusable energy sources for fungal growth and cell wall formation in the mutant lacking Tpy enzymes, it is not surprising that this mutant resulted in sensitivity to cell wall perturbing agents. Taken together, these results reveal that combinatorial inhibition of the TPS1/TPS2 pathway with the Tpy pathway in *A. fumigatus* may render this important human pathogen more susceptible to killing by cell wall perturbing antifungal drugs.

Trehalase enzymes are crucial to hydrolyze Trehalose as a carbon source in fungi [32,38]. As *A. fumigatus* appears to have both a neutral and acidic trehalase, the question arises why these enzymes appear to not be active in the OrlA mutant and Tpy/OrlA triple mutant. Trehalase requires cAMP dependent phosphorylation for its function [39]. Therefore, the decreased activity of trehalose hydrolysis found in the mycelial tissue of Δ*orlA* can also be a consequence of a major decrease in cAMP levels in this mutant. Along these lines, an Adenylyl cyclase mutant (resulting in loss of cAMP production) of *M. grisea* displays not only a delay in conidial germination but also overall colony conidiation [40]. These phenotypes of this cAMP deficient mutant are restored in the presence of exogenous cAMP derivatives. This finding indicates that cell signaling involving cAMP plays a central role in regulating many of the biological activities and development of fungi. In agreement, the abolished conidiation of Δ*orlA* was partially restored in cAMP substituted liquid GMM (data not shown). However, despite the partial restoration of conidiation, trehalose breakdown was not increased in the presence of cAMP. Regardless, we cannot rule out the possibility that the significant delay in trehalose breakdown in Δ*orlA* is in part due to insufficient cAMP levels as a result of T6P accumulation. A further detailed examination of cAMP levels and trehalase enzyme activity is needed in the OrlA null mutant and *tpy* mutants to reach additional definitive conclusions about the mechanisms behind the OrlA and Tpy mutant phenotypes.

Intriguingly, an essential role of Tpy pathway is primarily involved in trehalose degradation rather than the anticipated role in trehalose biosynthesis in the absence of OrlA. The trehalose production via the canonical TPS1/TPS2 pathway has been shown to

be required for virulence in human fungal pathogens: in particular *C. albican, C. neoformans,* and *C. gattii* [24,26,27]. On the contrary, *A. fumigatus orlA* mutant has attenuated virulence with unaffected trehalose production. Whether trehalose plays a role associated with *in vivo* fungal virulence still remained. Therefore, we utilized the trehalose deficient Tps1 mutant to examine the role of trehalose in pathogenesis of *A. fumigatus* in immune compromised murine models of IPA. The data from virulence test in both insect and murine models are consistent, and strongly conclude that trehalose storage sugars are not involved in the infectivity and pathogenesis of *A. fumigatus*. The Tps1 double mutant (Δ*tpsA*/Δ*tpsB*) was unable to synthesize trehalose as characterized in Chapter 3 and this finding was consistent with previously published data in the *A. fumigatus* AF293 strain [29]. However, the *Tps1* mutant is likely as virulent as the wild type strain in all three IPA murine models.

Contrary to my findings, Al-Bader *et al.* found an increased virulence phenotype in a corticosteroid model inoculated with a *Tps1* mutant, and a loss of trehalose production. Differences in the report by Al-bader *et al*. may be due to the different strains of *A. fumigatus* utilized or a different murine model. Taken together, loss of trehalose production itself does not impair its virulence *in vivo* in three murine models inoculated with *A. fumigatus tps1* mutant. These findings confirm that the attenuated virulence phenotype of Δ*orlA* is primarily due to the host response against the T6P mediated cell wall alteration. In addition, the phenotype of the Δ*orlA*/Δ*tpyA*/Δ*tpyB* mutant and its impaired trehalose breakdown activity would also have *in vivo* defective growth because of the inability to utilize storage trehalose as a G1P energy source under the glucose

deprived host environment. Moreover, accumulation of T6P dramatically influences alteration of the cell wall in a similar effect to Δ*orlA* on the cell wall perturbing agents media which could possibly increase the recruitment of leukocytes and host antifungal activity against this mutant. Due to the cell wall defect data, it is plausible that Δ*orlA*/Δ*tpyA*/Δ*tpyB* would have attenuated virulence in murine models of IPA, and possibly a non-virulence phenotype due to fungal growth defect and host response based on the phenotype and attenuated virulence results of Δ*orlA*.

Unlike the dispensable role of trehalose in virulence, we found that the accumulation of trehalose does play a role as a stress protectant in high temperature growth (Chapter 3) and in increased survival after prolonged storage in the refrigerator. The degree of increased survival seems to reflect the amount of accumulated trehalose in conidia. The *orlA* mutants with high trehalose production survive cold storage longer than the wild type strain that has accumulated lower amount of trehalose. In addition, high sensitivity to cold storage was observed in *Tps1* mutants although similar trehalose production to wild type was observed in single mutants of Tps1 orthologs. A longer period of storage may be necessary to better determine the role of trehalose in the survival rate of these mutants.

In conclusion, the investigation of an alternate trehalose biosynthesis pathway in *A. fumigatus* confirmed that the TPS1/TPS2 pathway is the main route of trehalose synthesis in this mold. Thus, persistent trehalose production in the *orlA* mutant is not synthesized from the Tpy pathway. However, this reversible enzyme is strongly regulated by free Pi, and results in activation of trehalose phosphorolysis, yielding one molecule of

each G1P and glucose end product. Under the inhibitory effect of T6P, trehalose phosphorolysis is likely one metabolic mechanism to be utilized for energy generation to maintain fungal growth. Therefore, this study highlights the importance of trehalose and trehalose metabolism in *A. fumigatus*. Since the main hypothesis of this study was based on the phenotype of Δ*orlA*, further characterization and investigation of a physiological significance of Tpy in *A. fumigatus,* and evolution of this alternate trehalose biosynthesis pathway needs to be considered in the presence of OrlA. In addition, one aspect that might be considered in future work is the possibility that several additional pathways, which have not yet been investigated in *A. fumigatus*, may possibly be involved in trehalose synthesis in the absence of OrlA.

Table 4.1. Genome analyses reveal genes involved in trehalose biosynthesis and hydrolysis pathways found in *A. fumigatus* regarding the similar amino acid sequences to fungal model *S. cerevisiae* and filamentous fungal model *A. nidulans*.

Function	Locus ID	Organisms	Gene name	ORF length	References
Trehalose 6 Phosphate	TPS1	*S. cerevisiae*	Sc-tps1	495 aa	
Synthase	AFUB_001790	A1163	Af-tpsA	515 aa	Chapter 3
	AFUB_021080	A1163	Af-tpsB	479 aa	Chapter 3
	AFUB_099940	A1163	Af-tpsC	475 aa	
	AFUB_062010	A1163	Af-tpsD	476 aa	
Trehalose 6 Phosphate	TPS2	*S. cerevisiae*	Sc-tps2	896 aa	
Phosphatase	AN3441	*A. nidulans*	An-orlA	882 aa	
	AFUB_043350	A1163	Af-orlA	949 aa	Chapter 2
Regulatory Subunit	TSL1	*S. cerevisiae*	Sc-tsl1	1098 aa	
	TPS3	*S. cerevisiae*	Sc-tps3	1054 aa	
	AFUB_089470	A1163	Af-tslA	919 aa	Chapter 3
	AFUB_021090	A1163	Af-tslB	918 aa	Chapter 3
Trehalose	AFUB_037080	A1163	Af-tpyA	694 aa	This study
Phosphorylase	AFUB_062450	A1163	Af-tpyB	667 aa	This study
Trehalase	AFUB_046050	A1163	Af-treA	1072 aa	
	AFUB_070450	A1163	Af-treB	775 aa	

Table 4.2. *Aspergillus fumigatus* mutant and complement strains are created and used in this study.

Strain	Genotype	References
Δ*orlA*	CEA17 *orlA*::PYRG	Chapter 2, [1]
Rec-*orlA*	CEA17 *orlA*::PYRG, *orlA*:HPH	Chapter 2, [1]
Δ*orlA* pyrG-	CEA17 *orlA*::PYRG$^-$	Chapter 3 and 4
Δ*orlA*Δ*tpyA*	CEA17 *orlA*::PYRG$^-$, *tpyA*::PYRG	This study
Δ*orlA*Δ*tpyB*	CEA17 *orlA*::PYRG$^-$, *tpyB*::PYRG	This study
Δ*orlA*Δ*tpyA*Δ*tpyB*	CEA17 *orlA*::PYRG$^-$, *tpyB*::PYRG, *tpyA*::HPH	This study
Δ*tpsA*	CEA17 *tpsA*::PYRG	Chapter 3 and 4
Δ*tpsB*	CEA17 *tpsB*::PYRG	Chapter 3 and 4
Δ*tpsA* pyrG-	CEA17 *tpsA*::PYRG$^-$	Chapter 3 and 4
Δ*tpsA*Δ*tpsB*	CEA17 *tpsA*::PYRG$^-$, *tpsB*::PYRG	Chapter 3 and 4
Δ*tpsA*Δ*tpsB*+*tpsA*	CEA17 *tpsA*::PYRG$^-$, *tpsB*::PYRG *tpsA*:HPH	Chapter 3 and 4
Δ*tpsA*Δ*tpsB*+*tpsB*	CEA17 *tpsA*::PYRG$^-$, *tpsB*::PYRG *tpsB*:BLE	Chapter 3 and 4

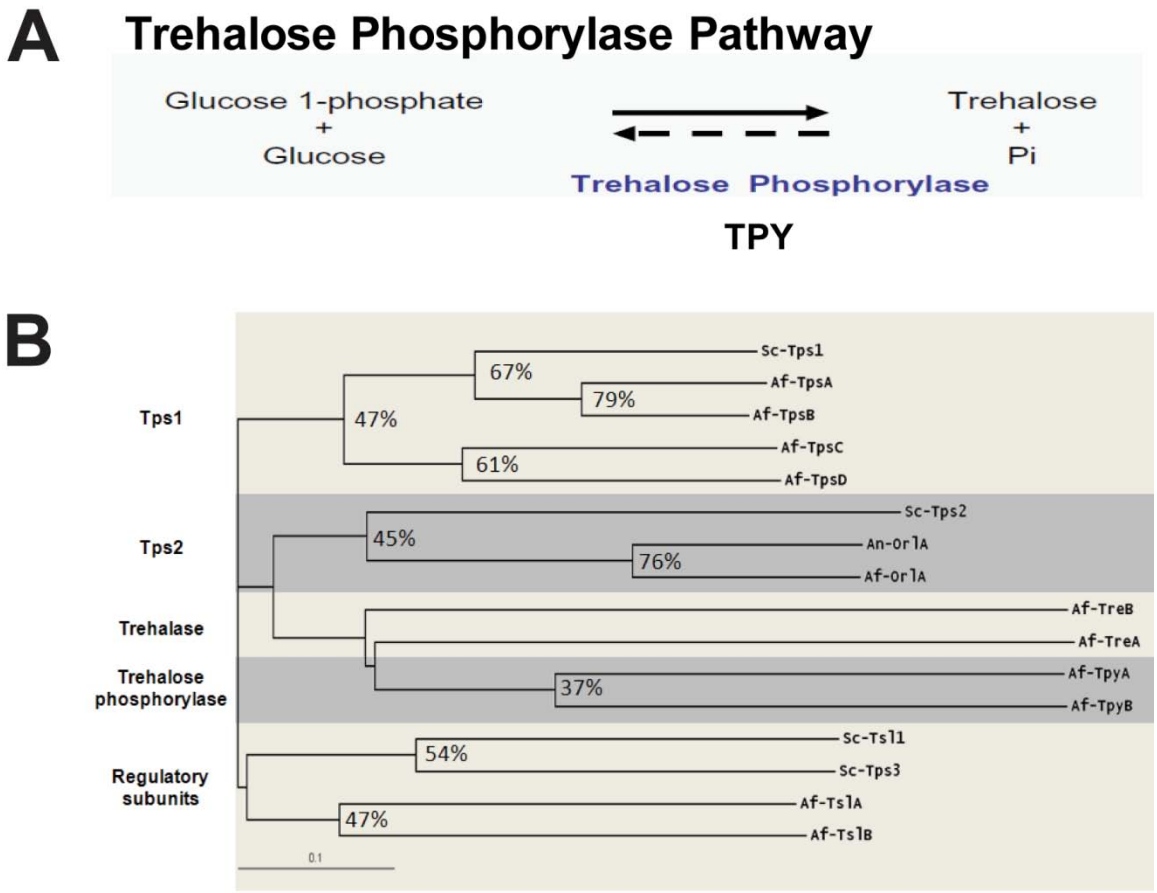

Figure 4.1. Trehalose Phosphorylase pathway and Phylogenetic tree. A) Trehalose Phosphorylase Pathway is characterized by the reversible Trehalose Phosphorylase enzyme (TPY). Glucose-1-Phosphate (G1P) and Glucose are substrates for trehalose biosynthesis (solid arrow). The trehalose phosphorolysis or breakdown of trehalose (dashed arrow) is catalyzed by TPY enzyme to obtain one molecule of G1P and Glucose as products. Free Pi is critical for the regulation of TPY enzyme activity: low Pi stimulates the activation of trehalose biosynthesis where high Pi promotes degradation. B) A phylogenetic tree of amino acid sequences of all predicted putative proteins involved in trehalose biosynthesis pathways of *A. fumigatus* (Af) showing the clusters of each protein compared against the closely related fungal organisms; *S. cerevisiae* (Sc), and *A. nidulans* (An).

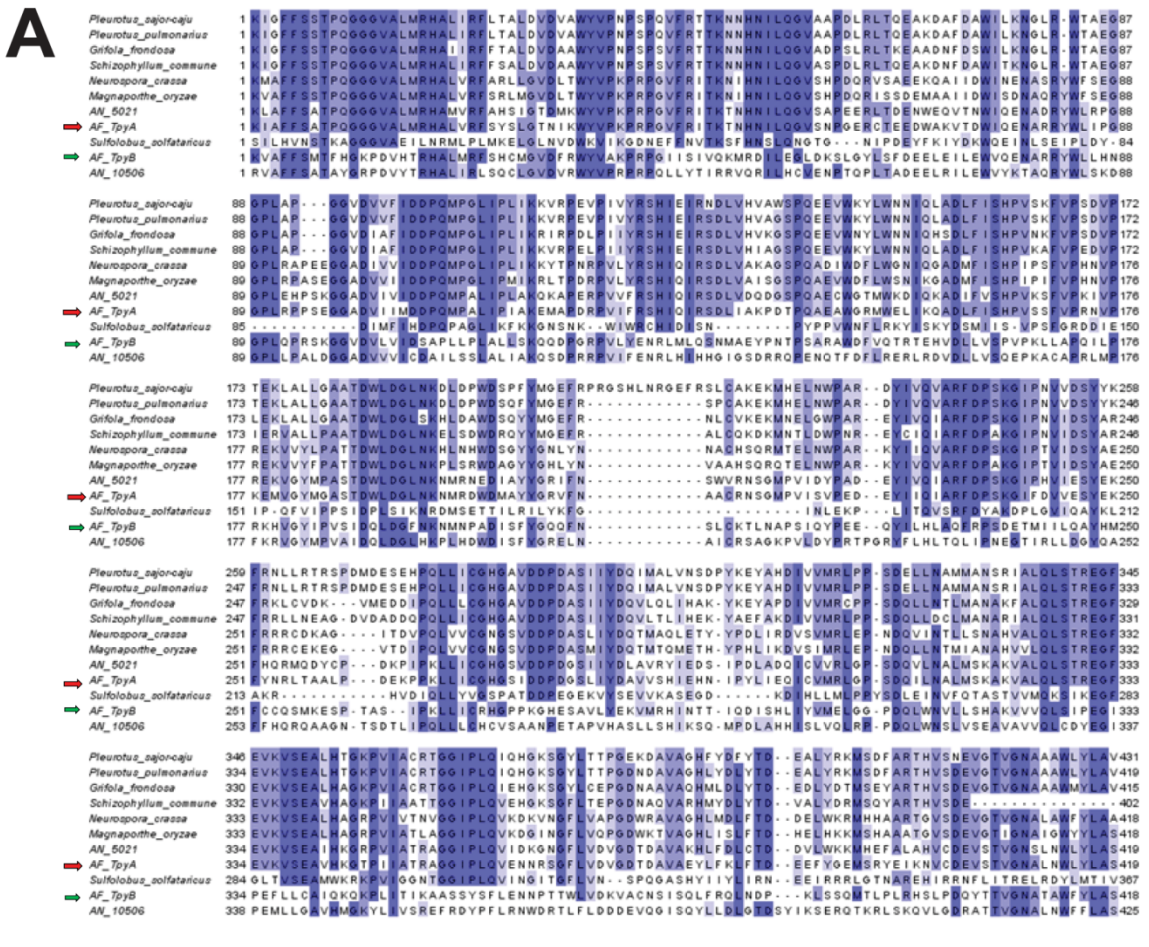
A
Pleurotus_sajor-caju
Pleurotus_pulmonarius
Grifola_frondosa
Schizophyllum_commune
Neurospora_crassa
Magnaporthe_oryzae
AN_5021
AF_TpyA
Sulfolobus_solfataricus
AF_TpyB
AN_10506

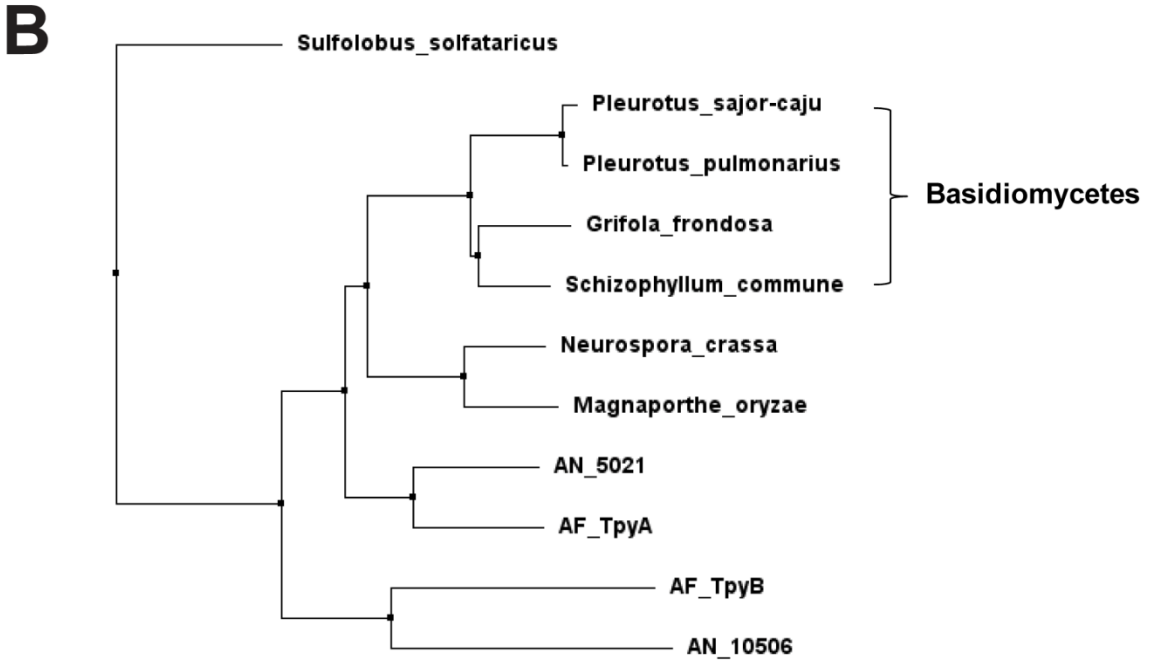
B
Sulfolobus_solfataricus
Pleurotus_sajor-caju
Pleurotus_pulmonarius
Grifola_frondosa
Schizophyllum_commune
Basidiomycetes
Neurospora_crassa
Magnaporthe_oryzae
AN_5021
AF_TpyA
AF_TpyB
AN_10506

Figure 4.2. Conservation of trehalose phosphorylase enzymes. A) Multiple alignment of amino acid sequences showing the relationship between the predicted Glycosyltransferase_GTB_type domain of *A. fumigatus* (AF_TpyA, AF_TpyB), and *A. nidulans* (AN_5021, AN_10506) in comparison to GT1 Trehalose phosphorylase domain of Basidiomycetes; *Pleurotus spp.*, *Grifola frondosa*, and *Schizophyllum commune* and representative strain of bacteria; *Sulfolobus solfataricus* and Clock-controlled-9 protein of *Neurospora crassa*, and *Magnaporthe oryzae*. The darker color represents the higher identical amino acids between groups of orthologs. B) Phylogenetic analysis of multiple alignment result in (A) was performed with CLUSTALX (1.83) and displayed with Jalview (2.7).

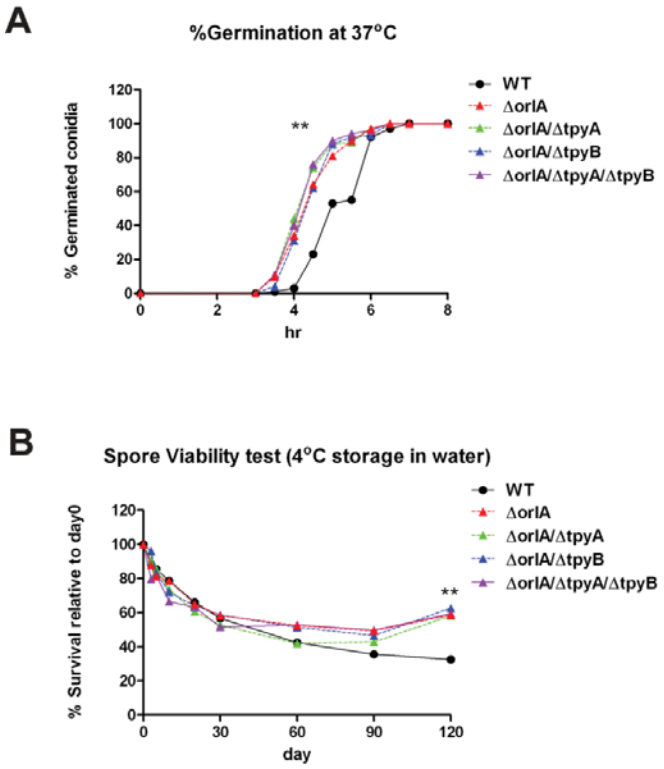

Figure 4.3. Early germination and increased prolong viability during cold storage is observed in all Tpy mutants. A) Germination of wild type and mutant strains in liquid glucose minimal medium (LGMM) culturing at 37°C/300 rpm, germinated conidia were monitored per indicated time under microscope. Percentage of germinated conidia was calculated from 200 total conidia. All mutants germinated faster than the wild type strain ($P \leq 0.05$). B) Viability during storage at 4°C was assessed in tested strains. At the indicated time point of cold storage, 100 µl of 200 conidia were plated on Sabouraud media and incubated at 37°C until colonies appeared on plates. The percent survival of each time point was calculated as a percentage of the actual survival colonies to the colony count on day 0. All mutants had an increased ability to survive the cold storage greater than wild type strain after 4 months ($P \leq 0.05$).

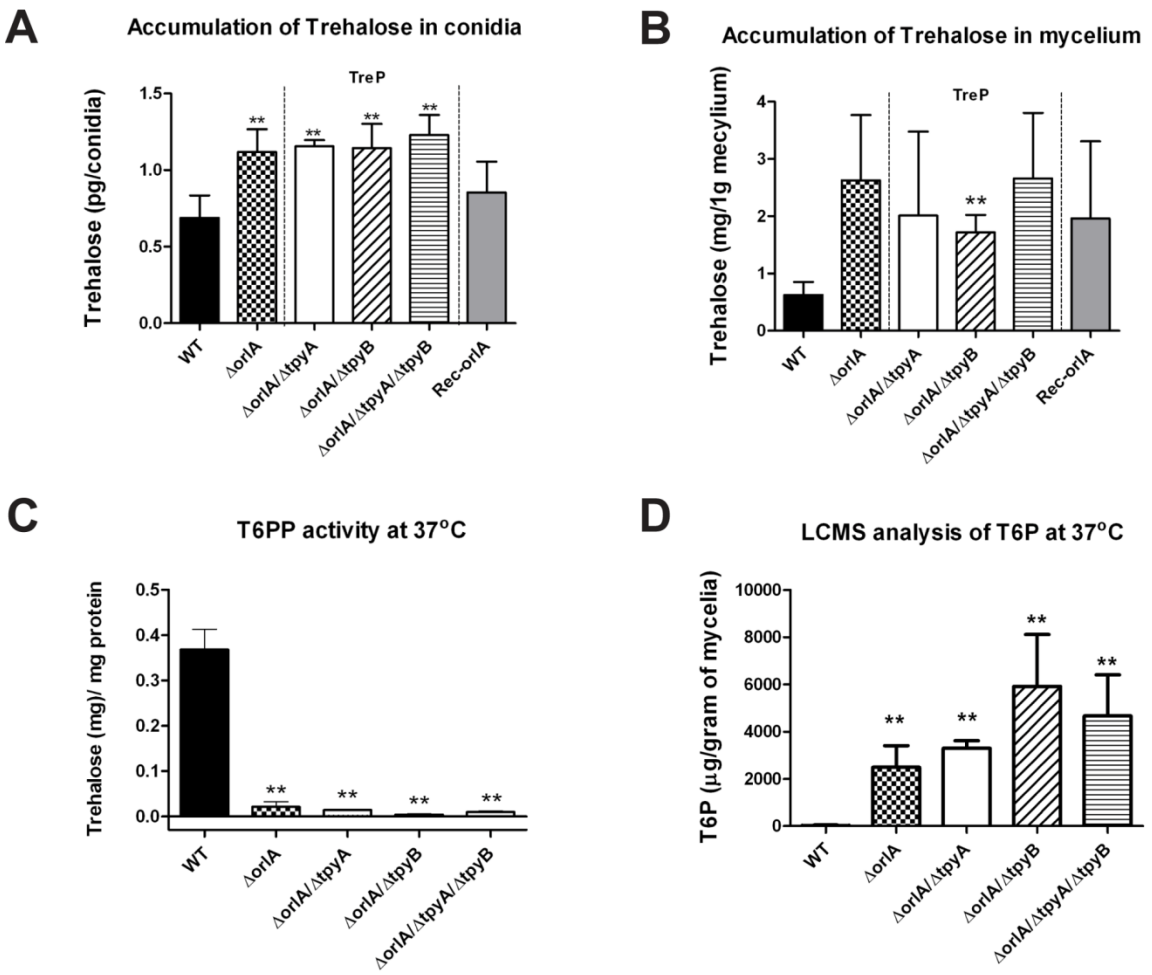

Figure 4.4. Accumulated trehalose in conidia (A) and mycelium (B) of mutants lacking Tpy encoding genes (*tpyA*, *tpyB*). Trehalose levels were increased compared to the wild type (** $P \leq 0.05$ in comparison to WT) but not significantly different to the Δ*orlA* background strain. C) T6PP enzyme activity was measured in respective strains and a trace activity of T6PP enzyme was detected in all strains derived from Δ*orlA* background strain whereas high activity was shown in wild type (** $P \leq 0.05$). D) T6P intermediate levels are similar to the trehalose production results, all mutant strains lacking OrlA, and Tpy have a significant accumulation of the T6P intermediate compared to the wild type. Data are represented as mean+/- SD of three biological replicates.

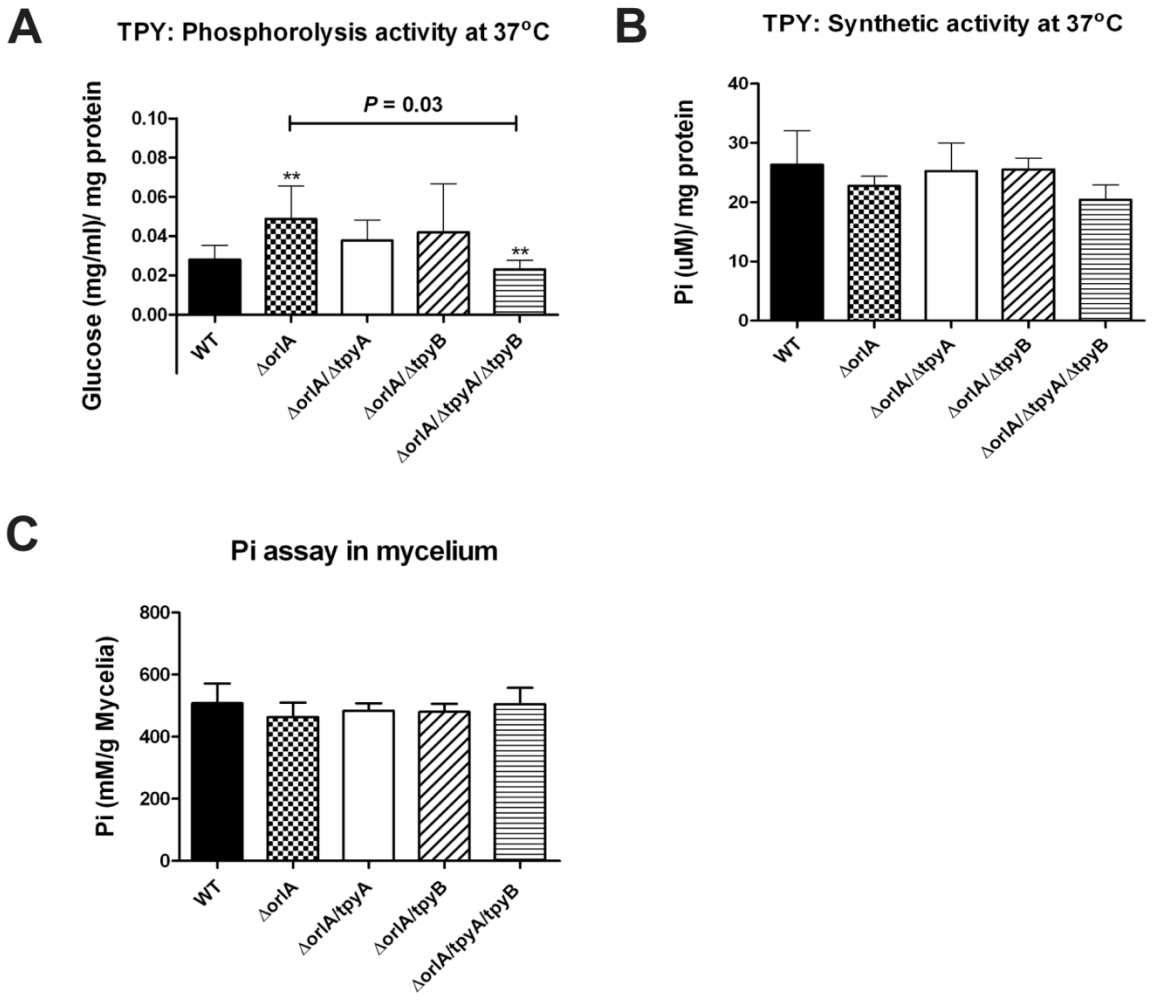

Figure 4.5. Trehalose phosphorylase enzyme activity in both directions was determined with cell free extracts. A) Trehalose phosphorolysis activity was significantly decreased in the mutants lacking functional trehalose phosphorylases (Δ*orlA*Δ*tpyA*Δ*tpyB*, ***P*=0.03). B) Synthetic activity of trehalose phosphorylase was not significantly changed in all tested strains. C) A high amount of available free inorganic phosphate was found and similar in the mycelium of all tested strains.

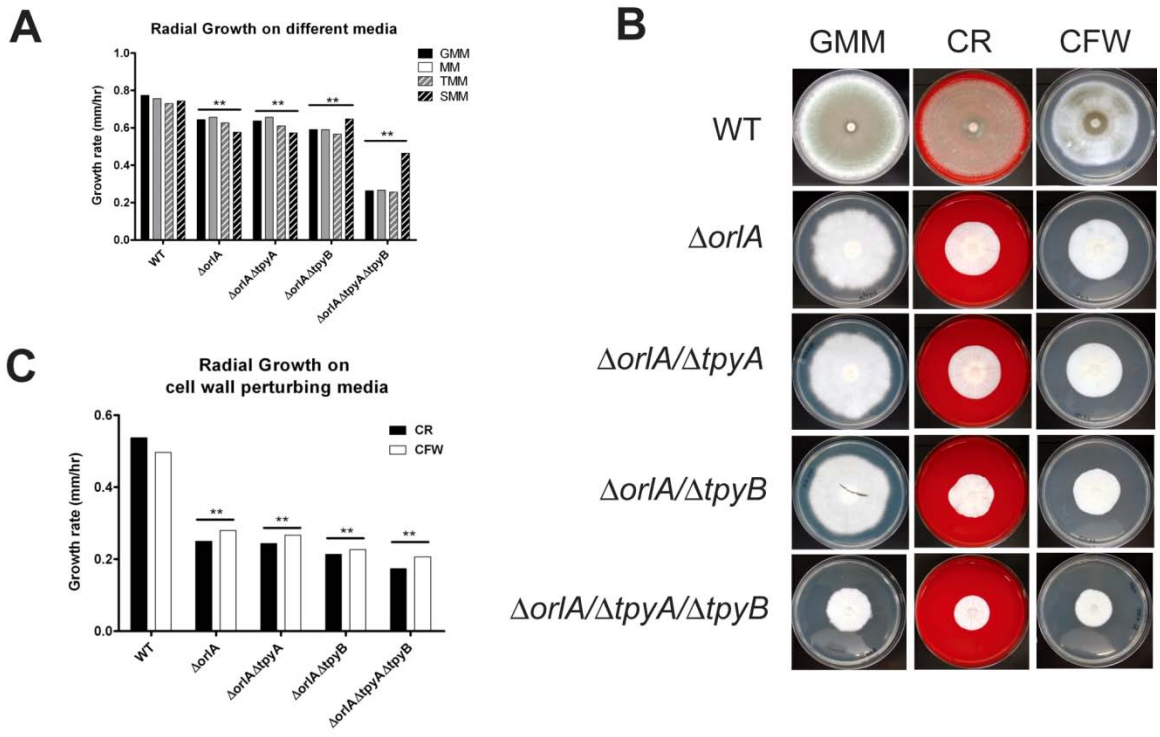

Figure 4.6. Defective mobilization of intracellular (MM) and extracellular (TMM) trehalose in the mutant strain lacking OrlA and TpyA/TpyB. A) Radial growth was measured everyday after 5□l of $1x10^6$ Conidia of test strains were placed in the center of the specified media, MM; minimal media without carbon source, TMM; 0.5% Trehalose minimal media, GMM; 1% Glucose minimal media and SMM; 1.2 M Sorbitol minimal media. All mutants lacking OrlA and Tpy were significantly reduced in growth on tested media ($P \leq 0.05$) and the impaired growth of Δ*orlA*/Δ*tpyA*/Δ*tpyB* strain was restored on SMM media. Data are represented as mean of three biological replicates. B) Cell wall perturbing assay showed an impaired cell wall integrity in all mutants lacking OrlA and Tpy encoding genes (*tpyA*, *tpyB*). Known cell wall perturbing agents CR; 1mg/ml congo red and CFW; 25µg/ml Calcofluor White were added in GMM media at the indicated concentrations. Plates were incubated at 37^{o}C for 6 days with the exception of all strains on GMM control plates that were earlier captured due to extensive growth. C) Growth rates of respective strains were generated from daily radial growth measurement as shown in B. A similar impaired growth rate on cell wall perturbing media was observed for all mutant strains compared to the WT ($P \leq 0.05$).

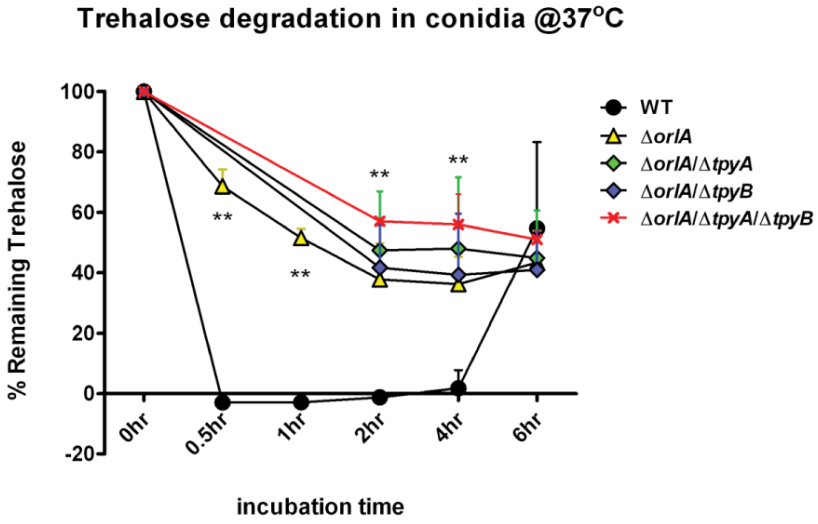

Figure 4.7. Breakdown of intracellular trehalose during conidia germination of *A. fumigatus* wild type (CBS 144.89) and mutant strains in LGMM at 37°C. Conidia were collected at the indicated time during germination, and trehalose was extracted and assayed using an enzymatic procedure. A significant decrease in mobilization of trehalose in all mutant strains relative to wild type was observed (** $P \leq 0.05$). The Δ*orlA*/Δ*tpyA*/Δ*tpyB* strain showed a more pronounced decrease in activity of trehalose degradation in the swollen conidia after 4 hr incubation. Each value is the mean of three independent replicate measurements.

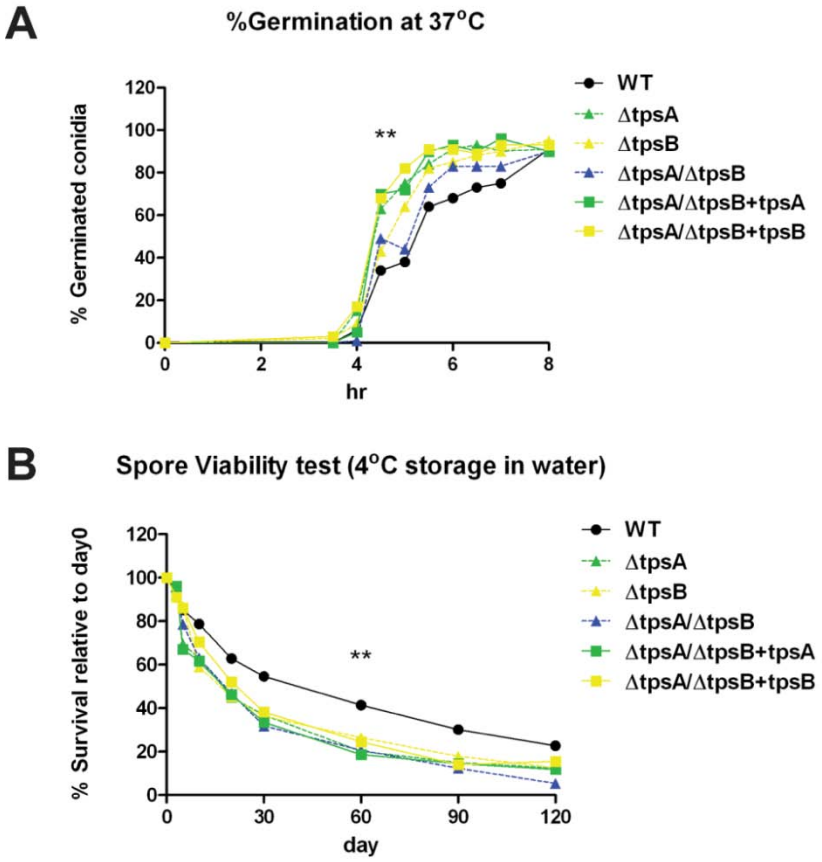

Figure 4.8. Germination and viability assays of trehalose synthase mutants. A) Germination of wild type and trehalose synthase mutant strains in LGMM cultured at 37°C/300 rpm, germinated conidia were monitored at indicated times under the microscope. The percentage of germinated conidia was calculated from total 200 conidia. All mutants germinated significantly faster than the wild type strain ($P \leq 0.05$). B) Viability during storage at 4°C was accessed in tested strains. At indicated timepoints of prolonged cold storage, 100 µl containing 200 conidia were plated on Sabouraud media and incubated at 37°C until colonies appeared on plates. The percent survival of each time point was calculated as a percentage of the actual surviving colony count to the colony count on day 0. All mutants had a significant reduction in their ability to survive cold storage compared to the wild type strain ($P \leq 0.05$).

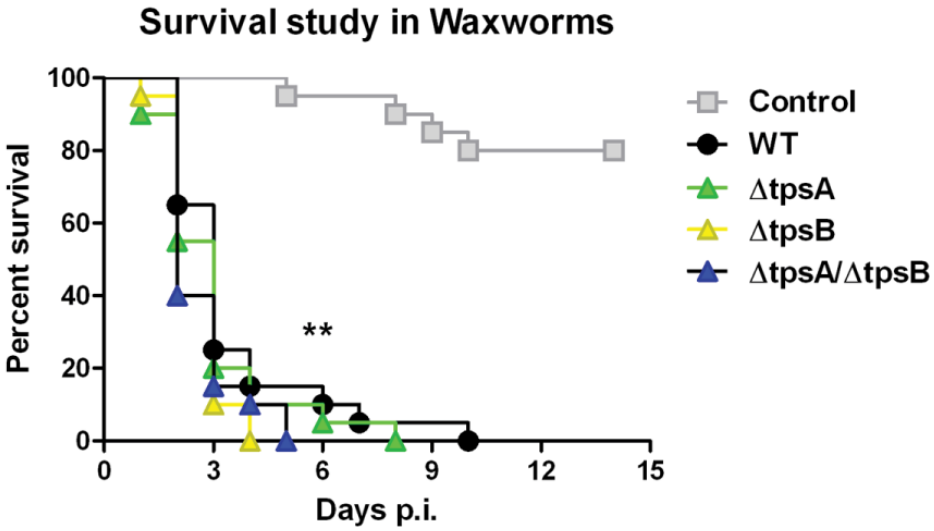

Figure 4.9. Survival of the Greater Wax Moth *Galleria mellonella* larvae infected with $1x10^5$ conidia of different *A. fumigatus* strains. Asterisk indicates a significant reduced survival of larvae inoculated with the Tps1 mutants and wild-type compared with control uninfected group, $P \leq 0.05$ by the log rank test, n = 20 worms per fungal strain and mean value of three separate experiments is presented.

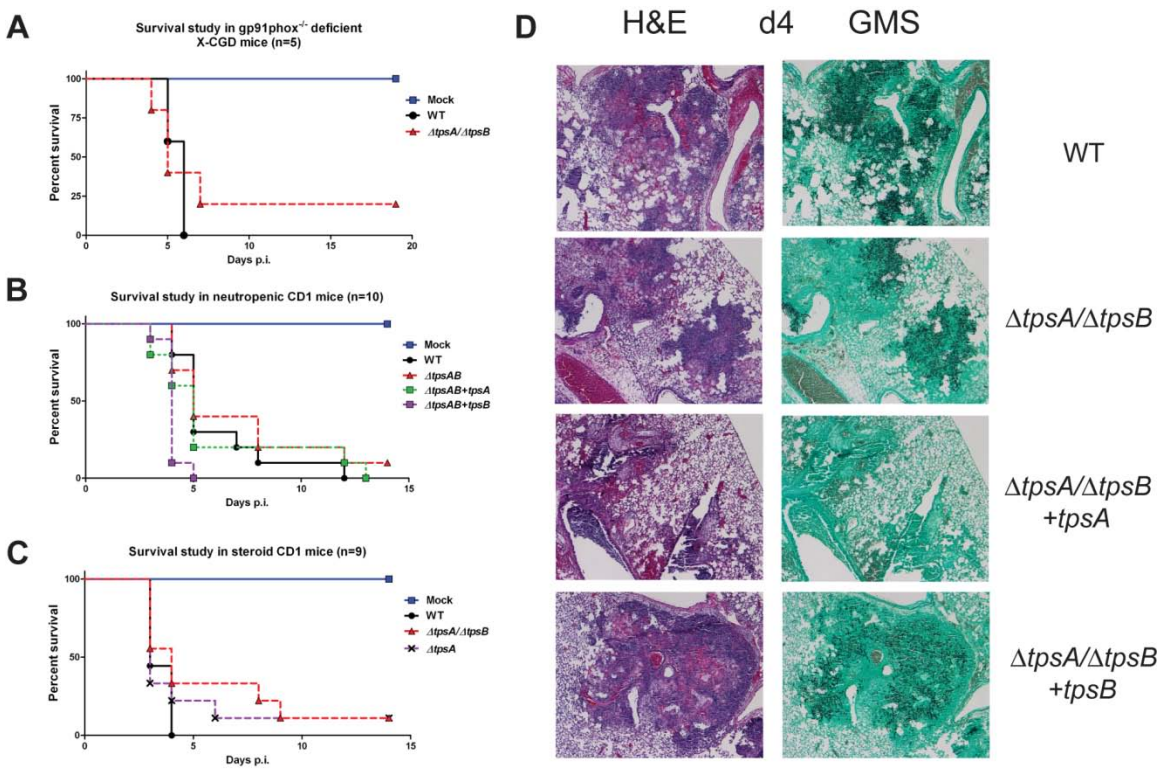

Figure 4.10. Trehalose is not required for virulence in the human fungal pathogen *A. fumigatus*. The Tps1 mutant strain that was unable to produce trehalose (Δ*tpsA*/Δ*tpsB*) showed wild type virulence in three distinct murine models of invasive pulmonary aspergillosis A) xCGD mice, gp91Phox -/- B) Chemotherapeutic treated CD1 mice, and C) Corticosteroid treated CD1 mice. Mice were intranasally inoculated with test strains including wild type, a double mutant strain lacking Tps1, reconstituted strains, and a mock control as indicated in the legend. D) Histopathology of infected chemotherapeutic CD1 mice showing the GMS stained tissue demonstrating extensive fungal growth in the lung airways and H&E staining on day4 post inoculation showing extensive tissue necrosis and lung damage with leukocyte infiltration, 40x magnification. The histopathological experiment was conducted separately from the survival study in B.

Literature Cited

1. Puttikamonkul S, Willger SD, Grahl N, Perfect JR, Movahed N, et al. (2010) Trehalose 6-phosphate phosphatase is required for cell wall integrity and fungal virulence but not trehalose biosynthesis in the human fungal pathogen *Aspergillus fumigatus*. Mol Microbiol 77: 891-911.

2. Wannet WJ, Op den Camp HJ, Wisselink HW, van der Drift C, Van Griensven LJ, et al. (1998) Purification and characterization of trehalose phosphorylase from the commercial mushroom *Agaricus bisporus*. Biochim Biophys Acta 1425: 177-188.

3. Avonce N, Mendoza-Vargas A, Morett E, Iturriaga G (2006) Insights on the evolution of trehalose biosynthesis. BMC Evol Biol 6: 109.

4. Kitamoto Y, Akashi, H., Tanaka, H. and Mori, N. (1988) α-Glucose-1-phosphate formation by a novel trehalose phosphorylase from *Flammulina velutipes*. FEMS Microbiology Letters 55: 147-150.

5. Eis C, Nidetzky B (1999) Characterization of trehalose phosphorylase from *Schizophyllum commune*. Biochem J 341 (Pt 2): 385-393.

6. Aisaka K, Masuda T (1995) Production of trehalose phosphorylase by *Catellatospora ferruginea*. FEMS Microbiol Lett 131: 47-51.

7. Schick I, Haltrich D, Kulbe KD (1995) Trehalose phosphorylase from *Pichia fermentans* and its role in the metabolism of trehalose. Appl Microbiol Biotechnol 43: 1088-1095.

8. Shinohara ML, Correa A, Bell-Pedersen D, Dunlap JC, Loros JJ (2002) *Neurospora* clock-controlled gene 9 (ccg-9) encodes trehalose synthase: circadian regulation of stress responses and development. Eukaryot Cell 1: 33-43.

9. d'Enfert C (1996) Selection of multiple disruption events in *Aspergillus fumigatus* using the orotidine-5'-decarboxylase gene, *pyrG*, as a unique transformation marker. Curr Genet 30: 76-82.

10. Shimizu K, Keller NP (2001) Genetic involvement of a cAMP-dependent protein kinase in a G protein signaling pathway regulating morphological and chemical transitions in *Aspergillus nidulans*. Genetics 157: 591-600.

11. Yelton MM, Hamer JE, Timberlake WE (1984) Transformation of *Aspergillus nidulans* by using a trpC plasmid. Proc Natl Acad Sci U S A 81: 1470-1474.

12. Grahl N, Puttikamonkul S, Macdonald JM, Gamcsik MP, Ngo LY, et al. *In vivo* hypoxia and a fungal alcohol dehydrogenase influence the pathogenesis of invasive pulmonary aspergillosis. PLoS Pathog 7: e1002145.

13. Yu JH, Hamari Z, Han KH, Seo JA, Reyes-Dominguez Y, et al. (2004) Double-joint PCR: a PCR-based molecular tool for gene manipulations in filamentous fungi. Fungal Genet Biol 41: 973-981.

14. Cramer RA, Jr., Gamcsik MP, Brooking RM, Najvar LK, Kirkpatrick WR, et al. (2006) Disruption of a nonribosomal peptide synthetase in *Aspergillus fumigatus* eliminates gliotoxin production. Eukaryot Cell 5: 972-980.

15. Fuller KK, Zhao W, Askew DS, Rhodes JC (2009) Deletion of the protein kinase A regulatory subunit leads to deregulation of mitochondrial activation and nuclear duplication in *Aspergillus fumigatus*. Eukaryot Cell 8: 271-277.

16. Gravelat FN, Ejzykowicz DE, Chiang LY, Chabot JC, Urb M, et al. *Aspergillus fumigatus* MedA governs adherence, host cell interactions and virulence. Cell Microbiol 12: 473-488.

17. Huppert M, Oliver DJ, Sun SH (1978) Combined methenamine-silver nitrate and hematoxylin & eosin stain for fungi in tissues. J Clin Microbiol 8: 598-603.

18. Mabey JE, Anderson MJ, Giles PF, Miller CJ, Attwood TK, et al. (2004) CADRE: the Central Aspergillus Data REpository. Nucleic Acids Res 32: D401-405.

19. Arnaud MB, Cerqueira GC, Inglis DO, Skrzypek MS, Binkley J, et al. The *Aspergillus* Genome Database (AspGD): recent developments in comprehensive multispecies curation, comparative genomics and community resources. Nucleic Acids Res 40: D653-659.

20. Altschul SF, Gish W, Miller W, Myers EW, Lipman DJ (1990) Basic local alignment search tool. J Mol Biol 215: 403-410.

21. Lombardi LM, Brody S (2005) Circadian rhythms in *Neurospora crassa*: clock gene homologues in fungi. Fungal Genet Biol 42: 887-892.

22. Brennan M, Thomas DY, Whiteway M, Kavanagh K (2002) Correlation between virulence of *Candida albicans* mutants in mice and *Galleria mellonella* larvae. FEMS Immunol Med Microbiol 34: 153-157.

23. Cabib E, Leloir LF (1958) The biosynthesis of trehalose phosphate. J Biol Chem 231: 259-275.

24. Zaragoza O, de Virgilio C, Ponton J, Gancedo C (2002) Disruption in *Candida albicans* of the TPS2 gene encoding trehalose-6-phosphate phosphatase affects cell integrity and decreases infectivity. Microbiology 148: 1281-1290.

25. Zaragoza O, Blazquez MA, Gancedo C (1998) Disruption of the *Candida albicans* TPS1 gene encoding trehalose-6-phosphate synthase impairs formation of hyphae and decreases infectivity. J Bacteriol 180: 3809-3815.

26. Petzold EW, Himmelreich U, Mylonakis E, Rude T, Toffaletti D, et al. (2006) Characterization and regulation of the trehalose synthesis pathway and its importance in the pathogenicity of *Cryptococcus neoformans*. Infect Immun 74: 5877-5887.

27. Ngamskulrungroj P, Himmelreich U, Breger JA, Wilson C, Chayakulkeeree M, et al. (2009) The trehalose synthesis pathway is an integral part of the virulence composite for *Cryptococcus gattii*. Infect Immun 77: 4584-4596.

28. Van Dijck P, De Rop L, Szlufcik K, Van Ael E, Thevelein JM (2002) Disruption of the *Candida albicans* TPS2 gene encoding trehalose-6-phosphate phosphatase decreases infectivity without affecting hypha formation. Infect Immun 70: 1772-1782.

29. Al-Bader N, Vanier G, Liu H, Gravelat FN, Urb M, et al. (2010) Role of trehalose biosynthesis in *Aspergillus fumigatus* development, stress response, and virulence. Infect Immun 78: 3007-3018.

30. Marechal LR, Belocopitow E (1972) Metabolism of trehalose in *Euglena gracilis*. I. Partial purification and some properties of trehalose phosphorylase. J Biol Chem 247: 3223-3228.

31. Luley-Goedl C, Nidetzky B Carbohydrate synthesis by disaccharide phosphorylases: reactions, catalytic mechanisms and application in the glycosciences. Biotechnol J 5: 1324-1338.

32. d'Enfert C, Fontaine T (1997) Molecular characterization of the *Aspergillus nidulans* treA gene encoding an acid trehalase required for growth on trehalose. Mol Microbiol 24: 203-216.

33. Hohmann S, Bell W, Neves MJ, Valckx D, Thevelein JM (1996) Evidence for trehalose-6-phosphate-dependent and -independent mechanisms in the control of sugar influx into yeast glycolysis. Mol Microbiol 20: 981-991.

34. Fleck CB, Brock M *Aspergillus fumigatus* catalytic glucokinase and hexokinase: expression analysis and importance for germination, growth, and conidiation. Eukaryot Cell 9: 1120-1135.

35. Flipphi M, van de Vondervoort PJ, Ruijter GJ, Visser J, Arst HN, Jr., et al. (2003) Onset of carbon catabolite repression in *Aspergillus nidulans*. Parallel involvement of hexokinase and glucokinase in sugar signaling. J Biol Chem 278: 11849-11857.

36. Panneman H, Ruijter GJ, van den Broeck HC, Visser J (1998) Cloning and biochemical characterisation of *Aspergillus niger* hexokinase--the enzyme is strongly inhibited by physiological concentrations of trehalose 6-phosphate. Eur J Biochem 258: 223-232.

37. Mesak LR, Dahl MK (2000) Purification and enzymatic characterization of PgcM: a beta-phosphoglucomutase and glucose-1-phosphate phosphodismutase of *Bacillus subtilis*. Arch Microbiol 174: 256-264.

38. d'Enfert C, Bonini BM, Zapella PD, Fontaine T, da Silva AM, et al. (1999) Neutral trehalases catalyse intracellular trehalose breakdown in the filamentous fungi *Aspergillus nidulans* and *Neurospora crassa*. Mol Microbiol 32: 471-483.

39. Thevelein JM (1984) Regulation of trehalose mobilization in fungi. Microbiol Rev 48: 42-59.

40. Choi W, Dean RA (1997) The adenylate cyclase gene MAC1 of *Magnaporthe grisea* controls appressorium formation and other aspects of growth and development. Plant Cell 9: 1973-1983.

CHAPTER FIVE

CONCLUSIONS

During the past 30 years, the incidence of invasive fungal infections (IFIs) has dramatically increased in immunocompromised hosts [1]. Recently, invasive pulmonary aspergillosis (IPA) has emerged as a leading cause of morbidity and mortality with the highest cumulative incidence in hematopoietic stem cell transplant (HSCT) recipients [2,3]. The emerging significance and high mortality rates associated with IPA have generated great interest in the scientific community to elucidate the pathogenesis mechanisms of *A. fumigatus*. With limited antifungal drugs available and poor outcomes with current antifungal treatments, much effort is being focused on developing new antifungal drugs targeting fungal specific pathways [4,5,6,7,8].

The goal of this dissertation was to characterize the role of the trehalose biosynthesis pathway in *A. fumigatus* due to its fungal specificity and role in fungal virulence in other human and plant fungal pathogens. Based on data from my dissertation research, the major findings are summarized in Figure 5.1. As one of the major goals of this work was to determine whether the trehalose pathway in *A. fumigatus* is a viable antifungal drug target, this chapter will discuss the significance of my findings in relation to this goal.

Data presented suggest that the TPS1/TPS2 pathway is the major route of trehalose synthesis in *A. fumigatus*. In addition, an alternate trehalose phosphorylase (TPY) pathway exists in this fungus that appears to have a specific role in trehalose

breakdown (Figure 5.1). My data suggest that trehalose biosynthesis in *A. fumigatus* is intimately linked to overall carbon metabolism in *A. fumigatus*. Glycolysis is the key metabolic pathway utilized by all living organisms, including *A. fumigatus*, to metabolize glucose. In fungi, glucose is phosphorylated to glucose-6-phosphate (G6P) by various glucokinases and hexokinases. In fungi, the G6P intermediate is not only isomerized to fluctose-6-phosphate (F6P), which is utilized to eventually produce pyruvate via glycolysis, but is also a precursor for trehalose biosynthesis by the TPS1/TPS2 pathway. Activity of the first catalytic enzyme in this pathway, Trehalose-6-Phosphate Synthase (Tps1), has been observed to be stabilized by the regulatory subunits (TslA and TslB) in *Saccharomyces cerevisiae* to form the T6P intermediate as a precursor to the trehalose product. My data revealed that in *A. fumigatus*, the absence of the second catalytic enzyme, Trehalose-6-Phosphate Phosphatase (OrlA/TPS2), resulted in the accumulation of the T6P intermediate that in some fungi acts as a specific inhibitor of hexokinase enzyme activity (Chapter 2). I observed a decrease in hexokinase activity in Δ*orlA* that I hypothesize results in a decrease in the carbon flux through glycolysis. This likely is at least part of the mechanism behind the observed defect in the cell wall of Δ*orlA* due to the reductions in Fructose-6-Phosphate (F6P), a precursor of chitin biosynthesis, and Glucose-1-Phosphate (G1P), a precursor of β-glucan biosynthesis. I hypothesize that the accumulated T6P intermediate acts as an internal stress mediator that may activate the cell wall integrity pathway (CWI). In addition, T6P accumulation or changes in levels of glycolytic intermediates likely lead to activation of cell wall biosynthesis transcriptional responsive genes including genes encoding chitin synthases (CHS) and glucan synthases

(FKS) as described in Chapter 2. Thus, these hypotheses are areas for further investigation in future research to definitively determine the relationship between trehalose biosynthesis, carbon metabolism and cell wall biosynthesis in *A. fumigatus*.

An intriguing finding with Δ*orlA* was the persistence of trehalose production despite the loss of trehalose-6-phosphate phosphatase activity in this mutant. This finding led me in Chapter 4 to try and discover the mechanism behind the observed unexpected trehalose accumulation in this mutant. Identification of two trehalose phosphorylase (TPY) encoding genes in the *A. fumigatus* genome presented a potential mechanism for the persistent trehalose production. Characterization of the TPY pathway in *A. fumigatus* identified a role for the TPY enzymes in the mobilization of trehalose to G1P and glucose products in the absence of a functional OrlA enzyme rather than a role in trehalose biosynthesis (Chapter 4). Thus, one potential mechanism by which Δ*orlA* is able to overcome the inhibitory effect of T6P on the hexokinase activity and supply of key precursors for downstream mechanisms, is through activation of these TPY enzymes (TpyA and TpyB). This activation can produce G6P from the G1P which is a product of TPY-mediated trehalose breakdown. Although the key sugar phosphorylation step (glucose → G6P) is specifically inhibited by T6P, G6P can still enter glycolysis or the pentose phosphate pathway to maintain metabolic flux and to provide key precursors of cell wall biosynthesis without a hexokinase- dependent process in Δ*orlA*. Chitin synthesis requires five enzymatic steps in order to convert F6P to chitin, whereas only a few steps are required for conversion of G1P to β-glucan. Therefore, it is possible that G1P was effectively converted to β-glucan rather than being utilized to achieve chitin biosynthesis

as demonstrated by the increased β-glucan and decreased chitin levels in Δ*orlA* (Chapter 3). This finding may explain how Δ*orlA* survives T6P accumulation while other fungal TPS2 null mutants such as *Cryptococcus neoformans* cannot. However, a precise role of the TPY pathway remains to be determined in the wild type, and further phenotyping of the TPY mutants would provide more information on the function of the TPY pathway in *A. fumigatus*. Thus, the specific mechanism behind the persistent production of trehalose in Δ*orlA* remains unknown. Exploring whether non-specific phosphatases, (undefined OrlA homologs) or another undefined trehalose biosynthesis pathway is involved in the maintenance of trehalose production will be an important research topic to address in further studies to gain a better understanding of *A. fumigatus* carbon metabolism. Complete loss of trehalose production was, however, observed in the mutant lacking the first catalytic Tps1 enzyme; trehalose 6 phosphate synthase (Δ*tpsA*/Δ*tpsB*) (Chapter 3 and 4). Intriguingly, the Tps1 mutant has a normal morphological phenotype on solid minimal media and importantly, its virulence as measured by murine mortality, resembled the wild type strain despite having no trehalose production. This result is surprising given the loss of virulence associated with TPS1 in other human and plant pathogenic fungi. In the rice pathogen, *Magnaporthe grisea* disruption of a *tps1* gene increases activity of hexokinase and results in loss of the ability to grow on glucose containing medium that is a similar to the phenotype of Δ*tps1* in *S. cerevisiae*. Plant fungal pathogens, including *M. grisea,* elaborated a specialized structure called an appresorium to breach the plant cuticle by generating mechanical force [9]. To generate the force, appressoria produce enormous hydrostatic turgor pressure by accumulating glycerol. Absence of Tps1 in *M. grisea*

results in abolished production of trehalose and shortage of available glucose in the cytoplasm, which leads to significantly decreased turgor pressure and thus attenuated pathogenicity [10]. Unlike *M. grisea* and *S. cerevisiae*, the Tps1 mutant of *A. fumigatus* has normal growth on glucose media and remains virulent. This data further illustrates the complexity and uniqueness of fungal metabolism in different fungal species. It is unclear how the Tps1 mutant in *A. fumigatus* is able to grow in the presence of glucose. As with data generated from Δ*orlA*, it seems clear that unique mechanisms of carbon flux regulation exist in *A. fumigatus* that remain to be elucidated. Identification of the compensatory signaling pathways induced in Tps1 and OrlA/Tps2 mutants in *A. fumigatus* may provide clues as to the identity of these mechanisms.

For example, Δ*orlA* has defective morphological growth on glucose media, but the defect is rescued on osmotically stable media (SMM). This may suggest that the High-Osmolarity Glycerol Pathway (HOG) involving a conserved mitogen-activated protein kinase, that regulates cellular turgor in fungi, is possibly activated in response to the increased extracellular osmolarity in the media because of decreased hexokinase activity [11]. Moreover, the defective growth of Δ*orlA* is also rescued on ethanol media, which suggests that *A. fumigatus* can utilize the glyoxylate pathway where two-carbon compounds are assimilated into the tricarboxylic acid cycle (TCA) to bypass the potential inhibitory affect on glycolysis by T6P accumulation. An intriguing experiment would be to grow Δ*orlA* in the presence of both glucose and a 2-carbon source such as ethanol and assess the growth and morphological consequences. These data may also suggest that the ability of Δ*orlA* to generally grow at a similar rate as the wild-type *in vivo* in murine

models of IPA may be directly tied to the availability of alternative carbon sources *in vivo* that allow the fungus to bypass the inhibition of glycolysis by T6P accumulation. Further studies are needed to definitively address this hypothesis, perhaps by making a double mutant in which both OrlA and a key enzyme in the glyoxylate pathway are deleted.

Taken together the above data suggest that fungal metabolism can be significantly altered by targeting OrlA in *A. fumigatus,* which provides support for my hypothesis that the TPS1/TPS2 pathway in *A. fumigatus* is a promising drug target. A clear take home message from these *in vitro* studies is that loss of OrlA/Tps2, while resulting in significant fungal metabolism changes, does not lead to fungal mortality under the conditions tested in theses studies. Thus, from the perspective of designing the ideal antifungal drug to treat invasive pulmonary aspergillosis, directly targeting this pathway in *A. fumigatus* may not be a sound approach. *In vivo*, I observed that loss of OrlA, however, does significantly affect the pathogenesis of IPA. Indeed, loss of OrlA function results in a strain of fungus that exhibits reduced virulence in immunologically distinct murine models of IPA. This loss of virulence in clinically relevant murine models of IPA thus warrants a further in depth examination of the potential of this pathway as an antifungal drug target.

An intriguing result with Δ*orlA* was that the *in vivo* attenuated virulence was at least partially due to increased susceptibility to neutrophil mediated killing of the fungus. Thus, targeting OrlA may help the compromised immune system overcome *A. fumigatus* infections. However, the increased inflammatory response observed in mice inoculated

with Δ*orlA* presents another challenge for targeting this pathway in immunocompromised patients that may have immune systems that have difficulty controlling inflammation. To potentially thwart this concern, the increased levels of β-glucan observed on the cell wall of Δ*orlA* could potentially be reduced by use of the clinically relevant echinocandin drugs that target β-glucan biosynthesis in fungi. It would be interesting to treat Δ*orlA* inoculated mice with caspofungin and determine whether this has an effect on the inflammatory response under these conditions that may improve infection outcome. Along these lines, whether the increased inflammation is due to the changes in the Δ*orlA* cell wall remains to be definitively determined. Besides the increase in β-glucan, the mutant also had a decrease in chitin and galactosaminogalactan (GAG) both of which may suppress inflammatory responses *in vivo* [12,13]. In addition, an alternate hypothesis is that Δ*orlA* secretes an extracellular factor that promotes inflammation and potentially leukocyte recruitment. This alternate hypothesis could be tested by utilizing heat killed Δ*orlA* conidia and/or culture supernatants from Δ*orlA* cultures that should contain the soluble factor. These future lines of inquiry will further define the impact of the trehalose pathway in *A. fumigatus* host interactions and may shed further clarity on the potential of targeting this pathway therapeutically.

Another area of future study is to definitively uncover the mechanism by which host leukocytes, particularly neutrophils, are able to mediate killing of Δ*orlA*. While the incidence of IPA in CGD patients is the most convincing evidence that phagocyte produced ROS are critical for controlling *A. fumigatus in vivo* growth, much remains to be learned about how phagocytes control and kill *A. fumigatus* [14]. RB6 depletion in our

CGD model of IPA resulted in increased mortality in Δ*orlA* inoculated animals, strongly suggesting that neutrophils are the main cell responsible for the attenuated virulence of Δ*orlA,* though we cannot rule out a role for other Gr1+ cells. Although my data strongly suggest that changes in the cell wall of Δ*orlA* increase recruitment of PMNs and provide additional antifungal activity against Δ*orlA*, I cannot rule out the possibility that the significant increase of neutrophils is solely due to recognition of specific receptors against increased β-glucan. Alternatively, the reduction of GAG in the Δ*orlA* cell wall may alter the induction of neutrophil apoptosis that could explain the increased neutrophil numbers. Moreover, it will be interesting to determine what specific changes in Δ*orlA* are responsible for its increased susceptibility to killing by neutrophils. Thus, this fungal mutant strain may provide a novel tool to uncover how *A. fumigatus* thwarts phagocyte killing in the immunocompromised patient setting. Consequently, this discovery could be used to design a novel antifungal therapeutic targeting this mechanism. Along these lines, discovering the mechanism by which neutrophils kill Δ*orlA* could identify a key phagocyte effector mechanism that could be used in combination with targeting OrlA to improve IPA patient outcomes. In addition to ROS dependent mechanisms, there are several mechanisms that neutrophils employ to provide antifungal activity against *A. fumigatus*. Mice deficient in the neutrophil granules serine proteases elastase (NE) and cathepsin G (CG) are susceptible to *A. fumigatus* and *M. bovis* infections [15,16]. Biochemical studies have demonstrated that NE and CG have microbicidal activities and an ability to degrade extracellular matrix components. Thus, NE and CG may have greater efficacy against the altered cell wall of Δ*orlA* compared to the intact cell wall of

wild type. Exploring the specific ROS independent antifungal pathways, such as NE and CG, might be a key to designing a potential combination therapy together with targeting OrlA. In support of this possibility, repetitive therapeutic application of liposomal encapsulated human CG/NE significantly reduced mycobacterial loads in the lungs of mice [16]. Thus, these findings may be relevant for the development of a novel antifungal treatment in immunocompromised patients that have leukocytes with deficient antifungal effector mechanisms such as those undergoing high dose corticosteroid therapies or graft versus host disease.

In conclusion, my dissertation research has provided new insights into how *A. fumigatus* causes lethal disease in clinically relevant murine models of IPA. While targeting the trehalose biosynthesis in this fungus for therapeutic development will be more complicated then in the pathogenic yeast *C. neoformans* and *Candida albicans*, my data suggest that further study of this pathway in *A. fumigatus* can potentially lead to development of a novel antifungal therapeutic regimen. Importantly, I have shown that alterations in fungal metabolism, such as through manipulation of the trehalose biosynthesis pathway, significantly alter the interaction of the fungus with its host. Further study of these mechanisms will undoubtedly lead to a greater understanding of IPA pathogenesis in addition to increasing our knowledge of fungal metabolism, cell wall biosynthesis and virulence. An intriguing final hypothesis for future exploration is that T6P itself may be secreted into the extracellular space by fungi that lack a functional trehalose-phosphate phosphatase and that T6P itself may have immunomodulatory activity that could perhaps be therapeutically exploited. Regardless, much remains to be

learned about this increasingly important human fungal pathogen in order to improve patient outcomes and minimize the incidence of this infection.

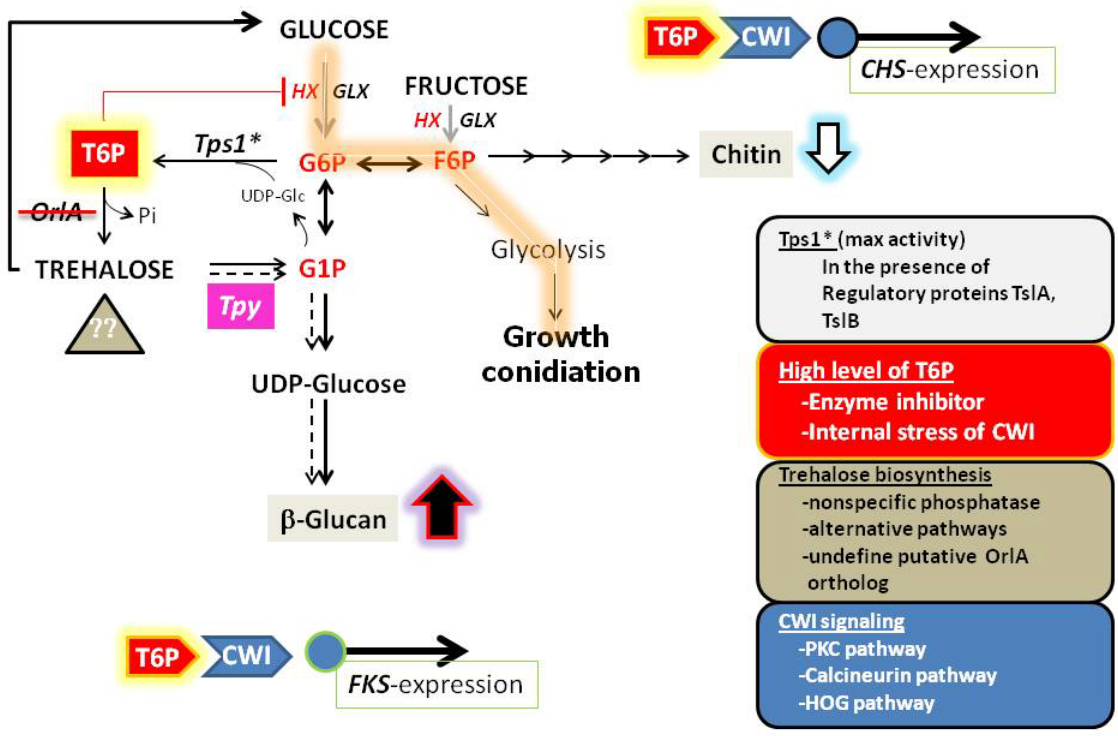

Figure 5.1. A schematic conclusion of regulatory circuits and interactions among glycolysis, trehalose biosynthesis (TPS1/TPS2), trehalose phosphorolysis (TPY), cell wall integrity, and cell wall biosynthesis pathways in *A. fumigatus* as elucidated in this dissertation.

Literature cited

1. McNeil MM, Nash SL, Hajjeh RA, Phelan MA, Conn LA, et al. (2001) Trends in mortality due to invasive mycotic diseases in the United States, 1980-1997. Clin Infect Dis 33: 641-647.

2. Pappas PG, Alexander BD, Andes DR, Hadley S, Kauffman CA, et al. Invasive fungal infections among organ transplant recipients: results of the Transplant-Associated Infection Surveillance Network (TRANSNET). Clin Infect Dis 50: 1101-1111.

3. Kontoyiannis DP, Marr KA, Park BJ, Alexander BD, Anaissie EJ, et al. Prospective surveillance for invasive fungal infections in hematopoietic stem cell transplant recipients, 2001-2006: overview of the Transplant-Associated Infection Surveillance Network (TRANSNET) Database. Clin Infect Dis 50: 1091-1100.

4. Kontoyiannis DP, Bodey GP (2002) Invasive aspergillosis in 2002: an update. Eur J Clin Microbiol Infect Dis 21: 161-172.

5. Walsh TJ, Anaissie EJ, Denning DW, Herbrecht R, Kontoyiannis DP, et al. (2008) Treatment of aspergillosis: clinical practice guidelines of the Infectious Diseases Society of America. Clin Infect Dis 46: 327-360.

6. Herbrecht R, Denning DW, Patterson TF, Bennett JE, Greene RE, et al. (2002) Voriconazole versus amphotericin B for primary therapy of invasive aspergillosis. N Engl J Med 347: 408-415.

7. Maschmeyer G, Haas A, Cornely OA (2007) Invasive aspergillosis: epidemiology, diagnosis and management in immunocompromised patients. Drugs 67: 1567-1601.

8. Latge JP (2007) The cell wall: a carbohydrate armour for the fungal cell. Mol Microbiol 66: 279-290.

9. Dixon KP, Xu JR, Smirnoff N, Talbot NJ (1999) Independent signaling pathways regulate cellular turgor during hyperosmotic stress and appressorium-mediated plant infection by *Magnaporthe grisea*. Plant Cell 11: 2045-2058.

10. Foster AJ, Jenkinson JM, Talbot NJ (2003) Trehalose synthesis and metabolism are required at different stages of plant infection by *Magnaporthe grisea*. EMBO J 22: 225-235.

11. Brewster JL, de Valoir T, Dwyer ND, Winter E, Gustin MC (1993) An osmosensing signal transduction pathway in yeast. Science 259: 1760-1763.

12. Fontaine T, Delangle A, Simenel C, Coddeville B, van Vliet SJ, et al. Galactosaminogalactan, a new immunosuppressive polysaccharide of *Aspergillus fumigatus*. PLoS Pathog 7: e1002372.

13. Mora-Montes HM, Netea MG, Ferwerda G, Lenardon MD, Brown GD, et al. Recognition and blocking of innate immunity cells by *Candida albicans* chitin. Infect Immun 79: 1961-1970.

14. Hasenberg M, Behnsen J, Krappmann S, Brakhage A, Gunzer M Phagocyte responses towards *Aspergillus fumigatus*. Int J Med Microbiol 301: 436-444.

15. Tkalcevic J, Novelli M, Phylactides M, Iredale JP, Segal AW, et al. (2000) Impaired immunity and enhanced resistance to endotoxin in the absence of neutrophil elastase and cathepsin G. Immunity 12: 201-210.

16. Steinwede K, Maus R, Bohling J, Voedisch S, Braun A, et al. Cathepsin G and neutrophil elastase contribute to lung-protective immunity against mycobacterial infections in mice. J Immunol 188: 4476-4487.

REFERENCES CITED

Aimanianda, V., J. Bayry, S. Bozza, O. Kniemeyer, K. Perruccio, S. R. Elluru, C. Clavaud, S. Paris, A. A. Brakhage, S. V. Kaveri, L. Romani & J. P. Latge, (2009) Surface hydrophobin prevents immune recognition of airborne fungal spores. *Nature* **460**: 1117-1121.

Aisaka, K. & T. Masuda, (1995) Production of trehalose phosphorylase by Catellatospora ferruginea. *FEMS Microbiol Lett* **131**: 47-51.

Aisaka, K., T. Masuda, T. Chikamune & K. Kamitori, (1998) Purification and characterization of trehalose phosphorylase from Catellatospora ferruginea. *Biosci Biotechnol Biochem* **62**: 782-787.

Al-Bader, N., G. Vanier, H. Liu, F. N. Gravelat, M. Urb, C. M. Hoareau, P. Campoli, J. Chabot, S. G. Filler & D. C. Sheppard, (2010a) The role of trehalose biosynthesis in Aspergillus fumigatus development, stress response and virulence. *Infect Immun*.

Al-Bader, N., G. Vanier, H. Liu, F. N. Gravelat, M. Urb, C. M. Hoareau, P. Campoli, J. Chabot, S. G. Filler & D. C. Sheppard, (2010b) Role of trehalose biosynthesis in Aspergillus fumigatus development, stress response, and virulence. *Infect Immun* **78**: 3007-3018.

Almyroudis, N. G., S. M. Holland & B. H. Segal, (2005) Invasive aspergillosis in primary immunodeficiencies. *Med Mycol* **43 Suppl 1**: S247-259.

Alp, S. & S. Arikan, (2008) Investigation of extracellular elastase, acid proteinase and phospholipase activities as putative virulence factors in clinical isolates of Aspergillus species. *J Basic Microbiol* **48**: 331-337.

Altschul, S. F., W. Gish, W. Miller, E. W. Myers & D. J. Lipman, (1990) Basic local alignment search tool. *J Mol Biol* **215**: 403-410.

Anderson, P. J., L. N. Karageuzian, H. M. Cheng & D. L. Epstein, (1984) Hexokinase of calf trabecular meshwork. *Invest Ophthalmol Vis Sci* **25**: 1258-1261.

Arnaud, M. B., G. C. Cerqueira, D. O. Inglis, M. S. Skrzypek, J. Binkley, M. C. Chibucos, J. Crabtree, C. Howarth, J. Orvis, P. Shah, F. Wymore, G. Binkley, S. R. Miyasato, M. Simison, G. Sherlock & J. R. Wortman, The Aspergillus Genome Database (AspGD): recent developments in comprehensive multispecies curation, comparative genomics and community resources. *Nucleic Acids Res* **40**: D653-659.

Aufauvre-Brown, A., E. Mellado, N. A. R. Gow & D. W. Holden, (1997) Aspergillus fumigatus chsE: A Gene Related to CHS3 of Saccharomyces cerevisiae and

Important for Hyphal Growth and Conidiophore Development but Not Pathogenicity. *Fungal Genet Biol* **21**: 141-152.

Avonce, N., A. Mendoza-Vargas, E. Morett & G. Iturriaga, (2006) Insights on the evolution of trehalose biosynthesis. *BMC Evol Biol* **6**: 109.

Babenko, V. N. & D. M. Krylov, (2004) Comparative analysis of complete genomes reveals gene loss, acquisition and acceleration of evolutionary rates in Metazoa, suggests a prevalence of evolution via gene acquisition and indicates that the evolutionary rates in animals tend to be conserved. *Nucleic Acids Res* **32**: 5029-5035.

Balloy, V. & M. Chignard, (2009) The innate immune response to Aspergillus fumigatus. *Microbes Infect* **11**: 919-927.

Balloy, V., M. Huerre, J. P. Latge & M. Chignard, (2005) Differences in patterns of infection and inflammation for corticosteroid treatment and chemotherapy in experimental invasive pulmonary aspergillosis. *Infect Immun* **73**: 494-503.

Bell, W., P. Klaassen, M. Ohnacker, T. Boller, M. Herweijer, P. Schoppink, P. Van der Zee & A. Wiemken, (1992) Characterization of the 56-kDa subunit of yeast trehalose-6-phosphate synthase and cloning of its gene reveal its identity with the product of CIF1, a regulator of carbon catabolite inactivation. *Eur J Biochem* **209**: 951-959.

Bell, W., W. Sun, S. Hohmann, S. Wera, A. Reinders, C. De Virgilio, A. Wiemken & J. M. Thevelein, (1998) Composition and functional analysis of the Saccharomyces cerevisiae trehalose synthase complex. *J Biol Chem* **273**: 33311-33319.

Bellocchio, S., C. Montagnoli, S. Bozza, R. Gaziano, G. Rossi, S. S. Mambula, A. Vecchi, A. Mantovani, S. M. Levitz & L. Romani, (2004) The contribution of the Toll-like/IL-1 receptor superfamily to innate and adaptive immunity to fungal pathogens in vivo. *J Immunol* **172**: 3059-3069.

Belocopitow, E. & L. R. Marechal, (1970) Trehalose phosphorylase from Euglena gracilis. *Biochim Biophys Acta* **198**: 151-154.

Belocopitow, E. & L. R. Marechal, (1974) Metabolism of trehalose in Euglena gracilis. Partial purification and some properties of phosphoglucomutase acting on beta-glucose 1-phosphate. *Eur J Biochem* **46**: 631-637.

Bergmeyer, H. U., M. Grassl & H. E. Walter, (1983). In: Methods of Enzymatic Analysis (Bergmeyer, H.U.ed) 3rd ed. Deerfield Beach, FL: Verlag Chemie, pp. Volume II, 222-223.

Bernard, M. & J. P. Latge, (2001) Aspergillus fumigatus cell wall: composition and biosynthesis. *Med Mycol* **39 Suppl 1**: 9-17.

Bhabhra, R. & D. S. Askew, (2005) Thermotolerance and virulence of Aspergillus fumigatus: role of the fungal nucleolus. *Med Mycol* **43 Suppl 1**: S87-93.

Bianchi, M., A. Hakkim, V. Brinkmann, U. Siler, R. A. Seger, A. Zychlinsky & J. Reichenbach, (2009) Restoration of NET formation by gene therapy in CGD controls aspergillosis. *Blood* **114**: 2619-2622.

Bianchi, M., M. J. Niemiec, U. Siler, C. F. Urban & J. Reichenbach, Restoration of anti-Aspergillus defense by neutrophil extracellular traps in human chronic granulomatous disease after gene therapy is calprotectin-dependent. *J Allergy Clin Immunol* **127**: 1243-1252 e1247.

Blazquez, M. A., R. Lagunas, C. Gancedo & J. M. Gancedo, (1993) Trehalose-6-phosphate, a new regulator of yeast glycolysis that inhibits hexokinases. *FEBS Lett* **329**: 51-54.

Blazquez, M. A., R. Stucka, H. Feldmann & C. Gancedo, (1994) Trehalose-6-P synthase is dispensable for growth on glucose but not for spore germination in Schizosaccharomyces pombe. *J Bacteriol* **176**: 3895-3902.

Bok, J. W., S. A. Balajee, K. A. Marr, D. Andes, K. F. Nielsen, J. C. Frisvad & N. P. Keller, (2005) LaeA, a regulator of morphogenetic fungal virulence factors. *Eukaryot Cell* **4**: 1574-1582.

Borgia, P. T. & C. L. Dodge, (1992) Characterization of *Aspergillus nidulans* mutants deficient in cell wall chitin or glucan. *J Bacteriol* **174**: 377-383.

Borgia, P. T., Y. Miao & C. L. Dodge, (1996) The *orlA* gene from *Aspergillus nidulans* encodes a trehalose-6-phosphate phosphatase necessary for normal growth and chitin synthesis at elevated temperatures. *Mol Microbiol* **20**: 1287-1296.

Brakhage, A. A., S. Bruns, A. Thywissen, P. F. Zipfel & J. Behnsen, Interaction of phagocytes with filamentous fungi. *Curr Opin Microbiol* **13**: 409-415.

Brakhage, A. A. & K. Langfelder, (2002) Menacing mold: the molecular biology of Aspergillus fumigatus. *Annu Rev Microbiol* **56**: 433-455.

Brakhage, A. A. & B. Liebmann, (2005) Aspergillus fumigatus conidial pigment and cAMP signal transduction: significance for virulence. *Med Mycol* **43 Suppl 1**: S75-82.

Brennan, M., D. Y. Thomas, M. Whiteway & K. Kavanagh, (2002) Correlation between virulence of Candida albicans mutants in mice and Galleria mellonella larvae. *FEMS Immunol Med Microbiol* **34**: 153-157.

Brewster, J. L., T. de Valoir, N. D. Dwyer, E. Winter & M. C. Gustin, (1993) An osmosensing signal transduction pathway in yeast. *Science* **259**: 1760-1763.

Brown, G. D. & S. Gordon, (2001) Immune recognition. A new receptor for beta-glucans. *Nature* **413**: 36-37.

Brown, G. D., J. Herre, D. L. Williams, J. A. Willment, A. S. Marshall & S. Gordon, (2003) Dectin-1 mediates the biological effects of beta-glucans. *J Exp Med* **197**: 1119-1124.

Brun, Y. F., C. G. Dennis, W. R. Greco, R. J. Bernacki, P. J. Pera, J. J. Bushey, R. C. Youn, D. B. White & B. H. Segal, (2007) Modeling the combination of amphotericin B, micafungin, and nikkomycin Z against *Aspergillus fumigatus in vitro* using a novel response surface paradigm. *Antimicrob Agents Chemother* **51**: 1804-1812.

Bruns, S., O. Kniemeyer, M. Hasenberg, V. Aimanianda, S. Nietzsche, A. Thywissen, A. Jeron, J. P. Latge, A. A. Brakhage & M. Gunzer, Production of extracellular traps against Aspergillus fumigatus in vitro and in infected lung tissue is dependent on invading neutrophils and influenced by hydrophobin RodA. *PLoS Pathog* **6**: e1000873.

Cabib, E. & L. F. Leloir, (1958) The biosynthesis of trehalose phosphate. *J Biol Chem* **231**: 259-275.

Cabib, E., D. H. Roh, M. Schmidt, L. B. Crotti & A. Varma, (2001) The yeast cell wall and septum as paradigms of cell growth and morphogenesis. *J Biol Chem* **276**: 19679-19682.

Calvo, A. M., R. A. Wilson, J. W. Bok & N. P. Keller, (2002) Relationship between secondary metabolism and fungal development. *Microbiol Mol Biol Rev* **66**: 447-459, table of contents.

Cao, Y., Y. Wang, B. Dai, B. Wang, H. Zhang, Z. Zhu, Y. Xu, Y. Jiang & G. Zhang, (2008) Trehalose is an important mediator of Cap1p oxidative stress response in *Candida albicans*. *Biol Pharm Bull* **31**: 421-425.

Casadevall, A., (2005) Fungal virulence, vertebrate endothermy, and dinosaur extinction: is there a connection? *Fungal Genet Biol* **42**: 98-106.

Chai, L. Y., M. G. Netea, J. Sugui, A. G. Vonk, W. W. van de Sande, A. Warris, K. J. Kwon-Chung & B. J. Kullberg, Aspergillus fumigatus conidial melanin modulates host cytokine response. *Immunobiology* **215**: 915-920.

Chai, L. Y., A. G. Vonk, B. J. Kullberg, P. E. Verweij, I. Verschueren, J. W. van der Meer, L. A. Joosten, J. P. Latge & M. G. Netea, Aspergillus fumigatus cell wall components differentially modulate host TLR2 and TLR4 responses. *Microbes Infect* **13**: 151-159.

Choi, W. & R. A. Dean, (1997) The adenylate cyclase gene MAC1 of Magnaporthe grisea controls appressorium formation and other aspects of growth and development. *Plant Cell* **9**: 1973-1983.

Clark, A. F. & C. L. Villemez, (1972) The Formation of beta, 1 --> 4 Glucan from UDP-alpha-d-Glucose Catalyzed by a Phaseolus aureus Enzyme. *Plant Physiol* **50**: 371-374.

Cooney, N. M. & B. S. Klein, (2008) Fungal adaptation to the mammalian host: it is a new world, after all. *Curr Opin Microbiol* **11**: 511-516.

Cornish, E. J., B. J. Hurtgen, K. McInnerney, N. L. Burritt, R. M. Taylor, J. N. Jarvis, S. Y. Wang & J. B. Burritt, (2008) Reduced nicotinamide adenine dinucleotide phosphate oxidase-independent resistance to Aspergillus fumigatus in alveolar macrophages. *J Immunol* **180**: 6854-6867.

Cramer, R. A., Jr., M. P. Gamcsik, R. M. Brooking, L. K. Najvar, W. R. Kirkpatrick, T. F. Patterson, C. J. Balibar, J. R. Graybill, J. R. Perfect, S. N. Abraham & W. J. Steinbach, (2006) Disruption of a nonribosomal peptide synthetase in *Aspergillus fumigatus* eliminates gliotoxin production. *Eukaryot Cell* **5**: 972-980.

Cramer, R. A., Jr., B. Z. Perfect, N. Pinchai, S. Park, D. S. Perlin, Y. G. Asfaw, J. Heitman, J. R. Perfect & W. J. Steinbach, (2008) Calcineurin target CrzA regulates conidial germination, hyphal growth, and pathogenesis of Aspergillus fumigatus. *Eukaryot Cell* **7**: 1085-1097.

Cramer, R. A., A. Rivera & T. M. Hohl, Immune responses against Aspergillus fumigatus: what have we learned? *Curr Opin Infect Dis* **24**: 315-322.

Crowe, J. H., F. A. Hoekstra & L. M. Crowe, (1992) Anhydrobiosis. *Annu Rev Physiol* **54**: 579-599.

Crowe, L. M., D. S. Reid & J. H. Crowe, (1996) Is trehalose special for preserving dry biomaterials? *Biophys J* **71**: 2087-2093.

Cunha, C., M. Di Ianni, S. Bozza, G. Giovannini, S. Zagarella, T. Zelante, C. D'Angelo, A. Pierini, L. Pitzurra, F. Falzetti, A. Carotti, K. Perruccio, J. P. Latge, F. Rodrigues, A. Velardi, F. Aversa, L. Romani & A. Carvalho, Dectin-1 Y238X polymorphism associates with susceptibility to invasive aspergillosis in hematopoietic transplantation through impairment of both recipient- and donor-dependent mechanisms of antifungal immunity. *Blood* **116**: 5394-5402.

d'Enfert, C., (1996) Selection of multiple disruption events in *Aspergillus fumigatus* using the orotidine-5'-decarboxylase gene, *pyrG*, as a unique transformation marker. *Curr Genet* **30**: 76-82.

d'Enfert, C., B. M. Bonini, P. D. Zapella, T. Fontaine, A. M. da Silva & H. F. Terenzi, (1999) Neutral trehalases catalyse intracellular trehalose breakdown in the filamentous fungi Aspergillus nidulans and Neurospora crassa. *Mol Microbiol* **32**: 471-483.

d'Enfert, C. & T. Fontaine, (1997) Molecular characterization of the Aspergillus nidulans treA gene encoding an acid trehalase required for growth on trehalose. *Mol Microbiol* **24**: 203-216.

Da Silva, C. A., C. Chalouni, A. Williams, D. Hartl, C. G. Lee & J. A. Elias, (2009) Chitin is a size-dependent regulator of macrophage TNF and IL-10 production. *J Immunol* **182**: 3573-3582.

Dagenais, T. R. & N. P. Keller, (2009) Pathogenesis of Aspergillus fumigatus in Invasive Aspergillosis. *Clin Microbiol Rev* **22**: 447-465.

Daley, J. M., A. A. Thomay, M. D. Connolly, J. S. Reichner & J. E. Albina, (2008) Use of Ly6G-specific monoclonal antibody to deplete neutrophils in mice. *J Leukoc Biol* **83**: 64-70.

Damveld, R. A., M. Arentshorst, A. Franken, P. A. vanKuyk, F. M. Klis, C. A. van den Hondel & A. F. Ram, (2005a) The Aspergillus niger MADS-box transcription factor RlmA is required for cell wall reinforcement in response to cell wall stress. *Mol Microbiol* **58**: 305-319.

Damveld, R. A., P. A. vanKuyk, M. Arentshorst, F. M. Klis, C. A. van den Hondel & A. F. Ram, (2005b) Expression of agsA, one of five 1,3-alpha-D-glucan synthase-encoding genes in Aspergillus niger, is induced in response to cell wall stress. *Fungal Genet Biol* **42**: 165-177.

de Nobel, H., C. Ruiz, H. Martin, W. Morris, S. Brul, M. Molina & F. M. Klis, (2000) Cell wall perturbation in yeast results in dual phosphorylation of the Slt2/Mpk1

MAP kinase and in an Slt2-mediated increase in FKS2-lacZ expression, glucanase resistance and thermotolerance. *Microbiology* **146 (Pt 9)**: 2121-2132.

De Virgilio, C., N. Burckert, W. Bell, P. Jeno, T. Boller & A. Wiemken, (1993) Disruption of TPS2, the gene encoding the 100-kDa subunit of the trehalose-6-phosphate synthase/phosphatase complex in Saccharomyces cerevisiae, causes accumulation of trehalose-6-phosphate and loss of trehalose-6-phosphate phosphatase activity. *Eur J Biochem* **212**: 315-323.

De Virgilio, C., U. Simmen, T. Hottiger, T. Boller & A. Wiemken, (1990) Heat shock induces enzymes of trehalose metabolism, trehalose accumulation, and thermotolerance in Schizosaccharomyces pombe, even in the presence of cycloheximide. *FEBS Lett* **273**: 107-110.

Dennehy, K. M., G. Ferwerda, I. Faro-Trindade, E. Pyz, J. A. Willment, P. R. Taylor, A. Kerrigan, S. V. Tsoni, S. Gordon, F. Meyer-Wentrup, G. J. Adema, B. J. Kullberg, E. Schweighoffer, V. Tybulewicz, H. M. Mora-Montes, N. A. Gow, D. L. Williams, M. G. Netea & G. D. Brown, (2008) Syk kinase is required for collaborative cytokine production induced through Dectin-1 and Toll-like receptors. *Eur J Immunol* **38**: 500-506.

Denning, D. W., (1996) Therapeutic outcome in invasive aspergillosis. *Clin Infect Dis* **23**: 608-615.

Denning, D. W., (1998) Invasive aspergillosis. *Clin Infect Dis* **26**: 781-803; quiz 804-785.

Dixon, K. P., J. R. Xu, N. Smirnoff & N. J. Talbot, (1999) Independent signaling pathways regulate cellular turgor during hyperosmotic stress and appressorium-mediated plant infection by Magnaporthe grisea. *Plant Cell* **11**: 2045-2058.

Drent, M., N. A. Cobben, R. F. Henderson, E. F. Wouters & M. van Dieijen-Visser, (1996) Usefulness of lactate dehydrogenase and its isoenzymes as indicators of lung damage or inflammation. *Eur Respir J* **9**: 1736-1742.

Drickamer, K. & M. E. Taylor, (1993) Biology of animal lectins. *Annu Rev Cell Biol* **9**: 237-264.

Ebel, F., M. Schwienbacher, J. Beyer, J. Heesemann, A. A. Brakhage & M. Brock, (2006) Analysis of the regulation, expression, and localisation of the isocitrate lyase from Aspergillus fumigatus, a potential target for antifungal drug development. *Fungal Genet Biol* **43**: 476-489.

Edavana, V. K., I. Pastuszak, J. D. Carroll, P. Thampi, E. C. Abraham & A. D. Elbein, (2004) Cloning and expression of the trehalose-phosphate phosphatase of

Mycobacterium tuberculosis: comparison to the enzyme from Mycobacterium smegmatis. *Arch Biochem Biophys* **426**: 250-257.

Eis, C. & B. Nidetzky, (1999) Characterization of trehalose phosphorylase from Schizophyllum commune. *Biochem J* **341 (Pt 2)**: 385-393.

Ejzykowicz, D. E., M. M. Cunha, S. Rozental, N. V. Solis, F. N. Gravelat, D. C. Sheppard & S. G. Filler, (2009) The *Aspergillus fumigatus* transcription factor Ace2 governs pigment production, conidiation and virulence. *Mol Microbiol* **72**: 155-169.

El-Benna, J., P. M. Dang, M. A. Gougerot-Pocidalo & C. Elbim, (2005) Phagocyte NADPH oxidase: a multicomponent enzyme essential for host defenses. *Arch Immunol Ther Exp (Warsz)* **53**: 199-206.

Elbein, A. D., Y. T. Pan, I. Pastuszak & D. Carroll, (2003) New insights on trehalose: a multifunctional molecule. *Glycobiology* **13**: 17R-27R.

Elliott, B., R. S. Haltiwanger & B. Futcher, (1996) Synergy between trehalose and Hsp104 for thermotolerance in *Saccharomyces cerevisiae*. *Genetics* **144**: 923-933.

Erjavec, Z., H. Kluin-Nelemans & P. E. Verweij, (2009) Trends in invasive fungal infections, with emphasis on invasive aspergillosis. *Clin Microbiol Infect* **15**: 625-633.

Fedorova, N. D., N. Khaldi, V. S. Joardar, R. Maiti, P. Amedeo, M. J. Anderson, J. Crabtree, J. C. Silva, J. H. Badger, A. Albarraq, S. Angiuoli, H. Bussey, P. Bowyer, P. J. Cotty, P. S. Dyer, A. Egan, K. Galens, C. M. Fraser-Liggett, B. J. Haas, J. M. Inman, R. Kent, S. Lemieux, I. Malavazi, J. Orvis, T. Roemer, C. M. Ronning, J. P. Sundaram, G. Sutton, G. Turner, J. C. Venter, O. R. White, B. R. Whitty, P. Youngman, K. H. Wolfe, G. H. Goldman, J. R. Wortman, B. Jiang, D. W. Denning & W. C. Nierman, (2008) Genomic islands in the pathogenic filamentous fungus Aspergillus fumigatus. *PLoS Genet* **4**: e1000046.

Feng, X., K. Krishnan, D. L. Richie, V. Aimanianda, L. Hartl, N. Grahl, M. V. Powers-Fletcher, M. Zhang, K. K. Fuller, W. C. Nierman, L. J. Lu, J. P. Latge, L. Woollett, S. L. Newman, R. A. Cramer, Jr., J. C. Rhodes & D. S. Askew, HacA-independent functions of the ER stress sensor IreA synergize with the canonical UPR to influence virulence traits in Aspergillus fumigatus. *PLoS Pathog* **7**: e1002330.

Fillinger, S., M. K. Chaveroche, P. van Dijck, R. de Vries, G. Ruijter, J. Thevelein & C. d'Enfert, (2001) Trehalose is required for the acquisition of tolerance to a variety

of stresses in the filamentous fungus *Aspergillus nidulans*. *Microbiology* **147**: 1851-1862.

Fleck, C. B. & M. Brock, Aspergillus fumigatus catalytic glucokinase and hexokinase: expression analysis and importance for germination, growth, and conidiation. *Eukaryot Cell* **9**: 1120-1135.

Flipphi, M., J. Sun, X. Robellet, L. Karaffa, E. Fekete, A. P. Zeng & C. P. Kubiecek, (2009) Biodiversity and evolution of primary carbon metabolism in Aspergillus nidulans and other Aspergillus spp. *Fungal Genet Biol* **46 Suppl 1**: S19-S44.

Flipphi, M., P. J. van de Vondervoort, G. J. Ruijter, J. Visser, H. N. Arst, Jr. & B. Felenbok, (2003) Onset of carbon catabolite repression in Aspergillus nidulans. Parallel involvement of hexokinase and glucokinase in sugar signaling. *J Biol Chem* **278**: 11849-11857.

Flores, C. L., C. Gancedo & T. Petit, Disruption of Yarrowia lipolytica TPS1 gene encoding trehalose-6-P synthase does not affect growth in glucose but impairs growth at high temperature. *PLoS One* **6**: e23695.

Fontaine, T., A. Delangle, C. Simenel, B. Coddeville, S. J. van Vliet, Y. van Kooyk, S. Bozza, S. Moretti, F. Schwarz, C. Trichot, M. Aebi, M. Delepierre, C. Elbim, L. Romani & J. P. Latge, Galactosaminogalactan, a new immunosuppressive polysaccharide of Aspergillus fumigatus. *PLoS Pathog* **7**: e1002372.

Fontaine, T., C. Simenel, G. Dubreucq, O. Adam, M. Delepierre, J. Lemoine, C. E. Vorgias, M. Diaquin & J. P. Latge, (2000) Molecular organization of the alkali-insoluble fraction of Aspergillus fumigatus cell wall. *J Biol Chem* **275**: 27594-27607.

Foster, A. J., J. M. Jenkinson & N. J. Talbot, (2003) Trehalose synthesis and metabolism are required at different stages of plant infection by *Magnaporthe grisea*. *EMBO J* **22**: 225-235.

Fuller, K. K., W. Zhao, D. S. Askew & J. C. Rhodes, (2009) Deletion of the protein kinase A regulatory subunit leads to deregulation of mitochondrial activation and nuclear duplication in Aspergillus fumigatus. *Eukaryot Cell* **8**: 271-277.

Gancedo, C. & C. L. Flores, (2004) The importance of a functional trehalose biosynthetic pathway for the life of yeasts and fungi. *FEMS Yeast Res* **4**: 351-359.

Gastebois, A., T. Fontaine, J. P. Latge & I. Mouyna, (2010) beta(1-3)Glucanosyltransferase Gel4p is essential for Aspergillus fumigatus. *Eukaryot Cell* **9**: 1294-1298.

Gerson, S. L., G. H. Talbot, S. Hurwitz, B. L. Strom, E. J. Lusk & P. A. Cassileth, (1984) Prolonged granulocytopenia: the major risk factor for invasive pulmonary aspergillosis in patients with acute leukemia. *Ann Intern Med* **100**: 345-351.

Goodridge, H. S., A. J. Wolf & D. M. Underhill, (2009) Beta-glucan recognition by the innate immune system. *Immunol Rev* **230**: 38-50.

Graham, L. M., S. V. Tsoni, J. A. Willment, D. L. Williams, P. R. Taylor, S. Gordon, K. Dennehy & G. D. Brown, (2006) Soluble Dectin-1 as a tool to detect beta-glucans. *J Immunol Methods* **314**: 164-169.

Grahl, N., S. Puttikamonkul, J. M. Macdonald, M. P. Gamcsik, L. Y. Ngo, T. M. Hohl & R. A. Cramer, In vivo hypoxia and a fungal alcohol dehydrogenase influence the pathogenesis of invasive pulmonary aspergillosis. *PLoS Pathog* **7**: e1002145.

Gravelat, F. N., D. E. Ejzykowicz, L. Y. Chiang, J. C. Chabot, M. Urb, K. D. Macdonald, N. al-Bader, S. G. Filler & D. C. Sheppard, Aspergillus fumigatus MedA governs adherence, host cell interactions and virulence. *Cell Microbiol* **12**: 473-488.

Gugnani, H. C., (2003) Ecology and taxonomy of pathogenic aspergilli. *Front Biosci* **8**: s346-357.

Han, S. E., H. B. Kwon, S. B. Lee, B. Y. Yi, I. Murayama, Y. Kitamoto & M. O. Byun, (2003) Cloning and characterization of a gene encoding trehalose phosphorylase (TP) from Pleurotus sajor-caju. *Protein Expr Purif* **30**: 194-202.

Harris, J. L., (1986) Modified method for fungal slide culture. *J Clin Microbiol* **24**: 460-461.

Hasenberg, M., J. Behnsen, S. Krappmann, A. Brakhage & M. Gunzer, Phagocyte responses towards Aspergillus fumigatus. *Int J Med Microbiol* **301**: 436-444.

Heinsbroek, S. E., P. R. Taylor, M. Rosas, J. A. Willment, D. L. Williams, S. Gordon & G. D. Brown, (2006) Expression of functionally different dectin-1 isoforms by murine macrophages. *J Immunol* **176**: 5513-5518.

Henriet, S. S., P. W. Hermans, P. E. Verweij, E. Simonetti, S. M. Holland, J. A. Sugui, K. J. Kwon-Chung & A. Warris, Human leukocytes kill Aspergillus nidulans by reactive oxygen species-independent mechanisms. *Infect Immun* **79**: 767-773.

Henry, C., J. P. Latge & A. Beauvais, alpha1,3 glucans are dispensable in Aspergillus fumigatus. *Eukaryot Cell* **11**: 26-29.

Herbrecht, R., D. W. Denning, T. F. Patterson, J. E. Bennett, R. E. Greene, J. W. Oestmann, W. V. Kern, K. A. Marr, P. Ribaud, O. Lortholary, R. Sylvester, R. H. Rubin, J. R. Wingard, P. Stark, C. Durand, D. Caillot, E. Thiel, P. H. Chandrasekar, M. R. Hodges, H. T. Schlamm, P. F. Troke & B. de Pauw, (2002) Voriconazole versus amphotericin B for primary therapy of invasive aspergillosis. *N Engl J Med* **347**: 408-415.

Hohl, T. M., H. L. Van Epps, A. Rivera, L. A. Morgan, P. L. Chen, M. Feldmesser & E. G. Pamer, (2005) Aspergillus fumigatus triggers inflammatory responses by stage-specific beta-glucan display. *PLoS Pathog* **1**: e30.

Hohmann, S., W. Bell, M. J. Neves, D. Valckx & J. M. Thevelein, (1996) Evidence for trehalose-6-phosphate-dependent and -independent mechanisms in the control of sugar influx into yeast glycolysis. *Mol Microbiol* **20**: 981-991.

Horikoshi, K. & Y. Ikeda, (1966) Trehalase in conidia of Aspergillus oryzae. *J Bacteriol* **91**: 1883-1887.

Hottiger, T., C. De Virgilio, M. N. Hall, T. Boller & A. Wiemken, (1994) The role of trehalose synthesis for the acquisition of thermotolerance in yeast. II. Physiological concentrations of trehalose increase the thermal stability of proteins *in vitro*. *Eur J Biochem* **219**: 187-193.

Hottiger, T., P. Schmutz & A. Wiemken, (1987) Heat-induced accumulation and futile cycling of trehalose in Saccharomyces cerevisiae. *J Bacteriol* **169**: 5518-5522.

Huppert, M., D. J. Oliver & S. H. Sun, (1978) Combined methenamine-silver nitrate and hematoxylin & eosin stain for fungi in tissues. *J Clin Microbiol* **8**: 598-603.

Ishihara, R., S. Taketani, M. Sasai-Takedatsu, Y. Adachi, M. Kino, A. Furuya, N. Hanai, R. Tokunaga & Y. Kobayashi, (2000) ELISA for urinary trehalase with monoclonal antibodies: a technique for assessment of renal tubular damage. *Clin Chem* **46**: 636-643.

Ishihara, R., S. Taketani, M. Sasai-Takedatsu, M. Kino, R. Tokunaga & Y. Kobayashi, (1997) Molecular cloning, sequencing and expression of cDNA encoding human trehalase. *Gene* **202**: 69-74.

Jacobson, E. S., (2000) Pathogenic roles for fungal melanins. *Clin Microbiol Rev* **13**: 708-717.

Janeway, C. A., Jr., (1989) Approaching the asymptote? Evolution and revolution in immunology. *Cold Spring Harb. Symp. Quant. Biol.* **54**: 1-13.

Johnson, E. A., (1946) An Improved Slide Culture Technique for the Study and Identification of Pathogenic Fungi. *J Bacteriol* **51**: 689-694.

Kandror, O., A. DeLeon & A. L. Goldberg, (2002) Trehalose synthesis is induced upon exposure of Escherichia coli to cold and is essential for viability at low temperatures. *Proc Natl Acad Sci U S A* **99**: 9727-9732.

Kane, S. M. & R. Roth, (1974) Carbohydrate metabolism during ascospore development in yeast. *J Bacteriol* **118**: 8-14.

Kaur, R., B. Ma & B. P. Cormack, (2007) A family of glycosylphosphatidylinositol-linked aspartyl proteases is required for virulence of *Candida glabrata*. *Proc Natl Acad Sci U S A* **104**: 7628-7633.

Keller, N. P., G. Turner & J. W. Bennett, (2005) Fungal secondary metabolism - from biochemistry to genomics. *Nat Rev Microbiol* **3**: 937-947.

Kerrigan, A. M. & G. D. Brown, Syk-coupled C-type lectins in immunity. *Trends Immunol* **32**: 151-156.

Kitamoto, Y., Akashi, H., Tanaka, H. and Mori, N. , (1988) α-Glucose-1-phosphate formation by a novel trehalose phosphorylase from *Flammulina velutipes*. *FEMS Microbiology Letters* **55**: 147-150.

Kitamoto, Y., Osaki, N., Tanaka, H., Sasaki, H., Mori, N., (2000) Purification and properties of a-glucose 1-phosphate-forming trehalose phosphorylase from basidiomycete, Pleurotus ostreatus. *Mycoscience* **41**: 607-613.

Kontoyiannis, D. P. & G. P. Bodey, (2002) Invasive aspergillosis in 2002: an update. *Eur J Clin Microbiol Infect Dis* **21**: 161-172.

Kontoyiannis, D. P., K. A. Marr, B. J. Park, B. D. Alexander, E. J. Anaissie, T. J. Walsh, J. Ito, D. R. Andes, J. W. Baddley, J. M. Brown, L. M. Brumble, A. G. Freifeld, S. Hadley, L. A. Herwaldt, C. A. Kauffman, K. Knapp, G. M. Lyon, V. A. Morrison, G. Papanicolaou, T. F. Patterson, T. M. Perl, M. G. Schuster, R. Walker, K. A. Wannemuehler, J. R. Wingard, T. M. Chiller & P. G. Pappas, Prospective surveillance for invasive fungal infections in hematopoietic stem cell transplant recipients, 2001-2006: overview of the Transplant-Associated Infection Surveillance Network (TRANSNET) Database. *Clin Infect Dis* **50**: 1091-1100.

Koonin, E. V., N. D. Fedorova, J. D. Jackson, A. R. Jacobs, D. M. Krylov, K. S. Makarova, R. Mazumder, S. L. Mekhedov, A. N. Nikolskaya, B. S. Rao, I. B. Rogozin, S. Smirnov, A. V. Sorokin, A. V. Sverdlov, S. Vasudevan, Y. I. Wolf, J.

J. Yin & D. A. Natale, (2004) A comprehensive evolutionary classification of proteins encoded in complete eukaryotic genomes. *Genome Biol* **5**: R7.

Kupfahl, C., T. Heinekamp, G. Geginat, T. Ruppert, A. Hartl, H. Hof & A. A. Brakhage, (2006) Deletion of the gliP gene of Aspergillus fumigatus results in loss of gliotoxin production but has no effect on virulence of the fungus in a low-dose mouse infection model. *Mol Microbiol* **62**: 292-302.

Latge, J. P., (1999) Aspergillus fumigatus and aspergillosis. *Clin Microbiol Rev* **12**: 310-350.

Latge, J. P., (2007) The cell wall: a carbohydrate armour for the fungal cell. *Mol Microbiol* **66**: 279-290.

Latge, J. P., (2010) Tasting the fungal cell wall. *Cell Microbiol* **12**: 863-872.

Lee, J. H., K. H. Lee, C. G. Kim, S. Y. Lee, G. J. Kim, Y. H. Park & S. O. Chung, (2005) Cloning and expression of a trehalose synthase from Pseudomonas stutzeri CJ38 in Escherichia coli for the production of trehalose. *Appl Microbiol Biotechnol* **68**: 213-219.

Levin, D. E., (2005) Cell wall integrity signaling in Saccharomyces cerevisiae. *Microbiol Mol Biol Rev* **69**: 262-291.

Li, H., B. M. Barker, N. Grahl, S. Puttikamonkul, J. D. Bell, K. D. Craven & R. A. Cramer, Jr., The small GTPase RacA mediates intracellular reactive oxygen species production, polarized growth, and virulence in the human fungal pathogen Aspergillus fumigatus. *Eukaryot Cell* **10**: 174-186.

Lillie, S. H. & J. R. Pringle, (1980) Reserve carbohydrate metabolism in Saccharomyces cerevisiae: responses to nutrient limitation. *J Bacteriol* **143**: 1384-1394.

Livak, K. J. & T. D. Schmittgen, (2001) Analysis of relative gene expression data using real-time quantitative PCR and the 2(-Delta Delta C(T)) Method. *Methods* **25**: 402-408.

Lockington, R. A., G. N. Borlace & J. M. Kelly, (1997) Pyruvate decarboxylase and anaerobic survival in Aspergillus nidulans. *Gene* **191**: 61-67.

Lombardi, L. M. & S. Brody, (2005) Circadian rhythms in Neurospora crassa: clock gene homologues in fungi. *Fungal Genet Biol* **42**: 887-892.

Londesborough, J. & O. Vuorio, (1991) Trehalose-6-phosphate synthase/phosphatase complex from bakers' yeast: purification of a proteolytically activated form. *J Gen Microbiol* **137**: 323-330.

Lorenz, M. C. & G. R. Fink, (2001) The glyoxylate cycle is required for fungal virulence. *Nature* **412**: 83-86.

Lowell, C. A., L. Fumagalli & G. Berton, (1996) Deficiency of Src family kinases p59/61hck and p58c-fgr results in defective adhesion-dependent neutrophil functions. *J Cell Biol* **133**: 895-910.

Luley-Goedl, C. & B. Nidetzky, Carbohydrate synthesis by disaccharide phosphorylases: reactions, catalytic mechanisms and application in the glycosciences. *Biotechnol J* **5**: 1324-1338.

Lunn, J. E., R. Feil, J. H. Hendriks, Y. Gibon, R. Morcuende, D. Osuna, W. R. Scheible, P. Carillo, M. R. Hajirezaei & M. Stitt, (2006) Sugar-induced increases in trehalose 6-phosphate are correlated with redox activation of ADPglucose pyrophosphorylase and higher rates of starch synthesis in *Arabidopsis thaliana*. *Biochem J* **397**: 139-148.

Mabey, J. E., M. J. Anderson, P. F. Giles, C. J. Miller, T. K. Attwood, N. W. Paton, E. Bornberg-Bauer, G. D. Robson, S. G. Oliver & D. W. Denning, (2004) CADRE: the Central Aspergillus Data REpository. *Nucleic Acids Res* **32**: D401-405.

Mamishi, S., N. Parvaneh, A. Salavati, S. Abdollahzadeh & M. Yeganeh, (2007) Invasive aspergillosis in chronic granulomatous disease: report of 7 cases. *Eur J Pediatr* **166**: 83-84.

Marechal, L. R. & E. Belocopitow, (1972) Metabolism of trehalose in Euglena gracilis. I. Partial purification and some properties of trehalose phosphorylase. *J Biol Chem* **247**: 3223-3228.

Maruta, K., H. Mitsuzumi, T. Nakada, M. Kubota, H. Chaen, S. Fukuda, T. Sugimoto & M. Kurimoto, (1996) Cloning and sequencing of a cluster of genes encoding novel enzymes of trehalose biosynthesis from thermophilic archaebacterium Sulfolobus acidocaldarius. *Biochim Biophys Acta* **1291**: 177-181.

Maschmeyer, G., A. Haas & O. A. Cornely, (2007) Invasive aspergillosis: epidemiology, diagnosis and management in immunocompromised patients. *Drugs* **67**: 1567-1601.

McCormick, A., L. Heesemann, J. Wagener, V. Marcos, D. Hartl, J. Loeffler, J. Heesemann & F. Ebel, NETs formed by human neutrophils inhibit growth of the pathogenic mold Aspergillus fumigatus. *Microbes Infect* **12**: 928-936.

McDonagh, A., N. D. Fedorova, J. Crabtree, Y. Yu, S. Kim, D. Chen, O. Loss, T. Cairns, G. Goldman, D. Armstrong-James, K. Haynes, H. Haas, M. Schrettl, G. May, W. C. Nierman & E. Bignell, (2008) Sub-telomere directed gene expression during initiation of invasive aspergillosis. *PLoS Pathog* **4**: e1000154.

McIntosh, M., B. A. Stone & V. A. Stanisich, (2005) Curdlan and other bacterial (1-->3)-beta-D-glucans. *Appl Microbiol Biotechnol* **68**: 163-173.

McNeil, M. M., S. L. Nash, R. A. Hajjeh, M. A. Phelan, L. A. Conn, B. D. Plikaytis & D. W. Warnock, (2001) Trends in mortality due to invasive mycotic diseases in the United States, 1980-1997. *Clin Infect Dis* **33**: 641-647.

Medzhitov, R., (2007) Recognition of microorganisms and activation of the immune response. *Nature* **449**: 819-826.

Medzhitov, R. & C. A. Janeway, Jr., (1997) Innate immunity: impact on the adaptive immune response. *Curr Opin Immunol* **9**: 4-9.

Mellado, E., A. Aufauvre-Brown, N. A. Gow & D. W. Holden, (1996) The Aspergillus fumigatus chsC and chsG genes encode class III chitin synthases with different functions. *Mol Microbiol* **20**: 667-679.

Mellado, E., G. Dubreucq, P. Mol, J. Sarfati, S. Paris, M. Diaquin, D. W. Holden, J. L. Rodriguez-Tudela & J. P. Latge, (2003) Cell wall biogenesis in a double chitin synthase mutant (chsG-/chsE-) of Aspergillus fumigatus. *Fungal Genet Biol* **38**: 98-109.

Mesak, L. R. & M. K. Dahl, (2000) Purification and enzymatic characterization of PgcM: a beta-phosphoglucomutase and glucose-1-phosphate phosphodismutase of Bacillus subtilis. *Arch Microbiol* **174**: 256-264.

Micheli, P. A., (1729) Nova plantarum genera juxta Tournefortii methodum disposita. Florence, Italy: Bernardo Paperini.

Milewski, S., I. Gabriel & J. Olchowy, (2006) Enzymes of UDP-GlcNAc biosynthesis in yeast. *Yeast* **23**: 1-14.

Mora-Montes, H. M., M. G. Netea, G. Ferwerda, M. D. Lenardon, G. D. Brown, A. R. Mistry, B. J. Kullberg, C. A. O'Callaghan, C. C. Sheth, F. C. Odds, A. J. Brown,

C. A. Munro & N. A. Gow, Recognition and blocking of innate immunity cells by Candida albicans chitin. *Infect Immun* **79**: 1961-1970.

Morgenstern, D. E., M. A. Gifford, L. L. Li, C. M. Doerschuk & M. C. Dinauer, (1997) Absence of respiratory burst in X-linked chronic granulomatous disease mice leads to abnormalities in both host defense and inflammatory response to Aspergillus fumigatus. *J Exp Med* **185**: 207-218.

Mortensen, K. L., E. Mellado, C. Lass-Florl, J. L. Rodriguez-Tudela, H. K. Johansen & M. C. Arendrup, Environmental study of azole-resistant Aspergillus fumigatus and other aspergilli in Austria, Denmark, and Spain. *Antimicrob Agents Chemother* **54**: 4545-4549.

Mouyna, I., W. Morelle, M. Vai, M. Monod, B. Lechenne, T. Fontaine, A. Beauvais, J. Sarfati, M. C. Prevost, C. Henry & J. P. Latge, (2005) Deletion of GEL2 encoding for a beta(1-3)glucanosyltransferase affects morphogenesis and virulence in Aspergillus fumigatus. *Mol Microbiol* **56**: 1675-1688.

Munro, C. A. & N. A. Gow, (2001) Chitin synthesis in human pathogenic fungi. *Med Mycol* **39 Suppl 1**: 41-53.

Munro, C. A., R. K. Whitton, H. B. Hughes, M. Rella, S. Selvaggini & N. A. Gow, (2003) CHS8-a fourth chitin synthase gene of Candida albicans contributes to in vitro chitin synthase activity, but is dispensable for growth. *Fungal Genet Biol* **40**: 146-158.

Murphy, H. N., G. R. Stewart, V. V. Mischenko, A. S. Apt, R. Harris, M. S. McAlister, P. C. Driscoll, D. B. Young & B. D. Robertson, (2005) The OtsAB pathway is essential for trehalose biosynthesis in Mycobacterium tuberculosis. *J Biol Chem* **280**: 14524-14529.

Murray, I. A., K. Coupland, J. A. Smith, I. D. Ansell & R. G. Long, (2000) Intestinal trehalase activity in a UK population: establishing a normal range and the effect of disease. *Br J Nutr* **83**: 241-245.

Ngamskulrungroj, P., U. Himmelreich, J. A. Breger, C. Wilson, M. Chayakulkeeree, M. B. Krockenberger, R. Malik, H. M. Daniel, D. Toffaletti, J. T. Djordjevic, E. Mylonakis, W. Meyer & J. R. Perfect, (2009) The trehalose synthesis pathway is an integral part of the virulence composite for Cryptococcus gattii. *Infect Immun* **77**: 4584-4596.

Ni, M. & J. H. Yu, (2007) A novel regulator couples sporogenesis and trehalose biogenesis in *Aspergillus nidulans*. *PLoS One* **2**: e970.

Nierman, W. C., A. Pain, M. J. Anderson, J. R. Wortman, H. S. Kim, J. Arroyo, M. Berriman, K. Abe, D. B. Archer, C. Bermejo, J. Bennett, P. Bowyer, D. Chen, M. Collins, R. Coulsen, R. Davies, P. S. Dyer, M. Farman, N. Fedorova, T. V. Feldblyum, R. Fischer, N. Fosker, A. Fraser, J. L. Garcia, M. J. Garcia, A. Goble, G. H. Goldman, K. Gomi, S. Griffith-Jones, R. Gwilliam, B. Haas, H. Haas, D. Harris, H. Horiuchi, J. Huang, S. Humphray, J. Jimenez, N. Keller, H. Khouri, K. Kitamoto, T. Kobayashi, S. Konzack, R. Kulkarni, T. Kumagai, A. Lafon, J. P. Latge, W. Li, A. Lord, C. Lu, W. H. Majoros, G. S. May, B. L. Miller, Y. Mohamoud, M. Molina, M. Monod, I. Mouyna, S. Mulligan, L. Murphy, S. O'Neil, I. Paulsen, M. A. Penalva, M. Pertea, C. Price, B. L. Pritchard, M. A. Quail, E. Rabbinowitsch, N. Rawlins, M. A. Rajandream, U. Reichard, H. Renauld, G. D. Robson, S. Rodriguez de Cordoba, J. M. Rodriguez-Pena, C. M. Ronning, S. Rutter, S. L. Salzberg, M. Sanchez, J. C. Sanchez-Ferrero, D. Saunders, K. Seeger, R. Squares, S. Squares, M. Takeuchi, F. Tekaia, G. Turner, C. R. Vazquez de Aldana, J. Weidman, O. White, J. Woodward, J. H. Yu, C. Fraser, J. E. Galagan, K. Asai, M. Machida, N. Hall, B. Barrell & D. W. Denning, (2005) Genomic sequence of the pathogenic and allergenic filamentous fungus Aspergillus fumigatus. *Nature* **438**: 1151-1156.

Nishimoto, T., M. Nakano, T. Nakada, H. Chaen, S. Fukuda, T. Sugimoto, M. Kurimoto & Y. Tsujisaka, (1996) Purification and properties of a novel enzyme, trehalose synthase, from Pimelobacter sp. R48. *Biosci Biotechnol Biochem* **60**: 640-644.

Noubhani, A., O. Bunoust, B. M. Bonini, J. M. Thevelein, A. Devin & M. Rigoulet, (2009) The trehalose pathway regulates mitochondrial respiratory chain content through hexokinase 2 and cAMP in Saccharomyces cerevisiae. *J Biol Chem* **284**: 27229-27234.

Nwaka, S., B. Mechler, M. Destruelle & H. Holzer, (1995) Phenotypic features of trehalase mutants in Saccharomyces cerevisiae. *FEBS Lett* **360**: 286-290.

O'Gorman, C. M., H. T. Fuller & P. S. Dyer, (2009) Discovery of a sexual cycle in the opportunistic fungal pathogen Aspergillus fumigatus. *Nature* **457**: 471-474.

Orciuolo, E., M. Stanzani, M. Canestraro, S. Galimberti, G. Carulli, R. Lewis, M. Petrini & K. V. Komanduri, (2007) Effects of Aspergillus fumigatus gliotoxin and methylprednisolone on human neutrophils: implications for the pathogenesis of invasive aspergillosis. *J Leukoc Biol* **82**: 839-848.

Pahl, H. L., B. Krauss, K. Schulze-Osthoff, T. Decker, E. B. Traenckner, M. Vogt, C. Myers, T. Parks, P. Warring, A. Muhlbacher, A. P. Czernilofsky & P. A. Baeuerle, (1996) The immunosuppressive fungal metabolite gliotoxin specifically inhibits transcription factor NF-kappaB. *J Exp Med* **183**: 1829-1840.

Pan, Y. T., V. Koroth Edavana, W. J. Jourdian, R. Edmondson, J. D. Carroll, I. Pastuszak & A. D. Elbein, (2004) Trehalose synthase of Mycobacterium smegmatis: purification, cloning, expression, and properties of the enzyme. *Eur J Biochem* **271**: 4259-4269.

Panneman, H., G. J. Ruijter, H. C. van den Broeck, E. T. Driever & J. Visser, (1996) Cloning and biochemical characterisation of an Aspergillus niger glucokinase. Evidence for the presence of separate glucokinase and hexokinase enzymes. *Eur J Biochem* **240**: 518-525.

Panneman, H., G. J. Ruijter, H. C. van den Broeck & J. Visser, (1998) Cloning and biochemical characterisation of Aspergillus niger hexokinase--the enzyme is strongly inhibited by physiological concentrations of trehalose 6-phosphate. *Eur J Biochem* **258**: 223-232.

Pappas, P. G., B. D. Alexander, D. R. Andes, S. Hadley, C. A. Kauffman, A. Freifeld, E. J. Anaissie, L. M. Brumble, L. Herwaldt, J. Ito, D. P. Kontoyiannis, G. M. Lyon, K. A. Marr, V. A. Morrison, B. J. Park, T. F. Patterson, T. M. Perl, R. A. Oster, M. G. Schuster, R. Walker, T. J. Walsh, K. A. Wannemuehler & T. M. Chiller, Invasive fungal infections among organ transplant recipients: results of the Transplant-Associated Infection Surveillance Network (TRANSNET). *Clin Infect Dis* **50**: 1101-1111.

Paris, S., D. Wysong, J. P. Debeaupuis, K. Shibuya, B. Philippe, R. D. Diamond & J. P. Latge, (2003) Catalases of Aspergillus fumigatus. *Infect Immun* **71**: 3551-3562.

Patterson, T., F., (2003) *Aspergillosis*, p. 519. Oxford University Press, New York.

Patterson, T. F., W. R. Kirkpatrick, M. White, J. W. Hiemenz, J. R. Wingard, B. Dupont, M. G. Rinaldi, D. A. Stevens & J. R. Graybill, (2000) Invasive aspergillosis. Disease spectrum, treatment practices, and outcomes. I3 Aspergillus Study Group. *Medicine (Baltimore)* **79**: 250-260.

Perlin, D. S. & E. Mellado, (2008) Antifungal Mechanisms of Action and Resistance. In: *Aspergillus fumigatus* and *Aspergillosis.* J.-P. Latge & W. J. Steinbach (eds). Washington, DC: ASM Press, pp. 568.

Petzold, E. W., U. Himmelreich, E. Mylonakis, T. Rude, D. Toffaletti, G. M. Cox, J. L. Miller & J. R. Perfect, (2006) Characterization and regulation of the trehalose synthesis pathway and its importance in the pathogenicity of *Cryptococcus neoformans*. *Infect Immun* **74**: 5877-5887.

Philippe, B., O. Ibrahim-Granet, M. C. Prevost, M. A. Gougerot-Pocidalo, M. Sanchez Perez, A. Van der Meeren & J. P. Latge, (2003) Killing of Aspergillus fumigatus

by alveolar macrophages is mediated by reactive oxidant intermediates. *Infect Immun* **71**: 3034-3042.

Philpott, C. C., (2006) Iron uptake in fungi: a system for every source. *Biochim Biophys Acta* **1763**: 636-645.

Pitt, J. I., (1994) The current role of Aspergillus and Penicillium in human and animal health. *J Med Vet Mycol* **32 Suppl 1**: 17-32.

Pollock, J. D., D. A. Williams, M. A. Gifford, L. L. Li, X. Du, J. Fisherman, S. H. Orkin, C. M. Doerschuk & M. C. Dinauer, (1995) Mouse model of X-linked chronic granulomatous disease, an inherited defect in phagocyte superoxide production. *Nat Genet* **9**: 202-209.

Puttikamonkul, S., S. D. Willger, N. Grahl, J. R. Perfect, N. Movahed, B. Bothner, S. Park, P. Paderu, D. S. Perlin & R. A. Cramer, Jr., (2010) Trehalose 6-phosphate phosphatase is required for cell wall integrity and fungal virulence but not trehalose biosynthesis in the human fungal pathogen Aspergillus fumigatus. *Mol Microbiol* **77**: 891-911.

Qu, Q., S. J. Lee & W. Boos, (2004) TreT, a novel trehalose glycosyltransferring synthase of the hyperthermophilic archaeon Thermococcus litoralis. *J Biol Chem* **279**: 47890-47897.

Ram, A. F., M. Arentshorst, R. A. Damveld, P. A. vanKuyk, F. M. Klis & C. A. van den Hondel, (2004) The cell wall stress response in Aspergillus niger involves increased expression of the glutamine : fructose-6-phosphate amidotransferase-encoding gene (gfaA) and increased deposition of chitin in the cell wall. *Microbiology* **150**: 3315-3326.

Ram, A. F. & F. M. Klis, (2006) Identification of fungal cell wall mutants using susceptibility assays based on Calcofluor white and Congo red. *Nat Protoc* **1**: 2253-2256.

Ratledge, C. & L. G. Dover, (2000) Iron metabolism in pathogenic bacteria. *Annu Rev Microbiol* **54**: 881-941.

Reese, A. J., A. Yoneda, J. A. Breger, A. Beauvais, H. Liu, C. L. Griffith, I. Bose, M. J. Kim, C. Skau, S. Yang, J. A. Sefko, M. Osumi, J. P. Latge, E. Mylonakis & T. L. Doering, (2007) Loss of cell wall alpha(1-3) glucan affects Cryptococcus neoformans from ultrastructure to virulence. *Mol Microbiol* **63**: 1385-1398.

Reeves, E. P., H. Lu, H. L. Jacobs, C. G. Messina, S. Bolsover, G. Gabella, E. O. Potma, A. Warley, J. Roes & A. W. Segal, (2002) Killing activity of neutrophils is mediated through activation of proteases by K+ flux. *Nature* **416**: 291-297.

Reid, D. M., N. A. Gow & G. D. Brown, (2009) Pattern recognition: recent insights from Dectin-1. *Curr Opin Immunol* **21**: 30-37.

Reinders, A., N. Burckert, S. Hohmann, J. M. Thevelein, T. Boller, A. Wiemken & C. De Virgilio, (1997) Structural analysis of the subunits of the trehalose-6-phosphate synthase/phosphatase complex in Saccharomyces cerevisiae and their function during heat shock. *Mol Microbiol* **24**: 687-695.

Richards, A. B., S. Krakowka, L. B. Dexter, H. Schmid, A. P. Wolterbeek, D. H. Waalkens-Berendsen, A. Shigoyuki & M. Kurimoto, (2002) Trehalose: a review of properties, history of use and human tolerance, and results of multiple safety studies. *Food Chem Toxicol* **40**: 871-898.

Richie, D. L., L. Hartl, V. Aimanianda, M. S. Winters, K. K. Fuller, M. D. Miley, S. White, J. W. McCarthy, J. P. Latge, M. Feldmesser, J. C. Rhodes & D. S. Askew, (2009) A role for the unfolded protein response (UPR) in virulence and antifungal susceptibility in Aspergillus fumigatus. *PLoS Pathog* **5**: e1000258.

Romani, L., (2004) Immunity to fungal infections. *Nat Rev Immunol* **4**: 1-23.

Roos, D., M. de Boer, F. Kuribayashi, C. Meischl, R. S. Weening, A. W. Segal, A. Ahlin, K. Nemet, J. P. Hossle, E. Bernatowska-Matuszkiewicz & H. Middleton-Price, (1996) Mutations in the X-linked and autosomal recessive forms of chronic granulomatous disease. *Blood* **87**: 1663-1681.

Ruf, J., H. Wacker, P. James, M. Maffia, P. Seiler, G. Galand, A. von Kieckebusch, G. Semenza & N. Matei, (1990) Rabbit small intestinal trehalase. Purification, cDNA cloning, expression, and verification of glycosylphosphatidylinositol anchoring. *J Biol Chem* **265**: 15034-15039.

Ruijter, G. J., H. Panneman, H. C. van den Broeck, J. M. Bennett & J. Visser, (1996) Characterisation of the Aspergillus nidulans frA1 mutant: hexose phosphorylation and apparent lack of involvement of hexokinase in glucose repression. *FEMS Microbiol Lett* **139**: 223-228.

Saito, K., T. Kase, E. Takahashi & S. Horinouchi, (1998a) Purification and characterization of a trehalose synthase from the basidiomycete grifola frondosa. *Appl Environ Microbiol* **64**: 4340-4345.

Saito, K., H. Yamazaki, Y. Ohnishi, S. Fujimoto, E. Takahashi & S. Horinouchi, (1998b) Production of trehalose synthase from a basidiomycete, Grifola frondosa, in Escherichia coli. *Appl Microbiol Biotechnol* **50**: 193-198.

Sano, F., N. Asakawa, Y. Inoue & M. Sakurai, (1999) A dual role for intracellular trehalose in the resistance of yeast cells to water stress. *Cryobiology* **39**: 80-87.

Schick, I., D. Haltrich & K. D. Kulbe, (1995) Trehalose phosphorylase from *Pichia fermentans* and its role in the metabolism of trehalose. *Appl Microbiol Biotechnol* **43**: 1088-1095.

Schobel, F., O. Ibrahim-Granet, P. Ave, J. P. Latge, A. A. Brakhage & M. Brock, (2007) Aspergillus fumigatus does not require fatty acid metabolism via isocitrate lyase for development of invasive aspergillosis. *Infect Immun* **75**: 1237-1244.

Schrettl, M., E. Bignell, C. Kragl, C. Joechl, T. Rogers, H. N. Arst, Jr., K. Haynes & H. Haas, (2004) Siderophore biosynthesis but not reductive iron assimilation is essential for Aspergillus fumigatus virulence. *J Exp Med* **200**: 1213-1219.

Schrettl, M., E. Bignell, C. Kragl, Y. Sabiha, O. Loss, M. Eisendle, A. Wallner, H. N. Arst, Jr., K. Haynes & H. Haas, (2007) Distinct roles for intra- and extracellular siderophores during Aspergillus fumigatus infection. *PLoS Pathog* **3**: 1195-1207.

Segal, B. H., (2009) Aspergillosis. *N Engl J Med* **360**: 1870-1884.

Sharon, H., S. Hagag & N. Osherov, (2009) Transcription factor PrtT controls expression of multiple secreted proteases in the human pathogenic mold Aspergillus fumigatus. *Infect Immun* **77**: 4051-4060.

Shimizu, K. & N. P. Keller, (2001) Genetic involvement of a cAMP-dependent protein kinase in a G protein signaling pathway regulating morphological and chemical transitions in *Aspergillus nidulans*. *Genetics* **157**: 591-600.

Shinohara, M. L., A. Correa, D. Bell-Pedersen, J. C. Dunlap & J. J. Loros, (2002) Neurospora clock-controlled gene 9 (ccg-9) encodes trehalose synthase: circadian regulation of stress responses and development. *Eukaryot Cell* **1**: 33-43.

Singer, M. A. & S. Lindquist, (1998) Thermotolerance in Saccharomyces cerevisiae: the Yin and Yang of trehalose. *Trends Biotechnol* **16**: 460-468.

Snelders, E., S. M. Camps, A. Karawajczyk, G. Schaftenaar, G. H. Kema, H. A. van der Lee, C. H. Klaassen, W. J. Melchers & P. E. Verweij, Triazole Fungicides Can Induce Cross-Resistance to Medical Triazoles in Aspergillus fumigatus. *PLoS One* **7**: e31801.

Snelders, E., H. A. van der Lee, J. Kuijpers, A. J. Rijs, J. Varga, R. A. Samson, E. Mellado, A. R. Donders, W. J. Melchers & P. E. Verweij, (2008) Emergence of azole resistance in Aspergillus fumigatus and spread of a single resistance mechanism. *PLoS Med* **5**: e219.

St Leger, R. J., L. Joshi & D. W. Roberts, (1997) Adaptation of proteases and carbohydrates of saprophytic, phytopathogenic and entomopathogenic fungi to the requirements of their ecological niches. *Microbiology* **143 (Pt 6)**: 1983-1992.

Steele, C., R. R. Rapaka, A. Metz, S. M. Pop, D. L. Williams, S. Gordon, J. K. Kolls & G. D. Brown, (2005) The beta-glucan receptor dectin-1 recognizes specific morphologies of Aspergillus fumigatus. *PLoS Pathog* **1**: e42.

Steinbock, F., S. Choojun, I. Held, M. Roehr & C. P. Kubicek, (1994) Characterization and regulatory properties of a single hexokinase from the citric acid accumulating fungus Aspergillus niger. *Biochim Biophys Acta* **1200**: 215-223.

Steinwede, K., R. Maus, J. Bohling, S. Voedisch, A. Braun, M. Ochs, A. Schmiedl, F. Langer, F. Gauthier, J. Roes, T. Welte, F. C. Bange, M. Niederweis, F. Buhling & U. A. Maus, Cathepsin G and neutrophil elastase contribute to lung-protective immunity against mycobacterial infections in mice. *J Immunol* **188**: 4476-4487.

Stephens-Romero, S. D., A. J. Mednick & M. Feldmesser, (2005) The pathogenesis of fatal outcome in murine pulmonary aspergillosis depends on the neutrophil depletion strategy. *Infect Immun* **73**: 114-125.

Sugui, J. A., H. S. Kim, K. A. Zarember, Y. C. Chang, J. I. Gallin, W. C. Nierman & K. J. Kwon-Chung, (2008) Genes differentially expressed in conidia and hyphae of Aspergillus fumigatus upon exposure to human neutrophils. *PLoS One* **3**: e2655.

Sugui, J. A., J. Pardo, Y. C. Chang, K. A. Zarember, G. Nardone, E. M. Galvez, A. Mullbacher, J. I. Gallin, M. M. Simon & K. J. Kwon-Chung, (2007) Gliotoxin is a virulence factor of Aspergillus fumigatus: gliP deletion attenuates virulence in mice immunosuppressed with hydrocortisone. *Eukaryot Cell* **6**: 1562-1569.

Sun, W. Q., A. C. Leopold, L. M. Crowe & J. H. Crowe, (1996) Stability of dry liposomes in sugar glasses. *Biophys J* **70**: 1769-1776.

Sur, I. P., Z. Lobo & P. K. Maitra, (1994) Analysis of PFK3--a gene involved in particulate phosphofructokinase synthesis reveals additional functions of TPS2 in Saccharomyces cerevisiae. *Yeast* **10**: 199-209.

Tekaia, F. & J. P. Latge, (2005) Aspergillus fumigatus: saprophyte or pathogen? *Curr Opin Microbiol* **8**: 385-392.

Thevelein, J. M., (1984) Regulation of trehalose mobilization in fungi. *Microbiol Rev* **48**: 42-59.

Thevelein, J. M. & S. Hohmann, (1995) Trehalose synthase: guard to the gate of glycolysis in yeast? *Trends Biochem Sci* **20**: 3-10.

Tkalcevic, J., M. Novelli, M. Phylactides, J. P. Iredale, A. W. Segal & J. Roes, (2000) Impaired immunity and enhanced resistance to endotoxin in the absence of neutrophil elastase and cathepsin G. *Immunity* **12**: 201-210.

Tsoni, S. V. & G. D. Brown, (2008) beta-Glucans and dectin-1. *Ann N Y Acad Sci* **1143**: 45-60.

Tsunawaki, S., L. S. Yoshida, S. Nishida, T. Kobayashi & T. Shimoyama, (2004) Fungal metabolite gliotoxin inhibits assembly of the human respiratory burst NADPH oxidase. *Infect Immun* **72**: 3373-3382.

Urban, C. F., U. Reichard, V. Brinkmann & A. Zychlinsky, (2006) Neutrophil extracellular traps capture and kill Candida albicans yeast and hyphal forms. *Cell Microbiol* **8**: 668-676.

Van Dijck, P., L. De Rop, K. Szlufcik, E. Van Ael & J. M. Thevelein, (2002) Disruption of the *Candida albicans TPS2* gene encoding trehalose-6-phosphate phosphatase decreases infectivity without affecting hypha formation. *Infect Immun* **70**: 1772-1782.

Varkey, J. B. & J. R. Perfect, (2008) Rare and emerging fungal pulmonary infections. *Semin Respir Crit Care Med* **29**: 121-131.

Verweij, P. E., E. Mellado & W. J. Melchers, (2007) Multiple-triazole-resistant aspergillosis. *N Engl J Med* **356**: 1481-1483.

Verweij, P. E., E. Snelders, G. H. Kema, E. Mellado & W. J. Melchers, (2009) Azole resistance in Aspergillus fumigatus: a side-effect of environmental fungicide use? *Lancet Infect Dis* **9**: 789-795.

Volling, K., A. Thywissen, A. A. Brakhage & H. P. Saluz, Phagocytosis of melanized Aspergillus conidia by macrophages exerts cytoprotective effects by sustained PI3K/Akt signalling. *Cell Microbiol* **13**: 1130-1148.

Vuorio, O. E., N. Kalkkinen & J. Londesborough, (1993) Cloning of two related genes encoding the 56-kDa and 123-kDa subunits of trehalose synthase from the yeast Saccharomyces cerevisiae. *Eur J Biochem* **216**: 849-861.

Walsh, T. J., E. J. Anaissie, D. W. Denning, R. Herbrecht, D. P. Kontoyiannis, K. A. Marr, V. A. Morrison, B. H. Segal, W. J. Steinbach, D. A. Stevens, J. A. van Burik, J. R. Wingard & T. F. Patterson, (2008) Treatment of aspergillosis: clinical practice guidelines of the Infectious Diseases Society of America. *Clin Infect Dis* **46**: 327-360.

Wannet, W. J., H. J. Op den Camp, H. W. Wisselink, C. van der Drift, L. J. Van Griensven & G. D. Vogels, (1998) Purification and characterization of trehalose phosphorylase from the commercial mushroom Agaricus bisporus. *Biochim Biophys Acta* **1425**: 177-188.

Waring, P., R. D. Eichner, A. Mullbacher & A. Sjaarda, (1988) Gliotoxin induces apoptosis in macrophages unrelated to its antiphagocytic properties. *J Biol Chem* **263**: 18493-18499.

Werner, J. L., A. E. Metz, D. Horn, T. R. Schoeb, M. M. Hewitt, L. M. Schwiebert, I. Faro-Trindade, G. D. Brown & C. Steele, (2009) Requisite role for the dectin-1 beta-glucan receptor in pulmonary defense against Aspergillus fumigatus. *J Immunol* **182**: 4938-4946.

White, T. C., K. A. Marr & R. A. Bowden, (1998) Clinical, cellular, and molecular factors that contribute to antifungal drug resistance. *Clin Microbiol Rev* **11**: 382-402.

Willger, S. D., S. Puttikamonkul, K. H. Kim, J. B. Burritt, N. Grahl, L. J. Metzler, R. Barbuch, M. Bard, C. B. Lawrence & R. A. Cramer, Jr., (2008) A sterol-regulatory element binding protein is required for cell polarity, hypoxia adaptation, azole drug resistance, and virulence in Aspergillus fumigatus. *PLoS Pathog* **4**: e1000200.

Wilson, R. A., R. P. Gibson, C. F. Quispe, J. A. Littlechild & N. J. Talbot, An NADPH-dependent genetic switch regulates plant infection by the rice blast fungus. *Proc Natl Acad Sci U S A* **107**: 21902-21907.

Wilson, R. A., J. M. Jenkinson, R. P. Gibson, J. A. Littlechild, Z. Y. Wang & N. J. Talbot, (2007) Tps1 regulates the pentose phosphate pathway, nitrogen metabolism and fungal virulence. *EMBO J* **26**: 3673-3685.

Winkler, K., I. Kienle, M. Burgert, J. C. Wagner & H. Holzer, (1991) Metabolic regulation of the trehalose content of vegetative yeast. *FEBS Lett* **291**: 269-272.

Woodruff, P. J., B. L. Carlson, B. Siridechadilok, M. R. Pratt, R. H. Senaratne, J. D. Mougous, L. W. Riley, S. J. Williams & C. R. Bertozzi, (2004) Trehalose is

required for growth of Mycobacterium smegmatis. *J Biol Chem* **279**: 28835-28843.

Xiuli, W., D. Hongbiao, Y. Ming & Q. Yu, (2009) Gene cloning, expression, and characterization of a novel trehalose synthase from Arthrobacter aurescens. *Appl Microbiol Biotechnol* **83**: 477-482.

Yamamoto, T., K. Maruta, H. Watanabe, H. Yamashita, M. Kubota, S. Fukuda & M. Kurimoto, (2001) Trehalose-producing operon treYZ from Arthrobacter ramosus S34. *Biosci Biotechnol Biochem* **65**: 1419-1423.

Yamamoto, Y. & R. B. Gaynor, (2001) Therapeutic potential of inhibition of the NF-kappaB pathway in the treatment of inflammation and cancer. *J Clin Invest* **107**: 135-142.

Yelton, M. M., J. E. Hamer & W. E. Timberlake, (1984) Transformation of *Aspergillus nidulans* by using a trpC plasmid. *Proc Natl Acad Sci U S A* **81**: 1470-1474.

Yu, J. H., Z. Hamari, K. H. Han, J. A. Seo, Y. Reyes-Dominguez & C. Scazzocchio, (2004) Double-joint PCR: a PCR-based molecular tool for gene manipulations in filamentous fungi. *Fungal Genet Biol* **41**: 973-981.

Yue, M., X. L. Wu, W. N. Gong & H. B. Ding, (2009) Molecular cloning and expression of a novel trehalose synthase gene from Enterobacter hormaechei. *Microb Cell Fact* **8**: 34.

Zaragoza, O., M. A. Blazquez & C. Gancedo, (1998) Disruption of the *Candida albicans TPS1* gene encoding trehalose-6-phosphate synthase impairs formation of hyphae and decreases infectivity. *J Bacteriol* **180**: 3809-3815.

Zaragoza, O., C. de Virgilio, J. Ponton & C. Gancedo, (2002) Disruption in *Candida albicans* of the *TPS2* gene encoding trehalose-6-phosphate phosphatase affects cell integrity and decreases infectivity. *Microbiology* **148**: 1281-1290.

Zuluaga, A. F., B. E. Salazar, C. A. Rodriguez, A. X. Zapata, M. Agudelo & O. Vesga, (2006) Neutropenia induced in outbred mice by a simplified low-dose cyclophosphamide regimen: characterization and applicability to diverse experimental models of infectious diseases. *BMC Infect Dis* **6**: 55.

APPENDICES

APPENDIX A

SOUTHERN BLOT ANALYSIS OF GENERATED STRAINS IN CHAPTER3

Generation and Confirmation of the *Pst*I truncated (pyrG-) *orlA* mutant for further generation of additional mutation in the Δ*orlA* background.

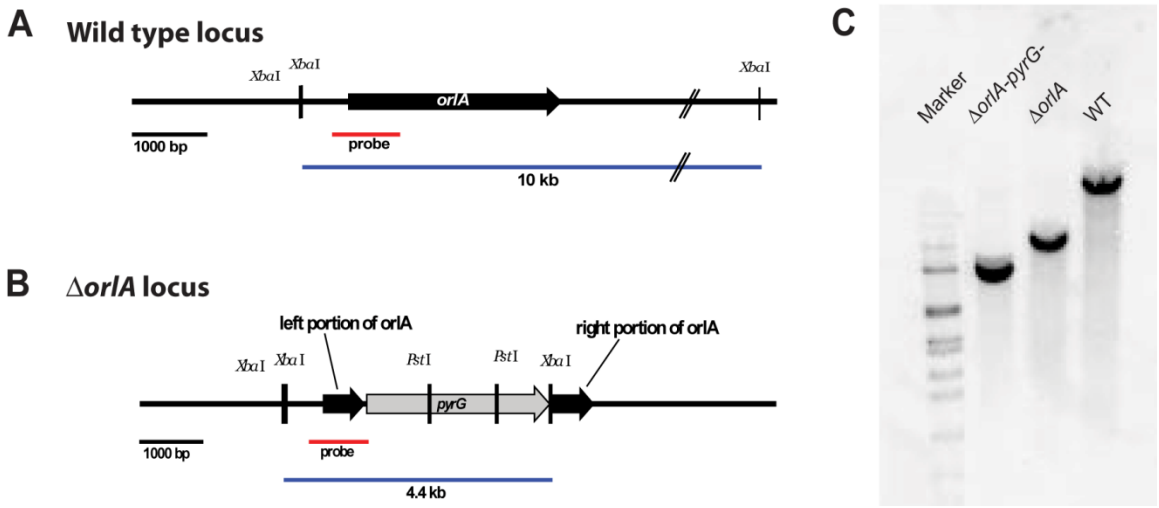

Figure A1. Schematic of genomic loci representing wild type *orlA* locus in *A. fumigatus* wild type CBS144.89 strain (**A**), and pyrG knockout locus of Δ*orlA*, and Δ*orlA*(pyrG-) null mutants (**B**). Genomic DNA from the respective strains was isolated and digested overnight with *Xba*I restriction enzyme. An approximate 1 kb genomic region was utilized as a probe. **C**) The expected hybridization patterns and sizes of the *orlA* locus in WT, Δ*orlA*, and Δ*orlA*(pyrG-) were observed and are 10kb, 4.4kb, and 3.4kb respectively.

Generation and Confirmation of the double mutant strain (Δ*orlA*/Δ*tslA*) that was generated from the Δ*orlA*(pyrG-) background strain.

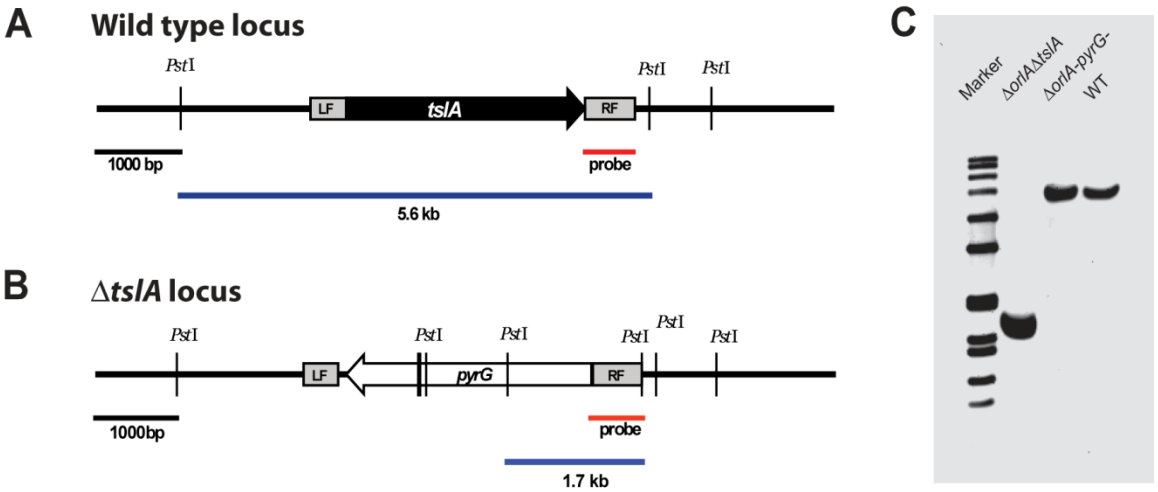

Figure A2. Schematic of genomic loci representing the wild type *tslA* locus in *A. fumigatus* wild type CBS144.89 and the Δ*orlA*(pyrG-) background strains (**A**), and pyrG knockout locus of Δ*tslA* in the Δ*orlA*/Δ*tslA* null mutant (**B**). Genomic DNA from the respective strains was isolated and digested overnight with *Pst*I restriction enzyme. An approximate 1 kb genomic region was utilized as a probe. **C**) The expected hybridization patterns and sizes of the *tslA* locus in WT, Δ*orlA*(pyrG-), and Δ*orlA*/Δ*tslA* were observed and are 5.6kb, 5.6kb, and 1.7kb respectively.

Generation and Confirmation of the triple mutant strain (Δ*orlA*/Δ*tslA*/Δ*tslB*) that was generated from the Δ*orlA*/Δ*tslA* background strain.

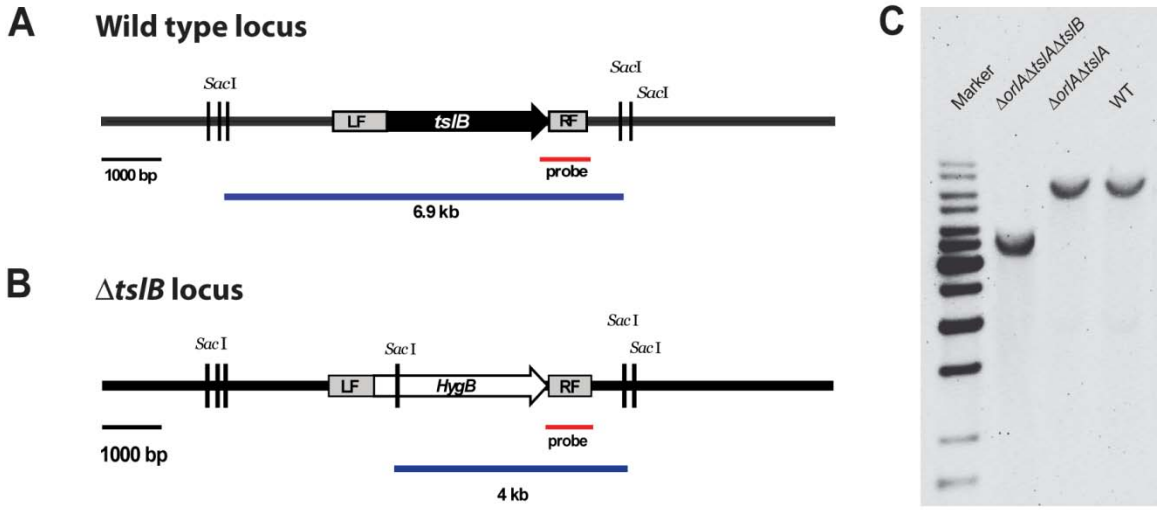

Figure A3. Schematic of genomic loci representing the wild type *tslB* locus in *A. fumigatus* wild type CBS144.89 and the Δ*orlA*/Δ*tslA* background strains (**A**), and HygB knockout locus of Δ*tslB* in the Δ*orlA*/Δ*tslA*/Δ*tslB* null mutant (**B**). Genomic DNA from the respective strains was isolated and digested overnight with *Sac*I restriction enzyme. An approximate 1 kb genomic region was utilized as a probe. **C**) The expected hybridization patterns and sizes of the *tslB* locus in WT, Δ*orlA*/Δ*tslA*, and Δ*orlA*/Δ*tslA*/Δ*tslB* were observed and are 6.9kb, 6.9kb, and 4kb respectively.

Generation and Confirmation of the reconstitution of *orlA* locus back into triple mutant strain (OrlA+Δ*orlA*/Δ*tslA*/Δ*tslB*) that was generated from the Δ*orlA*/Δ*tslA*/Δ*tslB* background strain.

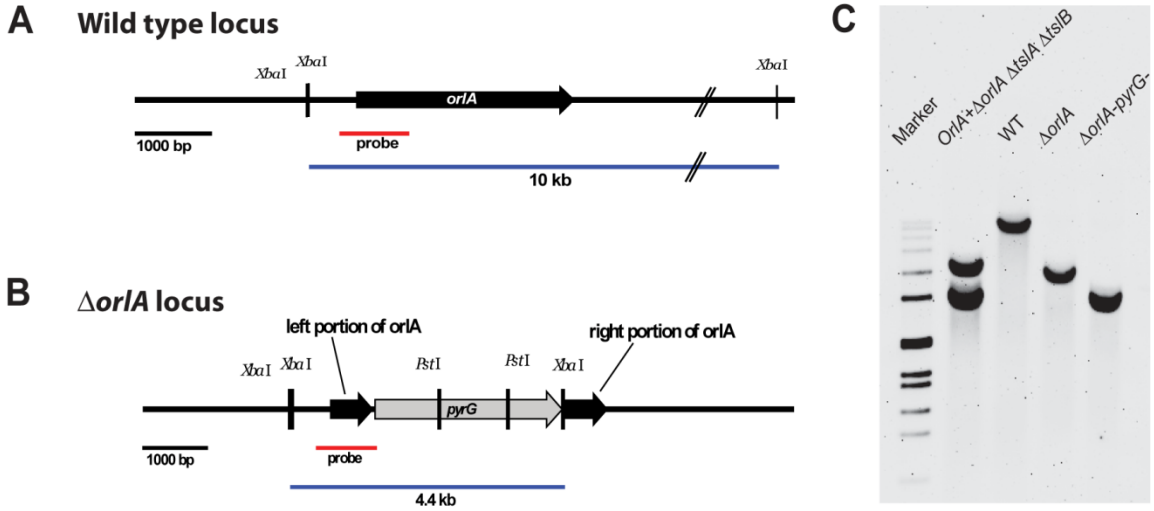

Figure A4. Schematic of genomic loci representing the wild type *orlA* locus in *A. fumigatus* wild type CBS144.89 strain (**A**), and pyrG knockout locus of Δ*orlA* in the Δ*orlA*, Δ*orlA(pyrG-)* null mutants and OrlA+Δ*orlA*/Δ*tslA*/Δ*tslB* strain (**B**). Genomic DNA from the respective strains was isolated and digested overnight with *Xba*I restriction enzyme. An approximate 1 kb genomic region was utilized as a probe. **C**) The expected hybridization patterns and sizes of the *orlA* locus in WT, Δ*orlA*, Δ*orlA(pyrG-)*, and OrlA+Δ*orlA*/Δ*tslA*/Δ*tslB* were observed and are 10kb, 4.4kb, 3.4kb and 3.4kb respectively. In additional, the reconstituted strain (OrlA+Δ*orlA*/Δ*tslA*/Δ*tslB*) contains a single ectopic insertion of wild type allele of *orlA* (top) and maintenance of the disrupted *orlA(pyrG-)* locus (bottom).

Generation and Confirmation of the single mutant strain (Δ*tpsA*) that was generated from auxotroph CEA17 (pyrG-) background strain.

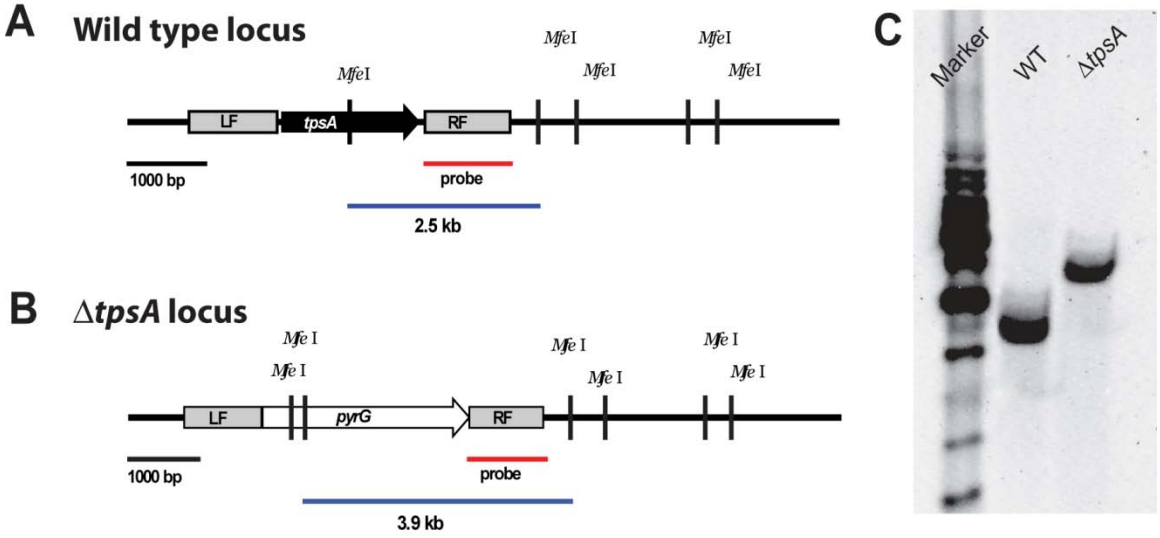

Figure A5. Schematic of genomic loci representing the wild type *tpsA* locus in *A. fumigatus* wild type CBS144.89 strain (**A**), and pyrG knockout locus of Δ*tpsA* null mutant (**B**). Genomic DNA from the respective strains was isolated and digested overnight with *Mfe*I restriction enzyme. An approximate 1 kb genomic region was utilized as a probe. **C**) The expected hybridization patterns and sizes of the *tpsA* locus in WT and Δ*tpsA* were observed and are 2.5kb and 3.9kb respectively.

Generation and Confirmation of the single mutant strain (Δ*tpsB*) that was generated from auxotroph CEA17 (pyrG-) background strain.

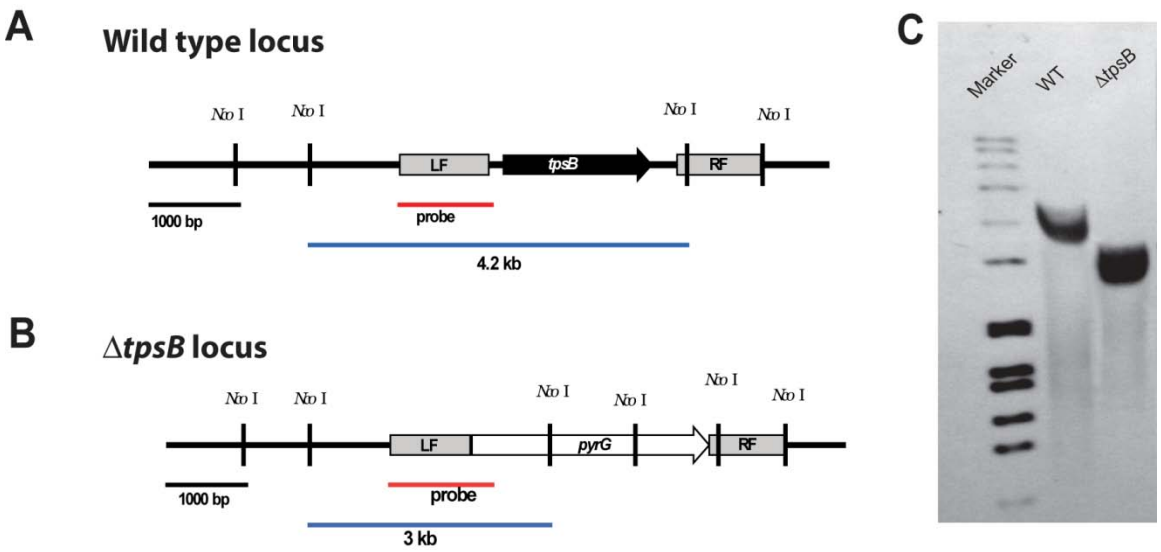

Figure A6. Schematic of genomic loci representing the wild type *tpsB* locus in *A. fumigatus* wild type CBS144.89 strain (**A**), and pyrG knockout locus of Δ*tpsB* null mutant (**B**). Genomic DNA from the respective strains was isolated and digested overnight with *Nco*I restriction enzyme. An approximate 1 kb genomic region was utilized as a probe. **C**) The expected hybridization patterns and sizes of the *tpsB* locus in WT and Δ*tpsB* were observed and are 4.2kb and 3kb respectively.

Generation and Confirmation of the *Nco*I truncated (pyrG-) *tpsA* mutant for further generation of additional mutation in the Δ*tpsA* background.

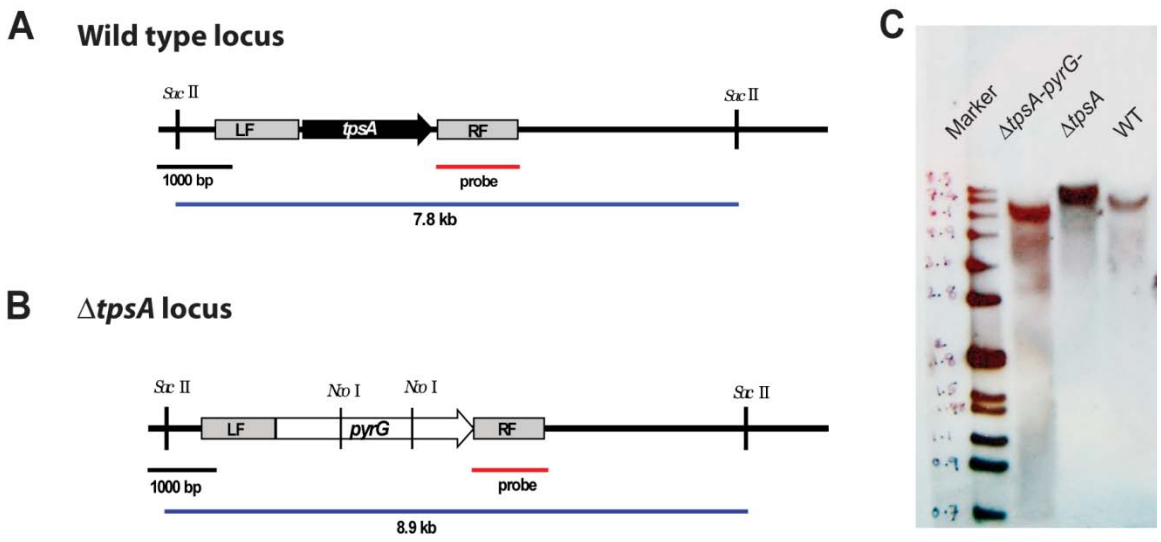

Figure A7. Schematic of genomic loci representing the wild type *tpsA* locus in *A. fumigatus* wild type CBS144.89 strain (**A**), and pyrG knockout locus of Δ*tpsA*, and Δ*tpsA*(pyrG-) null mutants (**B**). Genomic DNA from the respective strains was isolated and digested overnight with *Sac*II restriction enzyme. An approximate 1 kb genomic region was utilized as a probe. **C**) The expected hybridization patterns and sizes of the *tpsA* locus in WT, Δ*tpsA*, and Δ*tpsA*(pyrG-) were observed and are 7.8kb, 8.9kb, and 7.7kb respectively.

Generation and Confirmation of the double mutant strain (Δ*tpsA*/Δ*tpsB*) that was generated from Δ*tpsA*(pyrG-) background strain.

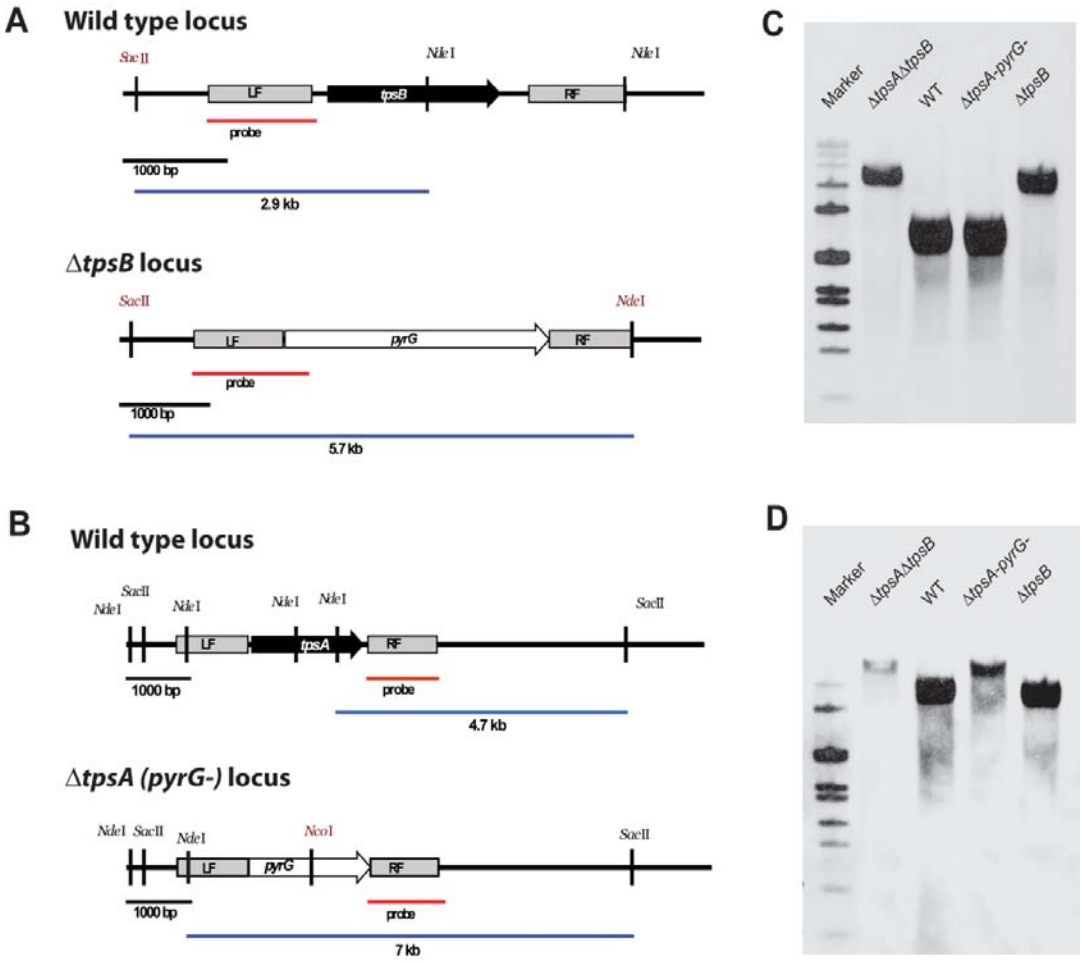

Figure A8. Schematic of genomic loci representing the wild type *tpsB* locus in *A. fumigatus* wild type CBS144.89 and Δ*tpsA*(pyrG-) background strains and the pyrG knockout locus of Δ*tpsB* in the single Δ*tpsB*, and double Δ*tpsA*/Δ*tpsB* null mutant (**A**). In addition, wild type *tpsA* locus in *A. fumigatus* wild type CBS144.89 and Δ*tpsB* strains and the truncated pyrG knockout locus of Δ*tpsA* in the Δ*tpsA(pyrG-)* background, and double Δ*tpsA*/Δ*tpsB* null mutant (**B**). Genomic DNA from the respective strains was isolated and digested overnight with *Nde*I+*Sac*II restriction enzymes. An approximate 1 kb genomic region was utilized as a probe. **C**) The expected hybridization patterns and sizes of the *tpsB* locus in WT and Δ*tpsA*(pyrG-) are 2.9kb similarly as well as the observed hybridization of Δ*tpsB* and Δ*tpsA*/Δ*tpsB* are 5.7kb similarly. **D**) The expected hybridization patterns and sizes of the *tpsA* locus in WT and Δ*tpsB* are 4.7kb similarly as well as the observed hybridization of Δ*tpsA*(pyrG-) and Δ*tpsA*/Δ*tpsB* are 7kb similarly.

Generation and Confirmation of the reconstitution of *tpsA* locus back into double mutant strain (Δ*tpsA*/Δ*tpsB*+*tpsA*) that was generated from Δ*tpsA*/Δ*tpsB* background strain.

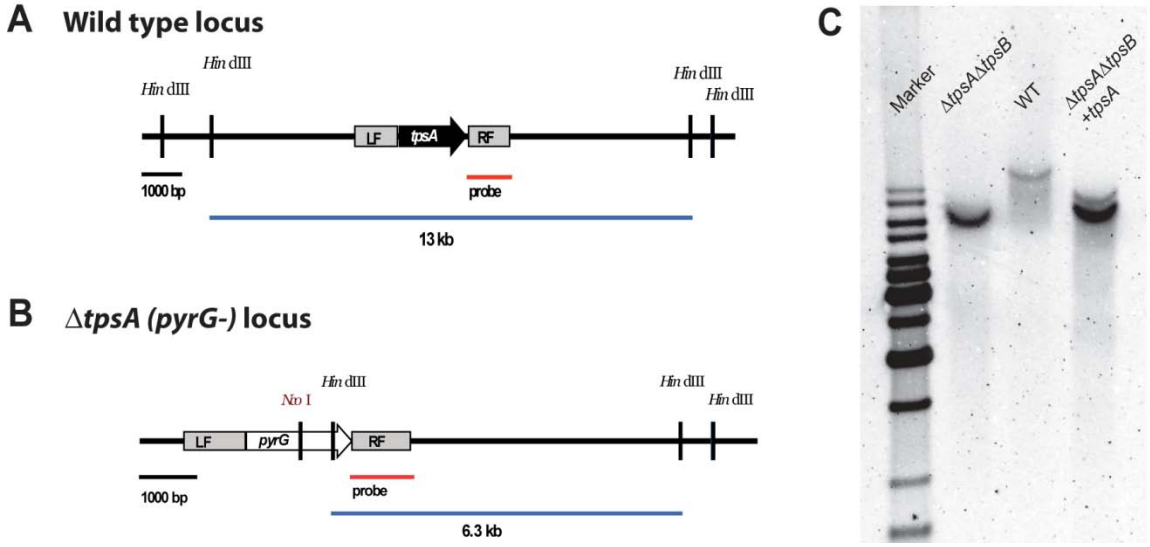

Figure A9. Schematic of genomic loci representing the wild type *tpsA* locus in *A. fumigatus* wild type CBS144.89 strain (**A**), and truncated pyrG knockout locus of Δ*tpsA* in the Δ*tpsA*/Δ*tpsB* background and Δ*tpsA*/Δ*tpsB*+*tpsA* strain (**B**). Genomic DNA from the respective strains was isolated and digested overnight with *Hind*III restriction enzyme. An approximate 1 kb genomic region was utilized as a probe. **C**) The expected hybridization patterns and sizes of the *tpsA* locus in WT, Δ*tpsA*/Δ*tpsB*, and Δ*tpsA*/Δ*tpsB*+*tpsA* were observed and are 13kb, 6.3kb and 6.3kb respectively. In additional, the reconstituted strain (Δ*tpsA*/Δ*tpsB*+*tpsA*) contains a single ectopic insertion of wild type allele of *tpsA* (top) and maintenance of the disrupted *tpsA(pyrG-)* locus (bottom).

Generation and Confirmation of the reconstitution of *tpsB* locus back into double mutant strain (Δ*tpsA*/Δ*tpsB*+*tpsB*) that was generated from Δ*tpsA*/Δ*tpsB* background strain.

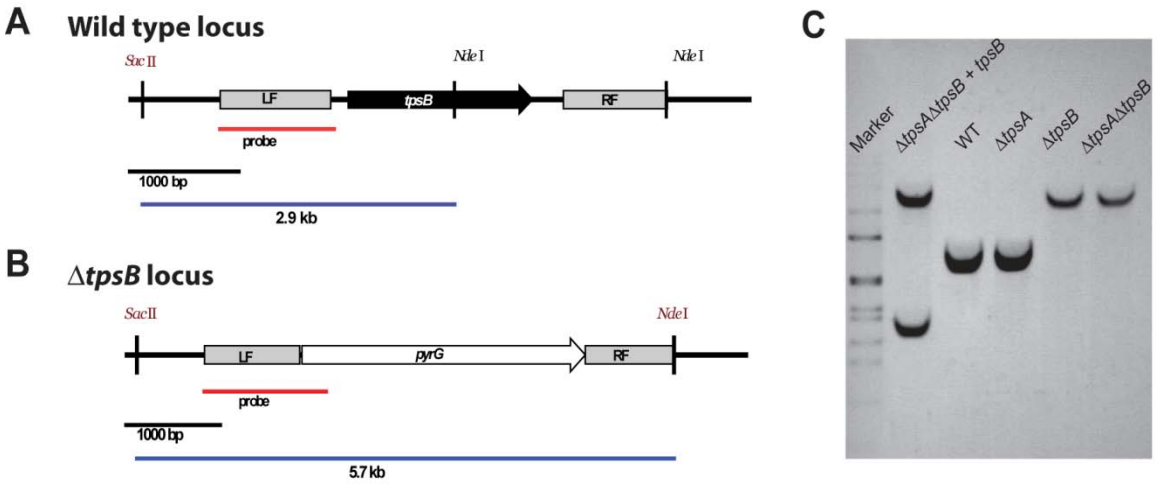

Figure A10. Schematic of genomic loci representing the wild type *tpsB* locus in *A. fumigatus* wild type CBS144.89 strain (**A**), and pyrG knockout locus of Δ*tpsB* in the Δ*tpsA*/Δ*tpsB* background and Δ*tpsA*/Δ*tpsB*+*tpsB* strain (**B**). Genomic DNA from the respective strains was isolated and digested overnight with *Nde*I+*Sac*II restriction enzymes. An approximate 1 kb genomic region was utilized as a probe. **C**) The expected hybridization patterns and sizes of the *tpsB* locus in WT and Δ*tpsA* are 2.9kb similarly as well as the observed hybridization of Δ*tpsB*, Δ*tpsA*/Δ*tpsB*, and Δ*tpsA*/Δ*tpsB*+*tpsB* are 5.7kb similarly. In additional, the reconstituted strain (Δ*tpsA*/Δ*tpsB*+*tpsB*) contains a single ectopic insertion of wild type allele of *tpsB* (bottom) and maintenance of the disrupted *tpsB* locus (top).

APPENDIX B

SOUTHERN BLOT ANALYSIS OF GENERATED STRAINS IN CHAPTER4

Generation and Confirmation of the double mutant strain (Δ*orlA*/Δ*tpyA*) that was generated from Δ*orlA*(pyrG-) background strain.

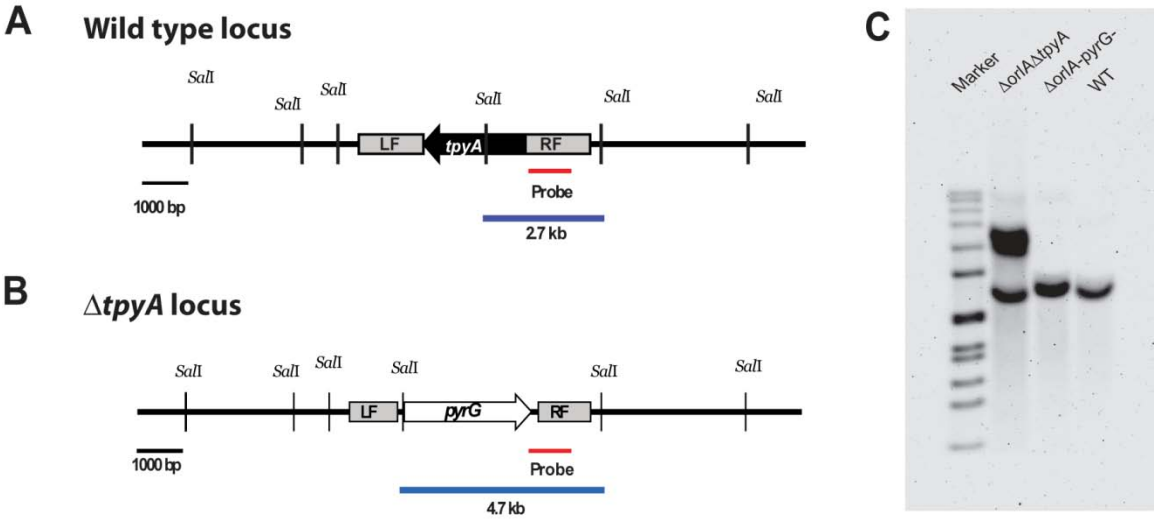

Figure B1. Schematic of genomic loci representing the wild type *tpyA* locus in *A. fumigatus* wild type CBS144.89 and the Δ*orlA*(pyrG-) background strains (**A**), and pyrG knockout locus of Δ*tpyA* in the Δ*orlA*/Δ*tpyA* null mutant (**B**). Genomic DNA from the respective strains was isolated and digested overnight with *Sal*I restriction enzyme. An approximate 1 kb genomic region was utilized as a probe. **C**) The expected hybridization patterns and sizes of the *tpyA* locus in WT, Δ*orlA*(pyrG-), and Δ*orlA*/Δ*tpyA* were observed and are 2.7kb, 2.7kb, and 4.7kb respectively. The Δ*orlA*/Δ*tpyA* double mutant showed an additional multiple insertion of knockout *tpyA* locus (bottom).

Generation and Confirmation of the double mutant strain (Δ*orlA*/Δ*tpyB*) that was generated from Δ*orlA*(pyrG-) background strain.

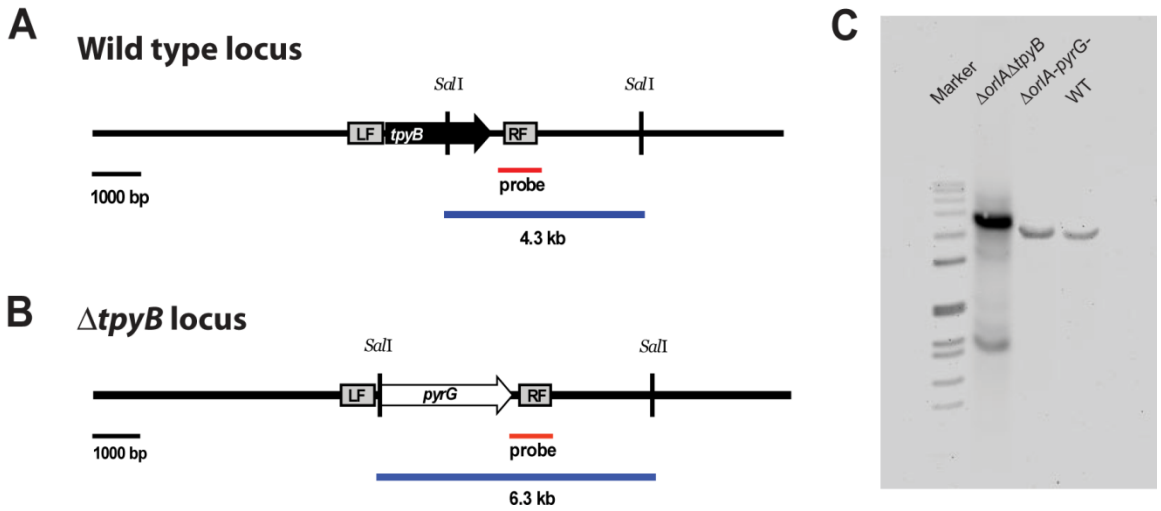

Figure B2. Schematic of genomic loci representing the wild type *tpyB* locus in *A. fumigatus* wild type CBS144.89 and the Δ*orlA*(pyrG-) background strains (**A**), and pyrG knockout locus of Δ*tpyB* in the Δ*orlA*/Δ*tpyB* null mutant (**B**). Genomic DNA from the respective strains was isolated and digested overnight with *Sal*I restriction enzyme. An approximate 1 kb genomic region was utilized as a probe. **C**) The expected hybridization patterns and sizes of the *tpyB* locus in WT, Δ*orlA*(pyrG-), and Δ*orlA*/Δ*tpyB* were observed and are 4.3kb, 4.3kb, and 6.3kb respectively. The Δ*orlA*/Δ*tpyB* double mutant showed an additional multiple insertion of knockout *tpyB* locus (bottom).

Generation and Confirmation of the triple mutant strain (Δ*orlA*/Δ*tpyA*/Δ*tpyB*) that was generated from Δ*orlA*/Δ*tpyB* background strain.

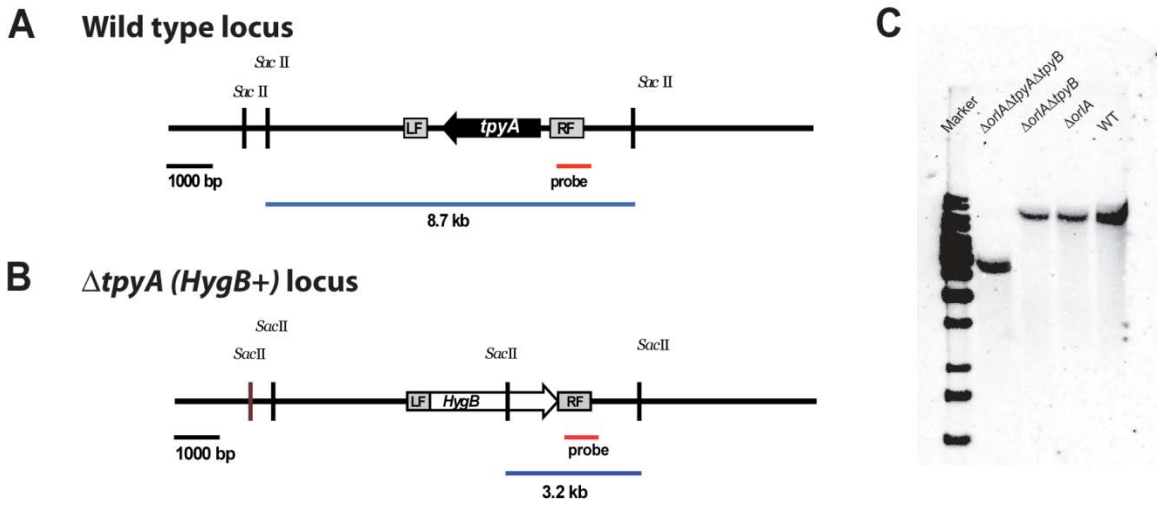

Figure B3. Schematic of genomic loci representing the wild type *tpyA* locus in *A. fumigatus* wild type CBS144.89 and the Δ*orlA*/Δ*tpyB* background strains (**A**), and HygB knockout locus of Δ*tpyA* in the Δ*orlA*/Δ*tpyA*/Δ*tpyB* null mutant (**B**). Genomic DNA from the respective strains was isolated and digested overnight with *Sac*II restriction enzyme. An approximate 1 kb genomic region was utilized as a probe. **C**) The expected hybridization patterns and sizes of the *tpyA* locus in WT, Δ*orlA*, Δ*orlA*/Δ*tpyB* and Δ*orlA*/Δ*tpyA*/Δ*tpyB* were observed and are 8.7kb, 8.7kb, 8.7kb and 3.2kb respectively.

APPENDIX C

TABLE OF PRIMERS USED IN CHAPTER 3

Table of nucleotide sequences of primers used for deletion and complementation strain constructions in Chapter 3

Primer	Description	Gene	Sequence (5'-3')
RAC93	tpsA left flank Fw	tpsA	TAGTCGACAACAGCCAGTCCATCTGAACCA
RAC94	tpsA left flank Rv	tpsA	CGGAATTCACCGGCGACAGAGTGTAATTGT
RAC95	tpsA right flank Fw	tpsA	ATGGATCCTTTGCAAGTTAGGCGCGGACAT
RAC96	tpsA right flank Rv	tpsA	TTGCGGCCGCAAACCCGACGAGAACTCGATGA
RAC99	tpsB left flank Fw	tpsB	TAGTCGACAAGCGTCCGTCTTGGCATTAGA
RAC100	tpsB left flank Rv	tpsB	CGGAATTCAGGCAACGAGACACGAAGCAAA
RAC101	tpsB right flank Fw	tpsB	ATGGATCCTTTCGTGTTCGTCGCCCAAACT
RAC102	tpsB right flank Rv	tpsB	ATGCGGCCGCATGGAACCTGCGTGCTTAGACA
RAC382	Fw-tpsA-recon	tpsA	GTAAGCTTAAGGCGCCATTCCAGTTAGTCAGA
RAC383	Rv-tpsA-recon	tpsA	TAGCGGCCGCCTCAACGGCTGTGTTTCCGTTGTT
RAC390	Fw-tpsB-recon	tpsB	TTGGGCCCACCGGTTTCTGATATCGACCGCAT
RAC391	Rv-tpsB-recon	tpsB	TAGAATTCATCAGGCCAAAGAGGTAAGCAGGT
RAC189	orlA_left flank_Fw	orlA	TCCTCGAGATCTATTGTCCTCTCAACGCCGCT
RAC190	orlA_left flank_Rv	orlA	ACGAATTCCTGCTTTGTTCAGTGGAACGGCAA
RAC191	orlA_right flank_Fw	orlA	TGTCTAGACGCAATGCGGTTTGGATCATCAGT
RAC192	orlA_right flank_Rv	orlA	CTGCGGCCGCAAGAAGAGGAAGATGAAGCGGCCT
RAC322	orlA-recon_FW	orlA	GAGCGGCCGCAAGAAACCGAGCCATGCTCAGAGA
RAC323	orlA-recon_RV	orlA	TGAAGCTTAAATTCCAGCCATGTGCCATCGTC
RAC1017	AF-tslA_LF_Fw	tslA	TTTCTAGACAGGGCCGAAGCTACCCTGGAA
RAC1018	AF-tslA_LF_Rv	tslA	GTACTAGTTTCACAGTGTATGGGAGGAATCTGGC
RAC1019	AF-tslA_RF_Fw	tslA	TCGAATTCTTGTCGTGCCATACTAGGCTTCCA
RAC1020	AF-tslA_RF_Rv	tslA	TAGTCGACTGCAGATTGACAGGTCAGGTCAGA
RAC1101	TslB_KO_LF_Fw	tslB	AACAGGGACATCGCAGTTTGATGC
RAC1102	TslB_KO_LF_Rv	tslB	ACCATCAGGGACAGCTTCAAGGATATCAGGCCAAAGAGGTAAGCAGGT
RAC1103	TslB_KO_Mid_Fw	tslB	ACCTGCTTACCTCTTTGGCCTGATATCCTTGAAGCTGTCCCTGATGGT
RAC1104	TslB_KO_Mid_Rv	tslB	AGGAAGTCAGGGTGTTGACAACGTTGCACGAGTGGGTTACATCGAACT
RAC1105	TslB_KO_RF_Fw	tslB	AGTTCGATGTAACCCACTCGTGCAACGTTGTCAACACCCTGACTTCCT
RAC1106	TslB_KO_RF_Rv	tslB	AAGTCTCATAATGCCGGCTTTGGC
RAC1107	TslB_KO_Nested_Fw	tslB	GGGGACAAGTTTGTACAAAAAAGCAGGCTAATACGCTGCCATTGGACCATTCC
RAC1108	TslB_KO_Nested_Rv	tslB	GGGGACCACTTTGTACAAGAAAGCTGGGTTGCTTCCATTCATCTAACTACGGCCC

APPENDIX D

TABLE OF PRIMERS USED IN CHAPTER 4

Table of nucleotide sequences of primers used for deletion and complementation strain constructions in Chapter 4

Primer	**Description**	**Gene**	**Sequence (5'-3')**
RAC702	TpyB_KO_LF_FW	TpyB	TATCGCAGTTTCGTGGATGGGACT
RAC703	TpyB_KO_LF_RV	TpyB	CCAACTTAATCGCCTTGCAGCACATTGCTG GCACAGATTCTCCTCTGA
RAC704	TpyB_KO_Mid_FW	TpyB	TCAGAGGAGAATCTGTGCCAGCAATGTGC TGCAAGGCGATTAAGTTGG
RAC705	TpyB_KO_Mid_RV	TpyB	ATGTCGATCCTGGACAACCAGCTTTCCGGC TCGTATGTTGTGTGGAAT
RAC706	TpyB_KO_RF_FW	TpyB	ATTCCACACAACATACGAGCCGGAAAGCT GGTTGTCCAGGATCGACAT
RAC707	TpyB_KO_RF_RV	TpyB	CCATCATGGCGCCGAATTTGTTCA
RAC708	TpyB_NESTED_FW	TpyB	GGGGACAAGTTTGTACAAAAAAGCAGGCT AGCCACTTTCACTTCCAGCCAGTA
RAC709	TpyB_NESTED_RV	TpyB	GGGGACCACTTTGTACAAGAAAGCTGGGT CCAAGGGCTCCATGATGCAACAAA
RAC755	TpyA_KO_LF_FW	TpyA	GCAAGTTATGCGAGCAACATGGGT
RAC779	TpyA_KO_LF_RV	TpyA	CCAACTTAATCGCCTTGCAGCACAAACAAC ACACCAGCTCGGCA
RAC780	TpyA_KO_Mid_FW	TpyA	TGCCGAGCTGGTGTGTTGTTTGTGCTGCAA GGCGATTAAGTTGG
RAC713	TpyA_KO_Mid_RV	TpyA	TGCGCCGACATGAAGGATGGATTATCCGG CTCGTATGTTGTGTGGAAT
RAC714	TpyA_KO_RF_FW	TpyA	ATTCCACACAACATACGAGCCGGATAATC CATCCTTCATGTCGGCGCA
RAC715	TpyA_KO_RF_RV	TpyA	TGTCTTCACGTCAGCTTGGGTTCT
RAC716	TpyA_NESTED_FW	TpyA	GGGGACAAGTTTGTACAAAAAAGCAGGCT AAACCAAGTCTAACCGCAGCGACT
RAC717	TpyA_NESTED_RV	TpyA	GGGGACCACTTTGTACAAGAAAGCTGGGT GTGGTTCAAACGTGGCAGCAGAAA
RAC855	TpyA_KO_LF_rv-HygB	TpyA	ACCATCAGGGACAGCTTCAAGGATAACAA CACACCAGCTCGGCA
RAC856	TpyA_KO_Mid_fw-HygB	TpyA	TGCCGAGCTGGTGTGTTGTTATCCTTGAAG CTGTCCCTGATGGT
RAC857	TpyA_KO_Mid_RV-HygB	TpyA	TGCGCCGACATGAAGGATGGATTATGCAC GAGTGGGTTACATCGAACT
RAC858	TpyA_KO_RF_fw-HygB	TpyA	AGTTCGATGTAACCCACTCGTGCATAATCC ATCCTTCATGTCGGCGCA